Microporous membranes as gas/liquid phase contactors for the use in aggressive colloidal solutions

Darragh, Brendan

Award date:
2007

Awarding institution:
University of Bath

Microporous membranes as gas/liquid phase contactors for the use in aggressive colloidal solutions

Brendan Darragh

A Thesis Submitted for the Degree of Doctor of Philosophy

University of Bath

Department of Chemical Engineering

January 2007

ProQuest LLC
789 East Eisenhower Parkway
P.O. Box 1346
Ann Arbor, MI 48106-1346

Abstract

Viscous glass coating solutions of high pH and containing colloidal solids require de-gassing prior to their use. In this study porous hollow fibre membranes were used to achieve desorption of dissolved gases by non-dispersive phase contacting. Membranes can offer the benefit of large surface area and remove dissolved gases by altering gas/liquid equilibrium.

Initially ceramic membranes were selected due to their resistance to the aggressive nature of the chemicals used. Ceramic hollow fibre membranes were produced via a phase inversion technique in which a polymer (polyethersulfone) and solvent (n-methyl-2-pyrrolidinone) were mixed and a ceramic powder of aluminium oxide was added to the mixture. This mixture was then extruded into water baths in which hollow fibre structures were formed as the solvent exchanged with the water bringing the polymer out of the liquid phase. Sintering of these structures at temperatures in excess of 1200°C caused burn out of the remaining polymer part of these structures. The result is a porous hollow fibre membrane. Fibres manufactured in this study showed typical pore diameters in the range 0.1 to 0.5μm.

Basic dip coating of the fibres in a simple water or alcohol based dispersion of alumina particles was employed to limit defects. Uncoated fibres frequently exhibited a handful of pores of sizes that were too large to determine by the methods used. Coating the fibres had the effect of minimising defects in the structures and hence limiting the maximum pore size of membranes to values in the range 0.3-0.4 μm.

An argon sweep gas was used to remove dissolved gas in the liquids tested. Modules produce from the prepared ceramic fibres exhibited mass transfer coefficients that were typically of the range 4 to 8×10^{-6} m/s when used with water. Use with glass coating solutions led to values in the range 8×10^{-7} to 1.5×10^{-6} m/s.

Due to the small size of the ceramic units produced a polymeric unit was introduced to demonstrate the concept of using membranes. The polymeric unit achieved mass transfer coefficients of 6×10^{-6} to 1.1×10^{-5} m/s in water. The same unit achieved typical mass transfer coefficients of 2 to 7×10^{-6} m/s in the glass coating solutions.

Another liquid tested included a neutral silica sol made up of far larger non-porous particles. This achieved similar results to the water tests.

Finally as an alternative to membranes the use of ultrasonic treatment and gas sparging was proposed. Ultrasonic treatment was demonstrated to be able to rapidly separate phases (remove bubbles) that become entrained in the viscous solution when gas is sparged. The results were compared on the basis of mass transfer per unit volume of the mass transfer unit (K_La). The ceramic and polymeric membrane units offered values of 0.0014 and 0.021 s^{-1} respectively while the sparge and ultrasound method achieved 0.033 s^{-1}.

All three methods were used in the intended application it was found that removal of dissolved gases to below 10% of their start concentration was not apparently sufficient to degas the coatings sufficiently for their intended use – the method of coating was however found to leave ample opportunity for re-absorption of gas.

The use of membranes was however clearly demonstrated to be able to lower the initial concentration of target gasses significantly in aggressive, colloidal and viscous solutions. This is achieved in a relatively short period given a suitable membrane unit size. In addition the use of ultrasound and sparging was also found to be a suitable method for reducing the concentration of undesirable dissolved gases in such liquids.

For Mum and Dad

Thanks for all your support in all my work

And to Dad especially I'm so very sorry you couldn't be here to see it finished, thanks for all the support you gave me through the highs and lows of the project. I will always love you Dad, and I will always remember you.

Bren

Contents

I Table of Figures

II Table of Tables

III Acknowledgements

I would like to thank the Engineering & Physical Sciences Research Council for their grant which enabled me to undertake this work, in addition I would like to thank my industrial CASE award sponsors Pilkington Group Limited.

On a professional level I would like to express my thanks to Dr Pawel Płucinski for his held and guidance throughout this project and in addition Dr Su Varma, David Holden and Stuart Dale of Pilkington Group Limited. for their helpful guidance through the project and in particular Stuart Dale for his practical assistance in my time at the Pilkington Group Limited. technology centre in Lathom.

On a personal level I would like to thank my family and my girlfriend Alina Iwan for their support, Dr May Ling Yeow and Mr Chin-Chih Tai for their help and discussions relating to hollow fibre manufacture. The technical staff of the Chemical engineering department and in particular Mr Fernando Acosta for their assistance in selecting equipment for construction of rigs. The technical staff in the Electron optics department for their help and assistance in SEM imaging. Dr Dmitri Bavykin for many many interesting discussions both relating to my work and not relating to my work that have allowed me to challenge the way I have looked at certain situations. And finally Richard Bull for always bringing me down to earth with his realist approach to life.

1 Introduction

This study is concerned with improving upon a process for the removal of dissolved nitrogen gas from a viscous solution that is used in the manufacture of fire safety glass. The existing process used by Pilkington Group Limited. is time consuming and a significant benefit may be obtained if the removal of dissolved gas can be achieved quickly. The current method employs natural degassing of the solution with oxygen once it has been applied to the glass. If the dissolved nitrogen is not removed from the solution bubbles will form once the solution has dried. This will result in lower quality glass products.

The motivation for the project is to find an alternative approach to removing the dissolved nitrogen from the glass solution which will offer a time saving over the existing method.

The general aims of the project were therefore as follows:

- To measure removal of dissolved nitrogen from the solution quantitatively
- To establish and investigate possible methods for removal of the dissolved gas including:
  - Hollow fibre membranes for non-dispersive phase contacting
  - Sparging the solution and removing entrained gas by ultrasound
- To construct suitable systems for testing the removal

On reviewing available methods and systems (see Chapter 2) the following approach to experimental work was developed and added to during the process of work:

- Develop hollow fibres which will be resistant to the chemical nature of the solution
- Investigate the removal of dissolved gas from water to assess performance of the contactor
- Investigate contactor performance on the coating solutions

- Investigate ultrasound and sparging as an alternative method making similar measurements
- Measure the performance of an industrially available contactor
- Attempt casting onto glass of treated solution and establish if blemish free glass is produced

2 Review of literature

2.1 Introduction to gas-liquid mass transfer

Gases and liquids will exchange mass according to concentration differences when they are in contact in order to establish equilibrium. The transfer takes place at the interface between gas and liquid and as such in order to make an effective process based on this mode of transfer the interface should be as large as possible.

2.1.1 Basic methods

The simplest method of allowing transfer between a gas and a liquid to take place is to expose them to each other. For example if it is assumed that temperature and pressure are constant and a tank of water is exposed to the atmosphere for a long period of time it will be in equilibrium with the atmospheric gasses around it. If the tank is then placed in a large sealed chamber with a different atmosphere (but the same temperature and pressure) the dissolved gas content of water in the tank will slowly alter to reach equilibrium with the new atmosphere (i.e. the chamber is sufficiently large that the gas is effectively a concentration sink). This process will take a different amount of time depending on a range of factors such as depth and amount of the water in the tank, the shape of the tank, in particular the shape of the tank at the liquid surface and hence the area of that surface. The key limiting factors in this process in addition to the size of the surface and total volume of water will be how quickly natural molecular diffusion occurs in the unstirred liquid and gas and how quickly mass transfer can take place across a unit of area, these parameters are fixed at the constant temperature and pressure but the limiting factors of molecular diffusion in the two phases can be overcome if the two phases are well mixed. Assuming the hypothetical situation where both the gas phase and the liquid phase in tank can be well mixed independently without dispersing the phases within one another the molecular diffusion ceases to be important so we can say the rate of mass transfer is related only to the ratio of the surface area and the volume of liquid (specific area). The absolute rate will be determined by this and the rate at which

transfer physically occurs over a known area. If it is assumed the volume of liquid is always the same then only the shape of the tank and hence the area of the liquid surface will control the rate of transfer. The best tank for fast mass transfer will be very shallow as shown in Figure 2.1 below

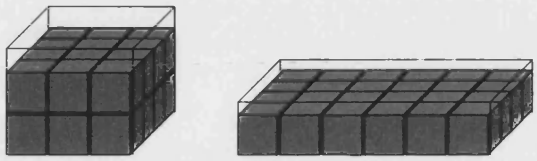

Liquid is represented by cubes to represent units of volume, both containers hold 24 units of volume but the container on the right has twice as much exposed surface area.

Figure 2.1 - Maximising surface area is the key to enhancing mass transfer

Of course no industrial process by design is quite as simple as a shallow tank as there are far better alternatives. However some processes are forced to be, in effect, very similar to a shallow tank. Blanketing of solutions applied to glass is currently the preferred method of dissolved nitrogen removal used in the application with which this work is concerned. This is in effect a very shallow tank with a controlled atmosphere above it. Blanketing is most often used to prevent undesired gases dissolving into liquids within processes but in this case is being used to extract undesired gases from the liquid.

2.1.2 Traditional dispersive methods

Methods of allowing mass transfer discussed so far have been focussed on the exposing of a liquid surface to a gas. This liquid surface is dependant on the nature of the equipment and how the liquid behaves in that equipment. The gas is simply flows through space in the equipment and is in contact with liquid wherever a liquid surface is formed. An alternative approach is to physically mix the bulk phases of the liquid and the gas. Conceptually this means one of two things putting bubbles of gas into a liquid or by putting drops of liquid into a gas.

There are many such processes in use in industry today the following overview includes those discussed in the literature[1].

- Distillation, flashing & rectification are all processes concerned with the separation of different components of a mixture by use of their differing volatility. The equipment itself is concerned with generating a gas phase from the mixture (i.e. the gas is itself formed from the liquid). Progressively contacting the gas phase with the liquid phase results in the more volatile components ending in the gas and the less volatile components in the liquid.
- Stripping and absorption are concerned with the removal or addition of components from or to a liquid stream into a gas stream. The work in this study will be concerned with stripping and hence equipment available for these operations is of interest here and will be discussed further.
- Evaporation and spray drying are also processes where gas and liquid contacting occurs and hence are worthy of mention however the principle itself is to remove liquid components from the liquid phase to leave usually either a solid or a concentrated component in the liquid.

Dispersive stripping and absorption equipment

The literature[1, 2] also lists equipment types used for the various processes Table 2.1 (below) includes those listed for stripping and or absorption processes or absorption dependant reaction processes.

Table 2.1 – Contacting equipment (based on literature[1, 2])

Equipment type	Continuous Phase	Contact type	Typical Specific Area, a (m^2/m^3)
Plate Column	Liquid and/or gas	Dispersive	150
Packed Column	Liquid and/or gas	Dispersive	220
Falling film contactor	Liquid and or gas	Non-dispersive	Widely variable
Spray Chamber	Gas	Dispersive	60
Agitated Tank	Liquid	Dispersive	500
Bubble Column	Liquid	Dispersive	200

Only one of the processes listed is non-dispersive, the falling film system the liquid and gas do not mix as bulk fluids in this system (see Figure 2.2). A film of liquid is poured down a surface and gas flows between surfaces to give contacting without dispersion.

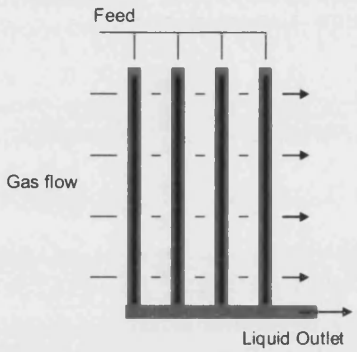

Figure 2.2 - Falling film contactor

This can, in certain circumstances, be a great advantage where the dispersive nature of the contact causes problems. Gabelman and Hwang[3] list some of the disadvantages of the bulk mixing process used in dispersive contacting they include the formation of emulsions or foaming and the problems of unloading or flooding of equipment. The liquids used in this study are viscous in nature and have a high solids content[4] and hence entrainment of the gas and flooding come into consideration as a high viscosity means that entrapped bubbles will remain in the liquid for long periods of time unless removed by the addition of a further separation procedure. The dispersive methods do have the advantage of being well mixed which is significant in that there is little use having a large surface area if the turnover of fresh fluid exposed to that surface is very low.

2.1.3 Non-dispersive methods

As discussed above it is important that any processes considered in this study are able to either perform gas/liquid contacting without dispersive mixing or that the problems

caused by mixing are overcome. The first situation, non-dispersive contacting is now discussed.

At this stage two possible methods of performing gas/liquid mass transfer without dispersion of one phase within the other have been considered, a simple shallow pool of liquid under a gas blanket or a falling film contactor. A falling film gives scope for treating liquid in a throughput style i.e. not all the liquid undergoes treatment at once. This means that the equipment can be smaller and cheaper and allows the liquid to be put through in either a single pass or by being recycled through until a desired level of stripping is achieved, though in theory this could be carried out with a shallow pool, the forced flow across the pool would make the process similar to a falling film. Falling film contactors do have a significant disadvantage however they require the liquid and gas to be present in the same space while the liquid flows. With a viscous liquid such as the one being treated in this study there is an appreciable film thickness. This means that the separation between surfaces within the equipment must be relatively high and hence the size of equipment increases. The surface of the falling film should also be stable to avoid any splashing which could entrain gas. This is likely to mean operation in laminar flow region with poor mixing in the liquid phase and hence limited mass transfer into any volume of the liquid not directly exposed at the film surface. As such a third method is now considered which offers operational benefits over a falling film while retaining the benefits of being non-dispersive. The use of hollow fibre membranes as contactors has been studied for non-viscous solutions by many workers and is well reported[3, 5-12].

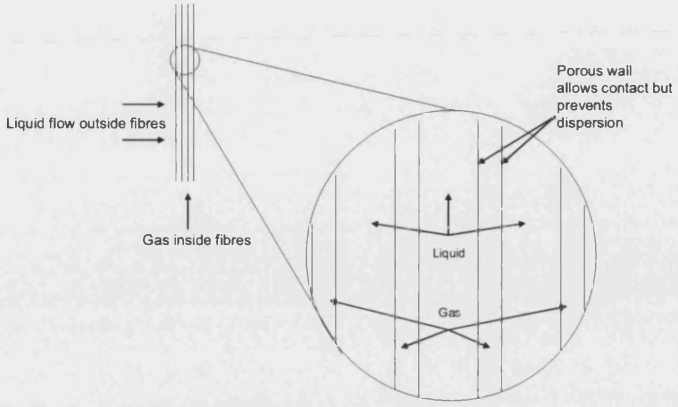

Figure 2.3 - Membrane contactor

Figure 2.3 shows a contactor system and how liquid and gas are in contact without risk of dispersion within one another – the membrane walls retain the liquid or gas either at their surface or within their cross section. Gabelman and Hwang[3] wrote of the advantages and disadvantages of such a system, those that are relevant in the case of this study are included here:

Advantages

- Most importantly there is no droplet formation or foaming as there is no actual dispersion of one phase within the other
- The available surface area is constant regardless of the flow of either gas or liquid
- Flooding and unloading do not occur in membrane module systems
- Scale up is typically linear with membrane systems when scale up is carried out by increasing number of modules. (Numbering up principle)
- There are no moving parts in the vessel (only relevant when compared to dispersive systems with agitated mixing).
- Area per unit volume is usually higher than in dispersive systems[25] (typical specific area can be 1000 m^2/m^3.
- Due to the constant area; measuring, calculating and predicting performance is more reliable and simpler.

Disadvantages

- Most significantly there is an additional resistance to mass transfer introduced, that of the membrane itself. Particularly significant in any part of the membrane that is liquid filled.
- Contactors can be susceptible to shell side bypassing, though industrially manufactured contactors can minimise this as will be discussed later in this chapter. (Some literature reports that channelling is not as likely in hollow fibre equipment as it is in conventional equipment[12])
- Membranes are subject to fouling, though this less of a problem in contactors as concentration difference rather than pressure difference drives the separation*.
- Potting adhesive used to seal the membranes in the unit may not be resistant to chemical attack.

* This statement has extra significance given the heavy solids content of the solution being used in this work – even though there is no pressure driven exchange between the two sides of the membrane the solids may have a tendency to gather on the membrane surface.

Zhang and Cussler[5, 7] commented on two facts from the above list the implication being that they are the key points: the increased surface area is an advantage leading to faster mass transfer however the added mass transfer resistance is a disadvantage leading to slower mass transfer.

In addition there is the further disadvantage that the vast majority of industrially available membranes are polymeric so care must be taken when choosing the material for the membrane.

2.1.4 Membrane operation and configurations

In a classic membrane separation, pressure is often the driving force. A process flow has components separated by the fact that the membrane permits different components to pass through the membrane at different rates, i.e. the membrane is selective. Because of the different rates of the transport of the components a degree of separation is achieved. A schematic of this process is shown in Figure 2.4.

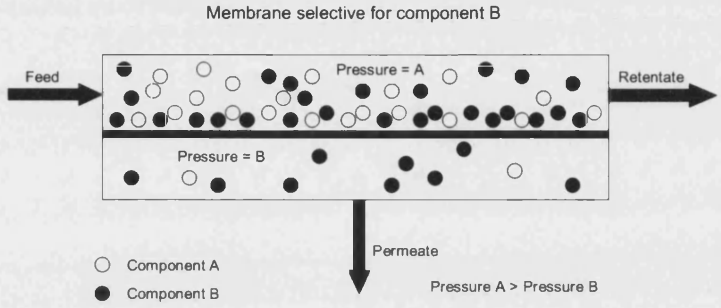

Figure 2.4 - Pressure driven membrane process

In the pressure driven process shown in Figure 2.4 two components enter in the feed fluid, and the fluid is driven through the membrane by the pressure difference, the membrane permits component B to pass through more easily than component A as a result more of component A passes out with the retentate and more of component B leaves as permeate. In most processes the difference in rate at which the components pass through the membrane allows a degree of separation hence in the diagram some of component A has passed through the membrane. It is possible to have a filtration situation in which one component will not cross the membrane at all though this is often due to the sheer size of the component. The alternative situation is the concentration driven process – these may or may not involve selectivity though the most common examples of purely concentration driven systems do not require a selective membrane and in fact the characteristic dense nature of a selective layer can hinder the process. In a porous membrane configuration with concentration as the driving force a component of components will cross the membrane in order to reach an equilibrium concentration. Figure 2.5 shows a schematic of a concentration driven separation process. If there is a solute which is present in two fluids which are in contact but do not mix such as an immiscible organic and aqueous system or a liquid and a gas (where a component of the gas dissolves in the liquid) the solute will reach

a concentration in both phases that satisfies equilibrium (so long as the fluids are in contact for a sufficiently lengthy period of time). In this process fluid 1 enters with a certain concentration of solute. Fluid 2 enters with no solute present. As fluid 2 is without solute on entry solute from fluid 1 will immediately move across the non-selective membrane in order to move the concentration in fluid 2 towards the equilibrium concentration.

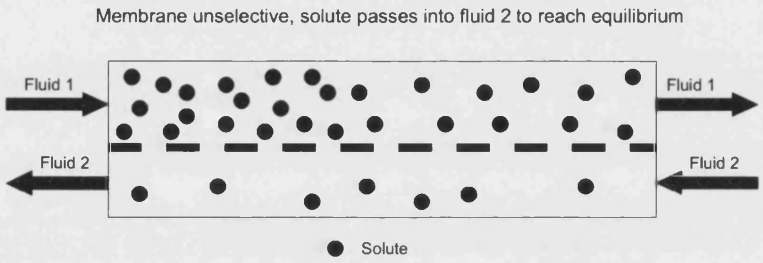

Figure 2.5 - Concentration driven membrane process

There are a range of possible membrane configurations available the most popular are outlined below:

Flat Sheet: The simplest type of membrane is a flat membrane sheet on which process streams can flow on either side separated by the membrane. In its simplest form a single flat sheet of membrane is sealed into a suitable unit. The result is a system which works as a in the example given in Figure 2.4 or Figure 2.5 depending on the nature of the process. A more realistic version of a flat sheet process is one in which several flat sheets are put together in a system which is not dissimilar to a filter press[13]. Several flat sheets are positioned in a stack the feed flow flows through a number of channels where it is exposed to the membrane on one side before leaving the unit. The permeate leaves after passing through the membrane into channels on the other side. In a concentration driven process there will be an inlet and outlet flow on both sides of the membrane layers.

Spiral wound: Spiral wound membranes are in effect flat sheet membranes formed into a space saving configuration. Several membranes are built together in layers separated by spacers which allow flow between the membranes. The membranes are

then sealed in a manner which makes flow possible for two fluids on opposing sides of the membrane. Finally the sandwiched separators and membrane are rolled into a cylindrical shape. The nature of the spiral flow and careful design of the spacers promotes turbulent flow which helps maximise performance[13]. Usually feed flows into the spaces between layers from one end to the other with permeate collecting and flowing towards the centre of the spiral. It is possible to flow fluid from the centre of the spiral outwards to the ends of the spiral for collection in the unit housing or vice-versa allowing contactor type operation.

Tubular: A configuration frequently mentioned in section 2.1 is hollow fibres; these are a subset of tubular membranes and will be discussed below. Tubular membranes are in effect structured in the same manner as shell and tube heat exchangers. Feed is commonly supplied to the shell side for pressure driven applications and both fluid steams are supplied in concentration driven processes. The equipment differs from a heat exchanger type design in that the tubes are themselves very openly porous the membrane is in fact a layer coated either on the inside or outside of the tube.

Hollow fibre: This membrane type is a subset of tubular membranes in terms of shape and usually module construction. It has been suggested that tubular membranes begin at a diameter of 10 mm rising towards 25 mm, while hollow fibres start at a maximum size of 2 mm and are any size below this[13]. This leaves a gap of 8 mm in diameter where no definition is applied. Other authors may define this differently and hence fill the gap with the definition of the capillary membrane – in effect a large diameter hollow fibre. The current author prefers to make an altogether alternative definition, that a hollow fibre is any tubular membrane smaller than 5mm in diameter in which the support material and the membrane are either produced together, are of the same material or are both in the pore size range below 10 μm. In other words a less clear definition but perhaps more useful definition is that the support if used alone would not be useful as a contactor let alone as a selective membrane in the tubular case. Or alternatively any tube that has potential as a membrane contactor is in effect classifiable as a hollow fibre so long as it is smaller than 5 mm in diameter. Anything else is a tubular membrane.

The advantages and disadvantages of each configuration have been summarised in the literature[13]:

Tubular

Advantages:

- Easy to use in a turbulent flow regime.
- Wide range of operational data available.
- They are easily cleaned and maintained.

Disadvantages:

- Large liquid hold up
- Low surface area per unit volume

Flat Sheet

Advantages:

- When stacked as in a filter press area per unit volume can be reasonably good
- Manufacture is relatively simple
- Collection can be made individually from each sheet of membrane making damaged sections easy to identify

Disadvantages:

- Often the whole unit may need to be dismantled to make repairs.
- While acceptable compared with large tubular membranes the area per unit volume is not as high as other units.

Spiral Wound

Advantages:

- High area per unit volume.
- Turbulence easily promoted
- Small footprint

Disadvantages:

- Prone to fouling
- Difficult to clean

Hollow fibre

Advantages:

- Highest area to unit volume ration
- Benefits from configuration being similar to tubular hence well known technology can prove to be analogous.
- Easier to seal in place than other configurations

Disadvantages:

- Unless feed is on the shell side pressure differences that are permitted are low.
- Tube side feed limits flow and pressure so results in laminar flow.
- Easily fouled and difficult to clean.

It is noted by the current author that there are some key points to address from the above list. There are significant differences in the advantages and disadvantages of some configurations in the case of a rigid ceramic membrane as opposed to a polymeric membrane. For example a flat ceramic membrane can prove to be very brittle and quite weak unless it is significantly thick in which case it will hinder permeation or mass transfer. In a tubular membrane there is added strength from the nature of the shape making ceramics a more feasible material particularly as there is a stronger resulting membrane for a given wall thickness as the diameter drops. This is indicated by simple stress calculations:

$$t = \frac{p_{\text{internal}} \cdot d_{\text{internal}}}{2f - p_{\text{internal}}} \qquad \textbf{(2.1)}$$

This governs internal pressure. In this equation t is the thickness of wall required to withstand internal pressure, d is diameter, p is pressure and f is the design stress. Hence as d is smaller so is e and hence a thinner membrane is able to withstand a larger internal pressure.

For external pressure we have a simplified worst case equation[13]:

$$p_{critical} = \frac{2E}{1-v^2}\left(\frac{t}{d_{external}}\right)^3 \qquad (2.2)$$

Here the additional symbols are: E, the Young's modulus and v, Poisson's ratio. Once again we can see for a given wall thickness reducing the diameter results in a higher critical pressure.

The result is that tubular membranes of small diameter, i.e. hollow fibres appear to be the most desireable configuration particularly if ceramic material is considered as a material.

2.1.5 Review of membrane contactor studies

There are a wide range of studies incorporating membranes as contactors the following part of this section is aimed at reviewing some of these studies with regard to identifying the scale of the studies conducted, the results achieved and the membrane types investigated. Firstly an introduction into the flow scheme in the most popular module configurations is given.

There are two main types of module configuration in bundles, parallel flow and cross flow. In addition some authors have investigated alternative configurations. Bundles can be made by placement of fibres into a bundle or by manufacture of a woven fabric and rolling of this fabric into a bundle[10]. Figure 2.6 shows the configuration of cross flow and parallel flow modules.

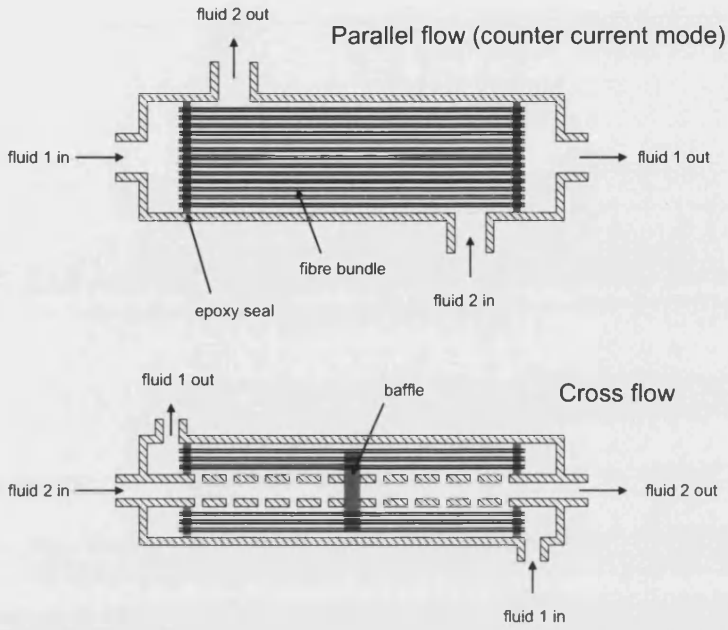

Figure 2.6 - Parallel and cross flow modules

Liquid-Liquid contacting

Though this study is concerned with gas liquid mass transfer, studies in liquid-liquid systems allow illustration of the nature of the interface in a contactor system so some studies are considered here.

Kiani *et al.*[14] studied the use of contactors for solvent extraction (a liquid-liquid contacting process). Flat polypropylene membranes manufactured by Celgard® were used the membranes have a wall thickness of 25.4 μm. Initially the authors define a micro porous membrane and hence a non-selective membrane as one which has pores from 0.1 μm to 0.001nm. A very wide definition though it is not clear weather the smaller size is the smallest that may be found in such a membrane or if membranes with such pore sizes as their average size are in fact suitable for non-selective contact – the former is more likely. A definition of liquid-liquid contact in a hydrophobic membrane is stated which can be well applied to gas-liquid contact in a hydrophilic membrane. In summary it is stated that with a hydrophobic membrane an organic phase will wet the membrane when it is allowed to contact one side of the membrane. If an aqueous phase then contacts the other side of the membrane the aqueous phase

is unable to wet the membrane and will not mix with the organic liquid in the pores. The organic phase will not emerge forming droplets so long as the pressure in the aqueous phase is maintained higher than in the organic phase. As such the liquids are in contact but not mixed hence they are in non-dispersive contact. In the same way in a hydrophilic membrane the aqueous phase will wet the membrane on contact but in the correct pressure conditions will not emerge from the other side of the membrane.

In the gas-liquid contact system there must be a pressure from the gas to prevent the aqueous phase from seeping through. This pressure can go up to but not exceed the bubble point of the gas in the largest pore – in other words there will be a minimum size at which a bubble of gas can be formed. As the pressure is raised this size is smaller, when the pressure reaches a point where this minimum bubble size is smaller than the largest pore then gas can come out of that pore into the aqueous phase. This idea can be used to determine size data in membranes and is discussed in more depth in sections 2.1.6 and 2.4.3. Figure 2.7 shows how fluids are distributed in different types of contactor.

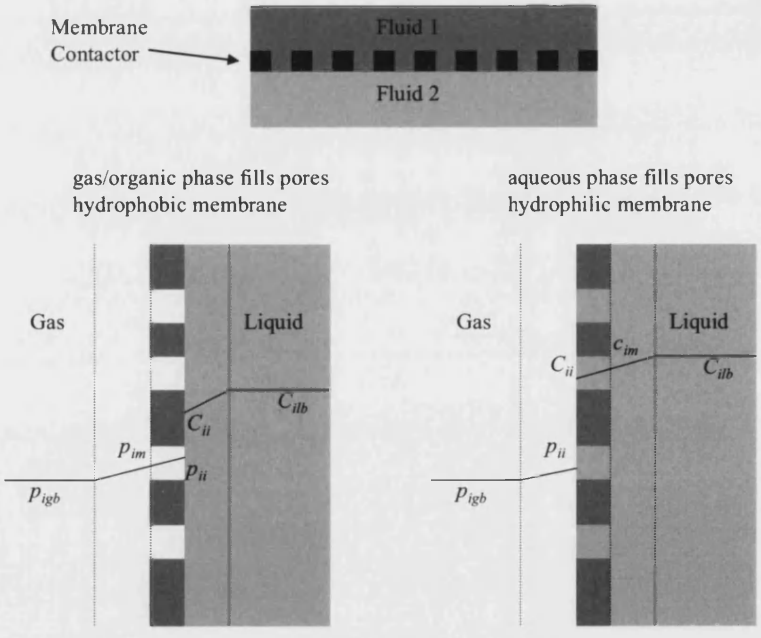

Figure 2.7 - Membrane contactor fluid locations

Kiani *et al.*[14] extracted acetic acid from an aqueous phase using non-aqueous solvent, the solvents used were xylene and methyl isobutyl ketone. It was shown that the extraction was easily achieved. It was demonstrated that at the relatively low pressures that were being used there was little or no effect from varying the pressure used to maintain the non-dispersive state. There was little or no dependence on the rate at which the aqueous phase was flowed at but that there was significant enhanced mass transfer if the rate of the organic phase was increased. This suggests the principle mass transfer resistance is in the organic phase.

Liquid-liquid extraction in hydrophilic and composite membranes[15, 16] has been studied by some workers. Membranes materials used include cellulose, glass and aluminium oxide. Though the system is not operating in gas/liquid mass transfer as is required in this work there are some interesting points to note firstly the pore size of aluminium oxide membranes used is variable across the membrane wall as it is a layered membrane[15]. The second point to note is that in using composite membranes a system which combines a hydrophobic and a hydrophilic layers allows the liquid-liquid interface within the membrane wall at the point where the two composite components meet. The key issues being the possibility of an interface within the membrane walls, the possibility of using aluminium oxide which offers greater resistance to chemical and thermal degradation than many polymeric materials. The varied nature of the pore size across a membrane is also raised as a concept and will be discussed further in section 2.1.6.

Gas/Liquid contacting

There have been several studies considering the use of membranes in a non-dispersive contacting role for gas and liquid. Many of these studies have focussed on absorption of a gas into a liquid system rather than desorption. Often this absorption can be for the use of the gas as a component in a liquid phase chemical reaction.

A patent exists under the title 'Gas transfer process with hollow fiber membrane' by Shindo *et al.*[17] in which there are the usual claims made in patent literature, these

provide a good list of definitions for a membrane contactor in a hollow fibre configuration the most general three points are as follows:

- Average pore diameter in the range 0.01 to 0.5 μm
- Internal diameter in the range 0.05 to 5 mm
- Porosity of the membrane higher than 0.1

The fibre type referred to is polypropylene. There are further definitions regarding open pore area and oxygen permeability, these data are both minimums specified for the patent and are more of an issue with small pore size membranes or membranes with directly manufactured straight pores i.e. track etched membranes where there could be either low permeability or low instance of open pores on the membrane surface.

The work of Zhang and Cussler[5, 7] looked at the concept of using non-selective membranes for gas absorption. Industrially available membranes in a hollow fibre configuration were used. The fibres were orientated in a module manufactured for co-current or counter-current flow. Figure 2.6 shows a schematic of a counter-current module. The fibres used had pores of 0.03 μm in diameter and were made from polypropylene the porosity of the membranes was 0.35. The transfer of carbon dioxide into sodium hydroxide was studied and mass transfer coefficients in the order of 1×10^{-5} to 5×10^{-5} m/s were calculated based on their data. The work then further studied several gasses in both sodium hydroxide and sulphuric acid mimicking some common gas/liquid absorption applications where packed towers had been used.

Costello *et al.*[18] studied the nature of flow in the shell side of hollow fibre contactors where flow was axial. The experiments conducted used hollow fibres with a pore size of 0.2 μm and a porosity of 0.5. The internal diameter was 0.3 mm and the external diameter 0.67 mm. Once again the preferred choice of test was stripping of oxygen from water using nitrogen as a sweep gas. A sweep gas was used counter-currently. Firstly pressure drop data was analysed and it was found that at packing densities below 50% there was turbulent flow and that at higher packing densities the pressure drop was more consistent with laminar flow. It is important to note the modules

prepared were made by random packing of the fibres used. It was postulated that the random packing assists in causing turbulent flow with lower densities as the fibres act as a static turbulence promoter. The mass transfer results reveal mass transfer coefficients in the range $6\text{-}10\times10^{-5}$ m/s. The mass transfer variation with packing density found that the coefficient went down as the packing density increased for a constant flow rate however when considering the pumping power required and running the equipment at a constant pumping power rather than flow rate the inverse was found and the higher the packing density the higher the mass transfer coefficient. The length of module used had little effect.

Crowder and Cussler[19] wrote a theoretical paper on mass transfer in contactors with an interesting aim. The aim was to establish that the average properties of hollow fibres in a module could be used to estimate the average mass transfer coefficient of that module. In order to do this the mass balance around a single hollow fibre was analysed. The analysis is extended to modules in which variable properties for the hollow fibres were allowed. As such the results obtained are good news for anyone wishing to build modules with fibres that are not strictly uniform as there are interesting conclusions relating to fibres with differing radii as well as differing wall thickness. This study will inevitably not produce perfectly identical fibres but will assume identical parameters for all fibres in modules used. As such the conclusions drawn by Crowder and Cussler are not discussed but the conclusions are of use to anyone making modules with fibres of widely varying quality with the intention of studying the effect of this.

There follows a review of a series of studies in which some mass transfer correlations to describe shell side mass transfer are presented. A summary of the equations presented is shown in Table 2.2.

Table 2.2 – Shell Side Mass Transfer Correlations

Geometry	Correlation	Flow Range	Comments	Ref.
Module Built Fibre by fibre – Crossflow (72 fibres) Wide Spacing	$Sh = 0.90\,\mathrm{Re}^{0.40}\,Sc^{0.33}$	10^{-2}<Re<10	Similar to heat transfer in a single tube	12
Module Built Fibre by fibre - Crossflow (750 fibres) Close Spacing	$Sh = 1.38\,\mathrm{Re}^{0.34}\,Sc^{0.33}$			12
Module built Fibre by fibre - Parallel flow 2100 fibres	$Sh = 0.24$			12
Module built Fibre by fibre - Parallel flow 2100 fibres	$Sh = 1.25\left(\mathrm{Re}\frac{d_e}{l}\right)^{0.93} Sc^{0.33}$		$d_e = 4XA / p_w$ where XA = cross sectional area, p_w = wetted perimeter	12
Axially wound fibres	$Sh = 0.49\,\mathrm{Re}^{0.53}\,Sc^{0.33}$	0.03<Re<3	Modules assembled by hand	10
Fabric	$Sh = 0.82\,\mathrm{Re}^{0.49}\,Sc^{0.33}$	0.1<Re<10	Relatively easy to manufacture	10

Geometry	Correlation	Flow Range	Comments	Ref.
Vane	$Sh = 0.80\,\mathrm{Re}^{0.46}\,Sc^{0.33}$	0.1<Re<10		[10]
	$Sh = 0.80\,\mathrm{Re}^{0.47}\,Sc^{0.33}$		Suggested average for fabric type modules	[10]
Bundle – Crossflow 2800 fibres	$Sh = 0.15\,\mathrm{Re}^{0.8}\,Sc^{0.33}$	Re>2.5		[9]
Bundle – Crossflow 11000 fibres	$Sh = 0.12\,\mathrm{Re}^{1.0}\,Sc^{0.33}$	Re<2.5		[9]
Bundle – Parallel flow	$Sh = 0.019Gr^{1.0}$	Gr<60		[9]
Crossflow	$Sh = 1.76\,\mathrm{Re}^{0.82}\,Sc^{0.33}$		suitable for range of modules	[8]

The definition of Sherwood (*Sh*), Reynolds (*Re*), Schmidt (*Sc*) and Grasshof (*Gr*) in references [9, 10, 12] is as follows:

$$Sh = \frac{kd}{D}$$

$$\mathrm{Re} = \frac{dv}{\upsilon}$$

$$Sc = \frac{\upsilon}{D}$$

$$Gr = \frac{d^2 \upsilon}{Dl}$$

Where:

k = mass transfer coefficient

d = diameter

D = diffusivity

v = flow velocity

υ = kinematic viscosity

l = length

in reference 8 the definitions of Sh and Re differ and are as follows:

$$Sh = \frac{kd_e}{D}$$

$$\mathrm{Re} = \frac{4Qd_e\rho}{A_k\mu}$$

Where:

d_e = hydraulic diameter

Q = volumetric flow rate

ρ = fluid density

A_k = Active interfacial area

μ = dynamic viscosity

Parallel and cross flow modules in a shell and tube arrangement:

Schöner *et al.*[8] studied mass transfer in hollow fibre modules constructed with cross-flow as the basis for their direction of flow. Industrially available modules supplied by Liqui-Cel® were used. These modules achieve this cross flow by feeding the module from a central inlet tube which runs to the centre of the module where it is blocked. Along the length of this feed tube there are several holes allowing outflow of the feed fluid forcing it to flow across the fibre bundle. Located in the centre of the

module and protruding radially from the central tube is a baffle, as such all the liquid which flows outward from the feed tube must cross the whole fibre bundle before rounding the baffle it can then only leave the module by crossing the fibre bundle once again where it can re-enter the central tube downstream of the centrally located block. Figure 2.6 shows a schematic of a cross flow module. The aim of the study was to develop a shell side mass transfer correlation suitable for single baffle cross flow modules. Liquid-liquid extraction was studied in their system. The fibres used were polypropylene, with average diameters of 0.26 – 0.31 mm. The porosity was 0.3-0.4 and pore size was 0.03 μm for some fibres rising to 0.05 μm for others. The result of the work is the proposal of a shell side correlation shown by 2.3 (a full definition of the dimensionless groups was given following Table 2.2). This correlation gives good agreement over the range of modules they use. The fluids used are an aqueous phase containing metal sulphate and an organic phase of bis(2-ethyl-hexyl)phosphate in iso-dodecane.

$$Sh = 1.76 Re^{0.82} Sc^{0.33} \qquad \textbf{2.3}$$

Yang and Cussler[11] described the potential of hollow fibres as contactors. In an interesting application fibres were used as artificial gills, in that they could be used to breath oxygen dissolved in water by capturing this oxygen by mass transfer. Live subjects were used for their tests, a single module of fibres was used for a rat or hamster and forty parallel modules were used to supply air to a dog. There is added interest in that the contactor must perform a stripping operation removing the oxygen from water and in addition it must perform an absorption operation by putting carbon dioxide back into the water. Industrially available hollow fibres with diameter 200 μm and wall thickness 25 μm were used. The porosity was 0.3. Contactors were in both parallel and cross flow arrangements. The experimental set up was a gas loop system, tap water was passed through one side of the module and gas was circulated from a sealed chamber through the module and back to the box which was nitrogen filled initially. They measured the rate at which the oxygen concentration in the box rose towards ordinary atmospheric conditions. The authors found that the system could sustain the life of small animals. However most significantly good agreement was found between the results they had expected to get and the results they actually

got. Adding multiple modules to the system resulted in the scaled up performance expected. It was also shown that the only resistance that was significant to the rate of mass transfer was that of diffusion of gas in the water. The membrane resistance and the gas phase resistance were not important. It is stated that because of this the membrane pore size and porosity are not improvable, i.e. there is no advantage to having a more porous membrane or having larger mean pore size. There could be a slower mass transfer rate if non-porous i.e. selective membranes were used in that there would be a lower mass transfer. In this they imply that at a certain limit of porosity and pore size there will be a point where the magnitude of mass transfer resistance in both the liquid and membrane phases become close and hence the liquid boundary layer diffusion resistance is no longer dominant. This study applies to hydrophobic modules where the membrane wall is not filled by liquid and as such a different conclusion may be inferred if there is a liquid layer in the wall.

The same workers considered this resistance [12]. Mass transfer was studied with a view to comparing performance with heat and mass transfer problems that are analogous. It is reported in this paper[12] (as in that discussed above[11]) that the key mass transfer resistance is in the water and not in the membrane or gas. Some correlations are given in the paper relating to the mass transfer coefficient in the liquid phase, these are shown in Table 2.2. It is also stated in this paper that the reason for this is that the membrane used is hydrophobic and as such the pores in their membrane are dry and diffusion proceeds quickly as in the gas phase. It is stated that should a hydrophilic membrane be used there would be a significantly higher resistance from the membrane. There are implications relating to both of these situations. If membrane resistance is unimportant then membrane material is also unimportant. This is as one would expect in fact the only significant control one can impart on mass transfer coefficient is to alter the liquid conditions and by implication the bulk rate of mass transfer is most easily improved by either altering liquid conditions to enhance the mass transfer coefficient or by increasing the amount of membrane and hence the available area for mass transfer. However 'liquid conditions' is a wide term encompassing liquid rate, temperature and flow behaviour hence enhanced mixing can assist mass transfer. The fibres themselves can act as a static mixer for the liquid so long as the liquid is flowing in the shell of the module,

intuitively this mixing will be better if the flow is more disrupted hence flow across a bundle of fibres should be better than flow along a bundle of fibres orientated in line with the flow. The further conclusion is drawn by the authors is that in a membrane which is hydrophilic, i.e. liquid fills the pores and the membrane transfer resistance is dominant the system can have any module configuration and should yield the same results for the same area of the same membrane.

Analysis of performance in contactors has been compared to performance in heat transfer equipment more recently[20]. The units used for the study were as in many works hydrophobic polypropylene. The conclusion from this work is that at low removal rates and low solute concentrations the heat transfer performance predictors work well – however at higher solute concentrations and higher flows there is some disagreement between experimental results and predictions made.

Alternative geometries:

Wikramasinghe *et al.*[9] also studied module geometry using parallel flow, but in addition cross flow over a helical bundle, over a rectangular bundle and over a cylindrical bundle, as well as flow along a flat membrane folded several times to create 'v' shaped flow channels was studied. Figure 2.8 shows these configurations.

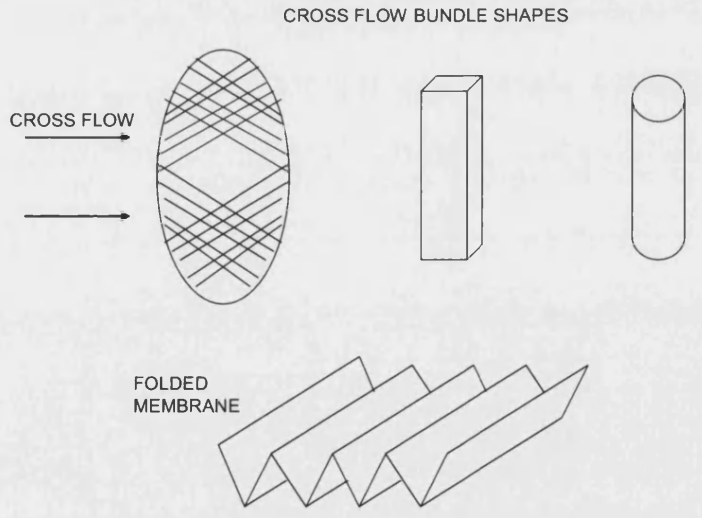

Figure 2.8 - Configurations used by Wickramasinghe *et al.*[9]

The study stripped oxygen from water using humidified nitrogen. The modules were constructed from micro-porous polypropylene membranes the modules used were industrially available modules. The range of sizes of the fibres was from 220 μm to 400 μm internal diameter, wall thicknesses of 25 to 30 μm. Flow with the liquid inside the fibres and outside the fibres was studied for the hollow fibre modules. Flow across the folded flat membrane was studied. An additional note to add to the fibre configuration is that some or the parallel flow contactors used employed hollow fibre fabric which was used more extensively in a further study by the same authors[10]. (This hollow fibre fabric study is discussed below). The results indicate better mass transfer in cross flow orientation than in parallel flow. The difference of the performance is as high as 12 to 14 times better. All cross flow results (for helically wound, cylindrical and rectangular cross flow) could be predicted with the same correlation so performance is in effect similar for all of them. The flat folded membrane was around ten times better than parallel flow.

The same workers studied modules made with hollow fibre fabric[10]. In brief the principle is the use of hollow fibres to make a woven material. Hollow fibres are used in one direction, nylon thread completes the weave in the other direction, this aids spacing of fibres and also aims to reduce channelling. The study reports correlations describing the mass transfer across the boundary layer present in the liquid phase in hollow fibre contactors. The workers re-iterate their observations that the boundary layer conditions are the controlling effect in membrane contactor work with hydrophobic micro porous membranes. It is also suggested that it may be a misconception of workers who use selective membranes to believe that dense selective membranes are unaffected by the boundary layer conditions and that only the membrane controls mass transport. The argument is supported with examples focussing on cases where selectivity of the membrane may be high for one component in a two component system such as water vapour and air. In this case it is possible to be selective for water vapour to an extreme ratio of selectivity though the resulting separation is a far lower ratio. This is due to the vastly higher permeability of the air. In cases such as this a combination of mass transfer resistances must be considered when predicting the performance of the contactor. The study focuses however on the conclusion from earlier work[12] that the performance of industrially

available contactors falls below the performance expected when compared to theories derived from heat transfer experiments and more significantly when compared to the performance of hand built contactors. The authors state that the reason industrially available contactors perform less well is that there is not such careful spacing of fibres. To test this modules with very carefully spaced fibres were built. The contactors used included axially wound fibres around a central porous feed pipe. The pipe is blocked and the liquid flow crosses the axially wound bundle and exits the contactor from the shell side of the module. Other contactors in this style included baffles to effectively make the crossing of the fibres effectively happen three times instead of once. Other modules consisted of hollow fibre fabric. As commented on above hollow fibre fabric is a woven mix of hollow fibres in one direction and nylon thread in the other. The result is well spaced hollow fibres in a sheet of fabric. From this fabric they manufactured multi-pass cross-flow modules using several baffles. A final module used a flat sheet of fibre fabric located diagonally across a box the liquid effectively flows along the box because the box is pulled through a static liquid. Fibres used were polypropylene, 250 μm internal diameter and wall thickness 25 μm. The porosity was 0.2. As in other studies the authors studied the removal of dissolved oxygen into a stripping gas of nitrogen. Results show that as expected carefully placed fibres give mass transfer results up to ten times faster at low flow rates than industrially available units. The authors propose that hollow fibre fabric is in fact very good at achieving this even spacing of fibres and offers greater ease of manufacture. However individually placed fibres in hand built modules still slightly outperformed the fabric or wound modules produced.

2.1.6 Hydrophilic membrane operation in gas-liquid mass transfer

As alluded to in section 2.1.5 it is possible to have a hydrophilic membrane operating as a gas/liquid contactor in this case there will be liquid in the pores of the membrane. In order for this operation to be successful there needs to be a higher pressure in the gas phase than in the liquid phase so as to prevent breakthrough of the liquid phase into the gas phase. As discussed there is a limit to the pressure that can be used. This pressure is known as the breakthrough pressure and is given by equation (2.4) this equation is known as the Laplace equation and it or versions of it are reported widely[3, 21-23].

$$\Delta p = \frac{2\sigma \cos \alpha}{r} \qquad \textbf{Laplace equation} \qquad (2.4)$$

Here Δp is the trans-membrane pressure difference, σ the surface tension, α the contact angle between the wetting fluid and the membrane pore and r the pore radius. A high breakthrough pressure is desirable as it permits a wide range of operating conditions or operational fluctuations. The implications of equation (2.4) are that the surface tension, the contact angle and pore radius affect the breakthrough pressure. If there is no option to alter the liquid then the contact angle can be altered by changing the chosen membrane or altering the membrane properties. Alternatively the pore size can be changed by changing the membrane or applying a coating to alter the pore size at a certain layer in the membrane. This raises an interesting point of operation. If the pores in a membrane are assumed to be cylindrical then pores will remain filled with liquid until the appropriate breakthrough pressure for that pore is reached. At this point the whole pore is emptied[24]. However if the pore is not cylindrical but is wider at one end than the other there it will possible to move the interface between the wide end at low pressure and the narrow end at just below the breakthrough pressure. At higher pressure the gas would then break through and remove the liquid from the pore completely. Alternatively if there is a layer of uniform pores and a layer of smaller pores on top of this then if gas is applied from the larger pored side then at a certain pressure (the breakthrough pressure of these pores the interface will move from the membrane edge to the border with the layer of smaller pores. At this location there will be a range of pressures, between p(breakthrough) for the large pores and p(breakthrough) for the smaller pores for which the interface should not move[3].

2.1.7 Commercial availability

There are a number of commercially available membranes available however several are in the form of units designed for pressure driven separations rather than concentration driven mass transfer processes i.e. they are selective membranes rather than micro porous non-selective membranes. Gabelman and Hwang[3] summarised some of the available units designed for concentration driven separations. Those that

could be used for gas stripping are considered below – in addition some other membrane manufacturers are also included which are not listed in the review.

Liqui-cel® range[25] manufactured by Celgard. These are baffled hollow fibre contactors they appear to be similar to parallel flow units but the internal baffles in fact provide cross flow in the same way as the cross-flow module shown in Figure 2.6 depicts. The membranes are manufactured from polypropylene or polyolefin.

Koch Membrane systems offer units designed for micro-filtration[26, 27] that could be used in a non-selective concentration driven process. These units are operated in a parallel flow method. The membranes available are manufactured from polysulfone or polyacrylonitrile.

Microdyn Technologies also offer some suitable membranes for contactor operations with a range of units from laboratory scale up to industrial units[28]. They have pore sizes in the range 0.1-0.2 μm and are mainly manufactured from polypropylene. They have units operating in simple parallel flow and in cross flow.

Millipore have a wide range of microfiltration filters in various configurations[29], the quoted pore sizes are in a suitable range for use as membrane contactors. The material of construction is polyvinylidinefluoride (PVDF).

In addition to those suggested by Gabelman and Hwang[3] there is an additional available membrane which can be used as a contactor though it is significantly different from the others available in that it is not a polymeric range of membranes but a ceramic range manufactured by Ceparation[30]. The pore sizes available cover a wide range including those suitable for working as a non-selective contactor.

2.1.8 Alternative method to membranes – Dispersive contact and ultrasound

As mentioned briefly above an alternative method to membranes is to be proposed this method involves dispersively contacting the sweep or stripping gas. As discussed above this will result in entrainment of the gas in the liquid. However studies have

shown that ultrasound can be used to remove bubbles from viscous liquids[31, 32]. The removal of bubbles is caused by the tendency of the ultrasound to cause a merging of bubbles within the liquid which raised their size and hence by gravity they float to the surface of the solution.

2.2 Membranes overview

Some membrane types are alluded to in the first part of this chapter when discussing non-dispersive mass transfer. However in order to establish the place of microporous membrane contactors in the field of membranes a brief discussion of various types will follow in this section.

The wide variety of membranes which exist can be classified in many ways, for example one can begin a classification based on material of construction, based on pore size, based on cross sectional structure or even other methods. A popular classification starts by separating natural membranes that exist in nature from synthetic membranes. A whole definition of synthetic membranes would need to include many that are still not relevant to this work so specifically the definition of types will begin from synthetic solid membranes hence eliminating liquid membranes. From this starting point we must now define our solid membrane types and for this task we must still select a first dividing definition, a popular method here is to look at a cross sectional structure an approach used by Mulder[33]. Here there is the classification of symmetric membranes, asymmetric membranes and composite membranes. Under this definition there are some subsets – cylindrical porous, porous and homogeneous (or non-porous) as subsets of symmetric membranes and porous with and without a dense top layer as subsets of asymmetric membranes. There are no immediate subsets in composite membranes. The homogeneous or non-porous membrane is a dense membrane which can be highly selective but will have low fluxes. Asymmetric membranes with a top skin and composite membranes also have a dense layer which although not as restrictive as a fully dense membrane are still low flux and selective. As mentioned in section 2.1 a porous membrane can be used for the concentration driven mass transfer providing that the interface between fluids can comfortably be maintained at the surface of the membrane or within the membrane

pores. As such the symmetric type membranes of porous and cylindrical porous in addition to the asymmetric porous are suitable for use as phase contactors. Cylindrical porous while suitable tend to be specialised membranes in which a dense non-porous film has pores cut or etched into it. This can be achieved in a number of ways however the process tends to be more expensive than preparation of asymmetric porous membrane or a symmetric porous membrane. As such we will focus on the remaining two membrane types and their position within the classification structure is shown in Figure 2.9.

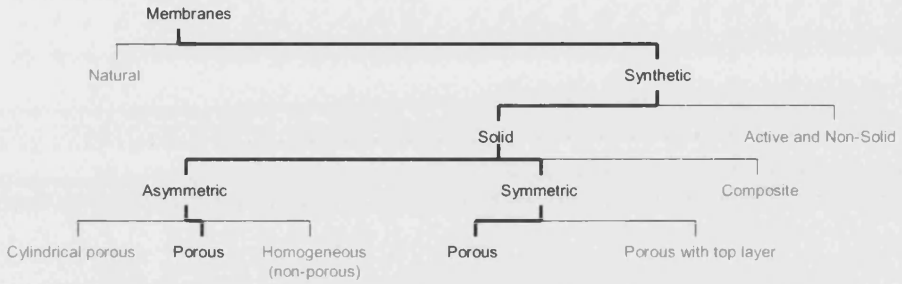

Figure 2.9 - Porous membranes within membrane classification

2.2.1 Basic membrane manufacture techniques

An overview of basic membrane manufacture is presented in this section. An excellent summary of methods is given by Mulder[34] and is summarised further here.

Sintering:

This technique can prepare membranes from both polymeric and ceramic materials and involves the heating of a powder compressed into the shape of the desired membrane. The heating then effectively merges the particles together at the points of contact and creates a solid structure from the powder. The powder does not melt as such because the melting point is not reached but material flows towards the contact points between particles and a neck is formed at the contact point this neck then grows. Mulder[34] continues in his summary listing materials suitable for sintering they include polyethylene, polytetrafluoroethylene polypropylene, steel, tungsten,

aluminium oxide, carbon and glass. The size ranges claimed are 0.1 to 10 μm with the lower limit determined by particle size. The porosity when using polymers is said to be low at 10-20%

Stretching

This is a method by which an extruded film made from a polymeric material is stretched perpendicular to the extruded direction. The stretching causes small tears in the film which if carried out in a careful controlled manner can yield uniform pores in the range 0.1 to 3 μm and very high porosity (up to 90%). Examples of stretched film polymers include Gore-Tex® developed by Gore[35].

Track etching

As briefly mentioned, above, this method produces cylindrical pores. In order to produce them a film is subjected to particle radiation of high energy which is focussed in spots. The polymer is disrupted creating 'tracks' the film is then drawn through a bath of acid or alkali where the 'tracks' are etched to form pores. The result is cylindrical pores through the film. The pore sizes possible are 0.02 to 10 μm.

Coating

Coating does not create the whole structure in itself but rather prepares the membrane layer by coating onto a substrate. Coating is often used in combination with porous layers prepared by other methods. Some coating methods can be used to refine the porosity of a porous structure i.e. to make a fairly varied surface on a porous structure more uniform. Other methods will deposit a dense layer the advantage here being that a thin dense coating can provide the selectivity desired in some membrane systems while the porous support does not restrict the flux like a thick dense layer would. It is commonly accepted that an openly porous layer has a small effect on rate of flux compared to the dense layer in this type of membrane structure. When preparing a membrane with a dense top layer the layer and porous support will usually differ in material so that the support material is of neutral selectivity to minimise the restriction to flux further. The combination of the two differing materials defines the produced membrane as a composite membrane. Coating techniques vary and those

suitable for preparing porous top layers suitable for phase contactors will be covered in depth below along with detailed manufacture of porous membranes.

Phase inversion

Phase inversion is a commonly used method for the production of polymeric membranes. The process forms a solid from a liquid. The liquid is prepared by dissolving the chosen polymer in a suitable solvent. The liquid which must be highly viscous is then shaped by certain means into the desired membrane configuration, flat sheet or hollow fibre (see section 2.1.4). Once shaped the liquid is transformed back to a solid by means of removing the solvent (or more accurately lowering the overall local solvent concentration, usually by solvent removal in addition to introduction of extra components called non-solvents). Once a critical point is reached the solvent is saturated with polymer and further solvent removal (or lowering of the local solvent concentration) results in a solid formation. This will be discussed in more detail below with emphasis on a specific method of solvent removal, there are however several methods by which the solvent can be removed. Mulder[34] provides a description which is summarised by the following:

Solvent evaporation: A process by which the liquid is cast onto a flat non-porous surface and the solvent used is allowed to evaporate. The process can form uniform dense membranes. This method can also apply layers of liquid by coating or spraying with evaporation allowing formation of a dense layer.

Precipitation from vapour: In this process the cast liquid is placed in an atmosphere of non-solvent and solvent vapour the non-solvent will diffuse into the film of liquid causing precipitation.

Precipitation by evaporation from a three component mixture: This process is similar in operation to ordinary solvent evaporation but a non-solvent is included in the liquid so as the solvent evaporates there is a further component which has a relative rise in concentration giving membranes with varied cross section usually involving a dense skinned portion.

Thermal precipitation: A method by which solvent/polymer mixture is prepared at an elevated temperature so that a higher amount of polymer can be dissolved. On cooling the critical point is reached as the solubility of the polymer in the solvent drops and as such a solid is formed.

Immersion precipitation: The most common method of phase inversion membrane manufacture. The polymer/solvent mixture is either cast or extruded and is placed in a bath of non-solvent. Local concentrations vary quickly at the surface with solvent diffusing into the bulk non-solvent and non-solvent diffusing into the polymer/solvent mixture. Often forming a skin at the surface the remainder of the membrane is formed by a slower process of diffusion of solvent and non-solvent.

2.2.2 Factors relating porous substructure and or support layers

It was stated above that the porous support layer or substructure in a composite or asymmetric membrane plays a role that is often seen as negligible compared to the selective layer. It does not always follow that this is the case and depends on configuration and the nature of the process. For example Loeb found that the openly porous support structure created a resistance[36] studying further Loeb *et al.*[37] report that even the support fabric on osmosis membranes provides a significant flux resistance this is presumably due to osmosis being partially concentration driven as well pressure as driven and the support fabric and porous substructures beneath the skin layer of a membrane retain a stagnant region of fluid which has a concentration profile such that the actual driving force is reduced due to the higher than bulk concentration held next to the skin layer of the membrane. Therefore it is important to appreciate that sublayers are important in membranes when the process is concentration driven.

2.3 Hollow fibre membrane manufacture

The manufacture of hollow fibre membranes is invariably performed by use of an extrusion process. The material that is extruded is where variations in method begin and then through a long course of variables in the manufacture of the fibres a wide

variety of different membranes can be made. In order to make a ceramic membrane some practices from the manufacture of ceramic structures will be used, these are discussed below.

2.3.1 Manufacture of ceramic structures

Slip casting is the most simple and classical method of the formation of ceramic bodies a slurry of ceramic material is poured into or onto a porous mould which absorbs the solvent and hence leaves a thin structure similar to a filter cake the excess slurry or 'slip' is then removed leaving this thin layer behind. This is then allowed to dry and a weak compact of ceramic powder results this can then be fired to form a final rigid ceramic structure[38].

Tape casting is a standard technique for the manufacture of more precise ceramic structures for use in industries such as the electronics industry[39]. The process of tape casting is very similar in principle to the process of slip casting. A slurry is cast on a surface with either the surface itself moving under a casting knife or the knife moving over the slurry the result is a thin layer of slurry which it dried to form thin sheets or 'tapes' of ceramic material. These tapes are then fired or sintered to form the permanent ceramic structure[40].

The basic principle of tape casting remains the same though there are a range of aqueous and non-aqueous solvents used. This basic principle can be applied to manufacture of extruded hollow fibres as will be outlined below.

2.3.2 Manufacture of hollow fibre membranes

The manufacture method of various membranes have been discussed (above) in this section a detailed study of the method chosen will be outlined.

The simplest method of producing a ceramic membrane may be to cast a slip or tape casting solution in a thin layer on a non-porous support – however as discussed a hollow fibre configuration has been selected and as such the cast shape must be

capable of being handled between processing steps. It could be possible to take a tubular support and coat a slip solution but a thin coating layer on the support would not be strong enough unless the support itself survived the later sintering of the ceramic layer. The best method would be to prepare a structure impregnated by ceramic material in which all but the ceramic is removed after sintering treatment leaving a strong fully ceramic structure. This can be achieved simply by taking a polymeric phase inversion technique and adding ceramic material to the mixture[41] or by adding ceramic powder to a polymer melt[42, 43].

Due to its simplicity and the availability of the equipment an immersion precipitation method is very suitable for manufacture of membranes in this project. However the formation of a thick dense layer restricting flux by limiting contact area is not suitable for a membrane phase contactor. It must be recalled at this stage that the intent is to produce a ceramic membrane which as discussed in section 2.3.1 employs the use of sintering. Recalling the brief introduction to sintering originally outlined by Mulder[34], in sintering the limitations of pore size are down to the particle size used. That said there is still an importance of understanding the immersion precipitation process and its effect on the likely polymeric structure. As such the method of manufacture itself is important as it introduces the variables that are encountered and that must be controlled or used to benefit the pre-sintered structure as well as the final membrane structure.

Manufacture of an immersion precipitation membrane can be as simple as casting a flat layer of polymer solution on a glass plate and then immersing the glass plate into a non-solvent bath. Even in this apparently simple process we have several variables to consider. The thickness of the cast film, the temperature of the surrounding atmosphere, the temperature of the glass, the period between casting and immersion, the speed at which the cast layer is spread upon the glass, the composition of the solution used, the list goes on. In more complex methods such as semi-continuous casting of flat membranes a support material may be drawn under a casting device which places a thin layer of solution on the support surface, the material can then be fed on rollers through a bath of non solvent and out again for collection and further treatment. As discussed the desired membrane for this study is in the hollow fibre

configuration this adds further complication in as much as the casting device for flat sheets can be a relatively simple device while an extrusion device producing an annular shape is not so simple. The lack of support means that the viscosity of the liquid must be higher so as the annular shape is able to withstand the forces it may be subjected to prior to solidification (that said once one has such a fibre there is the benefit that no support layer is present so there is no secondary support to remove prior to or during sintering – of course the main structural support prior to sintering is provided by polymer which will be 'burned' out as a result of sintering). It is important that once the polymer is burned away in sintering there that is enough material left to sinter and form a rigid structure

A simple diagram of spinning apparatus based on that presented in Mulder[34] is shown below (Figure 2.10), a more detailed diagram of the actual equipment used is presented in chapter 4 as Figure 4.2.

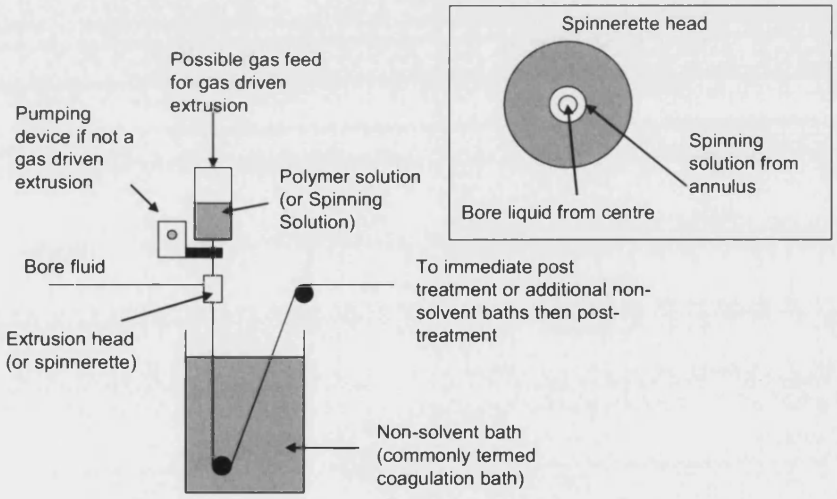

Figure 2.10 - Basic spinning process diagram based on that in the literature[34]

The solution is driven under gas pressure or pumped through the extrusion head which is commonly known as a spinnerette in hollow fibre manufacture. The solution flows out of an annular orifice. Inside of the annulus is a second orifice in most cases here a bore fluid flows – this can be a gas or a liquid but is most usually a non-solvent liquid[44-49]. The bore fluid effects phase inversion on the inner surface of the annular

tube of solution. At the outer surface there may or may not be a degree of evaporation based phase inversion or phase inversion caused by drawing of non-solvent water vapour into the polymer fluid from the atmosphere. Water vapour in the atmosphere can have enough of an effect that control of this atmosphere is undertaken[50]. This depends on the position of the extrusion head relative to the surface of the non-solvent bath. In some cases the extrusion head is located in the non-solvent so there is no contact between the outer surface and the atmosphere, this is known as wet spinning. When there is contact with the atmosphere the process is known as dry-wet spinning, the distance between the extrusion point and the surface of the non-solvent being termed the air gap. This terminology is used by many authors[48, 50, 51] and is appropriate for use to describe the position of the extrusion head in this work. Following the extrusion head and either direct entry into the non-solvent or a brief period in air before falling into the non-solvent the annular tube which is rapidly forming a solid fibre is looped around a roller in the bath and then by means of a motor is pulled at the same rate at which is falls from the extruder. This roller will draw the forming fibre through the non-solvent. It may be pulled direct to a wet collection point or pulled through several further baths of non-solvent and then to a wet collection point. The fibre is nearly always kept wet for some time following spinning for some time to allow full solidification of the polymer in the system and to allow solvent to leave the polymer matrix.

It is possible to operate the extrusion of fibres in other ways – melt extrusion and dry spinning are listed by Mulder[34]. Melt extrusion is not a form of phase inversion or immersion precipitation but rather a more traditional way of preparing a viscous liquid by simply melting the chosen material and extruding above the melting point. The method is not considered in this study but can be used for ceramic hollow fibres though not by direct melting of the ceramic but by melting a polymer and mixing in ceramic material then extruding the melt mixture before sintering[42, 43].

The exact means by which the polymer solidifies at first seems simple enough, the polymer is at some point of local concentration no longer fully soluble in the solvent due to addition of non-solvent into the system and so solidification occurs however the possible results of solidification can go in a number of directions. The

possibilities are outlined well in a work by Barth *et al.*[52] while a physical description of the process is provided by Mulder[53]. The composition of a three component system is best shown on a ternary diagram such as that shown in Figure 2.11.

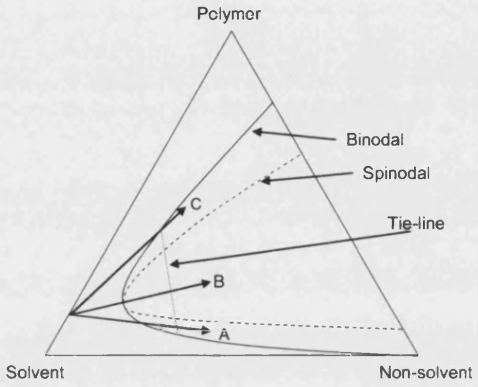

Figure 2.11 - Ternary diagram of a polymer/solvent/non-solvent mixture based on Barth *et al.*[52]

Three possible routes for solids formation are depicted on the diagram. Each route begins at the same point which is a binary mixture of polymer and solvent. The routes shown will either result in metastable nucleation and growth or thermodynamically unstable spinodal decomposition. Route A shows a form of nucleation and growth which is not useful for manufacture of membranes. The initial mixture of solvent and polymer moves towards the bimodal as non-solvent is introduced. On reaching the bimodal $\Delta G > 0$, the liquid-liquid demixing occurs only when stable nuclei are formed. These will form at points where the instantaneous local concentration at a point is polymer rich (i.e. at the opposite end of the tie-line shown in the diagram) the nuclei formed therefore have a composition high in polymer and are dispersed in non-polymer and solvent. The nuclei will grow forming a spongy very open, weak solid as phase inversion moves towards completion. If the route followed is route B then spinodal decomposition will follow. Here the composition moved towards the binodal and crosses immediately the spinodal such that the composition is in the unstable region and instantaneous liquid-liquid demixing occurs $\Delta G < 0$. The result is a disjointed mixture of small points with local compositions that lie on the binodal line (though the overall composition would lie within the unstable region enclosed by the spinodal). Route C once again gives us nucleation and growth however in this

position the nuclei formed are composed of non-solvent and solvent. These nuclei are dispersed within a region of mainly polymer. As the polymer region loses solvent to the nuclei the polymer solidifies and the nuclei form the pores within the structure. The result is a solid structure characterised by pores formed where the nuclei of solvent and non-solvent formed.

2.3.3 Past studies in polymeric flat sheet/fibre manufacture

Though the final membrane will not be a polymeric one there is value in studying the past work in the field of polymeric membrane manufacture as the expected structure has an important bearing on the expected structure of the final ceramic membrane on a macrostructure level. Therefore reviewing past work will enable a choice of polymer and solvent for manufacture of ceramic membranes in addition to the conditions in which the extrusion can be carried out. Essentially the following demands must be met; the polymer and solvent must be compatible, they must be compatible to a sufficient extent that the correct form of liquid-liquid demixing can be achieved to give a suitable structure. The structure that results should be suitable for the manufacture of ceramic membranes i.e. the macro-voids formed in the structure must not be too large or at worst the structure could collapse in the time between polymer burn out and the onset of sintering and at best the fibre produced will crumble easily.

Given that the properties of the polymer and solvent are not of concern for the final membrane it is logical to select a combination that is known and has been used successfully within the department of Chemical Engineering at the University of Bath. These combinations include the following; Polyvinylidinefluoride (PVDF) and *N,N*-dimethylacetamide (DMAc) and polyethersufone or polysulfone and *N*-methyl-2-pyrrolidinone (NMP) or DMAc. It was found that working with PVDF in extrusion could be difficult[54] but that said it is perfectly possible. In addition polyethersulfone and NMP was recommended by Li[55] who along with co-workers had previous experience of using polyethersulfone and NMP with ceramic material to produce ceramic fibres[41, 56]. The focus of this section will focus on the three possible polymers and two solvents mentioned above however some alternate combinations are included

as a demonstration of the alternatives or where the study is of importance in a general sense within the field of membrane manufacture by immersion precipitation.

The membrane types formed by immersion precipitation are often referred to as Loeb-Sourirajan type membranes[57]. The original Loeb-Sourirajan membrane was significant for more than just its manufacture technique and was in fact a cellulose acetate membrane formed by immersion precipitation of a four component mixture that included a pore forming agent. The membrane could be tailored to the specific demands of the separation by adjustment of operation temperature – a combination of this and other factors produced a successful reverse-osmosis membrane in which the asymmetry of the resulting membrane was important[57].

Formation of the characteristic structures within a phase inversion membrane:

The asymmetric nature of phase inversion membranes has been briefly mentioned above however there are several possibilities for the overall structure from varying thickness of any skin layer to the porosity and nature of the more porous region in the membrane. There have been some studies[58-61] attempting to model the phase inversion process and the general conclusions drawn from these studies is presented below:

A diffusion model proposed by Reuvers et al.[58, 59] concludes that there are two types of membrane formed by the suitable nucleation and growth method discussed in section 2.3.2 (Route C). Firstly membranes can form a skin layer where no nucleation could take place, beyond this is a thick sublayer of interconnected pores formed by the nucleation. Or alternatively there is a type formed where an additional layer is present between the skin and the porous layer, this is a dense layer of a few microns which is caused by a high polymer concentration which prevents pore interconnectivity associated with the more porous sub-layer. It is stated[58, 59] that the cause of this second membrane type is the failure of the composition to cross the binodal line. This type of membrane was only formed when using water as the non-solvent it is stated that solvents that are more miscible with water will allow this type

of membrane to be avoided. (The work studied a cellulose acetate, acetone, water system)

A further study[60, 61] by many of the above authors was published some five years later and drew some additional conclusions firstly on the formation of macro-voids within the cross section of the membrane which is a characteristic structure formed in immersion precipitation membranes. It was found that macrovoids result from instantaneous de-mixing of polymer and solvent – if there is delayed de-mixing there are no macro-voids. At certain concentrations of polymer and solvent there will not be macro-voids regardless of demixing timing. The study indicates that the delay in de-mixing can be influenced by a number of factors including the type of solvent, the amount of solvent in the coagulation bath and the amount of non-solvent in the initial casting solution. Generally de-mixing time increased when solvent concentration in the coagulation bath was increased. The results also imply that increased non-solvent in the initial casting solution will hasten de-mixing. The effect of a polymeric additive is found to also have an influence, investigating a PSF, NMP, PVP casting mixture with water added in some cases it was found that the presence of PVP can suppress the formation of macro-voids when the concentration reaches a critical point. The concentration being higher the lower the molecular weight of the additive. It is noted in this work that there are various theories put forward by other authors for the formation of macro voids the exact mechanism is not of such importance in this study as it is not the investigative focus of the work however understanding how to control the formation is important. The following studies are reviewed on the basis of the structures achieved and the way in which these structures were perceived by the authors however the above section on macro-void gives a basis for discussion of the following results. Though not all the studies are concerned with the manufacture hollow fibres the variables in production studied can be applied to hollow fibre manufacture. The studies are grouped based on the polymer solvent system used.

Polysulfone/Polyethersulfone based membranes:

Cabasso *et al.* published a two part study on polysulfone hollow fibres as early as 1976/77[62, 63]. Solvents including DMAc and DMF (N,N-dimethylformamide) were

used. DMAc was the preferred solvent with added PVP as a viscosity moderator. It was shown that PSF with DMAc and PVP is a suitable mixture, interestingly relatively large pore sizes were found when characterised using the bubble point method (see section 2.4.3) to determine maximum pore size, pores ranging from 0.19 to 0.44 μm were found. The morphology of the membranes produced is quite dense. With a ratio of solvent to other components of 1:1 of which 60% of the non-solvent was PSF and 40% was PVP. A one micron sized porous sponge structure (i.e. 1 μm is the size of the voids in the sponge structure) formed most of the cross section. When the solvent content was raised to 66% of the total with 24% PSF and 10% PVP there was some macro-void formation from the side of inner wall, sizes of the macro-voids were as high as 20 μm. When solvent content was raised to 75% of the total and PVP and PSF were 10% and 15% respectively there were macro-voids formed on both the inner and outer portions of the wall those on the inner were longer than from the previous solution while the outer macro-voids were particularly thin perhaps 5-10 μm though it is difficult to be certain at the magnification shown in images in the paper. The length of the outer macro-voids is around 30-40 μm. In summary it was found slower phase inversion and the higher viscosity in the spinning solution made it less likely macro-voids would be formed. This conclusion is consistent with the conclusions of Reuvers and various co-authors studies[58-61], discussed above.

Yamasaki *et al.*[64] used polysulfone with DMAc as the solvent. Two non-solvent baths in sequence were used. Flat film membranes were cast. The study investigated the effects of using 2-propanol in the first of the non-solvent baths. It was intended to study the permeation performance of the membranes produced as the work was specific to gas separation membranes. The membranes produced were laminated with a thin polydimethylsiloxane (PMDS) layer so as to prevent distortion of the permeation results caused by defects in their membranes. It was found that increasing the immersion time in the first bath could thicken the selective skin layer formed, but that this would, as one would expect reduce the overall permeability. The selectivity of the produced membrane was based both on initial polymer concentration as well as immersion time. Of significance for this work is the finding that a thicker skin layer could be formed as potentially this could assist in the formation of a more sound surface in a ceramic structure as too thin a layer could cause some of the underlying

macro-pores to become present at the surface after polymer burn-out. The authors conclude the effect of immersion in 2-propanol as the first non-solvent on the skin layer it that the layer can grown immersion is allowed to take place for longer. Selectivity is also higher except when the initial concentration of polymer in the casting solution exceeds 30% at which point the time spent in the 2-propanol no longer affected the selectivity. In addition the overall morphology of the membrane is altered quite significantly depending on time in the 2-propanol bath. Reviewing the SEM images presented in the study, the main body of the membrane appears consistent throughout for zero seconds and 300 seconds with few if any macro-voids. The characteristic void size in the sponge like structure seems to be as follows: For zero seconds the image is not clear the voids in the sponges are to small to be certain of a measurement. The voids are around 1-2 μm for 300s. The sample immersed for 5 seconds displays some macro-voids of over 5 μm and a characteristic size of voids in the sponge like area of 3-4 μm.

In a further study by the same authors[65] the same combination of polymer and solvent were used and based on the above study the possibility of improving upon the permeability of more selective membranes was studied. This was based on the assertion that the selectivity was relatively unaffected once the polymer concentration in the initial membrane casting solution was above 30%. Introducing a period of evaporation prior to the immersion in 2-propanol was investigated. It was found that the temperature at which the evaporation step was carried out could effect the permeance, in that a higher temperature led to a lower permeance up to a point at which the higher temperature was causing significant defects in the membrane. The study once again used SEM imaging to measure their definition of a skin layer and found a thicker skin layer when the evaporation time was longer however there are no SEM images are presented in the article in question as such no further analysis of their membrane morphology is possible.

Mok et al.[66] studied the effect of spinning conditions and some surface treatments on hollow fibres prepared from a polyethersulfone and NMP mixture. PVP was added as a pore forming agent into the casting solution. The study of the spinning conditions is of some interest as it demonstrates the possibility to manipulate the wall thickness,

and internal and external diameter of the produced fibre even though the extrusion head remains the same. It was found that the ratio of outer radius/inner radius decreased on increasing the flow of the bore liquid. The ratio also decreases when the casting solution temperature increases. It is stated that these findings are based on a constant internal diameter and flow rate of casting solution. The effect of temperature and bore flow rate seems to be expected however the constant internal diameter is interesting in that the expectation would be an increase of internal diameter on increasing the bore flow. One would expect raised temperature would have a similar effect due to lowered viscosity of the spinning solution making it more easily expanded by the bore fluid. Internal diameter is not stated for bore flow results however the variable temperature results do show a reasonably consistent internal diameter. It is also stated that the ratio decreases if internal diameter increases this is again to be expected at a constant casting solution flow rate. The ratio is also shown to decrease with increased solution viscosity though the authors state that this is due to an increase of inner radius caused by the viscosity increase this is interesting as one would expect the opposite as the higher viscosity will resist the influence of any internal flow pressure however the specific internal diameters are once again not quoted in favour of quoting the ratio. Reviewing the SEM micrographs presented in the study it can be seen that there are large finger like macro voids in the structure these appear to increase in size as the amount of PVP used in the spinning solution is increased.

The studies considered so far show a broad range of variables considered including the coagulation liquid and the composition of the spinning solution. It is an aim in this study to produce in a simple manner membrane contactors. As such of the above considered variables it is relatively simple to alter the spinning solution when compared to the composition of the coagulation bath which is a far larger volume which must then be stored or disposed of. There is still the possibility of limiting macro-void formation by adding PVP or by increasing the polymer content of the initial solution instead of using an alternative coagulation liquid. There are further studies on coagulation medium by several authors where the conclusions are similar – a longer immersion in a medium which causes less rapid immersion precipitation

reduces macro-voids and can cause thicker skin layers and or give rise to greater selectivity[67].

Unpurified tap water as coagulant has been used by Pesek and Koros[68, 69]. A two solvent system using THF (tetrahydrofuran) in addition to DMAc with polysulfone as the polymer. The SEM images presented show that even at reasonably high polymer concentrations some macro-void structures are present. They also show that even with the relatively fast phase inversion caused by the water they have a suitable skin layer as a result of the added THF.

Lafreniere *et al.*[70] studied polyethersulfone manufacture using PVP as an additive. It was found that the ratio of PVP/PES should approach one, if high product permeation is desired. Results for higher ratios are not presented. At an overall concentration of 20% PES this ratio showed a maximum, for lower ratios no maximum was observed and increasing PVP lowered permeability. It was also shown that there were anomalies in the solution viscosity and the pore size distribution as the ratio of PVP/PES approached one.

Wang *et al.*[71] studied the effects of different alcohols being added to the spinning solutions used in hollow fibre preparation. It was found that the permeability tended to be higher for higher alcohols. But that the permeability was still good for the lower alcohols while the selectivity was very high. Macro-voids within the structure were smaller and fewer as the alcohol used was changed progressively from C_1 to C_3 the use of 1-butanol saw return of large macro-voids. The move to pentanol saw few macro-voids again this anomaly was apparently explained by considering the intrinsic viscosity of the solution. The viscosities of the methanol and 1-butanol solutions in addition to an ethylene glycol and diethylene glycol based solution all had lower viscosities than solutions based on the other alcohols. The significance in this study is to look at the cross sectional structure and eliminating macro voids is not necessarily a desirable development when preparing a contactor rather than a selective membrane as a closer packed middle layer in the membrane results in a more stagnant region which will prevent mass transfer. As such alcohol addition does not seem worth perusing.

Wang *et al.*[72] and Wang *et al.*[71] both studied the used of polyethersulfone and in both papers the authors some of whom are the same introduce the concept of a precipitation value for assessment of the polymer/solvent/non-solvent balance. The measure is worth noting as it is valuable in determining the behaviour of these systems. However its use in preparing ceramic membranes based on filling a polymer/solvent system with ceramic powder is limited as the fine variations in selectivity and permeability will not apply and as such it is not used in this study

PVDF based membranes:

Khayet *et al.*[73] studied PVDF in DMAc. The effect of ethanol as a component in either the internal or external coagulant as well as the effects of ethylene glycol as a non-solvent additive in the casting solution were studied. Either water or a 50% ethanol 50% water mixture was used as a coagulant. The SEM images presented excellently demonstrate that when the mixture of ethanol and water was used the macro-void formation was reduced dramatically compared to solely water being used as the coagulant. In all the solutions used for the membranes shown in the images, 23wt% of polymer and 4wt% of ethylene glycol was used, the balance being DMAc. The effect of adding more ethylene glycol at the expense of solvent raised the pore size and porosity of the manufactured membranes.

Khayet and Matsuura[74] studied the effect of simply adding water to the polymer solvent mixture prior to casting membranes, this is similar to an effect studied to support macro-void formation theories as discussed[60, 61]. It was found that pore size and porosity increased when water concentration in the casting solution increased. This would seem to be consistent with the formation of macro-voids which was the expected result based on those earlier studies.

Yeow *et al.*[75] studied the manufacture of PVDF hollow fibre membranes using $LiClO_4$ as an additive to spinning solution in which DMAc was the solvent. It was shown that increasing the salt concentration (up to 3%) not only raised the viscosity of the solutions but also raised the mean pore size of the membranes made. The

higher the temperature of the water bath the lower the permeability of the membrane formed at high salt concentration (6%). At lower salt concentration (3%) the effect was the opposite. The difference in observed pore size between high and low temperatures for the low and high salt concentrations also correspond. Overriding this effect in both cases was the fact that the higher salt concentration (6%) lowered the permeability. The cross sectional structures shown in the study appear similar in all conditions from the SEM images presented which show the whole cross section. Closer views shows distinct differences particularly in the middle portion of the membrane. The higher the water bath temperature the more sponge like the middle structure while at lower temperatures the structure appeared more like an agglomeration of dense particles. The conclusions of the authors were that a careful selection of salt concentration and temperature allowed tailoring of the membrane. For this work the most significant fact is that there may be a possibility to use temperature to effect the way in which the central portion of the membrane is formed. The more open this portion of the membrane is in a ceramic structure the more easily it may be possible to control the location of the gas liquid interface.

Kong and Li[49] studied the manufacture of PVDF membranes using both DMAc and NMP as solvents and a range of variables including PVP, organic acids and LiCl as additives. Wide variability in the cross section was possible using these additives. PVP produced more porous membranes, organic acids could raise the porosity to a point at which there was an inflection and the porosity would decrease with further acid addition. Lithium chloride could also raise the porosity. There was also study of ethanol in the non-solvent baths into which the fibre was extruded as well as using ethanol as bore fluid. The ethanol tended to reduce the formation of a skin layer or even eliminate it. With regard to producing a ceramic membrane from a mixture of polymer solution and ceramic powder the lack of skin is undesirable. This is because the skin layer of polymer will orientate a quantity of ceramic material in a manner that will allow formation of a uniform surface where the packing of ceramic material should be highest in order to be able to control the gas liquid interface in this region.

Three further studies, Li *et al.*[47], Desmukh and Li[48] and Wang *et al.*[45] studied PVDF hollow fibre production and also showed that ethanol present as a component of the

non-solvent in baths or as bore liquid can limit skin formation. Li *et al.*[47] and Deshmukh and Li[48] also stated that the addition of PVP once again was shown to increase porosity.

2.3.4 Ceramic Membrane studies

Many ceramic membranes that are produced by combining the principles of tape casting and immersion precipitation go on to require a coating step – these coatings are used to reduce the pore size significantly which is something that may prove unnecessary for manufacture of contactors as such coatings will be treated separately in the next section – the focus here will be on the manufacture of a basic fibre by extrusion and sintering.

Liu *et al.*[76] studied manufacture of ceramic membranes by filling a polymer system with ceramic material and sintering the extruded fibre. The ceramic material used were $SrCe_{0.95}Yb_{0.05}O_{3-\alpha}$. These specialist materials are for conductive membranes by show clearly that the method of filling a polymer solution is valid for production of ceramic fibres (PES/NMP was used). In addition PVP was used as an additive. The morphology is as one would expect similar in appearance to a polymer fibre spun from a similar solution, the difference being that the fibre is far more porous as the polymer is no longer present in a sintered fibre. The authors present pre-sintering and post sintered fibres and outline some differences. It is stated that there are fewer finger shaped macro-voids after sintering. From the images presented there is some evidence of this but not strong evidence. The morphology in fact appears similar on a macro level. At a close magnification there is as expected significant difference between the polymer/ceramic mixture in the pre-sintering sample and the purely ceramic structure in the sintered sample.

Liu *et al.*[77] studied the manufacture of aluminium oxide membranes using immersion precipitation polymer solutions as a binder for the ceramic material. Sintering temperature and initial ceramic particle size mixtures were studied. Particle sizes of 1, 0.3 and 0.01 microns were used. Elevating the proportions of the smaller sizes was shown to reduce permeability and to increase fibre strength. Raising the temperature

at which fibres were sintered also reduced permeability and increased fibre strength. Comparing the morphology of these fibres with typical purely polymeric fibres from similar spinning solutions it must be said that the ceramic fibres exhibit fewer macro-pores. The structure is also different from the $SrCe_{0.95}Yb_{0.05}O_{3-\alpha}$ of Liu *et al.*[76] in as much as the precursor or unsintered fibre seems to show even fewer macro-voids than the sintered fibre.

An older study[78] incorporating some of the above authors[76, 77] also studied the manufacture of ceramic hollow fibres by the phase inversion and sintering process. The study has many of the same conclusions of that by Liu *et al.*[77] as the investigation studies the use of the same three particle sizes of aluminium oxide in the same polymer/solvent system. The later study simply presents more extensive results. What is shown is that the earlier study uses gas permeation data for ceramic membranes while the later does not appear to do so. It is not clear if this is for any significant reason but as will become clear in section 5.1.1 the current author feels that for several reasons the gas permeation method can be unreliable unless there is carefully designed and built equipment combined with carefully prepared samples.

As alluded to previously it is also possible to prepare ceramic membranes by melt extrusion from a polymer binder system[43, 79]. This is not feasible with the available equipment in this study the resulting fibres have a much more uniform cross section due to the lack of phase inversion effects. The results of Smid *et al.*[79] show that as with phase inversion based fibres there is no selectivity in un-coated fibres.

2.3.5 Ceramic coatings

Gas tight membranes in which there will be a dense skin layer and a potentially dense cross section of membrane are not desired for this study owing to the high physical contact area between gas and liquid hat is desired. As such in order to eliminate defects a simple dip coating process will be employed in which a particle dispersion will be made from alumina powder. It is more common to create a sol-gel type fluid by precipitating alumina from AlOOH[80] this tends however to result in the dense layer which is not desired here. The use of powder for the preparation of dip coating

solutions is however used in some studies, Falamaki *et al.*[81] for example used a powder in water and PVA mixture to successfully coat flat membranes using a very simple "dip in beaker" technique. There are pore sizes of 0.08-014 μm quoted which are expected to be perfectly acceptable for the membranes used in this study.

For completeness a short description of the sol preparation and sol-gel process is included based on the work of Smid *et al.*[79]. The process is however similar for many different authors[43, 82, 83]. Firstly a bohemite sol is produced by dispersing Al-tri-sec-butoxide in water at 90°C. PVA can be added to assist in avoiding cracking of the coatings. The sol is then peptized by adding HNO_3. Once prepared dip coating is by ordinary dip coating techniques or sometimes with vacuum coating[82].

2.4 Membrane characterisation

All membranes that are manufactured will need to have their properties defined in a manner that allows comparison of one membrane type to another. Simple facts about the membranes are obvious and can be simply stated such as material of construction and membrane configuration (i.e. flat, hollow fibre etc.). Often the most interesting details about a membrane are the analysis, to at least some degree, of the pores in the membrane. When discussing characterisation in this study in most cases the implication will be the determination of data with regard to pores in the membrane. The other data that may be determined is the diameter if hollow fibres both internal and external and scanning electron micrography (SEM) of the structure of hollow fibres.

2.4.1 Overview of available methods for membrane characterisation

There are several ways of determining data about the pores in a membrane Hernandez *et al.*[23] present a summary of some methods used. The following are some of the most popular methods:

- Bubble point: The bubble point method measures the required pressure to push a gas through liquid filled pores at various rates.

- Mercury porosimetry: This method is similar to the bubble point method in that the required pressure is measured for filling pores with mercury which will not wet the membrane.
- Solute retention: This measures the rejection of solutes of various molecular weights
- Electron microscopy (SEM): Simply analysis of the produced images to measure pore size is possible.
- Permporometry: This method measures gas flow through a membrane as pores are controllably blocked by condensation of a vapour in the pores.

In addition to the above methods listed by Heranadaz *et al.*[23] there are many other methods, the most significant of which with regard to pore size in hollow fibres is the gas permeation method of Yasuda and Tsai[84]. In this method the rate of gas flow through the membrane at various pressures is analysed resulting in data for mean pore size and effective surface porosity

Given the nature of the membranes expected in this study, the availability of the methods and the ease of use of the methods the following methods have been identified as potentially useful in this study. Gas permeation, bubble point and mercury porosimetry (on a back up basis as equipment was not available at the start of this study) and SEM.

2.4.2 Gas Permeation

The gas permeation method is the simplest of the methods to use experimentally. The method proposed by Yasuda and Tsai[84] defines the method of extracting data about the pore size of membranes based on the rate of permeation of a gas at a variety of pressures. The main function of their method is to describe the mean pore size of membranes. While the work in this study must make use of techniques for the characterisation of membranes the complexities of the method are of less importance to this study the derivation of the following equation is given by Yasuda and Tsai in their paper[84].

$$m = \left(\frac{B_0}{K_0}\right)\left(\frac{16}{3}\right)\left(\frac{2RT}{\pi}\right)^{\frac{1}{2}} M^{-\frac{1}{2}} \qquad 2.5$$

Where:

m = pore diameter

M = molecular weight of the permeating gas

B_0 and K_0 are defined in the following discussion.

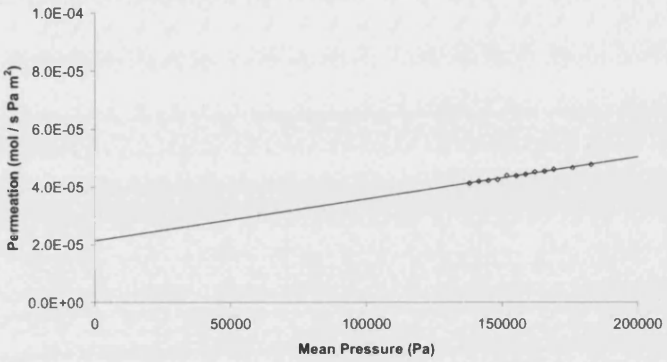

Figure 2.12 – Typical nitrogen gas permeation data in an uncoated ceramic membrane at 20°C

In equation 2.5 the parameters B_0 and K_0 are found by assessment of the permeability of gas through a sample of membrane over a range of pressures. This is illustrated in Figure 2.12 which depicts a typical gas flux (normalised to pressure as in some studies[45, 82]) vs. mean pressure data set. B_0 is the slope of the line and K_0 is the extrapolated value of permeation at a mean pressure of zero. However the equation given by Yasuda and Tsai[84] (represented here by equation 2.5) appears to be dimensionally incorrect, analysis of the units in the equation is presented below in equations 2.5a-c (units as presented in the original paper).

$$m = \left(\frac{B_0}{K_0}\right)\left(\frac{16}{3}\right)\left(\frac{2RT}{\pi}\right)^{\frac{1}{2}} M^{-\frac{1}{2}}$$

$$m = \left(\frac{cm^2 \cdot s}{s \cdot cm^2 \cdot Pa}\right)\left(\frac{-}{-}\right)\left(\frac{J \cdot K}{mol \cdot K}\right)^{1/2}\left(\frac{kg}{mol}\right)^{-1/2} \qquad 2.5a$$

$$note:\ J = \frac{kg \cdot m^2}{s^2} \ and \ Pa = \frac{N}{m^2}$$

Cancelling units within brackets leaves:

$$m = \left(\frac{-}{Pa}\right)\left(\frac{-}{-}\right)\left(\frac{kg \cdot m^2}{s^2}\right)^{1/2}\left(\frac{kg}{-}\right)^{-1/2} \qquad 2.5b$$

Cancelling all remaining cancellable units leaves

$$- = \left(\frac{-}{Pa}\right)\left(\frac{-}{-}\right)\left(\frac{-}{s}\right)\left(\frac{-}{-}\right) \qquad 2.5c$$

This means that dimensionally the right hand side of the original equation must be multiplied by something with units of *Pa s*, such as viscosity. This is demonstrated by an alternative work by Li *et al.*[47] which re-derives the equation giving a similar result (shown below as equation 2.6, the authors use P_0 rather than B_0 for one of the graphical parameters).

$$r = \left(\frac{P_0}{K_0}\right)\left(\frac{16}{3}\right)\left(\frac{8RT}{\pi M}\right)^{\frac{1}{2}} \mu \qquad 2.6$$

The small difference between equation 2.6 and 2.5 (aside from multiplying by viscosity as discussed) is the figure "8" rather than the figure "2" in the third bracket is due to equation 2.5 calculating pore diameter and equation 2.6 calculates pore radius. The method can also be used to give information regarding effective surface porosity by the following equation (presented by Li *et al.*[47])

$$\frac{\varepsilon}{L_p} = \frac{8\mu RTP_0}{r^2} \qquad 2.7$$

Where $\frac{\varepsilon}{L_p}$ is the effective surface porosity.

It should be noted that the original work by Yasuda and Tsai[84] along with several other studies[48, 49, 56] use the permeability coefficient rather than pressure normalised flux which is shown in Figure 2.12, their permeability coefficient had units of cm^2/s. This essentially does not make any difference to the result as the original authors suggested. This is due to the fact the intercept and gradient of the graph form a ratio that will be the same so long as the permeability is plotted in any form that is consistent with their original definition (i.e. there is a linear relationship between permeability as defined by the authors and the actual values used). For example one could even use electrical output measured as a voltage provided the relationship to a physical meaning of flow or pressure remains linear and that zero volts represented zero flow or zero pressure (allowing for adjustments for gauge pressure). The reason that this is in fact true is due to the important factor being the parameter of B_0 or P_0 divided by K_0 always cancelling any linear scalar quantities involved because it is a ratio. This can be shown by comparing the permeability coefficient method with the normalised flux method as follows:

Yasuda and Tsai[84] defined their permeability coefficient based on the permeability coefficient arising from:

$$K = K_0 + \left(\frac{B_0}{\mu}\right)\Delta\bar{p} \qquad 2.8$$

This equation defines the permeability coefficient K as that given in works including Hopfinger and Altman[85] the definition is quoted as follows:

"*RT times the molar flow rate per unit area of membrane divided by the pressure gradient*"

This would imply the following:

$$K = RT \cdot \frac{molar\ flow}{area \cdot time} \cdot \frac{1}{pressure\ gradient} = \frac{J}{mol \cdot K} \cdot \frac{K}{-} \cdot \frac{mol}{m^2 \cdot s} \cdot \frac{m}{Pa}$$

$$K = \frac{J}{Pa \cdot s \cdot m} = \frac{Nm \cdot m^2}{N \cdot s \cdot m} = \frac{m^2}{s}$$

So permeability coefficient as defined[85] is shown to have the same dimensions as those used by authors who work this way[48, 49, 56, 84]. Those who use pressure normalised flux appear to have a different system however as proposed by Yasuda and Tsai[84] we can remove all multipliers which are constant (i.e. we will linearly change the value of *K*. This includes R, T, area and the membrane thickness which forms part of the pressure gradient parameter. If we remove R, T and membrane thickness but keep the area we have the following definition of alternative *K*:

"*molar flow per unit area divided by pressure difference*" or

$$K_{alternative} = \frac{molar\ flow}{area \cdot time} \cdot \frac{1}{pressure\ difference} = \frac{mol}{m^2 \cdot s} \cdot \frac{-}{Pa} = pressure\ normalised\ flux$$

Both methods give the same result for pore size. Area is kept simply to define the system as pressure normalised flux rather than the more vague quantity of pressure normalised permeation rate which would not account for area.

2.4.3 Bubble point and Bubble point/gas permeation method

The test is a common method and is described by Mulder[86]. The bubble point method in its simplest form determines the maximum pore size of a membrane by displacement of a wetting fluid from the membrane using a non-wetting fluid. An extended version of the method uses gas permeation data obtained in a dry membrane

and permeation data in a wet membrane to provide a pore size distribution and the maximum pore size.

The theoretical basis for the extended bubble point method in ideal conditions does not require a gas permeation run and a wet permeation test but rather a single run of experiments run to a high input pressure as described by Jakobs and Koros[87]. The method relies on comparison of the flux of a liquid or gas through the membrane over a range of pressures. Starting at low pressures where the membrane is liquid filled through to high pressures at which progressively all the liquid filling the membrane's pores has been driven out of the pores and in effect the membrane is 'dry' or evacuated of the initial liquid. By observing the flux of the second fluid over a range of pressures the size of the pores being evacuated can be estimated. It should be noted that in the case of a two liquid method the liquids should be immiscible.

Observing the simplest case a hydrophilic membrane is flooded by water. Air is being used to evacuate the pores. If the pores are assumed to be straight (i.e. perpendicular to the membrane walls then each pore acts independently as an individual short capillary tube. There is an associated capillary pressure in each pore, this pressure must be exceeded on the 'dry' side in order to drive out the liquid filling that pore. The size of the pore can then be determined according to the Laplace equation (2.9) as reported in section 2.1.6.

$$\Delta p = \frac{2\sigma \cos\alpha}{r} \qquad \textbf{(2.9)}$$

Figure 2.13 gives a diagrammatic representation of how liquid is driven from the pores at an elevated Δp.

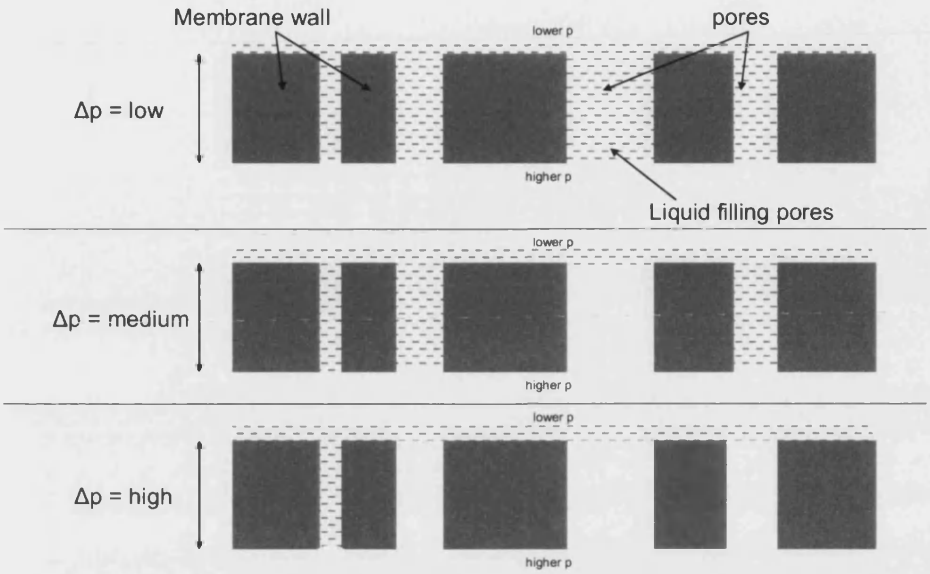

Figure 2.13 – Principle of the bubble point method

As the pores are emptied there will be an increasing measured gas flux until all the pores are empty at which point the gas flux increases linearly with increase in pressure as with the gas permeation method. The shape of a flux vs pressure curve in a bubble point test and a gas permeation test is as shown in Figure 2.14.

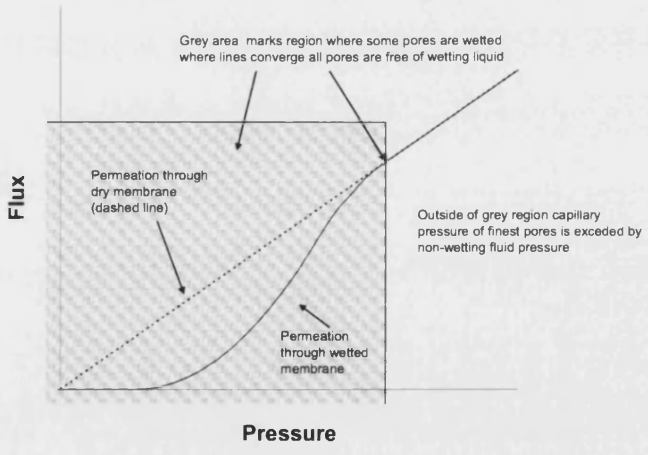

Figure 2.14 – Bubble point method output

By comparison of the permeation through the wetted membrane and the back extrapolated dry membrane data an 's' shaped distribution curve can be obtained. This gives the cumulative proportion of the maximum flow against pore size and is obtained simply by dividing the wet membrane flow by the extrapolated dry membrane flow. The result is a curve similar to those shown in Figure 2.15.

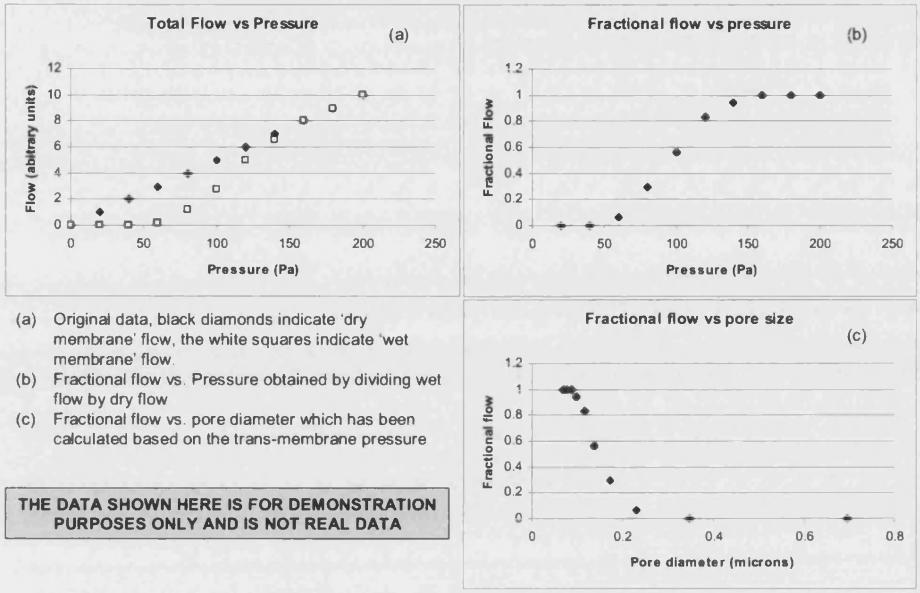

Figure 2.15 - Example of Bubble point/gas permeation data sets

The two curves (b&c) are in effect the same though curve (c) has had pressure replaced on the x-axis by pore size according to equation (2.9). Curve (a) shows the shapes similar to that in Figure 2.14.

Tests performed in this study use the gas permeation test and wet permeation approach as the pressure required to evacuate the smallest pores is very high. It is proposed that the Mulder[86] approach to obtaining dry permeation data is used and that bubble point data is measured up to the maximum allowable pressure or readable flow in the available apparatus. The result will be partial bubble point data and hence a partial distribution of pore sizes. The data obtained will be maximum pore size determined from the bubble point as standard and a mean pore size as determined by Jakobs and Koros[87], here the authors state a "flow weighted average pore size" at the point where flow through the wetted membrane reaches half that of the flow through

the dry membrane at the corresponding pressure. The authors also state that there is little practical value in converting the data obtained into distributions based on number of pores. The limitations of equipment used in this study would prevent full distribution analysis that said Jakobs and Koros[87] make a valid point in that the practical use of knowing the number of pores is limited compared to the expected flow through them. Whilst pressure driven flow is not the aim of contactor applications it must follow that a measure of this flow has a relation to the free area for contacting. That said the most important point of characterisation in this study is to find the maximum pore size which defines the operating limits. The mean pore size determined by this method will be most useful in allowing the method to be validated by comparing to methods which cannot be used on more than a few membrane samples due to time, cost and availability such as SEM and mercury porosimetry.

The bubble point method of analysing pore size data is mathematically a far simpler, and in the opinion of the author, a far more robust method. Further evidence is provided in a comparison of the gas permeation method and the bubble point method provided in section 5.1.1. The main disadvantage of the bubble point method is that it is more time consuming than the experimentally simpler gas permeation method. In effect a procedure similar to that of the gas permeation method is run twice or three times, each under slightly different conditions owing to operational difficulties caused by the available equipment (see section 4.3.3 for details of how the experiment was performed in this study).

2.4.4 Mercury Porosimetry

Mercury porosimetry also works on the basis of equation (2.9) and relies on the assumption of cylindrical pores. The method has disadvantages and advantages, it tends to be automated and can work at very high pressure giving good and extensive results provided the machine is in a good state of calibration. The high pressure can damage the membranes being tested[23, 88]. Some mercury always remains inside the membrane after testing. Most significant however is that the key fact relating to membranes as contactors is the size of the 'free for flow pores', i.e. pores that are open on both sides of the membrane. The bubble point method physically pushes

material through the membrane and hence gives data only on these pores, mercury porosimetry will also measure non-flow or 'dead-end' pores which will distort the pore size data gained with regard to the size of flow pores. Mercury porosimetry will also measure pore sizes throughout the full thickness of the walls of the membrane[88]. This problem is similar to the problem of measuring dead end pores but with the open porous structure of ceramic contactors there is no dramatically smaller sized pores at the surface of the membrane as compared with the structure in the main body of the wall and as such pore sizes measured will be not strongly affected by this. It can be a significant problem when testing other membrane types which have either a composite or asymmetric, selective or fine pored surface layer. The bubble point method does not suffer this problem owing to its measurement of 'free for flow' pores only.

2.4.5 SEM Imaging

With openly porous membranes the pore size and morphology can be assessed visually by use of SEM imaging. The details of the operation of the equipment and the method in which it works are not of great importance in this study. A good overview is provided by Mulder[86] in short however a high electron beam is aimed at the sample and the result is low energy electrons are liberated from the surface and detected forming an image. Key points in the method as regards the user involve the preparation of the sample – samples which do not conduct electricity should be coated with a thin layer of a suitable coating often gold. The sample must also be dry.

2.5 Dissolved nitrogen measurement

The problematic component within the glass coating solutions to be treated is dissolved nitrogen. The chemical stability of nitrogen makes it a difficult substance to measure reliably particularly in a high solids content solution for example measurement of DN could be carried out by gas chromatography(GC). However in the case of the liquid being laden with solids the GC column will be permanently clogged by the deposition of the particles[89].

One possible method exists for measuring DN directly in solution a device manufactured under the name Orbisphere[90]. The Orbisphere device potentially could be capable of making a measurement but flow to the component analyser would have needed to be higher (150-350 ml/min)[91] than some of our planned system circulation rates in our initial experiments. An alternative method of measurement is proposed below for which equipment was already available and as such the Orbisphere device was not selected.

In marine studies it is not uncommon to measure dissolved oxygen and estimate dissolved nitrogen based on the solubility of dissolved nitrogen and other dissolved gases and their proportions in the atmosphere[92]. Hence measurement and calculation of performance on dissolved oxygen can be related back to nitrogen concentration as follows based on the solubility of the two gasses. The mole fraction solubility of oxygen in water is 2.293×10^{-5} and of nitrogen is 1.183×10^{-5} as given by the literature[93].

2.6 Summary of project proposals

Having reviewed past work on mass transfer operations which concern gas stripping from liquids one of the best options available is the use of micro porous membranes in a contactor arrangement. Use of a sweep gas free of the dissolved gas to be removed will provide the driving force. The use of direct contact and mixing of gas and liquid will result in entrainment of the gas especially as the liquid is viscous. As such it is a less desirable method than non-dispersive contact. That said a proposed method of rapidly disengaging entrained gas from the liquid is discussed later in this chapter thus investigating an alternative to non-dispersive contact.

Having decided to use membrane contactors there is the consideration of what material should be used. Polypropylene membranes are widely available as can be seen from the number of studies which have used such fibres. Other popular polymeric materials are PVDF and polysulfone or polyethersulfone. These materials would all be hydrophobic and hence would have the advantage of having gas filled pores. Alternative to these or other polymers is the option of using ceramic materials – the simplest being aluminium oxide. This would however behave in a hydrophilic

manner and as such the liquid would fill the pores. As discussed however under certain circumstances the width of the wall that is filled by liquid could be limited.

Looking at the factors that concern the choice for material we have the following facts concerning the liquid to be stripped.

The liquid is approximately pH 11-12
Treatment may be useful at temperatures around 80-90 °C

Polypropylene does offer chemical and thermal resistance in theory but the maximum allowable temperature given in many manufacturers guidelines is 70 °C. There is a possibility that processing of the liquids in question in this study is best carried out at high temperature around or in excess of this temperature – as such polypropylene will be considered along with an alternative which is absolutely able to withstand temperatures in excess of 70 °C.

It is proposed that polypropylene membranes available commercially and aluminium oxide membranes manufactured in house be used to attempt removal of dissolved gasses by use of a sweep gas.

3 Mass transfer calculations

3.1 Mass transfer calculations

A measure of performance of mass transfer systems is the mass transfer coefficient this can be expressed in a number of ways such as moles of substance transferred per unit area per unit time. However one of the most common forms is volume based rather than molar based and as such the units cancel leaving length per unit time. This form of the coefficient with units, m/s will be used in this study.

3.1.1 Determination of mass transfer coefficient

In section 2.1.5 the concept of the changing concentration profile across the mass transfer region was introduced and shown in Figure 2.7 for ease of understanding part of the figure is reproduced and shown again below as Figure 3.1.

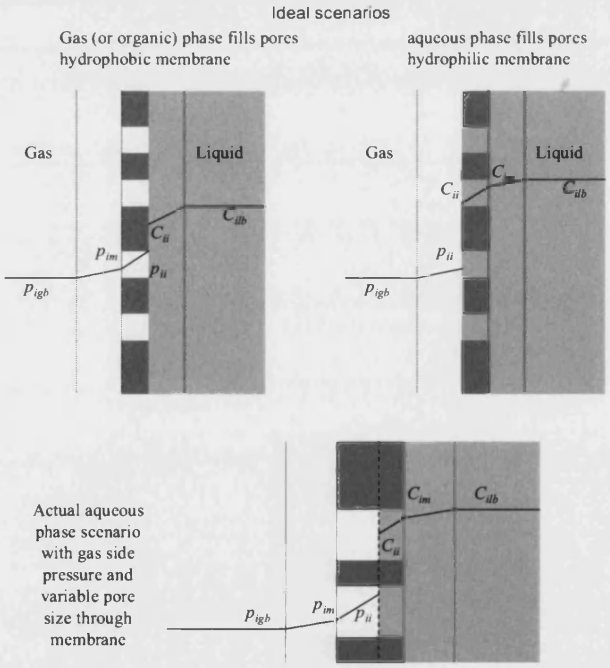

Figure 3.1 - Mass transfer regions and concentration gradients

In Figure 3.1 the symbols denote the following:

C = concentration
p = partial pressure

And the subscripts indicate:
igb = of component *i* in gas bulk
im = of component *i* at the membrane surface
ii = of component *i* at the gas liquid interface
ilb = of component *i* in the liquid bulk

In summary when extracting a gas component from the liquid there will be a certain concentration in the liquid phase. If liquid and gas are exposed to one another there will be a will be a concentration gradient between the two phases provided the partial pressure of the component does not match the equilibrium value. For example with regard to the diagram in Figure 3.1 the point where the concentration profile is discontinuous is the point where the line in the gas phase is marked p_{ii} and in the liquid phase is marked c_{ii} and it can be said that $c_{ii} = H\,p_{ii}$ where H is the equilibrium constant this is known as Henry's law and the value H is the Henry constant. In the ideal cases there is one fluid which fills the membrane pores. In the actual aqueous liquid and gas scenario with a hydrophilic membrane there will be a tendency for penetration of gas into the membrane layer resulting in a thinner liquid layer which will favour faster mass transfer compared to a totally liquid filled membrane. When modelling this system it is important to understand and account for the possibility of two mass transfer regions within the membrane wall.

It should be noted that the location of the interface will actually be varied throughout the membrane for a number of reasons. Firstly the membrane bore is unlikely to be perfectly centred within the structure though all calculations assume that it is. The result is that there is not a continuous wall thickness around the circumference of the membrane and therefore not a continuous position in which we will find the interface when its location is defined as distance from the wall (either outer or inner). An

alternative definition is possible which is to define its position as a fraction of the wall thickness which is or is not flooded by the liquid. However while this sounds like an appealing measure it can only be determined as a mean location based on assumption of equal wall thickness all around so in fact is not really any more useful a definition. Finally the location of the interface even in a perfectly uniform wall thickness membrane is unlikely to be a continuous line or flat plane, it will be determined by the somewhat chaotic arrangement of particles that make the internal membrane structure. In most cases porous membranes are modelled as a wall of continuous thickness through which there are cylindrical pores. Physically a preposterous notion for all but membranes where the pores are carefully formed to give this structure. However the assumption is a useful tool from which models of membrane performance may be developed and can in fact be modified to allow for the true structure by using parameters such as tortuosity. A further issue with the cylindrical pore assumption is the fact that it can give rise to assumptions on the nature of the membrane performance. If the user assumes cylindrical pores in the case of a gas liquid interface with a thin walled membrane in a physical sense then there is no choice but to assume that each pore is either filled with gas or with liquid. The membranes considered in this study are indeed not including carefully formed cylindrical pores and as such no pore will be a clear cut a situation as wholly filled or not filled with either phase. Throughout the structure of the membrane there will be connection and interconnection of pore structures there will be constriction and dilation of pore channels. If one assumes the structure is a hydrophilic material in which there are a number of non interconnected circular channels of varying diameter then each channel will have a different trans-membrane pressure beyond which it fully cleared of gas and a second trans-membrane pressure below which it will be fully liquid filled (in principle ignoring the curvature of the interface at the pore opening which would displace a tiny amount of liquid from the pore. Increasingly so with rise in pressure but assuming a pore wall at least ten times larger than the mean pore diameter then the displacement is unlikely to exceed 5% of the pore volume). The lower pressure determining the liquid filled region is in effect just higher than the bubble point of the widest point in the diameter of the pore, the higher pressure is just below the bubble point of the smallest diameter of the pore. The notion of perfectly circular channels and non-interconnectivity is clearly not accurate in the case of the

ceramic membranes in this study. However it provides a theoretical case which can be analysed to provide insight into the nature of the possibility of a discontinuous interface across the membrane wall. If one has a cluster of such pores next to each other in which the narrowest point in each is permitted to vary in location along its length then the position of the interface is different in each pore with regard to its position in the whole wall structure. Figure 3.2, shows a 2D example of the above theoretical circular pores and how interface position is not necessarily the same and then a 3D impression of how the actual interface position might be scattered given the real situation of interconnected pores.

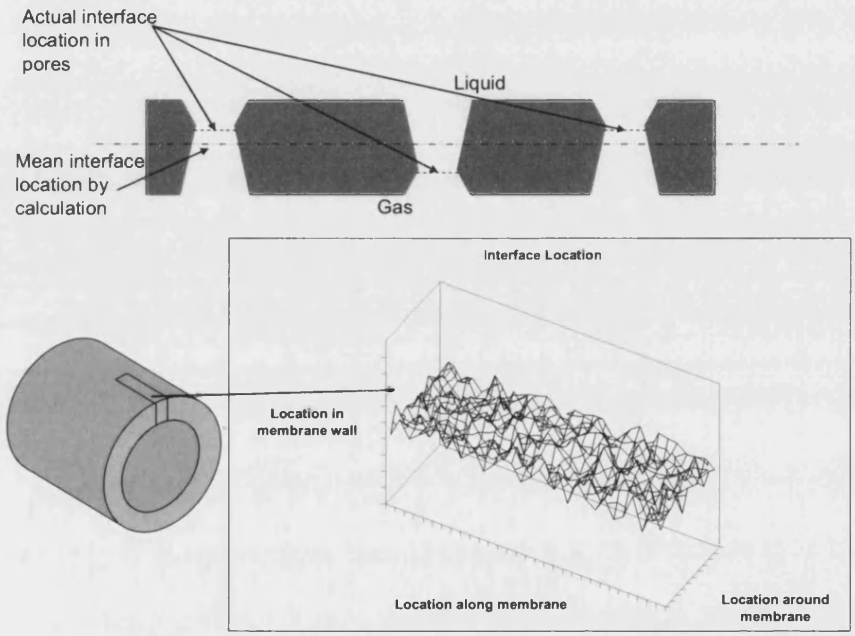

Figure 3.2 - Real and mean interface location

It is noted that although the cylindrical pores assumption is not accurate it does apply in principle to many equations used in this and other studies. It is therefore re-emphasised that modifications and factors such as allowing for two phases within the membrane wall can be allowed for. The following section describes how a liquid and gas filled region within the membrane wall is allowed for.

When finding the mass transfer coefficient directly from experimental data the overall mass transfer coefficient is assessed which combines the mass transfer regions together as a series of resistances. The individual mass transfer regions are assessed when predicting mass transfer based on physical data of the system and rely on an individual prediction of the mass transfer coefficient in each region. These can then be grouped together in series to calculate the overall mass transfer coefficient. The grouping together of mass transfer coefficients is by the same method as in heat transfer gives us the following equation[24]:

$$\frac{1}{K_l} = \frac{1}{k_g H_i} + \frac{1}{k_{mg} H_i} + \frac{1}{k_{ml}} + \frac{1}{k_l} \qquad \textbf{(3.1)}$$

Where:

K_l = overall mass transfer coefficient based on liquid (m/s)

k_g = mass transfer coefficient through gas side boundary layer (m/s)

H_i = Henry law constant in dimensionless form (-)

k_{mg} = mass transfer coefficient through gas filled portion of membrane (m/s)

k_{ml} = mass transfer coefficient through liquid filled portion of membrane (m/s)

k_l = mass transfer coefficient through gas side boundary layer (m/s)

The calculation of the mass transfer coefficients within the membrane is performed using the following equation:

$$k_m = D_e \varepsilon_m / (\tau_m \delta_{fl}) \qquad \textbf{(3.2)}$$

Where

k_m = mass transfer coefficient within the membrane in either gas or liquid phase:

D_e = effective diffusivity

ε_m = porosity of the membrane (-)

τ_m = tortuosity of the membrane

δ_{fl} = thickness of the layer of the fluid being assessed within the membrane wall

The wall thickness, δ_w, in an ideal scenario is the same as δ_{fl} and is equal to d_o - d_i where these are the outer and inner diameters of the membrane (i.e. the membrane is either not wetted or is fully wetted). The wall thickness is generally a known parameter while the position of the liquid gas interface within the wall may not be the comparison of the experimental results and correlated predictions of the shell and tube side mass transfer coefficients allow us to alter the membrane transfer coefficient to fit the data – the only parameter we have not defined in this is the location of the interface. Only estimates of porosity and tortuosity are available hence by using the value ε_m / τ_m as a fitting parameter with and experiment conducted at a very low trans membrane pressure we effectively can determine the location of the interface and measure the effect of adjusting gas side pressure on location of the interface.

Mass transfer on the tube-side:

The flow type within the lumen of hollow fibres is nearly always laminar flow the briefest of checks with regard to the Reynolds number can show this:

Looking at Nitrogen as an example using a typical lumen diameter of 1mm. the density of nitrogen is 0.716 kg/m^3 and the viscosity 1.78×10^{-5} Pas. To give a Reynolds number of just over 2000 the unrealistic tube side velocity of 50 m/s is required in a small unit of just 15 fibres such as those likely to be produced in this study the flow of gas through the unit would need to be nearly 36 l/min a more realistic normal flow would be 2 l/min (Re = 113) and a maximum flow of 8 l/min at at low pressure or 2 l/min at 8 bar would give Re < 1000. In industrial units the Reynolds number will be far lower due to the sheer number of fibres, i.e at 1000 fibres with a gas flows of up to 8 l/m and a lumen diameter of 0.15 mm, Re < 150.

Skelland[94] develops equations for determination of mass transfer within cylindrical tubes in a range of laminar flow conditions.

To establish the equation governing the overall continuity within the tube we consider an annular element of volume $2\pi r dr dx$ as in Figure 3.3.

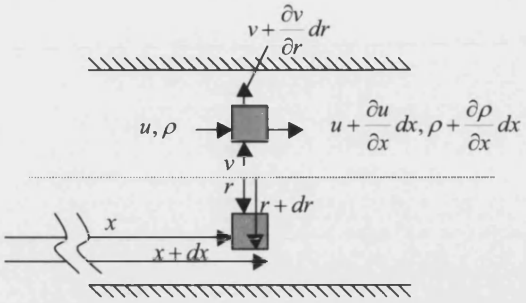

Figure 3.3 - Flow in a tube (redrawn based on[94])

Performing a mass balance we find that the mass flow into the element is:

$$2\pi r dr u\rho + 2\pi dx v\rho \qquad \textbf{3.3}$$

Where:

r = radius of the tube

u = axial flow velocity

v = radial flow velocity

ρ = fluid density

x = axial position in the tube

the rate of mass out is:

$$2\pi r dr\left(u\rho + \frac{\partial(u\rho)}{\partial x}dx\right) + 2\pi dx\left(rv\rho + \frac{\partial(rv\rho)}{\partial r}dr\right) \qquad \textbf{3.4}$$

and the accumulation is:

$$2\pi r dr dx \frac{\partial \rho}{\partial t} \qquad \textbf{3.5}$$

Where t = time.

the whole balance is therefore as in (3.6) expanding and dividing by r gives (3.7)

$$r\frac{\partial(u\rho)}{\partial x}+\frac{\partial(rv\rho)}{\partial r}+r\frac{\partial\rho}{\partial t}=0 \qquad \textbf{3.6}$$

$$\rho\left(\frac{\partial u}{\partial x}+\frac{v}{r}+\frac{\partial v}{\partial r}\right)+u\frac{\partial\rho}{\partial x}+v\frac{\partial\rho}{\partial r}+\frac{\partial\rho}{\partial t}=0 \qquad \textbf{3.7}$$

at steady state $\partial\rho/\partial t=0$, if the density is constant then for either steady or unsteady state we can reduce (3.7) to:

$$\frac{\partial u}{\partial x}+\frac{v}{r}+\frac{\partial v}{\partial r}=0 \qquad \textbf{3.8}$$

Making similar use of an annular element[94] obtains the equation to describe the distribution of a solute, A, in a binary system. The solute enters through the tube walls. Figure 3.4 shows the element.

The mass balance on component A is as follows for flow in, flow out and accumulation:

$$2\pi r dr n_{A_x}+2\pi\left(rn_{A_x}+\frac{\partial\left(rn_{A_r}\right)}{\partial r}dr\right)dx \qquad \textbf{in} \qquad \textbf{3.9}$$

$$2\pi r dr\left(n_{A_x}+\frac{\partial n_{A_x}}{\partial x}dx\right)+2\pi r n_{A_r}dx \qquad \textbf{out} \qquad \textbf{3.10}$$

$$2\pi r dr dx\frac{\partial\rho_A}{\partial t} \qquad \textbf{accumulation} \qquad \textbf{3.11}$$

The flux n, of species A in the r and x directions is defined as follows:

$$n_{A_r}=D\frac{\partial\rho_A}{\partial r}-v\rho_A \qquad \textbf{3.12}$$

$$n_{A_x}=-D\frac{\partial\rho_A}{\partial x}+u\rho_A \qquad \textbf{3.13}$$

Where D = diffusivity

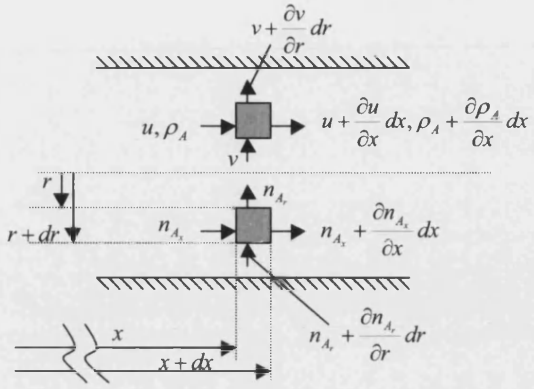

Figure 3.4 - Distribution of component A which enters through tube walls (redrawn based on [94])

Completing the mass balance:

$$\frac{\partial n_{A_x}}{\partial x}+\frac{\partial \rho_A}{\partial t}=\frac{1}{r}\frac{\partial\left(rn_{A_r}\right)}{\partial r} \qquad \textbf{3.14}$$

when combined with equations 3.12 and 3.13 we get:

$$u\frac{\partial \rho_A}{\partial x}+v\frac{\partial \rho_A}{\partial r}+\frac{\partial \rho_A}{\partial t}+\rho_A\left(\frac{\partial u}{\partial x}+\frac{v}{r}+\frac{\partial v}{\partial r}\right)=D\left(\frac{\partial^2 \rho_A}{\partial r^2}+\frac{1}{r}\frac{\partial \rho_A}{\partial r}+\frac{\partial^2 \rho_A}{\partial x^2}\right) \qquad \textbf{3.15}$$

Skelland[94] now points out that at steady state $\partial\rho_A/\partial t = 0$ and that based on equation 3.8 we can say that at constant density the final term on the left side of the equation = 0. If axial diffusion is neglected the term $\left(\partial^2\rho_A/\partial x^2\right)$ is removed resulting in a steady state equation as follows:

$$u\frac{\partial \rho_A}{\partial x}+v\frac{\partial \rho_A}{\partial r}=D\left(\frac{\partial^2 \rho_A}{\partial r^2}+\frac{1}{r}\frac{\partial \rho_A}{\partial r}\right) \qquad \textbf{3.16}$$

finally at points sufficiently distant from the entrance to the tube the velocity profile will be fully developed such that $v = 0$ resulting in:

$$u\frac{\partial \rho_A}{\partial x} = D\left(\frac{\partial^2 \rho_A}{\partial r^2} + \frac{1}{r}\frac{\partial \rho_A}{\partial r}\right) \qquad \textbf{3.17}$$

Equations 3.16 and 3.17 are solved with boundary conditions which are usually defined in one of two ways. Either a uniform concentration along the wall is assumed or there is a uniform mass flux at the wall. In the first case the solutions are expressed in terms of the average Sherwood number over the mass transfer section of the tube. In the second case the solution is defined in terms of a local Sherwood number. There are a number of situations that can arise when experiencing laminar flow in a tube[94] lists them as follows:

- Developing velocity and concentration profiles – near the tube inlet neither profile is yet developed but mass transfer occurs at the inlet.
- Fully developed velocity distribution and developing concentration distribution – This occurs when a length of tube exists in which no mass transfer occurs but obviously the velocity profile can develop.
- Fully developed velocity and concentration distributions – These conditions occur some distance downstream of the inlet.

For the modules constructed in this study there is a small distance of fibre for which no mass transfer occurs this accounts for around 1.5cm which is nearly 10% of their total length and is over 10 times the internal diameter as such the second possibility is closest to the true situation within the fibres. For the first possibility there are charts available in the literature presented by Skelland[94] based on those by Heaton *et al.*[95], Siegle[96] and Goldberg[97] which can give the Sherwood number in a range of conditions, the charts having been prepared by numerical solution of equation 3.16.

For the second case and hence the case most relevant to this study there is a detailed solution to equation 3.17 given by Skelland[94] the result being different depending on the velocity profile on which it is based. There is however an alternative considered by Skelland. An equation proposed by Lévêque[98] allows an approximation of the solution and is as follows:

$$Sh_{local} = \frac{k_p d_t}{D} = \frac{d_t}{0.893}\left(\frac{\beta_v}{9Dx}\right)^{1/3} \quad \textbf{3.18}$$

$$Sh_{average} = \frac{k_{pa} d_t}{D} = 1.615 d_t \left(\frac{\beta_v}{8DL}\right)^{1/3} \quad \textbf{3.19}$$

in both cases it is assumed that the concentration boundary layer is a thin zone near the wall and that linear velocity distribution exist across these thin boundary layers. Such that: (note subscript *t* denotes of the tube)

$$\beta_v = \frac{r_t - r}{u} \quad \textbf{3.20}$$

Skelland[94] replaces β_v in equations 3.18 and 3.19 by the following procedure:

Laminar flow velocity distribution for fully developed flow in a Newtonian fluid is:

$$u = 2V\left(1 - (r/r_t)^2\right) \quad \textbf{3.21}$$

assuming this holds in the laminar boundary layer:

$$\left(\frac{du}{dy}\right)_{y=0} = \left(-\frac{du}{dr}\right)_{r=r_t} = \frac{4V}{r_t} = \frac{8V}{d_t} \quad \textbf{3.22}$$

then substituting into equations 3.18 and 3.19:

$$Sh_{local} = 1.077\left(\frac{d_t}{x}\right)^{1/3} (\mathrm{Re}\cdot Sc)^{1/3} \quad \textbf{3.23}$$

$$Sh_{average} = 1.615\left(\frac{d_t}{L}\right)^{1/3} (\mathrm{Re}\cdot Sc)^{1/3} \quad \textbf{3.24}$$

Fully developed Profiles in both cases:

In this case all results give asymptotic figures these are shown by Skelland[94], and are summarised in Table 3.1 for example the condition for uniform wall concentration is based on the equation set below:

$$Sh(x) = \frac{\sum_{j=1}^{j=\infty} \frac{B_j}{2}\left(\frac{d\phi_j}{dr_+}\right)_{r_+=1} \exp\left(\frac{-\beta_j^2(x/r_t)}{Re \cdot Sc}\right)}{2\sum_{j=1}^{j=\infty} \frac{B_j}{2\beta_j^2}\left(\frac{d\phi_j}{dr_+}\right)_{r_+=1} \exp\left(\frac{-\beta_j^2(x/r_t)}{Re \cdot Sc}\right)} \qquad 3.25$$

where:

$$\beta_j = 4(j-1)+\frac{8}{3}; \quad j = 1,2,3,... \qquad 3.26$$

$$B_j = (-1)^{j-1} \times 2.84606\beta_j^{-2/3} \qquad 3.27$$

and

$$\frac{-\beta_j}{2}\left(\frac{d\phi_j}{dr_+}\right)_{r_+=1} = 1.01276\beta_j^{-1/3} \qquad 3.28$$

Table 3.1 – Sherwood numbers for fully developed profiles

Condition	Sherwood Number
Uniform Wall concentration	3.656
Uniform mass flux at wall	4.36
Assumed cubic polynomial concentration distribution	4.12

Mass transfer in shell side of module:

Shell side coefficients are a function of a number of factors which are difficult to assess analytically including most notably the geometry of the shell side region as such correlations are commonly used to assess the shell side mass transfer. These generally have the form:

$$Sh \propto Re^{\alpha} Sc^{\beta} f(geometry) \qquad 3.29$$

A number have been presented in the literature by various authors many of whose works were discussed in section 2.1.5. A summary of their tube side correlations is presented above in table Table 2.2:

The correlation used in this study is the following equation proposed by Yang and Cussler[12]. The study was based on a larger unit but the flow is of the correct orientation and the added flexibility owing to the wetted perimeter calculation allows for some adjustment to the module type.

$$Sh = 1.25\left(\mathrm{Re}\frac{d_e}{l}\right)^{0.93} Sc^{0.33} \qquad 3.30$$

3.2 Overall mass transfer coefficient

In order to achieve a calculation of overall mass transfer coefficient a mass balance across the contactor unit is required.

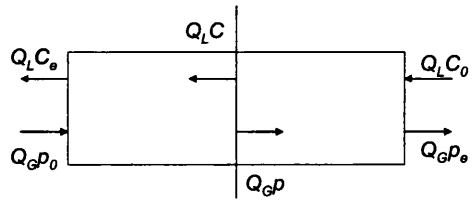

Figure 3.5 - Mass balance over a contactor

The mass balance for a specific component between the inlet and a point within the contactor is as follows (assuming the ideal gas law):

$$Q_L(C_0 - C) = Q_G \frac{1}{RT}(p_e - p) \qquad 3.31$$

Where:

R = universal gas constant

T = absolute temperature

G and L subscripts indicate gas or liquid phase and 0 and e subscripts denote inlet condition and exit condition respectively, where C and p do not have a subscript this denotes a location within the module.

The mass balance over the whole contactor is given by:

$$Q_L(C_0 - C_e) = Q_G \frac{1}{RT}(p_e - p_0) \qquad \textbf{3.32}$$

Rearranging both gives the following assuming the inlet partial pressure of the component is zero:

$$p = -\frac{Q_L RT}{Q_G}(C_0 - C) + p_e \qquad \textbf{3.33}$$

$$p_e = \frac{V_L RT}{V_G}(C_0 - C_e) \qquad \textbf{3.34}$$

Substituting 3.34 into 3.33 gives:

$$\begin{aligned} p &= \frac{Q_L RT}{Q_G}[(C_0 - C_e) - (C_0 - C)] \\ &= \frac{Q_L RT}{Q_G}(C - C_e) \end{aligned} \qquad \textbf{3.35}$$

The change in concentration in the liquid is proportional to the concentration in the gas this is related by the overall mass transfer coefficient as follows:

$$-Q_L dC = (K_L a) \cdot A_c dh(C - C^*) \qquad \textbf{3.36}$$

Where:

a = surface area per unit volume

A_c = cross sectional area of module

h = length of module

The concentration is marked C^* indicating that the concentration is that which would be in equilibrium with partial pressure p which is the partial pressure in the gas phase

at some point in the contactor. Substituting for partial pressure based on Henry's law gives this being valid owing to the low concentrations involved in this work:

$$C^* = \frac{p}{H} = \frac{Q_L RT}{Q_G H}(C - C_e) \qquad \textbf{3.37}$$

Where:

H is the Henry law constant

By using the substitution shown as equation 3.38 and combining equations 3.37 and 3.36 allows us to prepare a differential equation for the mass balance

$$y = \frac{Q_L RT}{Q_G H} \qquad \textbf{3.38}$$

$$-Q_L dC = (K_L a)\cdot A_c \cdot dh \cdot (C - y(C - C_e)) \qquad \textbf{3.39}$$

Rearranging gives:

$$-\int_{C_0}^{C} \frac{dC}{C(1-y) - yC_e} = \frac{K_L a \cdot A_c}{Q_L} \int_0^h dh$$

$$-\frac{1}{1-y}\int_{C_0}^{C} \frac{dc}{C - \frac{y}{1-y}C_e} = \frac{K_L a \cdot A_c}{Q_L} \int_0^h dh \qquad \textbf{3.40}$$

Integration gives us an expression for mass transfer:

$$-\frac{1}{1-y}\ln\left(C - \frac{y}{1-y}C_e\right)\Big|_{C_0}^{C} = \frac{K_L a \cdot A_c}{Q_L} h$$

$$\frac{1}{1-y}\ln\left[C - \frac{y}{1-y}C_e\right]_{C}^{C_0} = \frac{K_L a \cdot A_c \cdot h}{Q_L}$$

$$\ln\frac{C_0 - \frac{y}{1-y}C_e}{C - \frac{y}{1-y}C_e} = \frac{K_L a \cdot A_c \cdot h}{Q_L}(1-y)$$

$$K_L a = \frac{Q_L}{A_c h(1-y)} \ln \frac{C_0 - \frac{y}{1-y} C_e}{C_e - \frac{y}{1-y} C_e} \qquad 3.41$$

All required parameters for the mass transfer calculation are easily measured except C_e this can be calculated from known data in certain circumstances. The experiment is carried out by recycle of a liquid to through the mass transfer unit to and from a batch tank. If the tank concentration is measured the rate of change of that concentration allows calculation of C_e. This is limited to the situation where the change in concentration through the module is low i.e. less than 10%, Smith[99] presented the calculation of C_e based on rate of change of concentration in the tank and the basis is as follows based on the scheme in Figure 3.6:

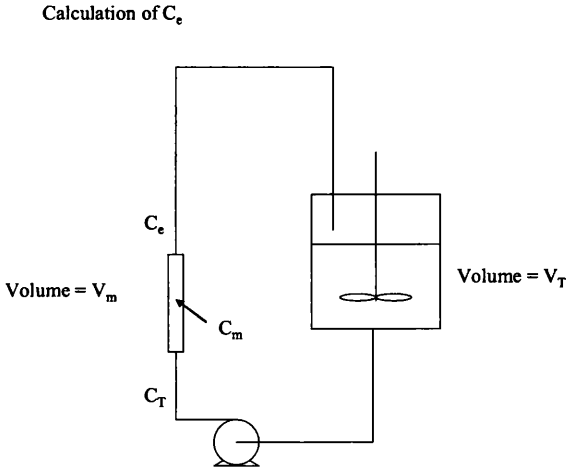

Figure 3.6 - Batch recycle system (based on Smith [99])

Mass balance for the overall system:

$$\int_0^{V_m} r dV_m = V_m \frac{dC_m}{dt} + V_T \frac{dC_T}{dt} \qquad 3.42$$

Where:

V = volume

r = rate of change of concentration in the tank

And subscripts m and T denote module and tank respectively.

By making suitable simplifications (i.e. the volume of the connective tubing in the system is assumed to be negligible and hence is excluded) and given the system limitations described above, we can say the rate of change, r, is approximately constant over the volume of the module, and C_m is approximately the same as C_T, hence we can say:

$$r = \left(\frac{V_m + V_T}{V_m}\right)\frac{dC_T}{dt} \qquad \textbf{3.43}$$

dC_T/dt is calculated experimentally. To determine C_e we must perform a mass balance over just the module:

$$QC_T - QC_e + \int_0^{V_m} r dV_m = V_m \frac{dC_T}{dt} \qquad \textbf{3.44}$$

Combining with equation 3.42 gives,

$$C_T - C_e = -\frac{V_T}{Q}\left(\frac{dC_T}{dt}\right) \qquad \textbf{3.45}$$

dC_T/dt is eliminated by substitution with equation 3.43 giving finally equation 3.46 which can be used to determine C_e this can then be used with equation 3.41 to determine the mass transfer coefficient.

$$C_T - C_e = -\frac{V_m}{Q}\left(\frac{V_T}{V_m + V_T}\right)r \qquad \textbf{3.46}$$

4 Experimental

The following chapter outlines the procedures and techniques used in this study for a range of processes. Starting with the manufacture of hollow fibre membranes from aluminium oxide, through the building of contactor units and the characterisation of the fibres finally there is a section on mass transfer measurements and glass coating.

4.1 Ceramic hollow fibre manufacture

Hollow fibre membranes are made by an extrusion process as discussed in chapter 2. The extruded material in this study was a polymer solvent system rather than a melt. This polymer solvent system is the start of the process for manufacture of hollow fibres which is outlined below.

4.1.1 Preparation of solution for extrusion

The starting material for preparation of hollow fibres is a viscous polymer/solvent solution or melt which can be extruded. This can take the form of a polymer melt or a polymer dissolved in solvent. In this work the starting material is exclusively a mixture of a polymer, polyethersulfone (PES)[Amoco Radel-A MW ca.40000], and (NMP) [Sigma Aldrich]. The two components are mixed on a Stuart SRT2 roller mixer for a minimum of 24 hours in a Duran Schott glassware bottle. On completion of the dissolving procedure (determined by visual inspection) the mixture can be left rolling for a period of time if it is so wished or ceramic powder can immediately be added. The desired quantities of ceramic powder added will vary depending on the desired make up of the fibre. There have been three sizes of alumina powder used in this study though the method employed permits the use of other sizes and other ceramic powders. The three sizes used have been α-alumina at a particle size of 1 μm[Alfa-Aesar], α-alumina at a particle size of 0.3 μm[Alfa-Aesar], and an α/γ-alumina mixture at a particle size of 0.01 to 0.02 μm[Alfa-Aesar]. From this point forward in the text they shall be referred to as Al_2O_3 (1 μm), Al_2O_3 (0.3 μm) and Al_2O_3 (0.01 μm). The addition of these powders proceeds as follows:

1. The solution bottle is taken from the roller mixer and an eight blade rushton type stirrer is inserted at approximately 1 cm above the base of the bottle and fixed at this height by tightening into and overhead mixer.
2. The stirrer is started at a speed of 300rpm.
3. The required amount of the selected particle size to be added is weighed out either in full or in a suitable portion for addition and the weights noted. The smallest sizes should be added first.
4. A paper funnel is inserted into the solution bottle between the stirrer shaft and the neck of the bottle, the ceramic powder is added through the funnel as shown in Figure 4.1.
5. After adding the portion weighed the funnel is removed and the stirrer speed increased to 1000rpm until all the floating powder is pulled under the solution surface. The stirrer is returned to 300 rpm and any further portions of alumina can be weighed and added by the same method.

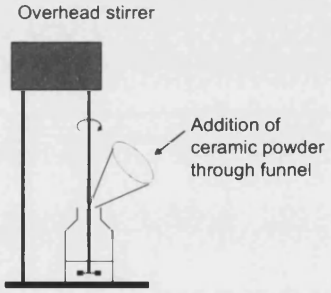

Figure 4.1 – Addition of ceramic powder to stirring mixture

4.1.2 Extrusion equipment and extrusion variables

Once prepared the spinning solution is extruded on the spinning rig. The spinning rig is designed for the wet or wet/dry extrusion of the spinning solution using the polymer/solvent/non-solvent phase inversion method. As such the rig has holding tanks which when in use contain non-solvent. The extruded fibre follows a path through two of these tanks and into a final third holding tank. The fibre reaches the

final tank by following a system of guide wheels. The rig is shown in Figure 4.2 and the key points are discussed below.

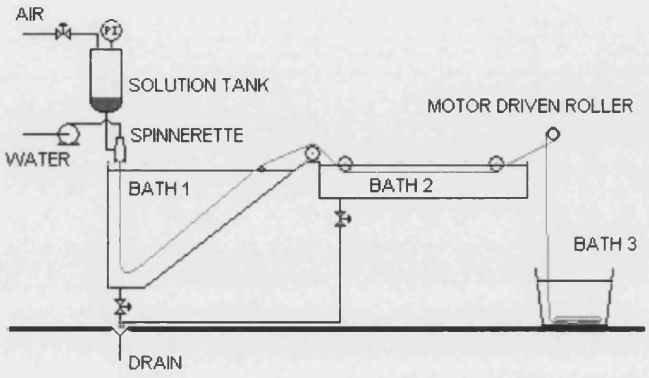

Figure 4.2 – Spinning Rig

Air – This is used to pressurise the solution tank and hence drive the solution through the spinning head. Usually 2 bar is used though in certain circumstances the pressure needs to be higher or lower to accommodate the extrusion properties of the spinning solution.

Solution Tank – The solution tank (in house manufacture) holds the spinning solution during the spinning process the capacity is one litre though normal charges of spinning solution are between 100 and 250 ml

Water – Water is used as the non-solvent bore liquid in all the experiments in this work. In some other studies discussed in chapter 2 have been other liquids used in the bore of the fibre. Water is fed to the bore tube of the spinnerette by a metering pump at rates usually between 2 and 15 ml/min.

Spinnerette – The spinnerette is so called from its standard name in association with manufacture of hollow fibres, though as is the case with most spinnerettes used in this field it does not spin in any way and is in fact a fixed extrusion head. The name is simply derived from the spinning heads used in the synthetic textiles manufacture industry. The device used in this study is based on a design used by Dr K. Li (and

was manufactured in house by Pilkington Group Limited.). The spinnerette internally has two discrete flow paths one for the spinning solution and one for the bore liquid. Figure 4.3 shows the spinnerette.

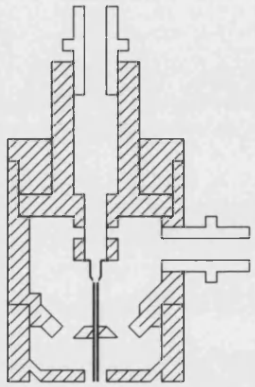

Figure 4.3 – Spinnerette

The extruded result is an annular fibre of solution which forms a solid surface rapidly after contact with the non-solvent. The unshaded portions shown in the diagram are standard Swagelok fittings for connecting NPT type (spinnerette fitting) to compression fit tubing (used to connect all parts of the system where tubing is required).

Bath Assembly (Incorporating Bath 1, Bath 2 and Motor driven roller) – The bath assembly (in house manufacture) used in this study could allow the use of combinations or variations in non-solvent. This option was not used in this study and water was the only non-solvent used. The motor driven roller has a wet sponge surface which lightly grips the fibre and guides it from the bath assembly into bath 3.

Bath 3 – Bath 3 (standard 50-100 litre hardware store plastic container) is the holding bath and is used to store the fibres for 24 hrs following their extrusion.

The operator controlled variables are the pressure applied to the solution, the temperature of the water baths, the rate of the bore liquid and the air gap.

4.1.3 Extrusion procedure

Once prepared the spinning solution can be kept mixed on the roller mixer until it is required. Once it is required the extrusion equipment must be prepared and ready to use prior to transfer of the spinning solution. This is because the spinning solution will drain (slowly) from the solution tank towards the spinnerette. In certain circumstances it may be desirable to place a ball valve between the solution tank and the spinnerette to prevent the solution reaching the spinnerette before the user is ready to begin. The rig is prepared according to the rig preparation procedure (see Appendix III). The following steps are then used to carry out an extrusion:

1. To begin spinning open the air stop valve prior to the solution tank. The solution will move quickly towards the spinnerette and will fill the solution side of the spinnerette before emerging from the annular shape at the spinnerette base. On appearance of solution from the base of the spinnerette the metering pump should be switched on.
2. As the metering pump drives water towards the spinnerette, the air in the water side of the spinnerette causes the already falling solution to form beads. These will float near the spinnerette on the surface of the non-solvent. As water enters the spinnerette and fills the non-solvent side the beads will change to a continuous fibre which will not float on the surface. At this stage the formed beads can be cleared away and discarded and the fibre should be fed by hand around the guide wheels, care should be taken not to pull on the fibre but to allow it flow at its natural rate. Once the fibre reaches the motor driven roller it should be passed under the roller and then back over so the fibre is lightly gripped and passes to bath 3 where it should coil unassisted.
3. The motor should be adjusted quickly to a speed that is approximately correct for the rate of extrusion so that there is no tightening or slackening of the extruding fibre.
4. The pressure on the solution tank should be adjusted to ensure it is correct (in most cases there is little or no adjustment to be made.
5. Depending on desired variables other adjustments may need to be made, such as altering the bore liquid rate.

6. Once all adjustments are made the motor can be fine tuned to give the exact take up rate for the extruding fibre and the extrusion should continue unaided save for minor motor speed adjustments. At this point the fibre should be kinked by hand just after the outlet from the spinnerette. When the kink reaches tank 3 the fibre should be cut after the kink and all the fibre in tank 3 discarded. All subsequently collected fibre will now be under the same conditions unless deliberate changes are made to conditions in which case these instructions should be followed again from the rough adjustment of the motor.
7. If large unexpected adjustments need to be made to motor speed then other conditions such as pressure or bore liquid rate may have changed unexpectedly or the solution for whatever reason is not well mixed.
8. Once all is working well the exact temperature of the three baths can be checked again.

The extrusion will continue until the level of solution in the tank gets low enough for gas to break through into the solution tank's outlet tube and hence to the spinnerette. At this stage the shut down and clean down procedure begins (see Appendix III).

4.1.4 Post Treatment of extruded fibres

The method presented here is the final settled method for post treatment used in this study and goes hand in hand with sintering of fibres supported by monolith. Prior to monolith sintering a simplified version of post treatment was used – this is summarised at the end of the section.

Fibres that have been extruded remain in water for 24 hrs after extrusion in order to allow complete exchange of solvent and non-solvent. The extruded fibres spend this 24 hr period in bath 3 on the extrusion rig. If it is not possible to carry out post treatment after 24 hrs the fibres should have their water changed regularly until post treatment can begin. Post treatment is the process by which the fibres are dried and cut ready for their next main treatment stage, sintering. The main problem with the fibres is that they will tend to curl when they begin to dry this curling effect is partly induced by the fact hat they have been curled on collection from the spinning rig and

so form their final structure in a curled shape. The fibres are however flexible and can have their shape relaxed by using hot tap water. Then by straightening the fibres and drying them in a holder in a straight orientation they can be far straighter than they would be if they were simply taken from bath three and dried. The procedure for post treatment is as follows:

1. A paper lining should be inserted into the fibre holder
2. The extruded fibre should be cut into lengths of approximately 40 cm lengths and gathered into a bundle of 20-30 fibres. The natural curvature of the fibres should be orientated such that all the fibres curve the same way.
3. A prepared bundle should then be held under running hot tap water for approximately two minutes.
4. The fibres should then be laid out on a holder such that their natural curvature is straightened by their position. Subsequent bundles can be laid on top of the preceding bundles or in a new holder if the first holder is full. Fibre holders hold the fibres at three points and have a paper lining bridge between the points as shown in Figure 4.4.
5. Once all the extruded fibre has been cut and laid into the holder the ends of the bundle should be loosely tied and the bundle labelled.
6. The fibres should be dry after 24-48 hrs of drying at room temperature.

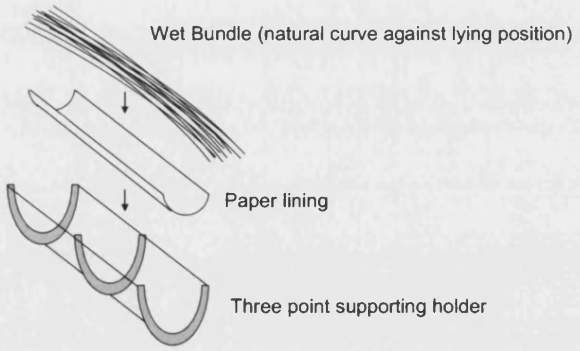

Figure 4.4 – Post treatment set up

Simplified post-treatment (used prior to the method detailed above)

The simplified method involved cutting to approximate lengths of 40 cm as before but fibres were cut direct from storage in cold water unless they were deemed particularly curled, when warm water was used. Bundles of fibres were tied and dried simply resting on absorbent paper. The result would be fibres which curled up as drying progressed.

4.1.5 Coatings

The coatings used are slurry dispersions of a fine alumina powder in either water or water and a combination of other components like poly(vinyl-alcohol) (PVA) [Fluka MW 72000] and ethanol or 1-propanol [Fisher chemicals analysis grade]. The desired amount of distilled water is added to a standard glassware bottle. If required the correct amount of PVA is then added to the bottle and the bottle is heated to between 85 and 90°C under reflux with moderate stirring by magnetic stirrer in order to dissolve the PVA. Once dissolved the contents should be cooled. The desired amount of ethanol or 1-propanol should be added once the mixture is cold. The addition should be carried out slowly tending towards drop-wise if the level of PVA is causing visible precipitation on the addition of amounts of the alcohol. Once prepared the solution is placed on a roller mixer until the addition of solids is carried out. The desired amount of aluminium oxide should be weighed out in full or in portions as appropriate (adding smaller particle sizes first). The addition can be carried out by pouring through a funnel while the mixture is stirred magnetically. Once the addition is complete the bottle should be returned to the roller mixer and left for a minimum of 24hrs before use. Solutions may be used repeatedly and can be kept dispersed by keeping them on the roller. If they contain PVA and are removed from the roller they should be returned for 24hrs prior to use. Solutions which have only water and/or ethanol or 1-propanol are easily re-mixed in a few minutes by direct stirring or stirring with a magnetic stirrer.

Once prepared and well mixed solutions are applied to the membranes by a dip coating method. The solution is transferred to a tall container such as a measuring cylinder which is placed on a magnetic stirrer. The fibres to be coated are prepared for coating by blocking the lower open end with putty. The stirrer is stopped and after

a few seconds the fibre is lowered into the solution where it is held for a pre-decided amount of time and is then raised out of the solution. The fibre stands on end to dry and the stirrer is switched back on until the next fibre is ready. Each fibre is coated using the same procedure. Following coating all the fibres are allowed to dry for a minimum of 8 hrs.

4.1.6 Sintering of fibres

Sintering is the process by which fibres are transformed from a partially polymeric, partially ceramic structure with some flexibility to a rigid strong ceramic structure. This is achieved by heating the polymer/ceramic structure to temperatures in excess of 1200°C. The fibre firstly looses its polymeric part during a phase known as 'burn out'. Following this the is in effect a powder compact of aluminium oxide. Once 1200°C is reached the powder making up the fibre will begin to fuse together making the rigid structure. During this process the fibres must be supported along their length to avoid bending.

Four types of support method have been used in this study each being a development from the previous method. The majority of fibres have been prepared using the last of the three methods presented below.

Method 1: flat grooved ceramic. This method used a piece of ceramic material with a groove cut into it. The fibre is laid out along the grove with minimal effort to straighten the fibre before placement – reliance was on the groove to hold the fibre in a straight position. The intended mechanism for support is that the fibre will soften and 'relax' into the groove under heating until the polymeric part of the fibre is burnt away the fibre will then take the shape of the groove as sintering occurs. The resulting fibres from this method tended to curl under the forces of sintering though some remained reasonably straight.

Method 2: flat grooved ceramic with fibre straightening. This approach ensured straighter fibres prior to sintering by hand straightening them. When worked gently by hand the fibres, which are usually flexible but hold their shape, can become pliable

and can be worked so they hold a new shape. Careful working can give a fibre which will be straight prior to placement in the grooved support. This means the grooved support is no longer relied upon to hold the fibre straight. The results from this method yielded slightly straighter fibres than the first method though fibres were often still far too curved to make into multi-fibre modules. It was seem that the fibres could curl upwards under sintering and as such an "all around the fibre" holder would be required

It should be noted that both the previous methods produced enough fibre in straight sections to provide samples for characterisation.

Method 3: ceramic monoliths. This method moved away from the use of a flat grooved support and utilised one or more ceramic monoliths for holding the fibres. There are massive advantages to be gained from such supports. The first advantage is that a fine size of monolith channels results in exceptionally straight hollow fibres. The second is that while the flat support could hold five fibres, the monoliths can hold up to 30-50 fibres of 30cm in length depending on which monoliths are used. The first monoliths used in tandem were a fine channelled cordierite monolith (which could be used up to 1350 °C) and a wider channelled alumina monolith (up to 1600 °C). The fine channelled monolith is used for burn out and 'pre-sintering' This removes the polymer component of the spun fibre and begins the sintering process. The result is a brittle and extremely porous structure that is only strong enough to be handle able. This is then coated with any desired coating as described in section 4.1.5 and placed in the wider channelled alumina monolith for final sintering. A later development and the final procedure arrived upon was to use a finer channelled alumina monolith for both stages – pre-sintering and final sintering. This allowed higher temperatures to be used for pre-sintering resulting in a more robust stock of base fibres which could be coated with fewer breakages.

Sintering procedure:

The procedure for sintering in monoliths is as described below: the only differences for other supports are that instead of inserting fibres into the monoliths the fibres

were laid out on the support or hand straightened and laid out on the support. The sintering is achieved using a tube furnace [Carbolite, CTF 17/75/300] with a 30 cm uniform temperature zone (+/- 5 °C). The furnace has a horizontally mounted tube.

1. The support should be selected and ensured that all fibre fragments/dust/debris that may be on or in the support is cleared out.
2. Fibres should be taken from their bundle and inspected for defects visually and by feeling the fibre along its length. Obviously defective fibres should be discarded.
3. Fibres were placed into the support monolith (cordierite) and trimmed to the exact length of the monolith (30 cm). If other monoliths are being used the fibres should be trimmed prior to insertion as other monoliths exceed this length.
4. Coated fibres must be inserted with great care to avoid damaging the un-sintered coatings.
5. Once full all the fibres were aligned with one end of the monolith and the monolith was inserted to the work tube of the furnace. Some degree of care should be taken to ensure that the 30 cm of fibres within the monolith are aligned such that they are occupying the uniform temperature zone. Note: the first and last 1-2 cm of each fibre is always discarded by the characterisation and/or module making procedure but poor alignment in the furnace could affect more than this length.
6. The furnace must now be programmed in accordance with the programming procedure, this is outlined in Appendix I along with the programs used. Once programmed the program can be started.

Notes on sintering:

Programs will typically take 24-36 hours before the fibres can be retrieved. Though programs may indicate that they finish faster than this the rate of actual cooling is far slower than the programmed cooling below 800 °C due to the well insulated nature of the furnace

There are restrictions on heating rate so no higher than 5 °C/min can be used to protect the work tube. Above 1100 °C the rate is limited by the heat input to the furnace so the rate drops to as little as 1 °C/min above 1550 °C.

Typical programs will hold a maximum temperature for a length of time and some include a temperature hold at lower temperature to facilitate 'burn out'.

Sintering of coated fibres outside of a monolith may appear appealing as there is less risk of damaging the coatings. There are however two problems with this approach firstly the monolith allows many more fibres to be sintered and more importantly the fibres can still bend under the forces endured during sintering of the coating.

4.1.7 Preparation of random packed module

The preparation of a random packed module involves creating a seal between a fibre bundle and a "t"-piece tube fitting initially before building the module around the fibres and sealing the opposing end of the fibres in a 't'-piece at the other end of the module. In order to achieve this two ½ inch Swagelok stainless steel 't'-pieces and the appropriate compression fitting parts and appropriate length of tubing are required. The chosen fibres were then checked for visible pinholes or defects. The fibres selected were also approximately 2 inches longer than the desired overall module length. Following the initial checking a further inspection by touch can locate imperfections on the fibre surface these can then be inspected under magnification. Any fibres with suspected weak points or pin-holes were not used. Once enough apparently defect free fibres were gathered their ends are aligned and placed through the first "t"-piece such that approximately an inch of fibre should protrude from the NPT connection on the "t"-piece. The appropriately sized tubing is tightly attached to this 't'-piece, the tubing helps to retain the fibres in a straight alignment within the first "t"-piece. Epoxy resin (standard commercially available fast setting Araldite®) was prepared for sealing fibres into place. The resin is applied around the fibre bundle approximately one inch from the end of the fibres and was thoroughly worked between the fibres such that there are no gaps between the fibres where the resin is present, further resin should be added as required. The covering of resin extended 5 to 10 mm along the length of the fibres. Once there was sufficient resin between the

fibres a further amount of resin was applied around the bundle as before. Instead of working this resin between the fibres the fibres are slid back into the "t"-piece such that the resin formed a seal between the fibres and the "t"-piece – once again further resin was applied if required. Once the seal is complete the "t"-piece holding the fibres was held horizontally and rotated around the circumference of the bundle until the resin begins to set hard (approximately six to ten minutes). After this the module was left for a minimum of one hour laid in a horizontal position before further construction of the module took place.

To finish preparation of the module the second end of the fibres is glued into the second "t"-piece. Prior to the final sealing of the fibres the second "t"-piece was attached to the tubing around the fibres. Great care was taken to avoid damaging the fibres while attaching this part. The "t"-piece was aligned such that the perpendicular outlet of the t-piece is aligned in the opposite direction to the first 't'piece. Figure 4.5 shows the alignment and also a cross section of the finally glued fibres prior to trimming.

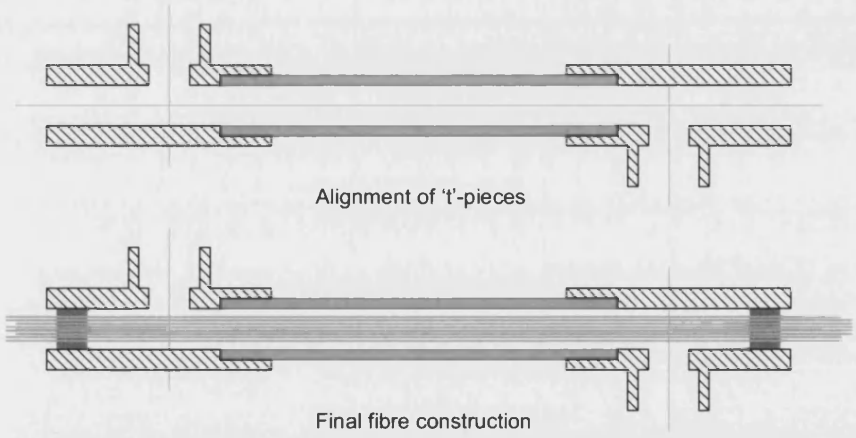

Figure 4.5 – Random packed model construction

Once the "t"-piece is aligned correctly and all the tube fittings are tightened the unglued fibre ends can be sealed in place using the same resin as before. The resin was worked into the gaps between fibres with the aim of placing the glue around the

fibres such that the glue occupied the mouth of the "t"-piece in which the unglued fibres were located. There was some flexibility in the position of the fibres at this end of the module which allowed resin to be worked between the fibres more easily. Once the fibres were all sealed together a further application of resin around the bundle assisted in sealing the bundle into the "t"-piece. Setting of the resin took approximately six to ten minutes. The module was once again rolled by hand horizontally until the resin was set. Following this the module was left overnight.

The final stage on the construction of the module is to remove the excess fibre protruding from the ends. This is usually achieved by breaking away the fibres where they emerge from the resin by careful fracturing with pincers or tweezers.

4.1.8 Preparation of structured module

The preparation of a structured module is a slightly different process to that of an unstructured module. Both ends of the module are glued at the same time to create a fibre bundle. The fibre bundle is then sealed into the module housing, which as with the unstructured module consists of two Swagelok "t"-pieces and the appropriate length of tubing with compression fit components. In order to prepare the fibre bundle end ensure structured spacing of the fibres along with good sealing between the fibres the bundle is built in layers. Each layer is inserted into two bundle supports (in house construction) at which point epoxy resin is applied between the fibres. The bundle consists of 17 fibres and follows the pattern shown in Figure 4.6.

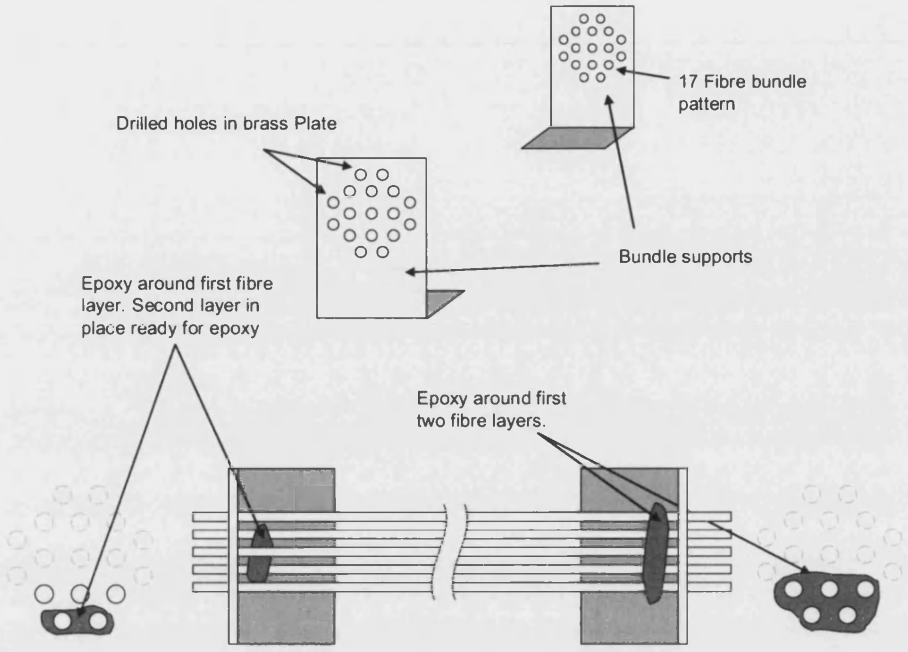

Figure 4.6 – Structured module construction

The bundle is built in 5 layers, two fibres, three fibres, two uneven layers of five fibres and a final layer of two fibres. The fibres to be used were carefully inspected before construction beginan as with the unstructured module. The first layer of fibres was placed in the supports by sliding the supports on from each end of the fibres, following this layer the fibres were inserted to both supports from one end of the construction (i.e. the fibres were passed through one support before entering the second). Epoxy resin was prepared as required for each layer rather than for the whole module. Ten minutes was allowed as a minimum between the construction of each layer.

Once construction of the bundle was complete the bundle supports remained in place to hold the bundle overnight, this allowed thorough drying of the resin. Following this the bundle supports were carefully removed, it was normal for one or two fibre ends to break during this removal this was acceptable so long as no fracture occurred on the fibre sections between the resin bonds. Care was taken to ensure no torsional stress was applied to the fibres as this would damage the section between the resin seals. The module parts were constructed and fully tightened as for the unstructured

module with "t"-piece outlets facing in opposite directions (see Figure 4.5). The bundle was inserted to the module and fresh resin was prepared. One end of the bundle was pulled out of the module housing slightly so it could have resin applied around the existing bonds between fibres. Care was not to block any fibres whose ends may have broken off when removing the bundle supports. Once a good coating was applied the bundle it was slid back into place in the housing and a seal made between the bundle and the housing using the applied resin. Once this was achieved the same rolling by hand technique used in preparation of a random packed module was used to allow the resin to dry evenly. After six to ten minutes the resin was set firmly enough to permit sealing of the second end of the bundle. Once again a good amount of resin was applied around the bundle until a seal was created between the housing and the bundle. Extra was taken not to block fibre ends that are close to the area of gluing as the resin must be pushed into the gap between the housing and the bundle which could result in excess resin spilling out onto the fibre ends. Drying of the resin was carried out by rolling the module as before. Once set the module was left overnight. Finally, as with the random packed module the excess fibre protruding from the module ends was trimmed by fracturing with pincers or tweezers.

4.2 SEM Characterisation

Scanning Electron Microscopy (SEM) imaging was used to study the morphology of the prepared fibres. The equipment used was principally a JEOL 6310 Scanning Electron Microscope and in some instances a JEOL T330. This allowed comparison of the evaluated pore sizes using permeation characterisation and the apparent pore sizes evident on the fibre surface. It is not the place to present a study of the workings of scanning electron microscopy – a brief summary of sample preparation and the image types taken is presented below.

4.2.1 SEM sample preparation

Sample for SEM are normally short lengths of the subject fibre mounted onto a sample plate. The images taken focus on the cross section through a fibre and the outer wall surface. As such two lengths of the fibre are used. One mounted vertically so as to be presenting its cross section and one laid flat so as to show the outer wall.

The exact lengths used were unimportant but for the vertically mounted samples something less than 5mm was desirable to ensure that there was no fouling of the sample on the imaging equipment which comes close in approach to the sample plate. The samples must then be coated with gold [Edawrds Sputter Coater] in order to be conducting.

4.2.2 SEM imaging

The images taken of the samples usually involve a full cross section, a cross section of just the wall and possible in addition a cross section close up at the wall outer and wall inner. The wall surface was usually imaged twice once at close for viewing apparent pore size and once at a wider angle to view the general wall smoothness/rougness.

4.3 Permeation Characterisation

Permeation characterisation is the process of establishing information about the pores in a membrane sample by permeating a fluid through the membrane under certain conditions. The known properties of the permeating fluid, and the method used allow some calculation relating to membrane pore size subject to certain assumptions.

4.3.1 Sample Preparation

Both the gas permeation method and the gas permeation/bubble point combined method use the same test modules and can be carried out one after the other as the method does not damage the membrane. Samples were prepared in single fibre modules in a dead end configuration. This means that one end of the fibre sample is open and sealed into a test module the other end is sealed and free within the test module. Typically samples were between 1 and 4 cm in length. Smaller samples result in more easily taken results and lower experimental error, though larger samples will be more representative of the fibre properties. To prepare a sample a fibre should was selected and a section of fibre which is defect free was identified. The fibre was fractured either side of the chosen section. In the case of most fibres (those which were sintered from a start length of 30 cm) the first and last 1-2 cm were

avoided as the fibre may have been located slightly off centre in the sintering furnace. The fibre sample was then be potted into a permeation test module. In order to pot the fibre sample epoxy resin was used (identical resin to that used in module preparation). A simple holder was also used to assist, it was constructed of a wooden block with a 3-5 mm deep hole drilled into it slightly wider than the diameter of a fibre. The hole had a wide paper based tape such as masking tape placed over it to make a minimum of 1 cm of tape in all directions from the hole. The fibre was then pushed through the tape into the hole so it was held vertically by the hole. The resin was prepared by mixing together the components as normal. A small amount was applied to the end if the fibre that was not inserted into the holder. The remainder of the resin was applied around the base of the fibre so as to be in contact with the fibre and to extend from the fibre at least 5 mm in all directions. The resin layer around the fibre was at least 1.5 mm thick checked by visual estimate. The module tube was then placed over the fibre into the epoxy. There was excess resin all around the outer diameter of the module on placement of the tube, i.e. it is certain that epoxy extends from the fibre to the inner diameter of the tube. The module was left in this state to dry overnight and then the paper tape was peeled from the wooden block. This freed the module from the block and a rim of paper and resin was left attached around the tube. This rim of resin was fractured all around the tube edge leaving the fibre and epoxy within the tube intact and flush with the tube end. This construction allowed the tube to be used as normal within compression fit components without the epoxy preventing proper connections. Any excess fibre outside of the module (the 3-5 mm which was beneath the tape within the block) was broken off with tweezers. The construction process is shown in Figure 4.7.

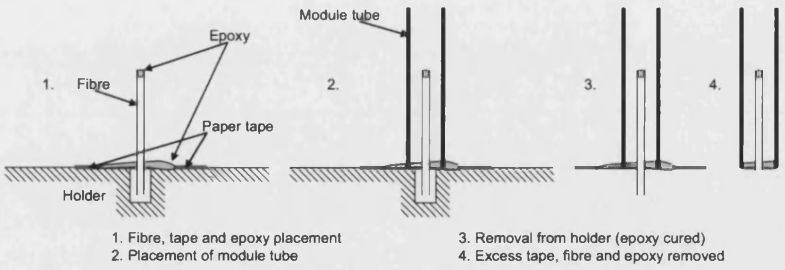

Figure 4.7 - Permeation characterisation module preparation

Re-use of test module tubes was desirable and removal of the previous sample was accomplished in two ways, the simplest method was to remove the membrane by fracturing it where it was held by the resin (in cases where a measurement of the sample size is needed this will reveal the exact length that was open as prior to this it cannot be certain how much of the sample was wetted by resin). Once only resin was left applying strong point pressure at the intersection of the resin and the tube wall or at the hole where the fibre had been would remove the whole circular resin piece. In certain cases where there is a thicker than expected resin layer this method did not work and the module was be placed in a lab bottle filled with NMP. After 24-48 hours the resin piece would become loose.

4.3.2 Gas permeation

The module manufactured as described in section 4.3.1 is inserted into the test rig see Figure 4.8. The rig uses a standard gas regulator to control the pressures for the test module and the rate of permeation is measured simply using a soap bubble flow meter (100 ml capacity) . An Ashcroft test gauge is used to give an accurate pressure reading for the inlet side pressure. The gas flow can only pass through the wall of the membrane due to the blocked end of the lumen side of the membrane. The soap bubble flow meter measures directly the permeation flow. This is carried out by a measuring the time taken for a given amount to permeate. A range of pressures are used and no pressures below 10 psi (68.94 kPa) are used. Details of the calculation method have been given in section 2.4.2.

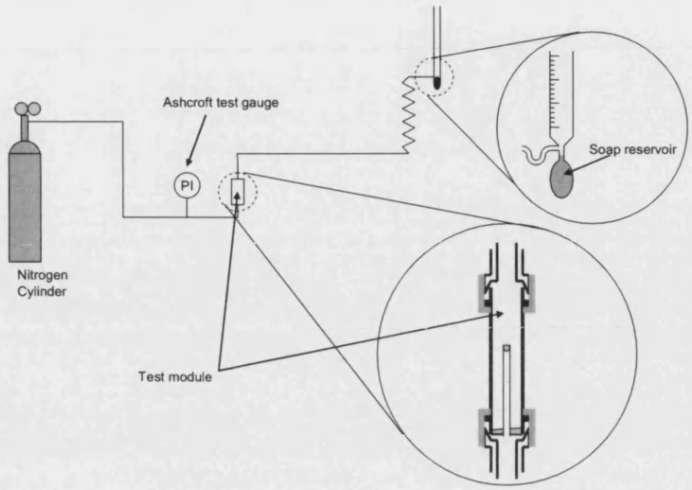

Figure 4.8 - Basic permeation characterisation set-up (used for gas permeation)

4.3.3 Gas permeation/bubble point combined method

A detailed description of the theory of the bubble point method is given in section 2.4.3. The operational method is in effect similar to the gas permeation test. Two versions of the bubble point method have been used in this study. The first simply compares permeation measurements taken in a gas permeation test with permeation methods taken for a wetted membrane – the second evolution of the method uses a saturated gas to carry out an identical test to the gas permeation test and then a saturated gas to carry out the wetted membrane test.

To carry out a wetted membrane test the set-up is the same as for a simple gas permeation test with one exception, either ethanol or 1-propanol is charged to the test module so that the test module is filled above the height of the membrane sample.

A disengagement column is also added to the equipment to prevent carry over of liquid alcohol into the soap bubble meter. The column as a 15cm length of ½" stainless steel tubing.

The alteration made to the method in the latter part of the project used a vessel filled with the same alcohol as the module through which the permeating gas was fed. This saturated the gas to minimise evaporative losses of alcohol from the module. Without

this there can be distortion of the results. It should be noted that there is a need to run the gas permeation test with this vessel removed from the system if a pure gas permeation result is desired – however for the best bubble point/gas permeation combined results the vessel should be in line for both the dry permeation test and the wet permeation test.

The expected permeation from the wet and dry test is somewhat different and as such there are two additional bubble flow meters available in capacities of 1 ml and 5 ml.

4.3.4 Mercury Porosimetry

Some mercury porosimetry data was obtained for membranes used in this study. The details of mercury porosimetry as a method are outlined in section 2.4.4. In this section I would like to acknowledge workers at the Technical University of Munich who carried out the mercury porosimetry measurements in Germany.

4.4 Mass transfer measurements

The aim of this study is to investigate the use of membranes to remove dissolved nitrogen from a liquid used as the precursor for a layer in the manufacture of safety glass. Measurement of dissolved nitrogen is somewhat difficult as outlined in section 2.5. Hence the measurement of dissolved oxygen (DO) will be used based on the assumption that the diffusivity of nitrogen and oxygen in the liquid is similar. Small contactors such as the ceramic membrane contactors manufactured in this study will not give high DO removal in a single pass so performance is measured in a batch recycle system.

4.4.1 Measurement method

Measurement of the dissolved oxygen content is carried out using a dissolved oxygen meter. The probe is recalibrated for 100% DO every day and recalibrated for 0% DO weekly during periods of use. The probe is used in a variety of ways depending on the system being tested – for example in water systems the probe is located in the batch

recycle tank whilst in tests on silicate solution the probe is located in a smaller test cell in line between the main tank and membrane module. Specific details are outlined in the following sections.

4.4.2 Mass transfer in membrane module systems

The rig for testing mass transfer performance is as discussed operated in a recycle system as such the liquid is drawn by pump from the batch recycle tank, possibly through a DO test cell (dependant on set-up). Following the pump the liquid feeds to the membrane module where it flows on the shell side of the module. Following the module the liquid is returned to the main tank. The set up is illustrated in Figure 4.9.

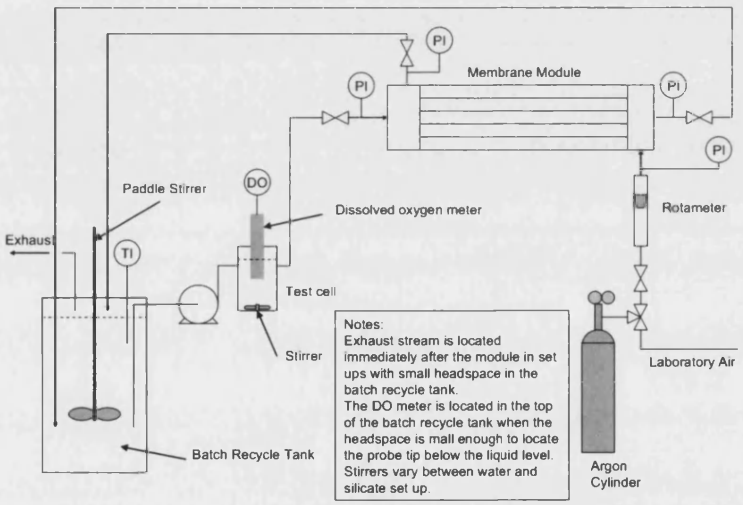

Figure 4.9 - Mass transfer measurement set-up

Notes on the mass transfer rig:

As indicated in Figure 4.9 there are a number of variations in set up depending on the circumstances of testing. For example there were three differently sized batch recycle tanks, one of 150 cm^3 capacity, one of 1.5 dm^3 and one of 5 dm^3 were used. The key points are that testing with water rather than silicate solution was carried out using a magnetic stirrer in the case of the smaller batch recycle tanks and an overhead paddle

stirrer when the larger batch recycle tank was used. For silicate solution a magnetic stirrer was used only for the 150 cm^3 tank. When testing with the 5 dm^3 the charge to the tank was not sufficient that the liquid level was close enough to the tank ports for placement of the DO probe into the solution. As such when using this tank the DO probe was placed in a test cell between the pump and the batch recycle tank. Because of the larger headspace the exhaust from the system was fed through the headspace to give an argon blanket. It should be noted the tank used had a tapering upper section and as such the area of the liquid surface was relatively small though there will have been an additional mass transfer effect encountered due to this headspace purge. It is also noted this set up was only used in conjunction with the commercial Liqui-Cel® module and not the smaller in-house constructed ceramic membrane modules. The exact set-up shown in Figure 4.9 is that used when using the larger tank only, though from the notes in this section the set-up for other instances should have been made clear. In addition not shown on the diagram cylinder supplied air has been used in some ceramic membrane experiments as it offers higher possible pressures than laboratory tap air.

Mass transfer experimental procedure

Notes on compatibility of fluids: prior to starting a silicate solution based series of experiments the system should be washed through with sodium hydroxide at 5 wt%. Solids will be formed from the silicate solutions on contact with water. As such if the system requires a full wash after silicate solution has been used it must also be carried out with sodium hydroxide. To prevent the use of large quantities of sodium hydroxide two 1 dm^3 batches of solution were prepared – one labelled "coarse wash" and one labelled "fine wash". The coarse wash was used after silicate solution as a clean down liquid to remove residual silicate and the fine wash to provide a clean flush of the system. The fine wash was used prior to start up with a silicate solution. After five uses the coarse wash was disposed of and the existing "fine wash" re-labelled as "coarse wash". A new fine wash solution was made to replace the old one.

For mass transfer rig start up refer to Appendix III. The DO measurement method outlined below details the method used to obtain the experimental results.

DO measurement procedure:

1. Once start up is complete or a run of DO measurements is complete there should be air running through the gas side of the membrane module.
2. Any adjustments to flow conditions, inlet/outlet pressures etc. that must be carried out to prepare the rig for the run under the variables to be tested were completed.
3. The DO level would be allowed to reach a point which was believed to be in excess of 85% of the maximum value for silicate solutions and for water the value would be greater than 95%. The change in DO level was noted against time during this phase of DO saturation for previously untested solutions such that a reasonable estimate of the maximum DO concentration could be made.
4. Once the DO measurement reached a satisfactory start point for desorption, the gas side was switched from air to argon a timer was started (or a continuation of timing was used if DO rise was monitored).
5. The DO level and solution temperature were recorded minute by minute or at another suitable time interval based upon the rate of desorption.
6. When desorption reached a level at which no further measurements were required (frequently below 10% of original value in polymeric membrane tests and after several hundred minutes in ceramic membrane tests) the gas side was switched to air and the next measurements could be taken by starting the "DO measurement procedure" instructions again. If shut down was desired or a change of test liquid is required then the "shut down" instructions (below) were followed

Note silicate solution could be left in the system for several days provided the gas side of the system was not flowing and all parts of the liquid system (except obviously the membranes themselves) are gas tight and liquid filled. The system was simply circulated with silicate solution in a loop for 10-20 minutes before restarting measurements after any static liquid filled shut down lasting longer than an hour. For full shut down/clean down of the mass transfer rig refer to Appendix III.

4.4.3 Mass transfer in sparge and ultrasound system

As discussed in chapter 2 an alternative method of removal of DN is to perform a dispersive contact and then remove the resulting entrained bubbles. This removal could be carried out using ultrasound. This was performed with the aim of comparing membrane methods and the sparge ultrasound method. The experimental set up was a modification of the membrane mass transfer rig in which the gas was fed direct to the batch recycle tank and the pump simply drove the liquid around a measurement loop for the purposes of testing since the probe could not operate in a liquid with entrained bubbles or in an ultrasound affected environment. The test cell was positioned prior to the pump which drew liquid from the cell returning it to the main tank which was sealed well save for a partially controllable opening to prevent overpressure in the tank. The slightly elevated pressure resulted in a flow if liquid driven via a submerged outlet tube to a second cell like tank located in an ultrasonic bath. This bath when switched on provided ultrasound treatment to remove the entrained gas from the liquid so that it could be tested in the test cell – the degree of phase separation was visible with entrained bubbles rapidly rising to the liquid surface. The liquid was drawn from the ultrasound tank into the test cell by a further tube the driving force being provided by the pump on the basis the test cell was air tight sealed. The ultrasound cell was open to atmosphere to vent the entrained gas. The set-up is shown in Figure 4.10.

For start up and shut down procedures refer to Appendix III

Once start up was complete mass transfer experiments could continue with exactly the same method as employed with the membrane module experiments (DO measurement procedure) starting at instruction 2.

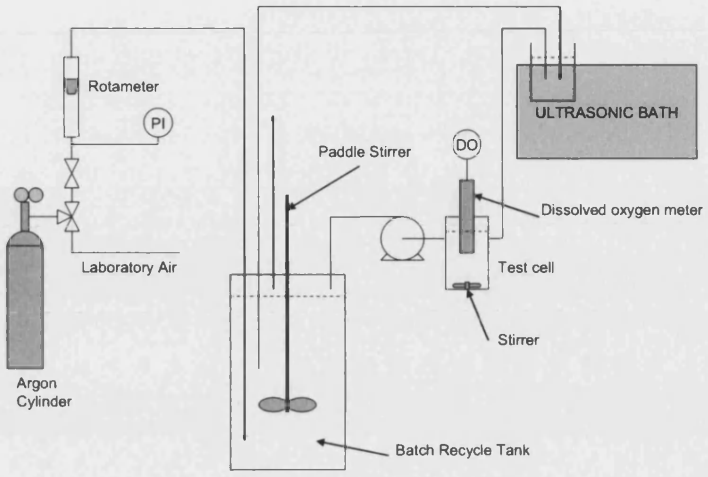

Figure 4.10 – Sparge and ultrasound set-up

4.5 Glass coating casting methods

Glass coating casting is the final stage in the process and was carried out at Pilkington Group Limited. labs in Lathom, Lancashire. The intricacies of the method are not important to the result of this work but the transfer of the liquid from membrane or sparge and ultrasound rig to the glass is a key issue as will be discussed in chapter 5 hence only a brief overview of the casting is provided and a detailed description of the transfer is covered.

4.5.1 Pour & dry/Tek Dry

Under normal conditions the Pour & Dry (PD) method involves the pouring of the silicate solution onto the glass. The glass is placed in an oven with a controlled atmosphere which is humid and contains oxygen. DN will transfer from the surface of the glass coating due to the lack of nitrogen in the surrounding atmosphere. After a period of time a skin forms on the surface of the solution and mass transfer ceases. Following completion of the run a second piece of glass is laminated on top of the coating to make a sandwich of two pieces of glass around the silicate coating layer. The glass is static in this process and runs for a time.

Tek Dry (TD) is similar in that the coating is poured on and dried in an oven however the atmosphere is not controlled. Tek Dry is designed for layers of silicate to be poured onto a moving substrate. This process is dynamic in that the coated glass moves through the oven so its control is based on the speed of the substrate movement.

In experiments for PD and TD glass plates were used. In the case of TD the plate was placed on the plastic film and hence moved through the oven as is normal for TD. The solution was treated as in the labs at the University of Bath and the liquid was then bottled in a manner that excluded air from the bottle. Liquid was poured from the bottle onto glass plates when required and placed in the appropriate machine from where Pilkington Group Limited. engineers completed the process.

4.5.2 Cast in Place

Cast in place (CIP) is a method by which silicate solution is injected directly between two pieces of glass and is chemically cured.

Here the current DN removal procedure is to treat half of the liquid by leaving under vacuum for a period of time and to heat the other half to a temperature so as to minimise the dissolved gas content. The two halves when mixed will form the final self setting solution.

This has been approached two ways with regard to DN removal. Once the mixture was fully prepared and treated by the membrane system and once two halves of the mixture were prepared such that the final setting mixture would only be formed on mixing of the two halves as with the current standard procedure. The highest DN carrying half was treated with the membrane rig and the second half of the mixture was slowly added to the batch recycle tank. Once fully mixed the liquid was tapped off into a bottle from the module outlet and sealed under argon until ready for CIP treatment.

4.6 Safety, Chemicals, Equipment

4.6.1 Safety

Safety assessments were carried out as per the University regulations and details are included in the appendix.

4.6.2 Chemicals

The chemicals used are summarised in Table 4.1 in the form of description, details and supplier. The glass coating liquids used for mass transfer experiments have been summarised separately.

Table 4.1 – Chemicals List

Description	Details	Supplier
Polyethersulfone	MW 40,000 Da	Amoco Radel-A
NMP	-	Sigma Aldrich
Al_2O_3 [(a)]	α alumina (1 μm)	Alfa-Aesar
Al_2O_3 [(b)]	α alumina (0.3 μm)	Alfa-Aesar
Al_2O_3 [©]	α/γ mix alumina (0.01-0.02 μm)	Alfa-Aesar
Compressed Air (cylinder)		BOC
Argon (cylinder)	Pureshield	BOC
Nitrogen (cylinder)		BOC
Poly-vinyl-alcohol	MW 72,000 Da	Fluka
1-propanol	Analysis grade	Fisher Scientific
Ethanol	Analysis grade	Fisher Scientific

The glass coating solutions tested were as shown in Table 4.2.

Table 4.2 - Glass solution data

Soln No.	% Na_2O	% K_2O	% SiO_2	Glycerol added	Notes	Viscosity mPas
1	8.63	-	27.6	yes	-	100
2	11.2	-	31.9	yes	-	600
3	8.63	-	27.6	no	-	100
4	11.2	-	31.95	no	-	600
5	-	-	40	no	12nm particles	-
6	-	-	50	no	50nm particles	-
7	-	21.6	30.8	no	-	150

5 Results and discussion

5.1 Membrane Manufacture and Characterisation

5.1.1 Validation of characterisation methods

Though manufacture of membranes is required before it is possible to characterise anything, it is important to understand the behaviour of the characterisation methods available and to validate them or they have no meaning. As such the first samples produced were characterised by more than just a single method and the results of the methods were compared. It is therefore useful to present a study of the characterisation methods prior to investigating results from membrane manufacture and hence this study is presented first.

Validation methods:
SEM imaging gives a clear image of the membrane surface but relative to other simpler tests is expensive and inconvenient unless a dedicated machine is available. As such there have been relatively few SEM images taken in this study but where they are available comment may be made on the validity of pore sizes that have determined by other methods.

Mercury porosimetry has itself validity issues as discussed in section 2.4.5. The method was also unavailable for regular use during this study. However an 's' distribution is given by the method and in cases where there are a large number of smaller dead end pores (which may be present within alumina particles rather than formed from spaces between the particles) this will show as a peak of smaller pore sizes or as a step in the 's' distribution. As such the main "open for flow" pore size should be possible to estimate based on the data. Because of this the method is chosen as a 'validating' method and some samples were sent to the Technical University of Munich, Germany, where they were tested.

The body of testing work on the membranes produced is to be based either upon the gas permeation test or the combined gas permeation and bubble point test. The results will be compared to those for the samples sent for mercury porosimetry analysis.

Methods of assessing true pore size will be as follows:

By mercury porosimetry the maximum pore size is given directly as a result of the test and will be taken as the figure given – in addition a second figure will be given to denote the point on the results curve where an estimated maximum pore size would be given simply by viewing the results – this allows permeation obviously caused by a defect in the membrane to be neglected. The mean pore size given by the results of the test is quoted as is the estimated mean pore size of flow pores based on 50% of cumulative total pore volume. By flow pores it is meant that in cases where there are two sections of 's' curve an end point for the first section is determined and the mean size based on 50% of the scale of just the first section of curve. As such the second s-curve is assumed to be dead end pores within alumina particles. These dead end pores would not be detected by the gas permeation or combined bubble point/gas permeation method.

Six fibres were assessed in this way – three of which were subjected to an attempt to coat them with γ-alumina direct from a powder based slurry – these coatings had then been sintered at relatively low temperature and hence it was expected that these samples would have a secondary pore size range as discussed above due to porosity of the γ-alumina particles. To highlight this the three coated membranes have a differential pore size distribution shown as Figure 5.2 and the three uncoated as Figure 5.3. It can be seen all three coated membranes have two significant regions where there is a substantial volume of pores. The lower sized of these are expected to be dead end pores in the structure of the alumina. The larger sized area of pores is expected to be the 'flow pores' where material can pass from one side of the membrane to the other. The uncoated membranes only show one region of pores as expected. Sample 15 does show two peaks but there is no diameter between the peaks where there are no pores and it is expected that there are some minor membrane

defects causing the lower peak. It is also noted that two of the coated membranes show very small peaks at very large pore diameters theses are also caused by defects.

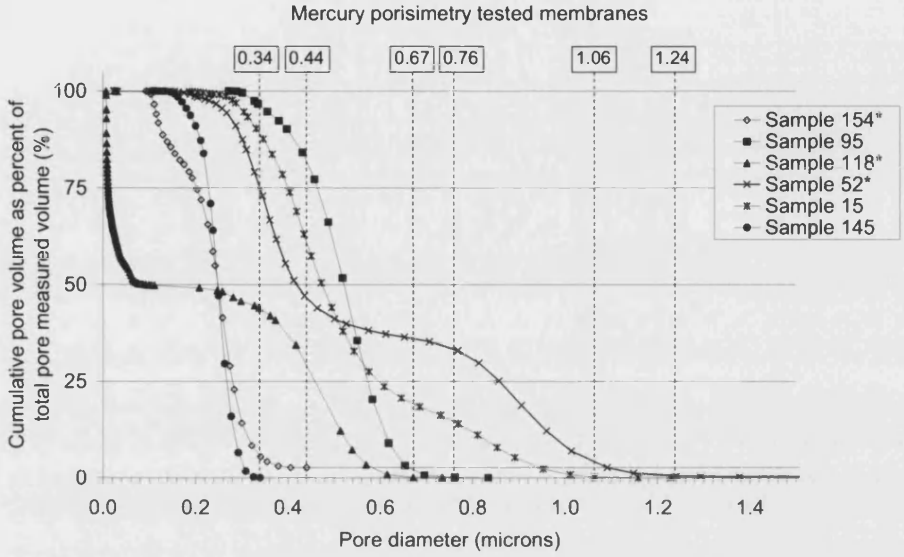

Figure 5.1 - Mercury porosimetry data for three coated and three uncoated ceramic membranes

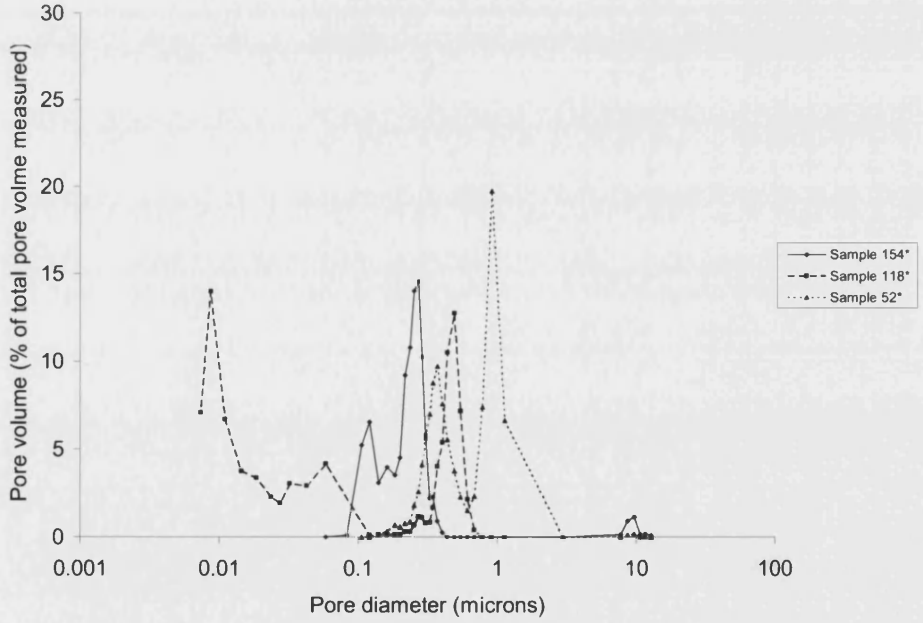

Figure 5.2 - Coated membrane pore size distribution based on mercury porosimetry data

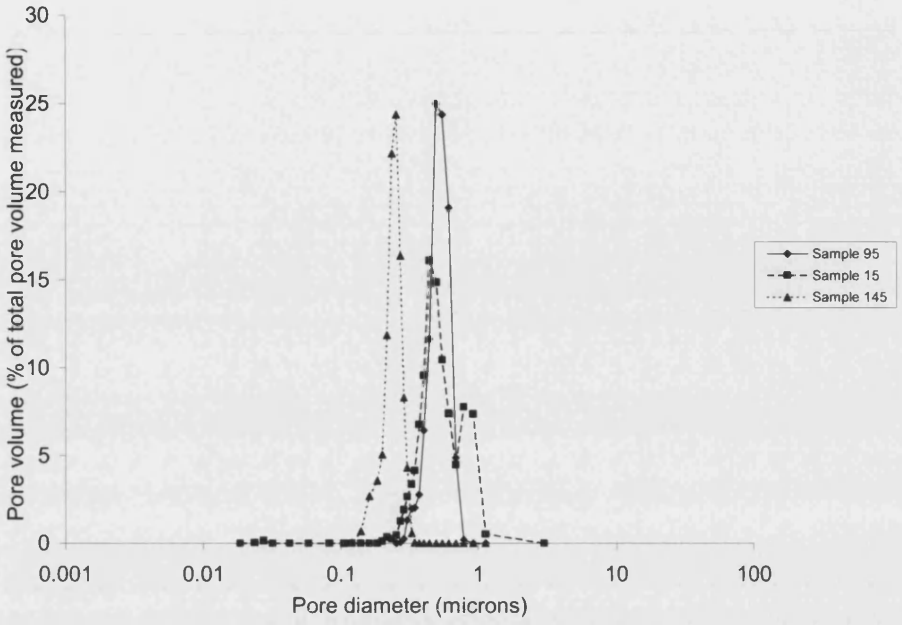

Figure 5.3 - Uncoated membranes pore size distribution based on mercury porosimetry data

It is noted at this point that a commonly used abbreviation is BP/GP, by this reference is being made to the combined bubble point/gas permeation method. Where this abbreviation is applied to data (for example in graph axis labels the definition directly means:

$$\frac{\text{Bubble Point Permeation rate}}{\text{Dry Gas Permeation Rate}} \Rightarrow \frac{BP}{GP}$$

The pore size data based on mercury porosimetry is presented in Table 5.1. The data given for these membranes by the combined bubble point/gas permeation (BP/GP) method and the gas permeation (GP) method is also included.

Table 5.1 – Pore size data by various methods comparing to mercury porosimetry data (all sizes given are pore diameter μm)

Sample ID	MP mean	FP median	MP max	ND max	BP/GP max	BP/GP median	GP mean
15	0.458	0.47	1.24	1.06	0.67	0.3[a]	n/a[b]
52*	0.447	n/a[c]	13.29	1.24	0.42	0.27	4.03
95	0.499	0.51	0.76	0.76	0.54	0.29	0.64
118*	0.0241	0.45	0.67	0.67	0.535	0.29	1.68
145	0.240	0.25	0.34	0.34	0.34	0.17	1.39
154*	0.218	0.25	13.43	0.44	0.33	0.19	0.64

(all data is pore diameter, μm)

* indicates samples which were subject to dip-coating in γ-alumina.

a, based on extrapolation of data in an apparently linear region of 's' curve

b, data resulted in a negative pore size when calculated

c, unusual distribution of pore sizes in which 2 steps are observed though neither would appear to be no-flow pores due to γ-alumina.

Table 5.2 shows the relative differences between median pore size by mercury porosimetry (indicated as FP as the results ignore pores that are not open for flow) and BP/GP, the mean pore size by MP compared with the mean size by GP and the median by BP/GP. The maximum pore sizes by MP (ND – the value taken assuming no defects) and the BP/GP max pore size are also compared.

Table 5.2 - Relative difference in pore size data, GP and BP/GP methods vs mercury porosimetry

Sample ID	Mean MP vs BP/GP	Mean MP vs GP	FP median vs BP/GP	FP median vs GP	ND max vs BP/GP
15	-34.5	n/a	-36.2	n/a	-36.8
52*	-39.6	801	n/a	n/a	-66.1
95	-41.9	28.3	-43.1	25.5	-29.0
118*	1103	6622	-35.6	260	-20.2
145	-29.2	479	-32.0	456	0
154*	-12.8	194	-24.0	156	-25.0

The γ-alumina involved in sample 118 appears to have skewed the mean pore size result to an unrealistically low value when considering the overall result hence the large errors compared with the "through flow" measurment methods of GP and BP/GP. Ignoring the second phase of the mercury porosimetry data seems to bring the data back into the expected flow pores size range.

The data shows that the BP/GP method consistently under sizes pores at around 30-40% on mean/median sizes but more critically for contactor operations is usually within 30% when estimating maximum pore size. The GP results varied wildly this is believed to be due to the sensitivity of the method as is shown below.

The following is an example of the fluctuation of mean pore size caused by sensitivity of the GP method – membrane samples 52 and 95 are used as an example and were tested prior to adjustments to the BP/GP method that required permeating gas to be bubbled through alcohol first. At the first stage two data points are included in the gas permeation data and both the gas permeation result and the median BP/GP result are shown (remembering that BP/GP relies on GP data and as such for the first BP/GP result only the two points in place are used). Subsequent stages in the test add a data point (in the order they were obtained, i.e. increasing pressure) to the GP data and the results are again calculated for both tests.

Table 5.3 - Variability of pore diameter based on GP and BP/GP methods

	Membrane 52			Membrane 95		
No of points in GP data	GP mean	BP/GP median	R^2 value of GP data	GP mean	BP/GP median	R^2 value of GP data
2	289	0.272	1	undefined	0.31	1
3	4.91	0.272	0.995	1.1	0.318	0.777
4	6.55	0.271	0.997	2.82	0.314	0.907
5	12.89	0.268	0.997	1.62	0.315	0.922
6	8.24	0.268	0.997	1.45	0.315	0.95
7	5.90	0.267	0.997	1.18	0.315	0.957
8	4.03	0.267	0.994	1.02	0.314	0.962
9	-	-	-	1.13	0.313	0.972
10	-	-	-	1.09	0.312	0.979
11	-	-	-	0.88	0.312	0.986

All data is pore diameter, μ

It is clear from the above data (Table 5.3) and the graphical representations below (Figure 5.5 and Figure 5.6) that there is considerable variability associated with the GP method while the GP/BP method is reasonably consistent. It does appear that the more data that is added to GP calculations the less variation there is – this is obviously to be expected as the effect of each new data point is less than that of the last. In both examples the R^2 value is reasonable throughout giving confidence in the straight line trend observed.

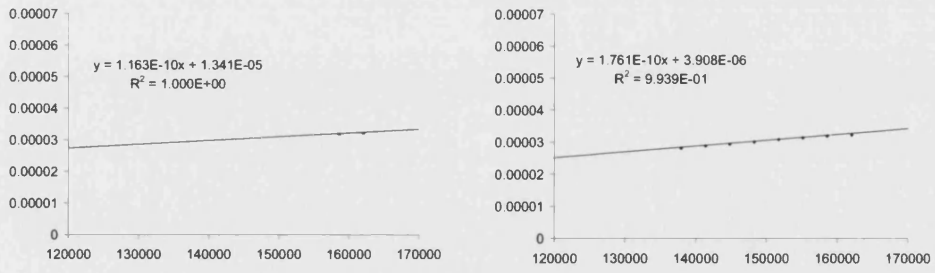

Figure 5.4 - Sample 52 GP data with two points and eight points illustrating result variability

Figure 5.4 shows that the variation between two data points and eight data points appears relatively small compared to the pore size result. The gradient is 30% lower and the intercept 4 times larger for the 2 data point example yet the calculated pore size is 290 μm while for 8 data points the result is 4 μm, this is a factor of nearly 75 times difference in the determined pore size. The eight data points also visually appear to be a trend of accurate data points (supported by R^2 data) however as discussed above and is shown by Figure 5.5 below calculated pore data from GP is very variable. The reasons for this are apparent when one analyses both the experimental method and more particularly the calculation involved. Also analysis of the method shows us why variability is low in the BP/GP method. The key parameters in the GP method are the value of the y-axis intercept and the slope of the straight line obtained. If one was to take five data points for example that are perfectly in line and have an R^2 value of 1.0 before adding a sixth experimental point which is of a lower value than expected, the line of best fit will be drawn at a fractionally lower slope. This in itself seems only a small difference, however the use of relatively low pressures required by the equipment and crucially the type of membrane assessed, added to the fact that the x-axis displays average pressure means that data points can only begin above atmospheric pressure and do not span a wide range beyond. Thus the adjustment of the line of best fit caused by the sixth data point is extrapolated back to the axis for a range often in excess of 200% of the range in which data can be taken making a large effect back at the intercept point. This is all accentuated by the fact that a lower slope will also yield a higher value of intercept. The fact that these values form a fraction rather than a product magnifies errors in the method and gives the wild fluctuation. It must be said in the method's defence that at lower pore size or over a range of higher measurable permeation rates and pressures these effects could be minimised and perhaps allow the method to be useful. However it must be concluded that in this study there was neither the equipment available to handle large flows nor the samples to test that would yield lower flows to bring the method into an acceptable range of reliability.

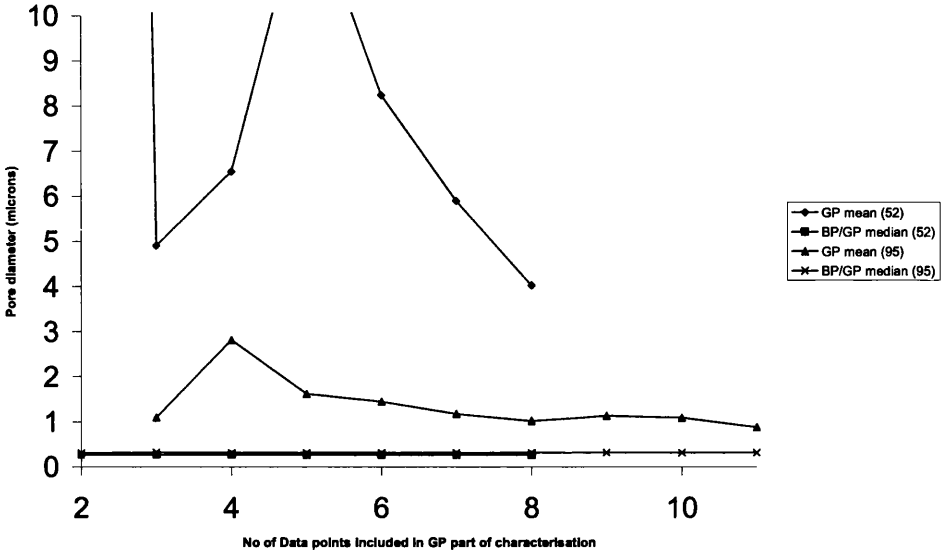

Figure 5.5 - Variability of result with amount of data GP method (BP/GP shown)

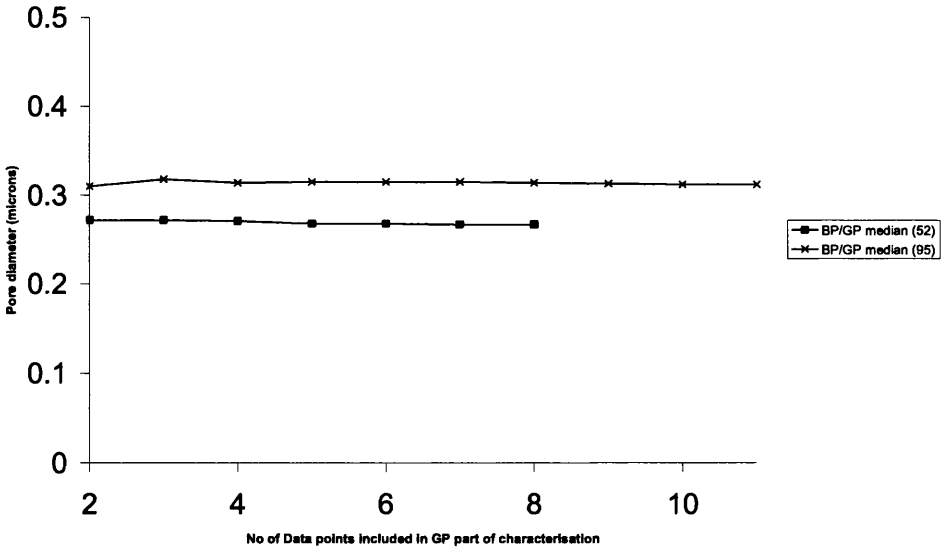

Figure 5.6 - Variability of result with amount of data BP/GP method

BP/GP method adjustments made late in the study

Some results from the BP/GP method showed the method to have errors when some samples allowed an apparent flow through a wet membrane (at higher pressures) which was higher than the expected flow from a dry membrane. This was attributed

to the evaporation of the wetting fluid from the reservoir of fluid surrounding the sample. The reservoir would typically show a loss of several millilitres of liquid after testing. An initial plan to saturate the gas with liquid was initially foiled due to no suitably pressure resistant vessel for saturation at pressures higher than 7 bar. Therefore initially 1-propanol replaced ethanol as the wetting fluid due to its higher boiling point. Later tests used on all samples involved with modules used for mass transfer studies introduced a saturation vessel while 1-propanol remained the wetting fluid of choice. Below follows a brief analysis of the effects of each variation.

1-propanol to ethanol

One would expect that changing the wetting fluid in the circumstances explained above that the maximum pore size should be maintained at the same position while the slope of the graph would change due to less evaporation of 1-propanol than ethanol. There is some difference in max pore size measured but this amounts to around 5-6 nm while at the measurement of mean pore size the difference has widened to around 10 nm. Figure 5.7 shows this effect.

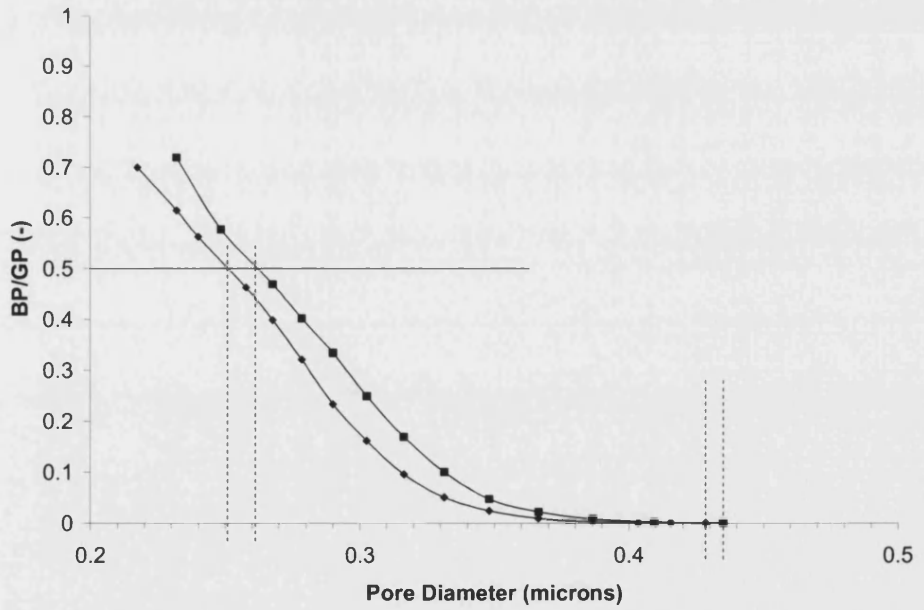

Figure 5.7 - Ethanol or 1-propanol as wetting fluid in the BP/GP test method (typical uncoated ceramic membrane sample)

Unsaturated permeating gas to saturated permeating gas

By saturating the permeant gas prior to feeding it to the module the evaporation of liquid is limited. Figure 5.8 shows the effects of saturation to either the bubble point test or both bubble point and gas permeation tests. This shifts the BP/GP curves to a more realistic position in terms of overall curve shape, the effect on results with regard to median pore size is limited to around 10-20 nm, or around 10%. There is no effect on maximum pore size.

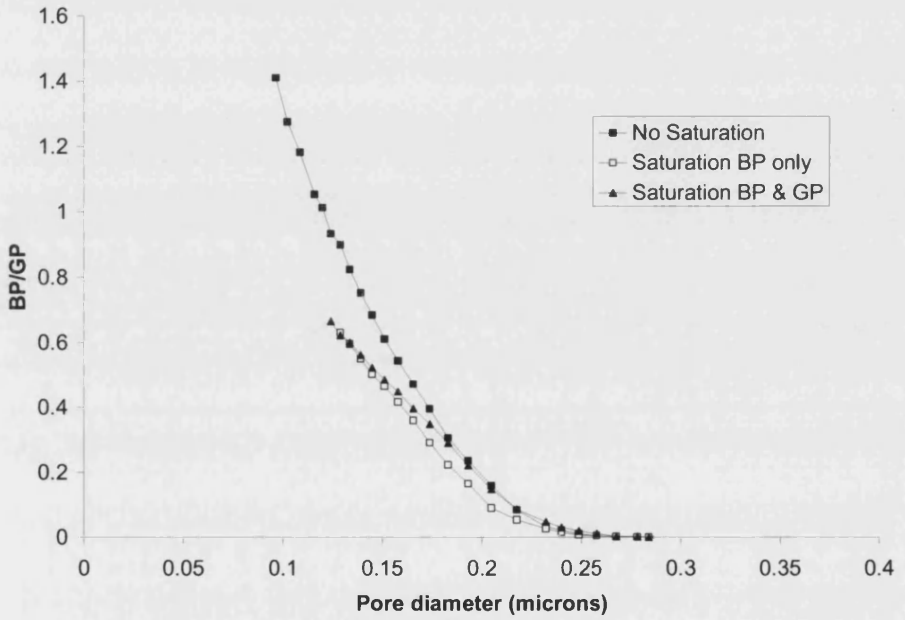

Figure 5.8 - Saturated gas improvement to BP/GP test (typical uncoated ceramic membrane sample)

In summary the BP/GP method is suitable for the characterisation of fibres in this study, the precise median pore size is not an essential factor but is instead a useful comparison between fibres. For usage as phase contactors data on maximum pore size is essential data as it governs operating conditions. As such the variability of method used is not of concern as the maximum pore size remains a direct measurement independent of any rate measurement or wetting fluids.

The gas permeation method is discounted as valid with regard to this study on the grounds discussed above it must be re-iterated that with sufficient time to take several measurements and with sufficiently accurately equipment the method is likely to be valid for a wide range of membranes.

5.1.2 Membrane Manufacture results

The solutions used for membrane manufacture were numbered during the study, these numbers remain to avoid errors when analysing the results hence the first solution encountered is solution 22.

Fibres from solution 22

Sintering was carried out using a monolith as support for the fibre.

Table 5.4 shows the solution composition of the extrusion solution, the produced fibre was sintered once at a temperature of 1500°C for 5 hrs with the associated heating times resulting in a full running time of more than 17 hrs though set cool down rates are not achieved giving a real time above normal temperatures (above 100°C) in excess of 20hrs with unloading not usually possible inside 24 hrs. This is because the work-tube holds a high temperature not measured well by the thermocouples at low temperature so the indicated temperature which is taken as real temperature is still below the work-tube temperature as the air around the outside of the tube is in fact where the thermocouple is located (see appendix on sintering programs – real vs. program temperature). Sintering was carried out using a monolith as support for the fibre.

Table 5.4 - Solution 22 composition

Component	wt% in Solution 22
NMP	39.56
PES	9.89
Al_2O_3 (1 μm)	39.56
Al_2O_3 (0.3 μm)	7.42
Al_2O_3 (0.01-0.02 μm)	2.47
PEG (mw 400)	1.10

The solution was extruded under 2 bar gas pressure, the temperature of all the water baths was 25°C and the internal coagulant rate was 5 ml/min. The rate at which solution falls from the extruder is variable dependant on the other conditions and in all sections of this work the pressure has been fixed at a chosen value with the rate determined by all the variables affecting it – for example in this case the uptake of fibre by the motorised guide roller was approximately the same for all air gaps excluding the zero air gap and this rate was around 2.75 times faster than the rate for zero air gap. The fibres analysed for variables other than air gap used a 60 mm air gap.

Effect of air gap

The effect of small variation in the air gap (distance between spinnerette and surface of water bath during spinning) was studied by measuring the median and maximum pore size (by BP/GP method) of a membrane produced. Other than the air gap all other variables were maintained as identical throughout the manufacture process. A summary of the production details of the fibre is presented below and the air gap was changed during the extrusion process.

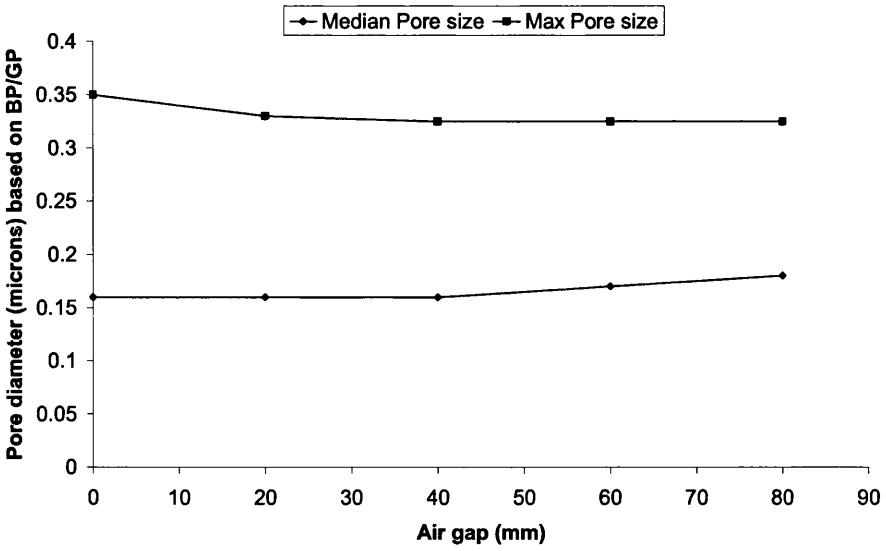

Figure 5.9 - Effect of air gap (Ceramic fibre sintered at 1500°C spun from solution 22 at varied air gap)

The air gap had little effect on the pore sizes in the produced membranes though there is some evidence to suggest that there is a tendency toward a slight narrowing of the pore size distribution at larger air gaps (i.e the median size remains the same but the maximum pore size is reduced see Figure 5.9) which indicates a more uniform fibre. The method of testing is measuring the flow pores of the membrane and given the likelihood of interconnected pores through the structure the actual measured pore sizes will most likely correspond to the pore openings in the region near the outer surface of the fibre. For this reason a more consistent fibre may be produced with a larger air gap as some initial setting of the surface may be occurring in the air drying phase. In the water phase the action of non-solvent and indeed bulk currents in the water bath are stronger and may disrupt the surface.

Effect of dip time when coating

Due to failure of the epoxy resin sealant during BP/GP characterisation of the samples the dip time effect can only be compared on the basis of maximum pore size. The samples do not provide a sufficiently extensive study of dip time to draw full

conclusions but were designed to see if there was an obvious variation worthy of further investigation.

The samples were prepared from solution 22 (detailed in Table 5.4), spun at the air gap of 60 mm. The other spinning variables are exactly the same as those for the samples used in the air gap investigation. With regard to sintering of the fibres there are two stages, the first is sintering following spinning and the second is sintering after coating. The first sintering process had a maximum temperature of 1400 °C and the second sintering after coating was at a maximum temperature of 1450 °C. In both cases the sintering was ramped to the maximum temperature where this temperature was sustained for 5 hours. The coating applied was coating solution 4 which is a mixture of 90 wt% distilled water and 10 wt% Al_2O_3 (0.01-0.02 μm). Recalling from chapter 4 that this grade of alumina is supplied as a mixture of alpha and gamma form. The applied coating was not allowed to dry before placement of the fibres in the furnace and application of the coating was carried out with the ends of the fibres both open. The fibres were sintered on a flat grooved ceramic support.

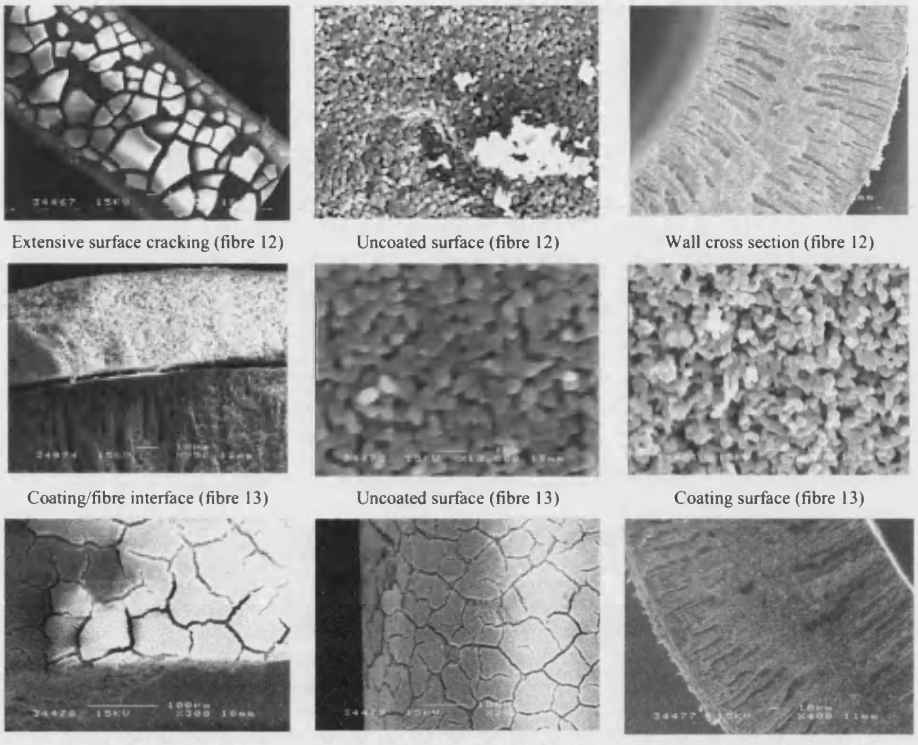

Figure 5.10 - Fibres coated for different lengths of time produced from solution 22 (sintered at 1400°C then dip coated for different lengths of time (fibre 12 – 45s, fibre 13 – 30s, fibre 14 – 15s), then re-sintered at 1450°C

The results showed that dip time gave rise to a maximum pore size of 0.35 μm for a dip time of 60 s (fibre 11), whilst the pore size increased to an apparent 0.38 μm for a dip time of 15 s (fibre 14), hardly a dramatic difference. Other fibres were created but not tested in this way once the fibre surface was examined. Figure 5.10 shows the surface of the fibre dipped for 15 s (fibre 14) the most significant finding is that there is extensive cracking of the coated surface other fibres in the study are also shown these include fibre 12 dipped for 45 s and fibre 13 dipped for 30 s. It can be seen that comparing fibre 12 to fibre 14 there is significantly less loss of coating on fibre 14 though extensive cracking exists in both cases. The reasons for significantly less loss of the coating are related to the shorter dip time involved with fibre 14 when compared to fibre 12. This resulted in a thinner layer which is less susceptible to actually falling away as the depth of cracked material is less, there may also be an increased bonding of the coating to the original fibre as the layer is thinner it would in

theory heat faster at the interface of the fibre and coating. However it must be said that the effect of this would not be expected to be significant over such a small difference in thickness (approximately 50 μm at the thickest for fibre 12 so one assumes slightly thicker for fibre 11 and down to 10 μm for fibre 14). The full cross sections shown in both fibre 12 and fibre 14 are similar as one would expect as the only differences were in the applied coating. The cross sectional view of the coating on fibre 13 shows the poor adhesion at the interface between the coating and the fibre which contributes to the flaking of the coating. It can be seen comparing the images of the coating and uncoated areas on fibre 13 that the coating is in fact more porous then the sintered sub fibre and that any open pore channels are larger. The conclusion drawn from this is that in fact the best effect that is achieved by this coating is to plug defects in the original fibre. It could be argued that if any defects in the original fibre are in fact plugged to the extent that ceramic material enters the large pores or pin-holes and is sintered firmly in place then it is desirable to loose the remainder of the coating as this is only adding to the wall thickness of the fibre and hence any membrane phase mass transfer resistance. Though the particle size of the alumina used in the coating is significantly smaller than the pores in the base fibre there is clearly what appears to be a reasonably uniformly distributed size of particle. This could be agglomeration of the alumina which was present in the original dip solution but is more likely (given the uniformity) to be an effect of the change of state of the alumna from gamma through to alpha. This change occurs because of the alumina finding its most stable state which is the alpha form. It cannot however reach this state until temperatures around 1100°C are reached. Before this a lower state is occupied these states are relatively stable under normal conditions but degradation to the more stable form occurs at the temperature concerned.

Fibres from solution 34

A wide range of fibres were prepared from solution 34 including those to be discussed next as such the details are presented below in Table 5.5.

Table 5.5 - Solution 34 composition

Component	wt% in Solution 34
NMP	44.45
PES	11.11
Al_2O_3 (1 μm)	44.44
Al_2O_3 (0.3 μm)	-
Al_2O_3 (0.01-0.02 μm)	-
PEG (mw 400)	-

The solution was extruded under the following conditions: Tap water was the liquid in all three baths the temperature in all the baths was 16°C. Distilled water was the bore fluid and was fed at 6 cm^3/min. The gas pressure to drive the extrusion was 0.8 bar. The air gap was zero.

Effect of sintering conditions on uncoated fibres

Six fibres were tested which had been prepared from solution 34 (see Table 5.5) and had not been coated, one of those tested had been sintered at a lower temperature (1450°C) than the others, while the others were made by using the same temperature (1550°C). These higher temperature fibres were either simply sintered by placement on a ceramic block or by pre-straightening by hand prior to placement on the block. Some of the fibres were sintered twice as well in an analysis of the effect of twice sintering which is required when coating a fibre. Since all the variable conditions are not so much numeric range of variables but a selection of processing options the best means for the presentation of the results is to display the relevant BP/GP curves. This gives some more information than the simple data extracted from the curves. The data is shown below in Figure 5.11. shows the conditions used to make the fibres and lists specifically the max pore size determined by the method.

Table 5.6 - Details of uncoated fibres from solution 34

Fibre No.	Max Pore diameter (μm)	Straightening method	Max. sintering temperature (°C)	No. of times sintered
15	0.66	GB	1450	1
28	0.56	GB	1550	1
44	0.45	GB+HS	1550	1
49	0.46	GB+HS	1550	1
54	0.41	GB+HS	1550	2

GB = Grooved Block (+HS = with Hand Straightening)

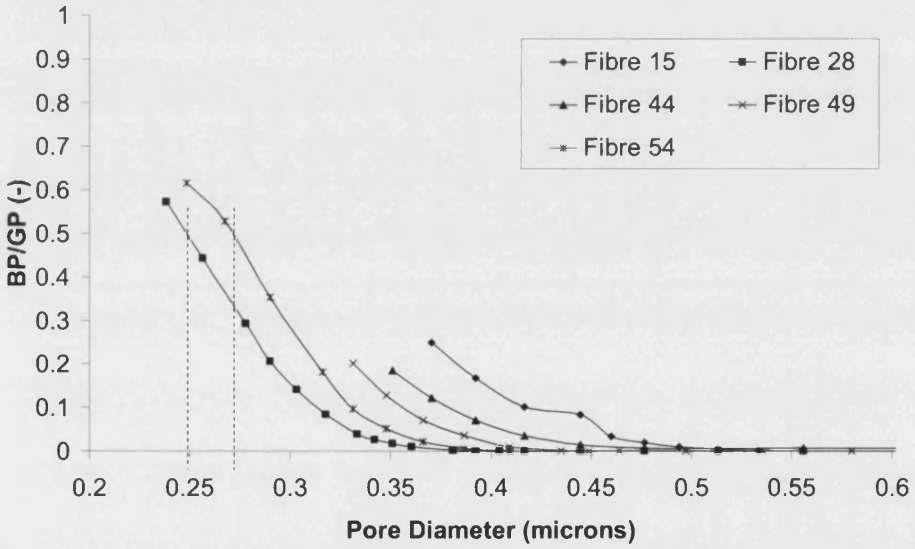

Figure 5.11 - Uncoated fibres based on solution 34 (preparation details outlined in Table 5.6)

It can be seen from the results for uncoated fibres from solution 34 that there is an experimental difficulty with the BP/GP method. These results are amongst the first to be taken by the method and the frequent difficulty in reaching the value of 0.5 (determined as the point at which the median pore diameter is read) is cause for concern. This was resolved by using smaller samples of fibre so that there would be less flow at the higher permeation pressures. It can be seen from those instances in which the median point is reached that the curve proceeds past BP/GP=0.5

approximately linearly once BP/GP=0.25 is exceeded. As such some fibres will have an extrapolated median pore size. This method is only considered when the last measured value of BP/GP exceeds 0.25.

The effects of the different conditions must therefore be assessed on the basis of the maximum pore diameter data and inferences drawn based on the limited curves available. One of the fibres clearly displayed behaviour consistent with a pinhole in the structure, this was fibre 44 which enters the portion of graph shown with a BP/GP value higher than zero. However, the listed maximum pore size is based on the point at which the curve begins to increase from this value. This leaves the fibre sintered at the lower temperature, Fibre 15, as the fibre with the largest maximum pore diameter, this is to be expected as the driving force for closing the pore diameter during sintering is the tendency for material to move towards points of contact between particles from the bulk of the particle more rapidly at higher temperature. The next expected conclusion is that there is a smallest maximum pore diameter in the fibre which was sintered twice (fibre 54). This fibre has been exposed for longer to the higher temperatures which allow pore closure and accordingly has indeed a slightly smaller pore diameter. The remaining three fibres one would expect to have similar maximum pore diameters on the basis that they all were sintered on a ceramic support and under the same sintering program. There is close agreement in fibres 44 and 49 but fibre 28 is significantly larger in the maximum pore diameter. Reviewing the actual curve shape reveals that there is in fact no great rise in the value of BP/GP until the pore value reaches between 0.45 and 0.48 μm (see Figure 5.12).

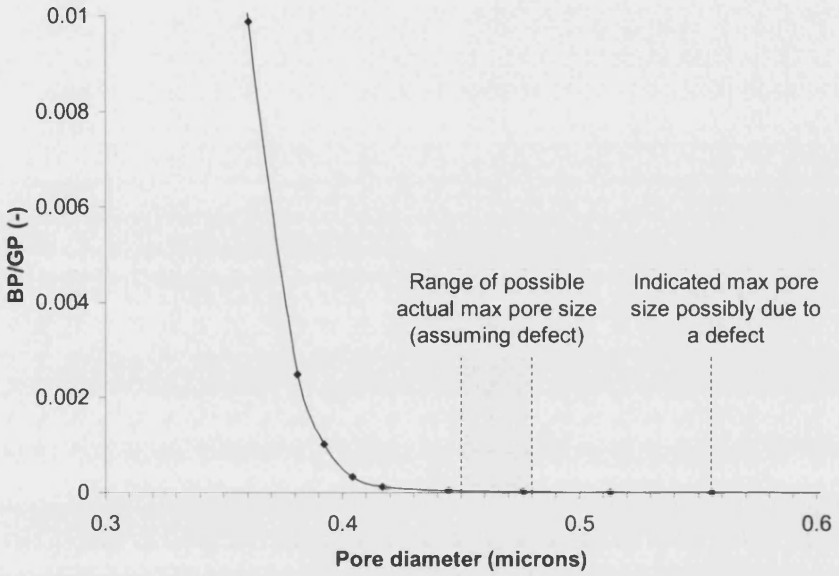

Figure 5.12 - Evidence of possible minor defect in fibre 28 (uncoated fibre prepared from solution 34 sintered once at at 1550°C)

This suggests that it is possible that the larger pore found is an isolated small pin hole or a defect and the normal resulting pore size is close to that of fibres 44 and 49. That said the shape and position of the curves for fibres 44 and 49 are quite close but that of fibre 28 is not so close indicating a slightly different structure. This can only be attributed to the hand straightening of the fibre carried out with fibres 44 and 49 but not with fibre 28, this may have disrupted some of the structure within the fibre resulting in a different curve shape. Intuitively disruption would cause the structure to become looser and hence the pore sizes slightly larger, this appears the likely case from the data for fibres 44 and 49 when looking at the pore distribution. The fact the apparent largest pore size of fibres 44, 49 and 28 remain close while the distribution is different could be due to the fact the largest pore size will always be a result of the loosest normal (non-defective) packing of the particles used (assuming fibre 28 is indeed displaying a small defect rather than an actual larger pore size).

Consistency of results based on BP/GP method

The method of BP/GP is largely used on one off samples given the time involved in the testing procedure. As such it is important to be confident in those results and confident that the fibres themselves are not widely variable along their length or from sample to sample. The following results show three fibres 32, 33 and 50. Fibres 32 and 33 were prepared in the same way while 50 was prepared in a very similar manner however when coating the fibre the fibre ends were sealed with putty and prior to first sintering the fibre was hand straightened. Two samples of fibre 32 were tested with ethanol as the wetting fluid, sample 33 was tested twice once with ethanol and once with 1-propanol, sample 50 was also tested with both fluids. Below is a summary of maximum and median pore size (Table 5.7) followed by the graphical results of the BP/GP test for the fibres (see Figure 5.13). In the following figures the letter in brackets following the fibre number indicates the wetting fluid used for the extended bubble point part of the characterisation. Where [e] is used this denotes ethanol, where [p] is used this denotes 1-propanol. The preparation details are as follows: all the fibres were prepared from base solution 34 (see Table 5.5 for composition details) the fibre was extrusion conditions are as detailed below Table 5.5. The applied coating was of the following composition: distilled water 95 wt%, aluminium oxide (0.01-0.02 μm particle size) 5 wt%. Fibres were dipped for 15 seconds.

Table 5.7 - BP/GP method integrity test comparing use of 1-propanol and ethanol as different wetting fluids on three different coated (coating 5wt% alumina in water) membranes prepared from spinning solution 34

Fibre	Wetting fluid	Max pore diameter (μm)	Median pore diameter (μm)
32 (sample 1)	Ethanol	0.535	0.245
32 (sample 2)	Ethanol	0.430	0.250
33	Ethanol	0.415	0.250
33	1-propanol	0.415	0.250
50	Ethanol	0.435	0.270*
50	1-propanol	0.420	0.270*

* by extrapolation

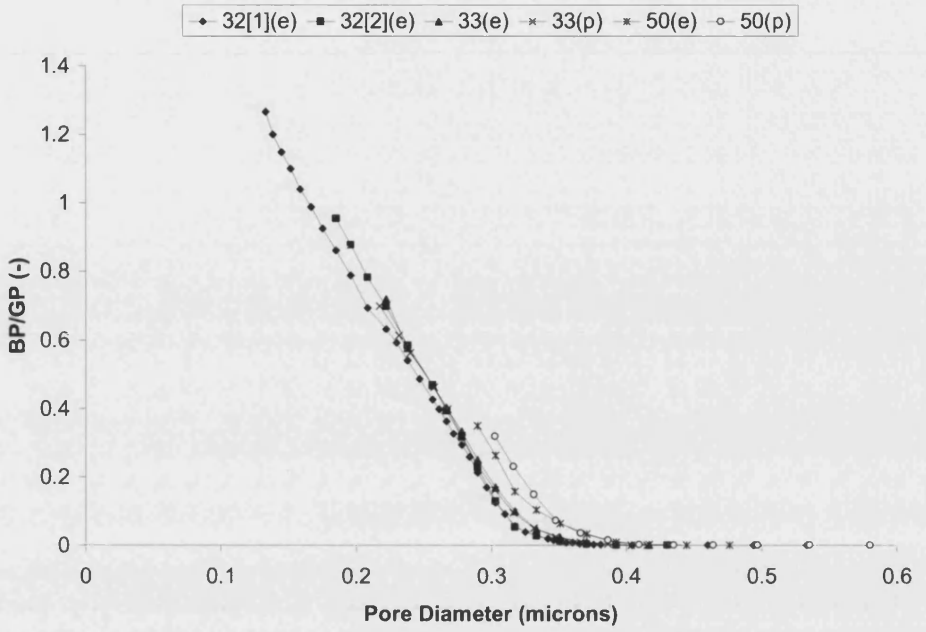

[e] ethanol is wetting fluid in BP test, [p] 1-propanol is wetting fluid in BP test

Figure 5.13 – BP/GP method integrity test comparing use of 1-propanol and ethanol as different wetting fluids on three different coated membranes prepared from spinning solution 34

The method shows excellent agreement in the pairs with regard to the sample median pore diameter. The agreement is good for fibre 50 and fibre 33 with regard to maximum pore size. However as we have seen with previous analysis there can be issues with maximum pore size analysis being distorted to larger sizes by defects. This is an issue for fibre 32 and is investigated below. The curve shapes also show excellent agreement between fibre 32 and fibre 33 suggesting consistency of manufacture, from fibre 32, both samples are very similar showing consistency in both manufacture and test method. The agreement between both tests on sample 33 shows that the switch to 1-propanol from ethanol does not drastically alter the results but the curves do become further apart as the curve proceeds to higher values of BP/GP. This was the desired effect of the switch to 1-propanol however the magnitude of the effect was not greatly significant. It can also be seen that the ethanol based results for fibre 32 show the flaw in the method first mentioned in section 4.3.3 and discussed in section 5.1.1, this is when the value of BP/GP exceeds a value of one due to evaporation of ethanol adding to the measured permeating volume. As discussed in section 5.1.1 a later alteration helped to correct this but gives rise to only

small changes in measured median pore size. The results for fibre 50 support the theory that hand straightened fibres suffer from loosening of their structure. This concurs with the results of fibres 49 and 44 vs. fibre 28 in the previous data set, the effect is not as great in this case as in the last this is due to the fact that a coating has been applied narrowing the pore distribution slightly.

Fibre 32 maximum pore size discrepancies

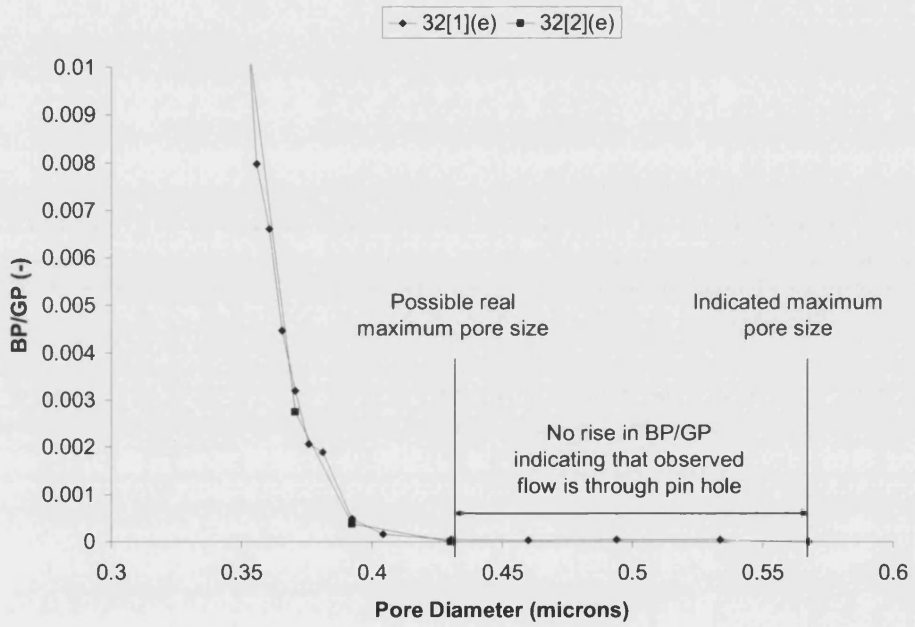

[e] ethanol is wetting fluid in BP test, [p] 1-propanol is wetting fluid in BP test

Figure 5.14 - Close analysis of apparent and real maximum pore size in Fibre 32 [1]

Looking at fibre 32 sample 1, it can be seen the apparent maximum pore size is 0.57 μm due to the observation of a low flow at this point. There is no increase in the value of BP/GP from this point until 0.43 μm. This brings the maximum pore size into line with the other fibres in this group.

Coating prior to sintering

In all the fibres encountered so far coatings have been applied by dip coating a sintered substrate fibre. A test to see if there was any merit in coating a non-sintered substrate was carried out, the expected conclusion being that there would not be any great difference made by coating a fibre before sintering as the polymer retained in the structure will prevent any significant application of ceramic material. As such the coated unsintered fibre should be similar in structure to an uncoated fibre. Given the expected limited coating ability of a water based dip coating solution an NMP solvent based solution was also used. This solution was expected to partially dissolve the surface of the fibre and as such immediately after coating the fibre was to be dipped in distilled water to quench the solvent action. Both dip coating solutions were 95 wt% liquid and 5 wt% aluminium oxide (0.01-0.02 μm particle size). Fibres were dipped for 15 seconds.

Table 5.8 – Details of preparation of fibres spun from solution 34 with regard to coating composition (NMP or water as solvent) and timing of coating (before or after first sintering)

Fibre	Median pore diameter (μm)	Maximum pore diameter (μm)	Coating solvent/water based, before/after sintering
28	0.245	(0.45-0.48)*	none
33	0.250	0.415	water/after
35	n/a	0.410	solvent/after
36	0.245	0.470	water/before
39	0.185	0.390	solvent/before

* based on analysis of possible pinhole, actual determined size 0.56 μm (see above)

Table 5.8 shows the BP/GP results for the fibres produced. The exceptional fibre is 39, discussing only the other results the maximum pore sizes achieved are smaller for the coatings applied after sintering and as expected the max pore size of the water based coating applied before sintering results in a similar fibre to the uncoated example. The median pore sizes remain largely unaffected. This shows that the coating is in effect narrowing the pore size distribution without moving the distribution to a lower size. This is a desirable effect as an open structure with pores in a range that allows contactor operation is desirable to allow maximum contact surface. Closing the pore size by a significant amount will reduce the direct physical contact area. Now attention is turned to fibre 39 in which there appears to be an effect

on median size and possibly a small effect on maximum size. Analysis of the curve that results allows shows no significant anomaly from the expected curve such as the flat line that is common with a pin hole. Lower than expected maximum pore size can sometimes occur due to experimental error in that the low flow is not observed initially so is first recorded at a higher pressure. This is usually apparent during the experimentation because the initial flow will be high (typical first observed flows are around 0.15-0.2 ml/min at the most for standard sample sizes). If abnormally high flow is observed initially the pressure is reduced and re-ramped to the point of onset of flow. The initial flow for this sample is very low at below 0.05 ml/min. This indicates a reasonably reliable result rather than an abnormally high flow which was missed during experimentation. The curve then continues in a classical 's' shape indicating no suspect result for median size. There is therefore the inference that the result is genuine and that using a solvent based coating prior to sintering can reduce pore size both maximum and particularly median. The effect is also desireable in this project in the event of difficulties in preventing gas breakthrough at the pore sizes used. There is however a problem with coating in this way, the fibre was nearly totally destroyed as the action of the solvent is so rapid, only barely enough fibre remained to perform the BP/GP test from an initial length of several centimetres. There was therefore a decision not to pursue this method as the fibres being obtained were in the pore range desired and the effect was minimal, in the event of dramatic pore size change being required other coating methods discussed in section 2.3.5 such as the sol-gel method could be used. It is noted that the damaging effect could have been limited by dilution of the solvent and this is suggested as worthy of some investigation in future studies.

Ceramic concentration in coatings

Once again fibres in this analysis are manufactured from Solution 34, the extrusion details can be found above. The variables in this analysis are the coating method and coating solution, one fibre has been coated with the same solution used in the above analysis (5 wt% solids in water) for 15 seconds. The other fibres were dipped in a solution with 10 wt% solids, for either 15 or 60 seconds. All solids in the coatings were aluminium oxide with particle size 0.01-0.02 μm. All fibres were subject to

straightening by hand prior to being sintered a first time. Maximum sintering temperature was 1550°C both before and after coating. The results are presented in Table 5.9 – Details of coated fibres spun from solution 34 with regard to solids content in the coating and duration of dip .

Table 5.9 – Details of coated fibres spun from solution 34 with regard to solids content in the coating and duration of dip coating

Fibre No.	Median pore diameter (μm)	Maximum pore diameter (μm)	Coating solids content (wt%)	Coating time (s)
50	0.270	0.420	5	15
51	0.270	0.420	10	15
52	0.270	0.410	10	60

There appears to be no significant effect of concentration of the coating or even the time for which samples are dipped. This would suggest that as concluded before for dip time, there is no significant effect on pore sizes and that in fact coatings of the type being applied merely plug defects and then crack and fall away from the fibre. It can be said that increasing the concentration of solids in the dip solution is similar to dipping for longer, there may be more deposited material but that material simply falls away unless it is trapped in macro-pores or pinholes.

5.1.3 Manufacture of aluminium oxide membrane (monolith support)

Owing to the ability of monoliths to provide much improved straightness in addition to a higher production rate a monolith support has been employed for all fibres manufactured in the remainder of the study. Flat ceramic supports have to date provided at best 10 small samples (3-4 cm) per sintering run or 5 larger samples (15-20 cm). Use of monoliths allows maximum length (30 cm) samples to be made the limit being determined not by the monolith but the size of the furnace. Monoliths also allow manufacture of in excess of 30 fibres per run depending on the monoliths used with as many as 70 possible in a single run. The monoliths used are discussed in section 4.1.6. The difference between straightness and potential length is demonstrated by the images in Figure 5.15. In both cases the fibres above the scale

are non-monolith supported fibres and below the scale are monolith supported fibres. The images are in inverted colour to improve contrast. The upper image demonstrates at a close range the curvature of non-monolith fibres, the lower image shows the length attained. Monolithic fibres demonstrating a typical 2-3 cm shrinkage from their initial length of 30 cm.

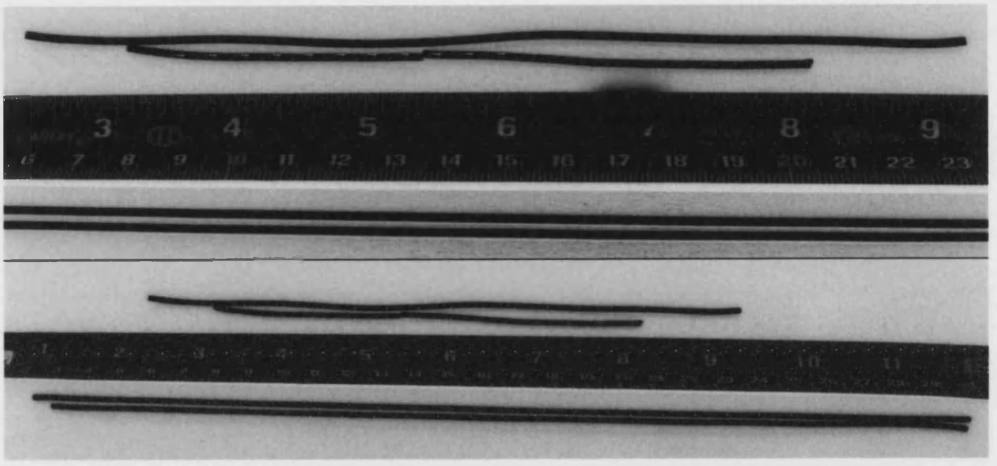

Figure 5.15 - Improvement of fibre straightness due to use of monolith as fibre support

In order to see if coatings could have a greater determination on pore size, i.e. to allow some easily managed flexibility in the max or median pore size it was decided to use a lower temperature for the pre-coating sinter step. This in theory leaves a more open structure with the aim being to allow better adhesion of the coating. It should penetrate further into the structure of the substrate, i.e. the solid material which up to now is retained at the outer surface unless encountering a pin-hole is given the opportunity to move into the structure providing an anchor for the coating on the surface. As has been seen however long dip time allows a substantial layer to build which is undesirable so dip times are reduced. The less sintered substrate should also allow better bonding of solids from the coating directly to the substrate as there is more sintering potential remaining in the substrate. The lower temperature will however leave weak substrate fibres which are susceptible to breakage.

Three different coating solutions have been used in the next section of results and to avoid repeating of their compositions they are presented in Table 5.10.

Table 5.10 – Composition of coatings associated with fibres from spun from solution 35 and 36

Coating No.	Water (wt%)	Ethanol (wt%)	Al_2O_3 [0.01-0.02 μm] (wt%)	Al_2O_3 [0.3 μm] (wt%)	PEG [m.w. 400] (wt%)
7	-	95.0	5.0	-	-
8	-	89.3	-	8.9	1.8
9	88.9	-	11.1	-	-

Ethanol was tried as a solvent to aid dispersion of the powder and poly ethylene glycol (PEG m.w. 400) was used to leave a polymer within the unsintered coating to help prevent cracking during drying and prior to sintering. The larger particle size alumina coating was employed as a basic coating that could minimise defects and standardise the fibre properties as has been shown to be possible. Following coating with this in some cases a low temperature sintering of gamma aluimna was tried as an alternative to previous methods.

Fibres from solution 35

Fibres in the next part of this study are based on solution 35 which was extruded under the following conditions: The water baths were at 14 °C, the extrusion pressure was 0.8 bar owing to the relatively low viscosity the intended pressure of 2 bar was too high. The air gap was set at 60 mm. The composition of the solution is shown in Table 5.11.

Table 5.11 - Solution 35 composition

Component	wt% in Solution 35
NMP	33.27
PES	8.32
Al_2O_3 (1 μm)	50.08
Al_2O_3 (0.3 μm)	-
Al_2O_3 (0.01-0.02 μm)	-
PEG (mw 400)	8.34

Structure of uncoated fibres based on solution 35

The uncoated structure will demonstrate the basic structure of the fibre given similar sintering conditions. However the final sintering step used for fibres from solution 35 ranged in temperature from 700 to 1500 °C. As such there is no ideal combination of sintering conditions to demonstrate the uncoated fibre properties. All the fibres were sintered first at 1300 °C, two uncoated fibres sintered at this temperature are tested and in addition one fibre sintered at 1300 °C and then sintered again at 1475 °C is tested, many fibres were sintered at this temperature and some were sintered at 1500 °C as an intermediate if not final step. No fibres were tested uncoated with three sintering runs though it is noted several coated fibres were subject to three runs. The data for the uncoated fibres is presented in Table 5.12.

Table 5.12 – Preparation details and pore size data for uncoated fibres from solution 35

Fibre No.	Median pore diameter (μm)	Maximum pore diameter (μm)	1st sintering run max. temperature (°C)	2nd sintering max. temperature (°C)
91	0.255	0.535	1300	1475
132	n/a*	0.500	1300	-
137	0.250**	0.605	1300	-

* insufficient data for extrapolation, **extrapolated from BP/GP method data exceeding 0.28

The maximum pore sizes observed are quite variable, but analysis of the permeation data around the max pore size point shows that the data appears to be genuine pores rather than pin-holes (as was the case of fibres 91 and 137).

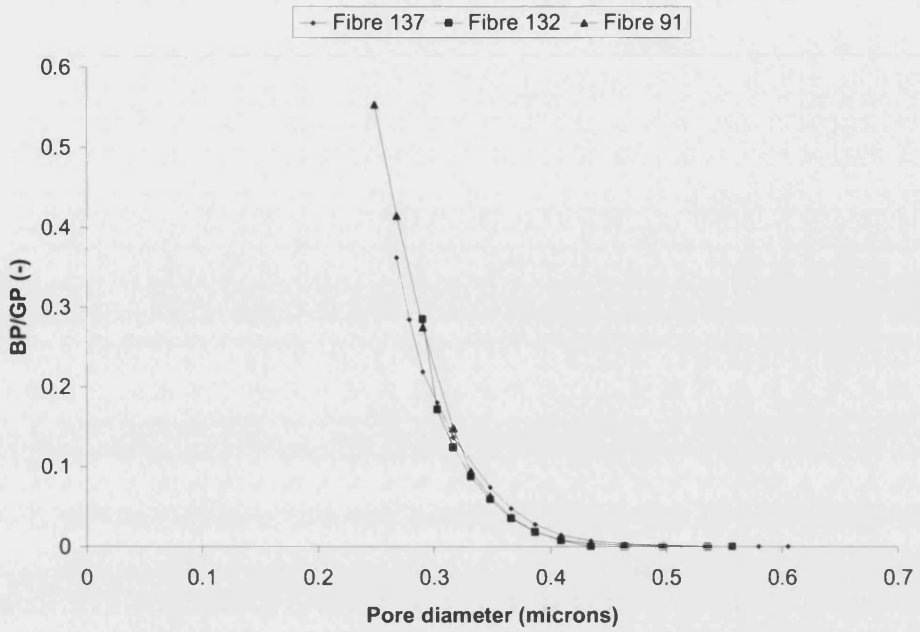

Figure 5.16 – BP/GP analysis for uncoated fibres based on solution 35 (for preparation details see Table 5.12)

There is however evidence to suggest that the pores are few compared to the overall pore distribution as can be seen from Figure 5.16 which shows the BP/GP data for the three fibres. There are several data points at pore sizes higher than 0.5 μm which remain close to a BP/GP value of zero. The curves only really break away from the x-axis below a pore size of 0.5 μm. As stated the analysis of the near zero points does indicate genuine pores as the value of BP/GP is in fact increasing between data points (as one moves toward a smaller pore size). On previous curves where pin-holes were identified the value of BP/GP was static in these flat regions.

In summary an uncoated fibre from solution 35 has a median pore size of around 0.25-0.26 μm. The maximum pore size though variable could be said to potentially be 0.45-0.50 μm, provided that a range of larger pores that are present in significant numbers can be plugged.

Coated fibres from solution 35

The aims of applying a coating to the fibres is to plug the pores that are few or even single pores but that are larger than the normal maximum size formed by the convergence of particles from the main spinning solution. A wide range of conditions were tried using the coatings shown in Table 5.10 with a range of sintering temperatures. The BP/GP curves have been analysed in such a way as to give three values for maximum pore size. The first shows the actual measured maximum, the second gives the maximum pore size with presumed pin-holes excluded and the third shows pore size that could be potentially achieved with effective blocking of a selection of larger pores or elimination of their formation. There is no conclusive result from the tests that one way of coating is better than another but by volume of results we can see that if one coating is applied there is less blocking of large pores or pin-holes than if two or more coatings are applied. This is to be expected.

It is also shown that pores are more effectively blocked by coatings based on a smaller particle size. Table 5.13 shows the data and the fibres have been ordered on the basis of maximum pore size excluding pin-holes running from largest to smallest. The parameters a,b,c and med indicate actual maximum observed pore diameter (a), maximum size excluding pin-holes (b), smallest maximum pore size which could be attained with effective coating (c) and median pore diameter (med). The sintering and coating data indicates the temperature of sintering and the number of the coating applied prior to the sintering treatment if a coating was applied – these numbers are appropriate to the coatings shown in Table 5.10.

Table 5.13 – Pore size data and coating details for fibres spun from solution 35

Fibre	Pore diameters (μm)				Sintering temp/coating data			
No.	a	b	c	med.	1st	2nd	3rd	4th
137	0.65	0.65	0.465	0.25*	1300	-	-	-
94	0.63	0.63	0.63	0.31	1300	1500/8	-	-
97	0.63	0.63	0.53	0.29	1300	1500/8	700/7	-
130	0.63	0.63	0.58	0.29	1300	1500/8	-	-
95	0.555	0.555	0.495	0.29	1300	1500/8	-	-
132	0.555	0.555	0.435	n/a	1300	-	-	-
87	0.55	0.55	0.495	n/a	1300	1475/7	-	-
133	0.55	0.55	0.465	n/a	1300	950/7	-	-
91	0.535	0.535	0.495	0.255	1300	1475	-	-
100	0.535	0.535	0.41	n/a	1300	700/7	-	-
110	0.535	0.535	0.465	0.25	1300	1500/8	1500/7	950/7
111	0.515	0.515	0.435	0.255	1300	1500/8	950/7	-
140_a	0.48	0.48	0.435	0.23*	1300	950/7	-	-
121	0.465	0.465	0.465	0.155	1300	1500/8	850/9	-
140_b	0.465	0.465	0.41	0.24	1300	950/7	-	-

As stated the fibres with more coatings and fibres made with coating 7 and 9 which used the smallest size particle are clustered toward the bottom of the table where the maximum pore diameters are the smallest. It is noted that the effect of number of coatings is proved by the fact that fibres coated once by coating 8 come before those coated once by coating 7 which in turn come before those coated once by coating 8 and then again by coating 7 or 9. There are two exceptions to this trend fibre 140 (samples a and b) and fibre 97. These could be explained by what appears to be some variability in the quality of the substrate fibre possibly due to poor mixing in the extrusion solution. This is shown by the flat regions in the BP/GP curves where there are few pores but clearly not isolated pin-holes.

As more coatings are applied the max size and max potential size become closer showing the coating effect but also showing that in this case one coating was leaving

some pores still in this region was not apparent with previous fibres so must be due to the substrate fibre. However the large maximum pore size associated with fibre 97 could also be due to low sintering temperature of the coating. The temperature used for the sintering of the small particle coatings does not appear to be greatly significant. This is probably due to the coating not being well enough dispersed in solution to create a very small pore size that would result from a true sol-gel coating sintered at low temperature. The higher temperature sintering of this material destroys the fine gamma structure but as the particles were not ultra finely dispersed there would have been agglomerated lumps behaving like particles of a size only slightly smaller than 0.3 μm hence the slightly more successful effect of coatings based on these particles than the coating (coating 8) based on the larger alpha alumina particles.

Fibres from solution 36

Prior to preparing fibres for use in modules a final group of fibres were made from solution 36 the composition is shown in Table 5.14.

Table 5.14 - Solution 36 composition

Component	wt% in Solution 36
NMP	36.63
PES	5.63
Al_2O_3 (1 μm)	37.32
Al_2O_3 (0.3 μm)	16.19
Al_2O_3 (0.01-0.02 μm)	2.82
PEG (mw 400)	1.41

The solution was extruded under the following conditions: extrusion pressure, 1.9 bar, water baths all at a temperature of 13 °C and the air gap was 50 mm. The fibres prepared were subject to a 1300°C sintering step and were then subject to combinations of sintering and coating using coatings 8 and 9 (see Table 5.10) one fibre (fibre 157) was also further coated with a polymer/solvent mixture to protect the ceramic coating. The results are graphically presented below in Figure 5.17 and numerically as Table 5.15.

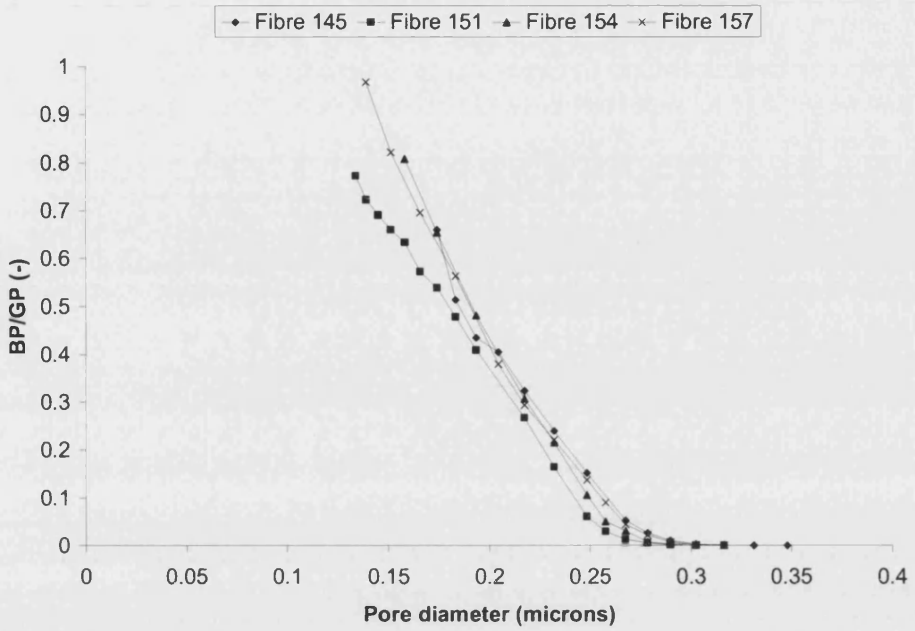

Figure 5.17 – BP/GP data for fibres from solution 36 various coated/uncoated fibres al sintered at a maximum temperature of 1500°C (for sintering and coating order refer to Table 5.15 for composition of coating solutions see Table 5.10)

The graphical representation shows the fibres have similar bulk structures whilst the numerical analysis of the maximum pore diameter is shown to be marginally reduced as more coating is applied thus once again the desired effect of minimisation of maximum pore size and limitation of defects. The uncoated fibre for example has a small range of larger pores as was displayed by fibres based on solution 35. As with fibres from solution 35 the pores are genuine and not a single pin-hole. It would appear based on the results of fibres 151,154 and 157 that this range of pores is closed by coating.

Table 5.15 – Pore size data, sintering details and coating selection for fibres from solution 36

Fibre No.	Maximum pore diameter (μm)	Median pore diameter (μm)	Sintering 1	Sintering 2 / coating 2	Sintering 3 / coating 2
145	0.350	0.185	1350	1500	-
151	0.315	0.180	1350	1500/8	-
154	0.315	0.190	1350	1500/8	850/9
157	0.305	0.190	1350	1500/8	850/9+pol.

Note fibre 157 was coated with polymer solution immediately after coating in solution 9.

5.1.4 Further developments in coatings

One further major development in coating was used but due to time constraints the effects were not extensively studied. The development was to add some Polyvinyl alcohol (PVA) to coatings this allowed drying prior to loading the fibres into the monolith supports without risk of loosing the delicate coating on insertion. No especially detailed study of this was carried out but the resulting pore diameters both maximum and median were not untypical of previously prepared fibres i.e. no adverse effect due the PVA was seen. Most significantly the coatings were not cracked. Figure 5.18 shows the lack of cracking strikingly as the boundary between the coated part of the fibre and the uncoated part of the fibre can be clearly seen. The surface of the coated region and the uncoated region is also shown close up to demonstrate the similarity in open pore size.

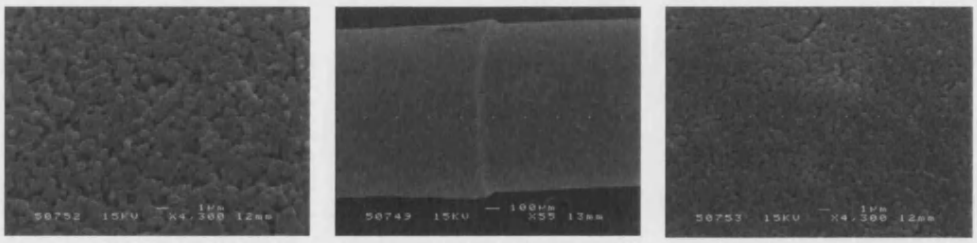

Coating surface Boundary of coating uncoated surface

Figure 5.18 – SEM images showing how PVA coating prevents cracking

5.1.5 Overview of membrane preparation.

Throughout all preparation of membranes there has appeared to be a characteristic maximum and median pore diameter based on the substrate fibre, coatings can then refine the structure eliminating defects and unusually large pores hence narrowing the pore size distribution. A quick summary of these characteristic sizes shows that as one would expect a higher concentration of particles and a higher concentration of the smallest particle types leads to smaller characteristic pore sizes. The expected packing of particles in the ceramic structure based on the particles used suggest that the particles are well packed in the final fibres. There are few serious defects and the defects that do exist are minimised by coating. It is noted that by experience the number of defects is still significant enough to potentially cause difficulty in building defect free modules where 15-30 fibres all defect free will be required.

5.2 Mass transfer in membrane modules

Modules were assembled from ceramic fibres. In total 9 modules were made and of them eight were used with one being damaged prior to use. Of the eight used three were quickly discarded owing to defects in one or more of the fibres within the module. A summary of the modules used is presented below. Table 5.16 refers to spinning solutions that were not detailed in the membrane characterisation section, details can be found in Appendix II.

Table 5.16 – Details of ceramic modules prepared, all fibres were sintered at 1350°C prior to second sintering at 1500°C (coatings where applicable were applied between sinterings dip times were 5s)

Module No	Spinning Soln No.	Coating Soln	details
1	various	none	start up module used often but for testing of system module was shorter than all other units. Was made with spare fibres from fibre characterisation work due to furnace being out of order for a period at the time.
2	36	uncoated	30 fibres used extensively with water
3	36	uncoated	module leaked immediately (29 fibres)
4	36	uncoated	damaged when cleaning by pressurising on the tube side after being blocked by glass solution (30 fibres)
5	36	uncoated	module damaged before use (15 fibres)
6	40	uncoated	module leaked immediately (15 fibres)
7	40	PVA based coating	blocked in early runs successfully cleaned then used to an extent with water (15 fibres)
8	41	PVA based coating	blocked in early runs cleaned and then used rarely (leaked at higher gas pressures) 15 fibres
9	41	PVA based coating	blocked after few runs leaked after cleaning (possibly through potting material) 15 fibres

5.2.1 Mass transfer results in ceramic modules

Stripping of oxygen from pure water

Initial experiments in the ceramic modules prepared were based on stripping of oxygen using argon with a one litre capacity tank as the main tank in a batch recycle

system. The dissolved oxygen content was measured directly in the tank which was agitated by magnetic stirring.

As outlined in section 3.1.1, C_T (tank concentration) is measured and the main details that must be extracted from the experimental data include: The exit concentration from the module, C_e, The main tank concentration and the rate of oxygen stripping, r, at a given point in the experiment. Determination of r is by fitting the experimental data to an exponential decay curve to find dC/dt and then using equation **5.1**. The concentration in the tank in an ideal situation follows this decay. There are small deviations in the actual experimental data as one would expect, this is due in part to the fact that there is a lag before the trend is established due to there being a time where the concentration gradients throughout the system are being established. There is also potential for some ingress of oxygen to the system from the atmosphere which can result in the main tank concentration being unable to reach an asymptote with zero but instead finding an asymptote at the point where the DO removal performance is matched by the ingress of oxygen. However as stated above for the purposes of modelling the process the system is assumed to be a perfect exponential decay. C_e is calculated from the following equation (5.2) as described in section 3.1.1.

$$r = \left(\frac{V_m + V_T}{V_m}\right)\frac{dC_T}{dt} \qquad \textbf{5.1}$$

$$C_T - C_e = -\frac{V_m}{Q}\left(\frac{V_T}{V_m - V_T}\right)r \qquad \textbf{5.2}$$

The prepared module used in the water tests was constructed by a random packing method and consisted of 30 fibres, at a length of 185 mm fibre ID was 678 μm, the fibre OD was 1.092 μm. The membrane area based on internal diameter is 0.0118 m^2.

In the experiments liquid flow rate, pressure and gas flow rate were varied.

Example of determination of the mass transfer coefficient

An individual result desorption of oxygen from water in a ceramic module (gas pressure 1 barg and liquid rate 250ml/min) is shown in Figure 5.19 below as an example of the handling of this data and its processing to the point of extracting the required information subsequent results will be shown in final form only.

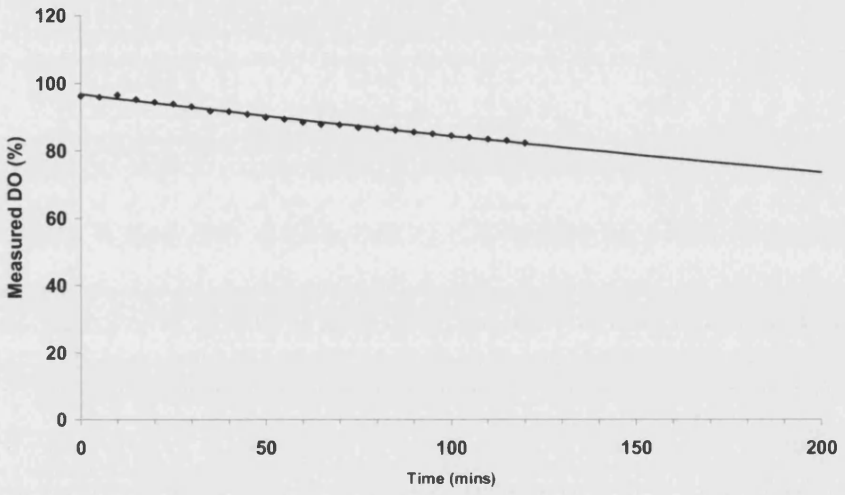

Figure 5.19 – Typical desorption of oxygen from water in ceramic module 2 at ambient conditions (example data set for example calculation)

Figure 5.19 shows the concentration of oxygen in the recycle tank as a function of time. When this concentration is normalised to a maximum value of 1 (by C/C_0) and plotted on a semi-logarithmic graph the result is Figure 5.20. Fitting to the data we obtain an equation of the decay and hence a value of dc/dt.

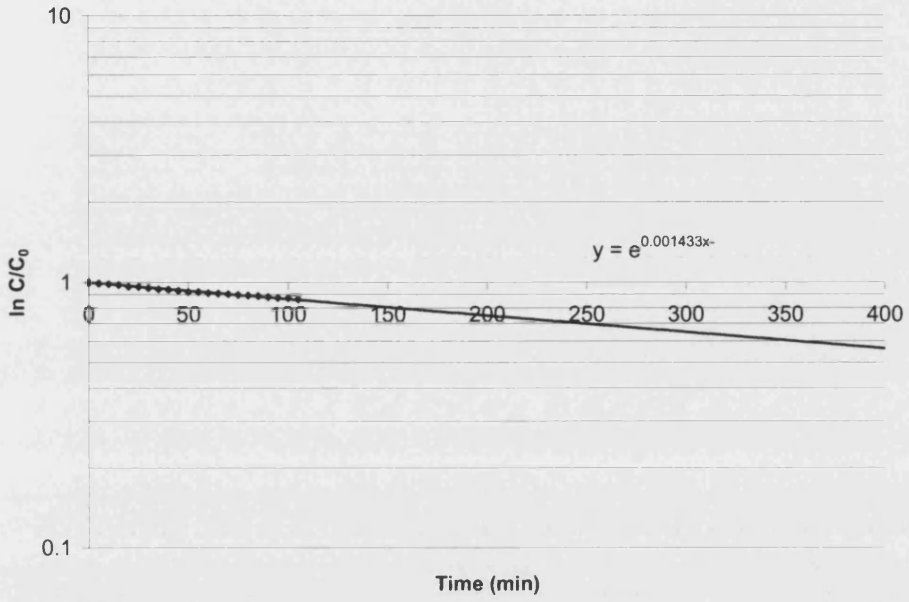

Figure 5.20 - Log plot of example data

The value of $d(C/C_0)/dt$ has the units min^{-1} as read from the graph, this is converted to units of s^{-1} which allows calculation of r and hence C_e. From this we can calculate the overall mass transfer coefficient K_l by use of equation **5.3** (for derivation see chapter 2).

$$K_L a = \frac{V_L}{A_c h(1-y)} \ln \frac{C_0 - \frac{y}{1-y} C_e}{C_e - \frac{y}{1-y} C_e} \qquad \textbf{5.3}$$

Where: $y = \frac{Q_L RT}{Q_G H}$ **5.4**

Module 2 results:

Module 2 was the only extensively tested membrane in which water was used owing to frequent damage to other ceramic modules when tested with glass coating solutions.

Varied liquid rate at constant gas rate and pressure

The following results show the effect of varying the rate at which liquid is put through the shell side of the module while maintaining a constant gas side feed pressure and mass flow rate of gas. One would expect that if there is a strong liquid (shell side) mass transfer resistance then the higher the flow rate of liquid the higher the rate of mass transfer [5, 7].

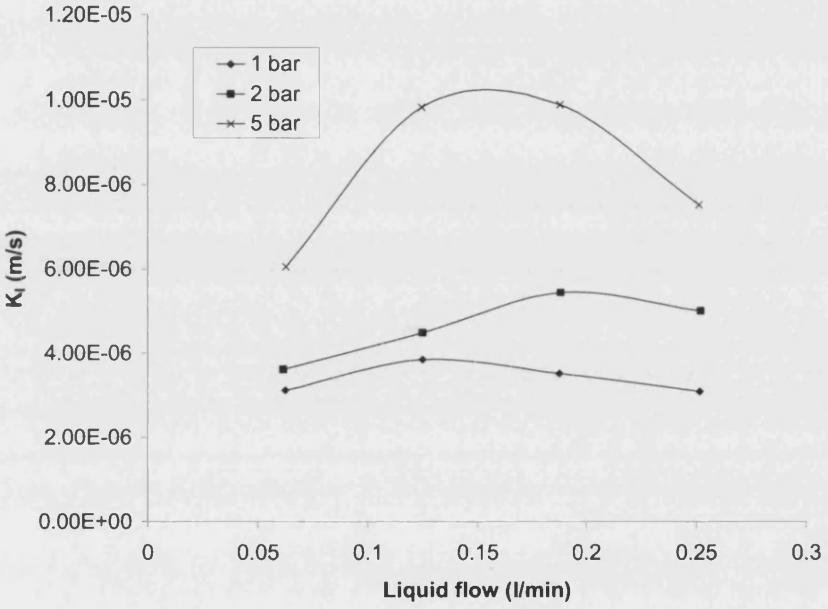

Figure 5.21 - Mass transfer coefficient for varied liquid flow at three different gas side pressures [module 2, gas rate 4.2 g/min, ambient conditions]

It appears from the results shown in Figure 5.21 that there is an optimum liquid flow rate at some point on each of the three curves. However due to the method used to vary flow rate there is a rise in liquid side pressure which was unavoidable. The rig used for these experiments did not have the facility to measure this effect accurately and hence it is proposed that the drop in measured K_l seen at the higher flow rates is attributed to a real terms lowering of trans-membrane pressure. It should be noted that the pressures listed refer to measured gas side outlet pressure rather than trans-membrane pressure. The reason why the mass transfer coefficient would drop with a lower trans-membrane pressure is believed to be due to there being a shift in the

gas/liquid interface location within the membrane wall. The magnitude of the mass transfer coefficient is lower than for literature values of polymeric modules where 1-6 $\times 10^{-5}$ is the norm [5, 18].

In order to study the location of the gas liquid interface data from a negligible gas side pressure run is used to define the value of ε_m/τ_m for the module. This is carried out by assuming the whole membrane wall is liquid filled and then adjusting the value of porosity and tortuosity so as to make the correlation based determination of the mass transfer coefficient equal to the experimentally determined one. The value of ε_m/τ_m is then maintained for all other predictions of mass transfer coefficient. The interface location is altered in the membrane mass transfer coefficient calculation so as to fit the calculated overall mass transfer coefficient with the experimentally determined one. The results are presented below with the interfacial location being given by the value, x, which is the fractional location of the interface within the wall, i.e. at x = 0, liquid fills the membrane and at x = 1, gas fills the membrane (i.e for the gas filled part of the membrane δ_{fl} = wall thickness × x and for the liquid filled region δ_{fl} = wall thickness × [1-x]). The value of ε_m/τ_m was determined as 0.341. A typical value for polymeric membranes may be 0.14 (based on a porosity of 0.35 and a tortuosity of 2.5[3]). With the assumption that a ceramic membrane will be less porous to the extent that parts of a polymeric membrane that would be solid will in a ceramic membrane be constructed from a compact of particles it is not unreasonable to propose a porosity of 0.6-0.7, the more open porosity would also lessen the tortuosity so a value between 1.5 and 2.5 could be reasonable. Values in these ranges allow a value of 0.341 for ε_m/τ_m. The correlation used for the determination of the mass transfer coefficient in the shell side of the module is shows as equation 5.5. For tube side and membrane coefficients the equations described in section 3.1.1 are summarised below:

$$Sh = 1.25\left(\mathrm{Re}\frac{d_e}{l}\right)^{0.93} Sc^{0.33} \qquad \textbf{5.5}$$

$$Sh_{average} = 1.615\left(\frac{d_t}{L}\right)^{1/3} (\mathrm{Re}\cdot Sc)^{1/3} \qquad \textbf{5.6}$$

$$k_m = D_e \varepsilon_m / (\tau_m \delta_{fl}) \qquad 5.7$$

The individual coefficients are combined by 5.8

$$\frac{1}{K_l} = \frac{1}{k_g H_i} + \frac{1}{k_{mg} H_i} + \frac{1}{k_{ml}} + \frac{1}{k_l} \qquad 5.8$$

Where:

K_l = overall mass transfer coefficient based on liquid (m/s)

k_g = mass transfer coefficient through gas side boundary layer (m/s)

H_i = Henry law constant in dimensionless form (-)

k_{mg} = mass transfer coefficient through gas filled portion of membrane (m/s)

k_{ml} = mass transfer coefficient through liquid filled portion of membrane (m/s)

k_l = mass transfer coefficient through gas side boundary layer (m/s)

The interfacial location for the data in Figure 5.21:

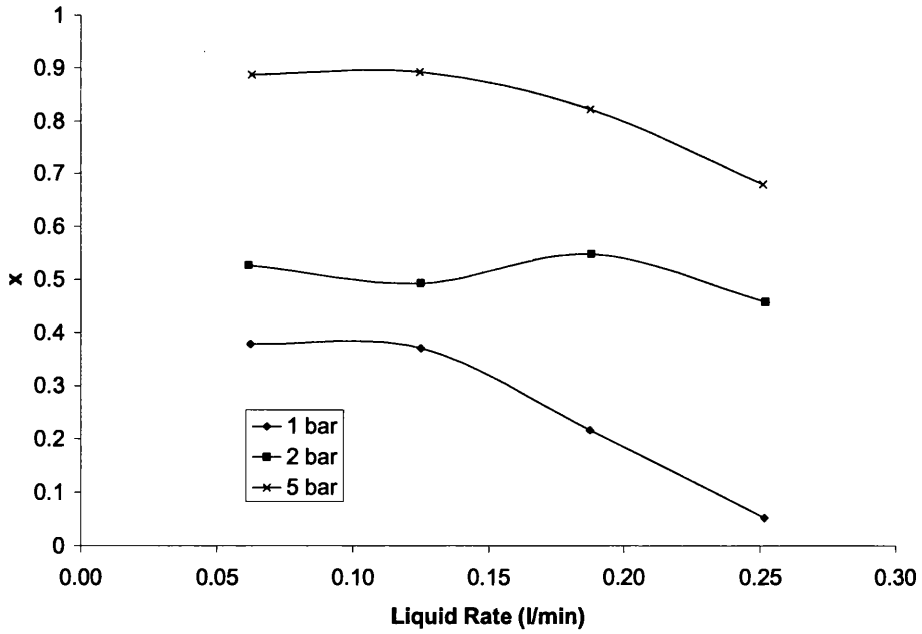

Figure 5.22 - Interfacial location vs liquid rate (module 2, desorption of oxygen from water)

The effect on interfacial position is shown by Figure 5.22. This shows that at higher pressures there is a shift in location of the interface towards the outside of the

membrane. The expected move of interfacial location towards the inner diameter as flow-rate increases is also observed. The fact that the interfacial location for the 1 bar tests moves to near the x = 0 point suggests that the pressure from the liquid side is around 1 bar and further analysis of the varied pressure data (see next section) shows that at a maximum pump flow rate the interface moves very little at a gas side pressure of 0.5 bar hence it is assumed that the pressure on the liquid side is between 0.5 and 1 bar with a likely case being nearer 0.5 bar given the movement of the interface at this pressure. For all experiments the rate of gas used was 4.2g/min, i.e. at higher pressures the volumetric rate was lower.

Varied gas side pressure with constant mass based gas rate and liquid flow

Variation of gas side pressure has been identified as possible means to increase the mass transfer capabilities of these membrane types by movement of the gas liquid interface. Figure 5.23 shows how this can work.

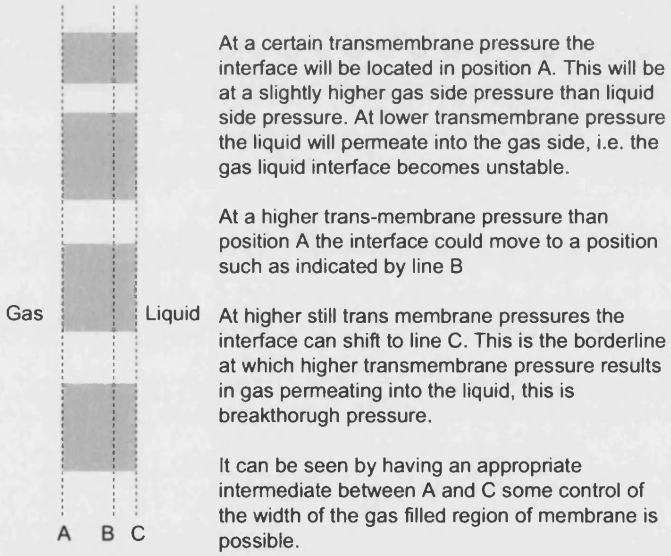

Figure 5.23 – Effect of trans membrane pressure on interfacial location

A study of gas side pressure effect is shown by Figure 5.24 and Figure 5.25.

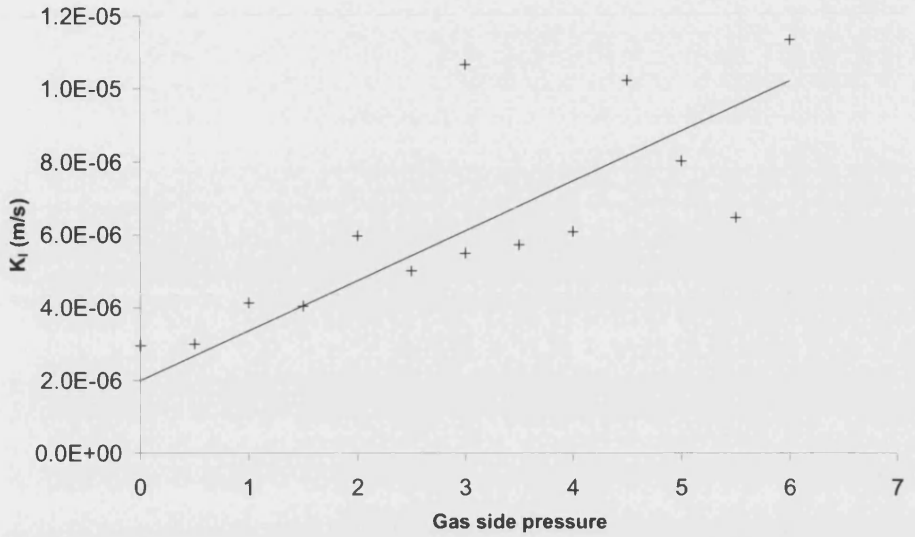

Figure 5.24 - K_l vs Gas side pressure (barg) [ceramic module 2, liquid rate fixed at 50ml/min, ambient temperature, desorption of oxygen from water]

The overall mass transfer coefficient is increased by raising gas side pressure, from a value of around 3×10^{-6} m/s to around 1.1×10^{-5} m/s. The oxygen removal per pass is up to a maximum of 3% at 6 bar gas side pressure, a typical value is 1.5 to 1.7% at pressures of 3-4 bar. The mass transfer itself is not influenced by the pressure the effect is purely a result of the movement of the interface. The effect of pressure on the interface is shown below in Figure 5.25. The data point from which the predicted interface position is based is that shown as point 0,0 in the chart. The gas side pressure was minimised to a level which the system gauges did not register, this combined with the liquid side pressure discussed in the previous section resulted in a small leakage of liquid into the gas side during this run (liquid breakthrough). The data point at 0.5 bar shows little movement in interfacial position and hence it is assumed the liquid side pressure is approximately balanced by the gas pressure at this point. The significant step at 1 bar suggests that there is significant trans-membrane pressure pushing from the gas side by this point. It is noted that one significant data point lies well out of the observed trend, this data point is one of two taken at 3 bar. It is believed that there may have been a probe error during this run. The data is subject to fluctuation at the higher pressures which could be attributed to small occasional break through of gas into the liquid side. While no significant leakage was observed it

casts some doubt over the extent to which the interface can be successfully moved without entrainment of gas in the liquid. The expected bubble point of water based on the 1-propanol BP/GP test is 9.95 bar owing to the significantly higher surface tension of water. The applied pressure if 6 bar was significantly lower but as the fibres were uncoated and that testing of each individual fibre for pinholes is not practical it is likely that there may have been a pin hole on one of the fibres. An basic bubble point test to see the point of gas intrusion to the liquid was carried out by 'dead-ending' the gas side and raising the gas pressure as in a normal bubble point test. Water was not pumped. Significant bubbling (gas breakthrough) began to be observed in the range 5-6 bar and hence results in this range are treated with caution. Even so it is reasonable to suggest that it is possible to drive a water interface to a mean position corresponding to x = 0.5-0.6, with potential for movement to a position of 0.8-0.85.

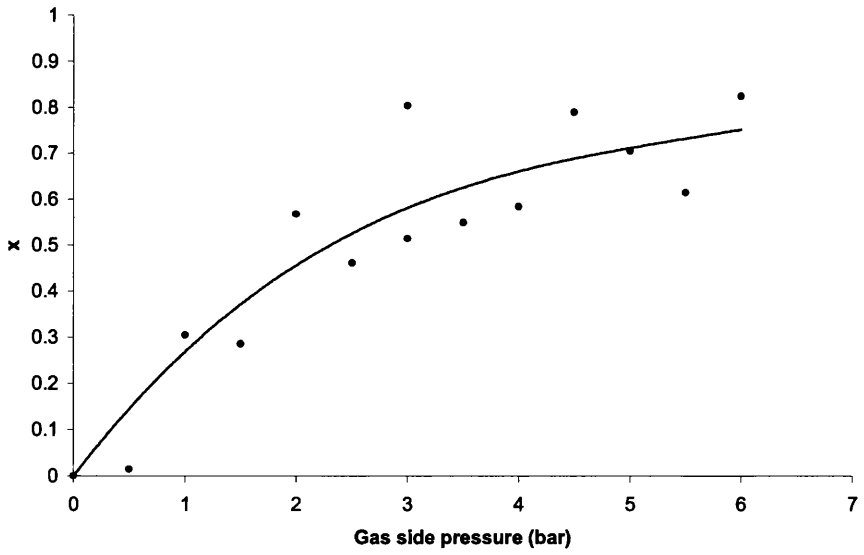

Figure 5.25 – Effect of Gas side pressure on interfacial location [module 2, liquid rate 50ml/min, ambient temperature, desorption of oxygen from water]

An analysis of the contribution of each mass transfer coefficient shows that the liquid based coefficients dominate as one would expect. The following figures show mass transfer resistance ($1/k$), where k is the individual mass transfer coefficient for each of the four mass transfer regions. These are shell side (MTC shell), liquid wetted

membrane (MTC ml), gas filled membrane (MTC mg) and tube side (MTC tube). Figure 5.26 would show the contribution of each of the 4 mass transfer resistances but the tube resistance and gas filled membrane resistance are too small to be seen. Hence Figure 5.27 focuses on the contribution of just the gas based coefficients. It can be seen that the overall mass transfer coefficient is still dominated by the liquid filled portion of the membrane even when the interface is moved to the region of x = 0.8. Though at least at this stage the contribution is just over half of the total mass transfer resistance as opposed to approximately seven eighths of the resistance when no gas side pressure is applied. Throughout these experiments the gas rate was 4.2 g/min once again. Liquid flow was 0.25 l/min

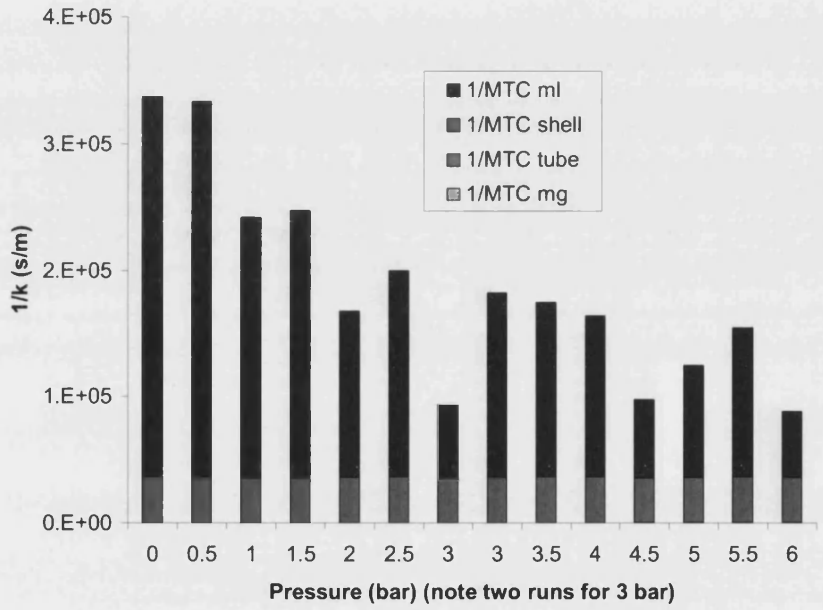

Figure 5.26 - Overall contribution of individual mass transfer coefficients (at various gas side pressures for the desorption of oxygen from water using module 2 at ambient temperature with liquid flow at 50ml/min)

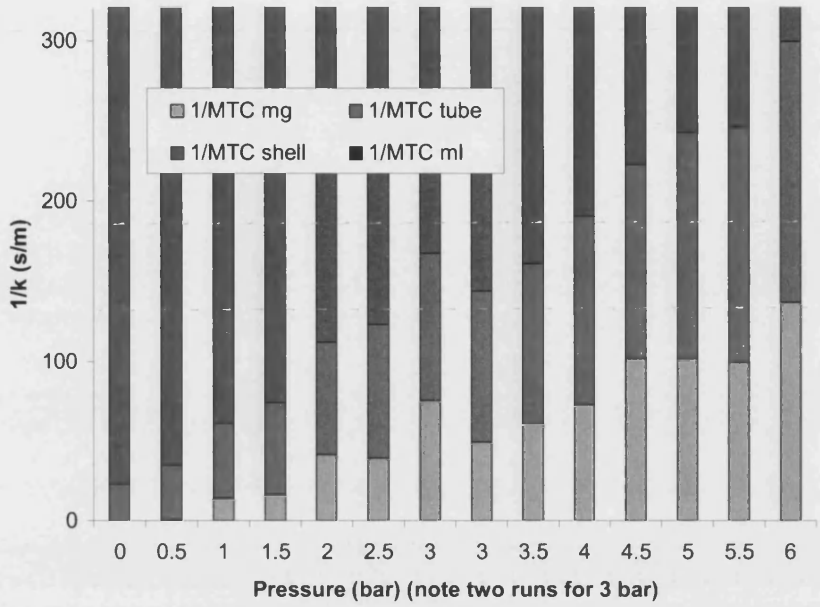

Figure 5.27 - Focus on contribution of gas based mass transfer coefficients (conditions as for Figure 5.26)

Varied gas rate with constant liquid flow and gas side pressure

Based on the individual contributions of mass transfer regions analysed in the above section it is expected that any variation of the gas flow with pressure maintained at a constant value should in theory result in very little effect upon the mass transfer results. This is because the resistance to mass transfer in the liquid mass transfer regions is far higher than in the gas based regions. Varying the gas rate will only influence the tube side coefficient which is gas based.

Figure 5.28 shows that there is no variation as expected. Experiments were conducted at 2 bar gas side pressure and a liquid flow of 0.25 l/min.

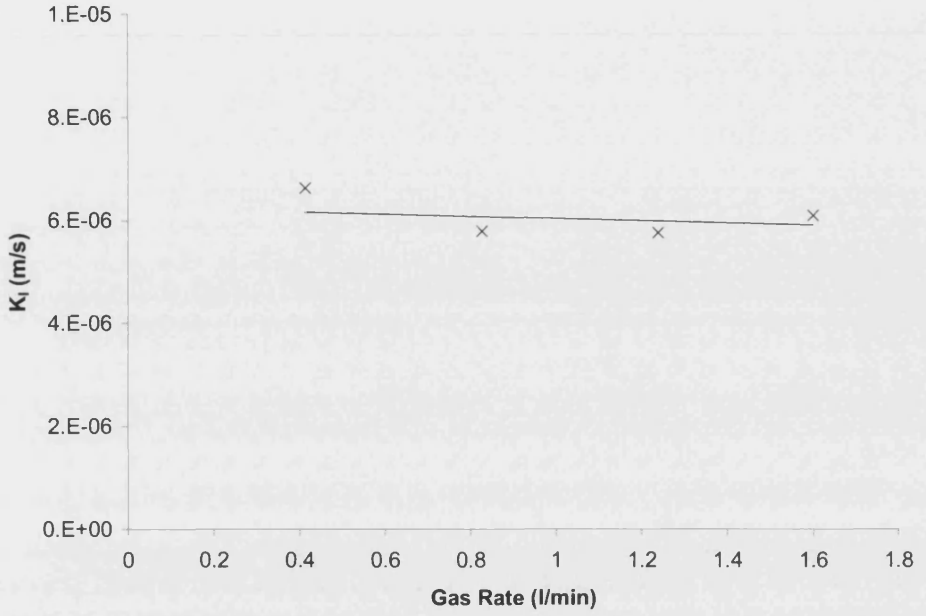

Figure 5.28 - K_l vs gas side flow rate [desorption of oxygen from water at ambient temperature in module 2, liquid rate = 50ml/min]

Other modules

Further Modules were prepared though several were used with glass solution before testing with water and this resulted in unexpected damage to the modules (see subsequent section). Module 7 had several water test results at varied pressures these results are shown below in Figure 5.29 and Figure 5.30.

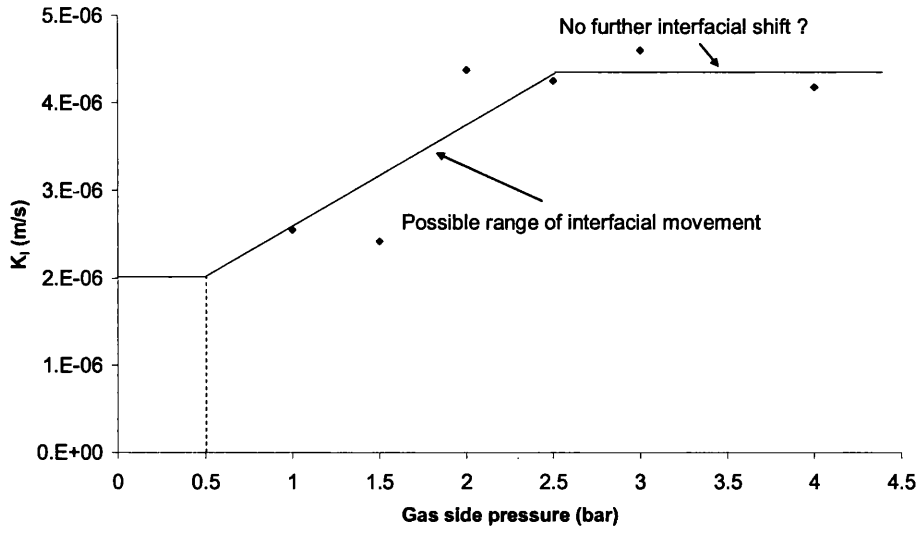

Figure 5.29 - K_l vs Gas side pressure for ordered packing module [desorption of oxygen from water at ambient temperature, liquid rate = 200ml/min)

Figure 5.29 shows the mass transfer coefficient data with some lines added for a proposed analysis of the data this line is based on the expected continuous shift of the interface until a certain point in the membrane. The data is too scattered to make a confident analysis of the results but between 1 bar and 2.5 bar there is clearly a rise in mass transfer it is proposed that there is no further interfacial movement beyond this pressure. If one assumes an approximately linear relationship drawn between the data points giving the least dramatic effect on mass transfer and one extrapolates back to 0.5 bar to give the mass transfer minimum (assuming this to be approximately the point of zero trans-membrane pressure due to the unmeasured liquid pressure). We can then perform an interfacial location fitting following the basis used for the random packed module above.

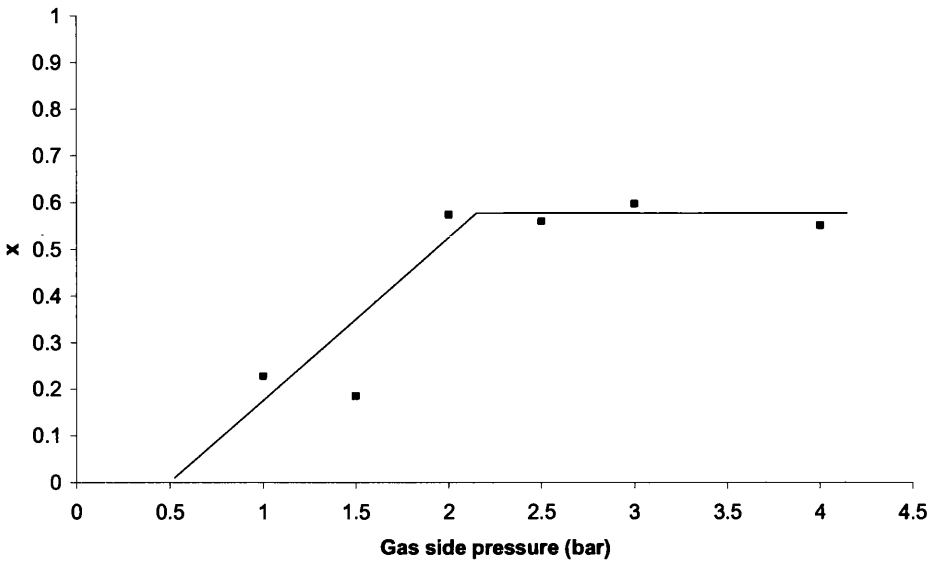

Figure 5.30 - Interfacial location vs pressure for ordered packing module (experimental conditions as for Figure 5.29)

The result of this is shown in Figure 5.30. Note a predicted point at zero pressure is included to represent the fitting of this point to x = 0. The flat region around x = 0.6 shows the end of interfacial movement with pressure, this could only be caused by a narrowing of the pores to the extent that a significantly larger rise in pressure is required to move the interface further. The fibre was coated which may explain the lack of further movement of water through the fibre wall. If the structure of the coating is essentially like that of a symmetric membrane, i.e. similar pore structure throughout and if the pore size is similar to or smaller than that of an uncoated membrane at the surface (as shown by BP/GP data on previous membranes tests) then this is not an unexpected result. However there needs to be caution at this point, the highest tested pressure was 4 bar which for the previous uncoated module also gave an interfacial shift value of approximately x = 0.6 (excluding one seriously outlying point). There are two possibilities that there will be a further shift at higher pressure but without breakthrough of gas into the liquid. Or that the coating has penetrated inward in the membrane wall sufficiently to create a basically uniform layer of pores between the position x = 0.6 and x = 1. The flatness of the data between 2 bar and 4 bar suggests that this is a possibility, especially as the uncoated membrane data is not flat in this region. SEM images reveal no obvious 'extra' thickness from the coatings

this is similar to the result from previous coatings in that any material not absorbed into the surface of the substrate falls away from the fibre or is only loosely attached and will be lost after light handling.

Results for glass solutions in various ceramic modules

The glass solutions used in testing were sodium or potassium silicate a further two were based on suspensions of silicon dioxide. Some solutions had glycerol added to them. Some basic composition data is given in Table 4.2.

The particles in solutions 1-4 and 7 are meso-porous with a large internal surface area to volume ratio. These solutions are also strongly basic. The particles in solutions 5 and 6 are dense and non-porous, the solutions are silica sols and are neutral.

There were a number of issues that became immediately apparent when treating the glass coating solutions with the membranes in question. Firstly was the difficulty in obtaining any confirmable data on desorption. The results with water were based largely on removal of dissolved oxygen from a position of 100% DO saturation in air which corresponds to a value of 9-10 ppm. The initial value in the glass coating solutions varied wildly depending on the solution with some appearing to have a measured saturated value of as little as 1-2 ppm and at the most a value of 4-5 ppm. Figure 5.19 and Figure 5.20 show that if these values of DO content are 'real' then there will be a very long timescale involved in assessing removal of DO as the rate was not 'fast' when starting from 10ppm. It is expected however that the values of DO shown are not necessarily real values but stable indicators of DO in an effectively arbitrary unit of measure. As with water there was an intent to normalise the data to a fractional DO_{max} figure. In addition magnetic stirring of 1.5 litres was not possible due to the high viscosity of the liquid and mechanical stirring with a grease based air seal was employed adding a new point of possible entry of air to the system. Further to this attempts to clean modules after use were insufficient and led to setting of the solution in the pores of the membrane, this was later rectified by flushing with NaOH though at an early stage attempts to backflush the membrane were leading to rupture of the potting material in a manner which made further use of the module impossible.

To overcome the DO removal/measurement issues a smaller volume tank was used 100-150 ml charge which in theory raised the observed rate of desorbtion owing to the lower volume. Magnetic stirring was able to maintain sufficient movement of liquid in order to give a stable DO reading.

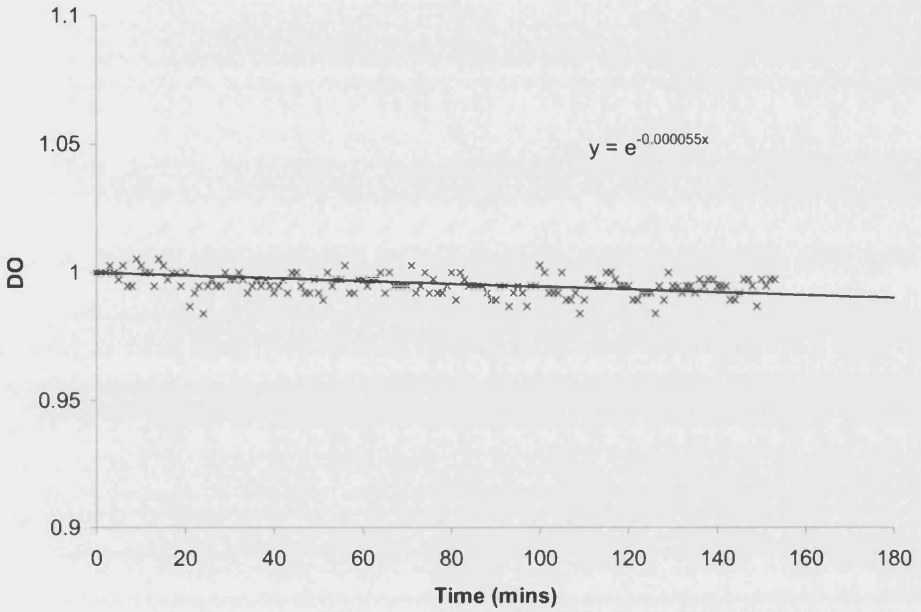

Figure 5.31 - Example of minimal DO removal in early experiments with ceramic module 7, liquid flow 200ml/min, ambient temperature.

A summary of the initial results is virtually worthless as there is no distinct movement in the DO concentration an example of this is given by Figure 5.31. The module used was the structured packing module used in the previous water based tests. The tank was 1.5 litres in capacity and the mass of liquid charged to the tank was 1890 g. As can be seen the rate is far slower than with water, it could be argued that within experimental variability there is no mass transfer at all. Other runs yielded no movement in DO concentration whatsoever though this was believed to be due to complete pore blocking by the glass coating material due to inadequate cleaning after use.

Observed rates of desorption improved somewhat with downsizing of the main tank and improved cleaning. Three modules yielded some data for glass solutions using

the smaller main tank the rates of observed desorption are very low and operational problems limited the number of runs that yielded data. Operational concerns focussed mainly on poor operability of the DO probe in the glass coating liquid. The second key problem was leaking of gas into the liquid side at pressures higher than about 2.5 – 3 barg. Leaking bubbles are far more detectable in the glass coating due to the viscosity entrapping the bubbles allowing them to be seen when they build up in significant numbers. The total volume of leaking gas remained low suggesting that it is possible that leaking was occurring in the water test but went undetected. The implication of this is important to consider as it will skew the results to a higher mass transfer coefficient. Results were only considered in runs where no confirmed leaking was detected (bubbles occasionally emerged from the modules due to gas bubbles being trapped in the unit on start up which can become dislodged this does not constitute leaking). Preparation of batches of solution in the system without a certain degree of bubble entrainment is also very difficult to achieve. Bubbles could be eliminated by the use of ultrasonic treatment of the main tank. Table 5.17 shows a summary of mass transfer values for ceramic modules operating with glass coating solution.

The following statements are applicable to the data.

- Bubbles in tank refers to a purely qualitative assessment of the amount of trapped bubbles in the tank during the run.
- Solution number refers to the type of solution tested details are given in Table 4.2
- M# refers to the module number used details were presented in Table 5.16.

Table 5.17 - Ceramic module mass results with glass solution showing experimental conditions

Run #	Tank charge (ml)	Gas Rate (l/min)	Pressure (barg)	Liquid rate (ml/min)	Bubbles In tank	Soln. No.	K_l (m/s)	M #
1	265	1	2.5	100.8	few	3	2.591E-06	7
2	265	1	2.5	100.0	few	3	1.634E-06	7
3	265	1	2.5	55.8	several	3	8.489E-07	7
4	265	0.7	2.6	19.2	few	3	7.699E-07	7
5	265	0.8	1.5	20	v few	3	1.460E-07	7
6	265	0.95	1.5	22.4	few	2	1.344E-06	8
7	265	0.9	4	51.6	few	1	4.746E-07	8
8	265	0.9	2	102.4	v few	1	7.824E-07	8
9	240	0.46	2	20.8	few	3	9.225E-07	9

The data is presented in relatively raw format and the calculations used are the same as those for runs with water where a larger tank was employed. This calculation may not be strictly valid due to the small size of the tank but enough of an indication is given to see that the mass transfer coefficients are low, compared to those of tests with water – approximately 4-5 times lower when comparing the best results obtained, this is problematic if one wishes to use such a system in practical application as the amount of mass transfer area will accordingly be large.

At this stage it was apparent that it would be impossible to treat sufficient glass coating solution to test in coating applications (approximately 3-5 litres is required) with any module manufactured within the scope of the project. Because of this a polymeric module was brought in to test the usefulness of membranes in a general sense with comparison of the polymeric module performance with water and the ceramic module performance of water allowing some assessment of their relative mass transfer capabilities. This would then allow a prediction of performance of a substantially larger ceramic module based on the polymeric module performance with glass solution. The intended approach is outlined in Figure 5.32.

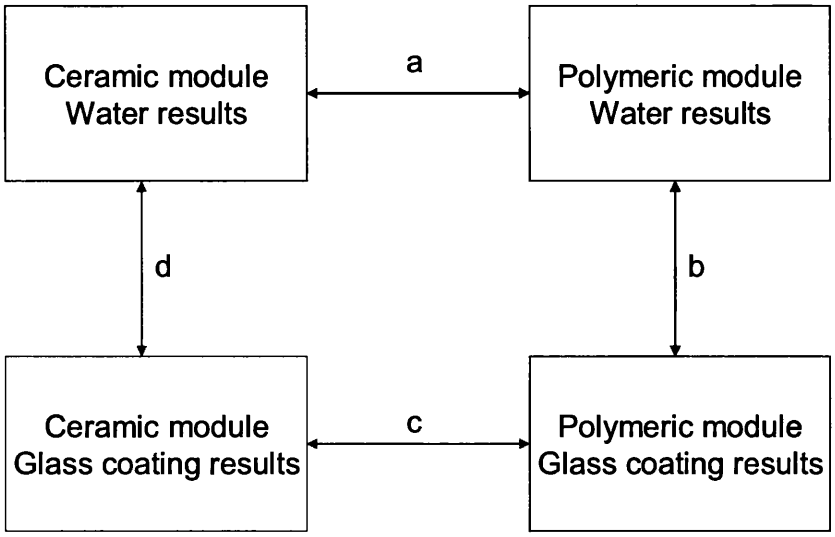

Figure 5.32 – Intended method of performance assessment by comparison of modules

The relationship between the ceramic module and polymeric module will be defined by results with water along line a, the relationship between water and glass coating will be defined along line b. By using relationships a and b it is proposed to make some conclusions about relationships c and d and hence predict performance of a full size ceramic module. It is also noted however that even with a large ceramic module the possibility that glass solution is dried at the gas/liquid interface resulting in blocking of the membrane.

5.2.2 Mass transfer results in polymeric module

A polymeric module was employed in order to prove the concept that membranes can or cannot be successfully used. The modules prepared in this study simply do not have enough efficient surface area to treat a significant enough quantity of liquid to test and hence results from a small commercial unit can provide a basis of evidence for what can be achieved in a large module as described above and in Figure 5.32. A polypropylene module was used as the liquid will not intrude into the pores due to its hydrophobic nature. There were several different liquids supplied for testing and all except one were extensively tested using this unit over ranges of liquid flow rate.

Pressure in this case is far less important as the membrane will not be liquid filled due to its hydrophobicity. Since gas rate is also deemed an insignificant factor in determining mass transfer coefficient a determination of the mass transfer coefficient can be made directly from an analysis of the decline in concentration in the recycle tank[8]. The bulk of results were taken by varying the liquid flow rate at a fixed feed liquid pressure of 1.38barg. There was a limiting condition on flow such that the outlet pressure remained above 0.69barg. This condition was applied after some results obtained with solution 3. These results and the limiting condition are discussed below.

The following demonstrates how analysis of the mass transfer coefficient was achieved:

The concentration of oxygen in the tank is reduced to a ratio of the concentration at time, t (C_t) to the initial concentration (C_0). The data is fitted to an exponential decline with approach to zero where k is the is the constant in the exponential decay. From the literature the following applies in a cross flow module neglecting tube side flow rate[8]:

$$\ln\frac{C_0}{C_t} = \frac{\dot{V}}{V_T}\left(1-\exp\left(-K_l\frac{A}{\dot{V}}\right)\right)t \qquad \textbf{5.9}$$

Where $\dot{V}$ is the volumetric flow rate, V_T is the volume of liquid in the main tank and A is the mass transfer area. Substitution of equations results in the following:

$$-K_l\frac{A}{\dot{V}} = \ln\left(1-\frac{V_T}{\dot{V}}k\right) \qquad \textbf{5.10}$$

An example of results obtained using the polymeric module is given below in Figure 5.33.

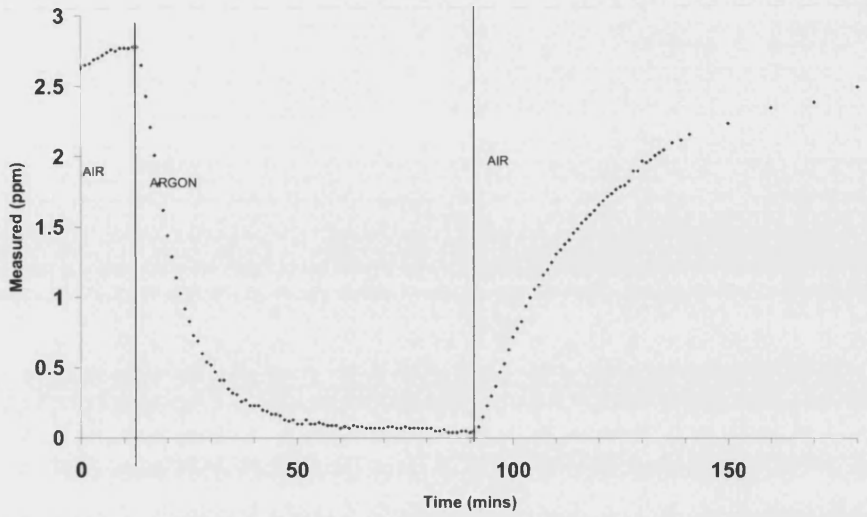

Figure 5.33 - Typical polymeric module desorption data with re-absorption following run at ambient conditions

The results are presented on a liquid by liquid basis. However varied gas rate was tested with liquid number 3 so liquid 3 is presented first to demonstrate the assumption that gas rate has no significant effect on mass transfer. Figure 5.34 comprehensively demonstrates this fact.

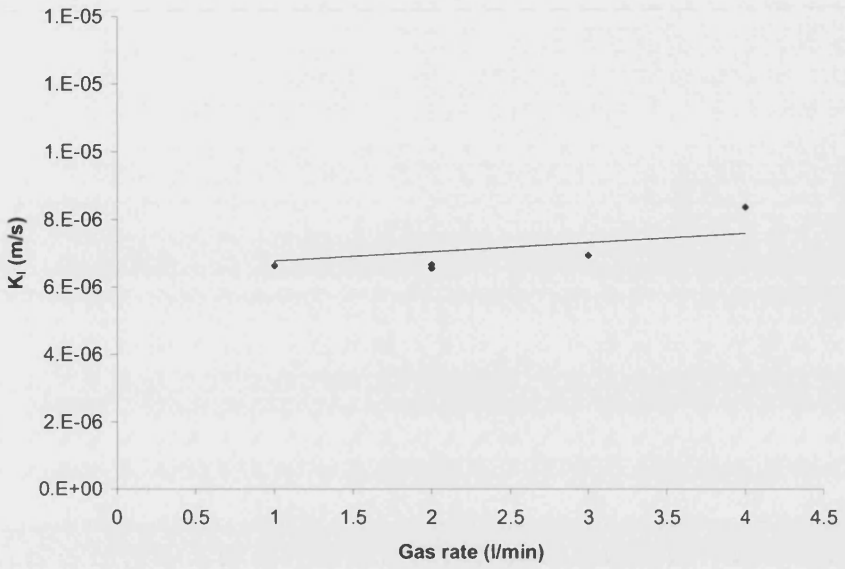

Figure 5.34 – Mass transfer coefficient calculated from the desorption of oxygen from solution 3 under varied gas rate (module liquid outlet pressure 0.7 bar, inlet pressure 1.4 bar, gas side pressure minimum possible, ambient temperature, liquid flow = 2.12 kg/min)

The varied gas rate can be said to have no effect on the mass transfer and hence it can be said that by far the dominating resistance to mass transfer is the liquid phase (or shell side resistance).

Varied liquid rate

The various glass coating solutions were tested at varying liquid flow rates, the results and a discussion of these is presented below. The results are presented on a basis of volumetric liquid rate versus mass transfer coefficient. In addition Figure 5.37 shows solutions 1&2 comparing liquid phase Reynolds number versus mass transfer coefficient.

Solution 3 (Figure 5.38), this solution is the same as solution 1 but without the additional glycerol. The mass transfer coefficient is slightly lower than in solutions 1 and 2 at similar liquid flow rates. It is noted that in this module some higher rate tests were carried out that demonstrated that higher mass transfer coefficients were

possible at higher rates. The result appear not to have the same characteristic shape as the other silicate solutions. It is possible that the different nature of the results is due to the lack of glycerol in this sample. However the results for this module are spread over a larger flow range than others due to these being the first results obtained. Later solutions showed that the pressure difference parameters used were not possible to maintain at such rates. In all subsequent runs a minimum of 0.69 barg liquid outlet was maintained to avoid gas leaking into the liquid side, this leakage could be observed clearly at 0.34 barg or lower, the two results for solution 3 at which there is a high value of mass transfer coefficient were obtained at 0.55 and 0.62 barg pressure on the outlet and hence they must be treated with a certain degree of caution. Ideally further results at lower flows would have been possible but time limitations prevented a return to this solution.

Solution 1 (Figure 5.35), this solution is a sodium silicate solution which has glycerol added. The variation of mass transfer coefficient above a liquid rate of 0.4 l/min is small suggesting that the mass transfer coefficient is no so dependant on the liquid flow beyond this point. This could be indicative of either a greater resistance elsewhere in the system, within the membrane for example. Or indicative that there is a limiting point to improvement of this resistance, the fact that the membrane is hydrophobic and that the results (particularly those with other solutions) appear to indicate the key resistance is in the liquid phase particularly at lower liquid rates. As such it is possibly that some bypassing, channelling, poor distribution or other physical effect which limits mass transfer is taking place. This could either be at low flow with rapid improvement to a point (i.e. fully distributed flow). Or at high flow channelling begins due to pressure drop across longer routes over the bundle of fibres. The circled points are lying outside of the trend of the other data points. These data points are both based on unusually short runs of data where the probe ceased responding.

Solution 2 (Figure 5.36), this solution like solution 1 is sodium silicate based with glycerol added. The variation of mass transfer coefficient with liquid flow rate is once again limited beyond a certain flow though there is not as much of an indication of this as there is with solution 1. The limit is once again around 0.4 l/min. The solution

has a higher solids content than solution 1 and hence a higher viscosity (6 times higher) the effect of this is not particularly apparent in the absolute value of K_l which are slightly lower but essentially of a similar magnitude to solution 1.

Variation of mass transfer coefficient with Reynolds number – Solutions 1&2 (Figure 5.37). Reynolds numbers were calculated based on mean flow velocity across the bundle as the liquid is assumed to flow radially across the bundle. The method for calculation of the Reynolds number is based on that used by Schöner *et al*.[8] in which a similar module was used.

The Reynolds numbers are low indication laminar flow. There is no change in flow regime indicated from the Reynolds numbers that would indicate why the variation of mass transfer coefficient is not linear this is particularly the case with solution 1 (as was observed when considering Figure 5.35). It can be argued that solution 2 could be a linear variation with Reynolds number. It was stated above that it appeared there is some reduction of the magnitude of the variation of mass transfer coefficient with increasing flow rate (and hence Reynolds number). Comparison of the two graphs makes this inconclusive. In effect the compressed scale of Figure 5.37 helps to make the case for a linear variation. The shape of the plotted data is similar to that plotted in Figure 5.36(variation of mass transfer coefficient versus liquid volumetric flow rate). When the scale of the Reynolds number analysis of just solution 2 is expanded the two analyses (liquid rate and Reynolds number) are almost identical in trend.

If it is assumed that the variation is indeed linear then the solution is behaving much more as one would expect for a liquid phase mass transfer dominated operation. Solution 2 would be closer in behaviour to solution 3 and different to solutions 1 and 4. This is somewhat perplexing given that solutions 2 and 3 have less in common with each other than they have in common with either of the other solutions. It must be concluded that the differences in behaviour between the solutions is due to a function of either the condition of the module at the time of testing or a variability in flow distribution within the module. This could be caused in some way by other effects stemming from the viscous nature of the liquid and the relatively tortuous path the liquid takes through the module. At different times the liquid may find routes

through the module that allow it to flow over less area. In other words there are lesser or greater regions of stagnant liquid in the module. The solutions which show a limited effect on mass transfer coefficients are experiencing large dead zones in the module whereas those closer to a linear variation are experiencing only small dead zones.

Solution 4 (Figure 5.39), identical to solution 2 but without added glycerol. Unlike the apparent relationship between solutions 1 and 3 there is little difference between solutions 2 and 4, once again it is stressed that there is some limitation to the comparability of results from solution 3. Solution 4 exhibits the implied fast rise in mass transfer coefficient up to 0.4 l/min of liquid before showing a slower rise in mass transfer coefficient. The rise is slightly more rapid than in solutions 1 or 2 but this may be because the slower rise in mass transfer coefficient appears to begin at a lower value. If the data point at a liquid rate of just below 0.3 l/min of liquid flow is considered to be part of the rapid rise phase then the subsequent slow rise inferred from the remaining results would be similar to that of solutions 1 and 2. The overall magnitude of the mass transfer coefficient like with solution 3 is slightly lower than the glycerol containing counterpart, solution2. The circled results for solution 4 were taken in one session together and were all lower than expected, the results for just below 0.7 l/min and just below 1 l/min were repeated later and found to be more in line with expected results. The low results are attributed to the fact that the probe was on some occasions prone to giving condensed reading due to upward drift of its zero set point.

Sodium silicate solutions in general

The sodium silicate solutions behaved similarly with the exception of solution 3 which was somewhat limited in analysis due to few results being available – the variation in mass transfer coefficient between solutions was minimal, what can be said is that the two solutions without glycerol experienced higher mass transfer coefficients by just a few per cent. The actual value of the mass transfer coefficient tended to be limited to approximately 6×10^{-6} m/s below liquid flow rates 1 l/min.

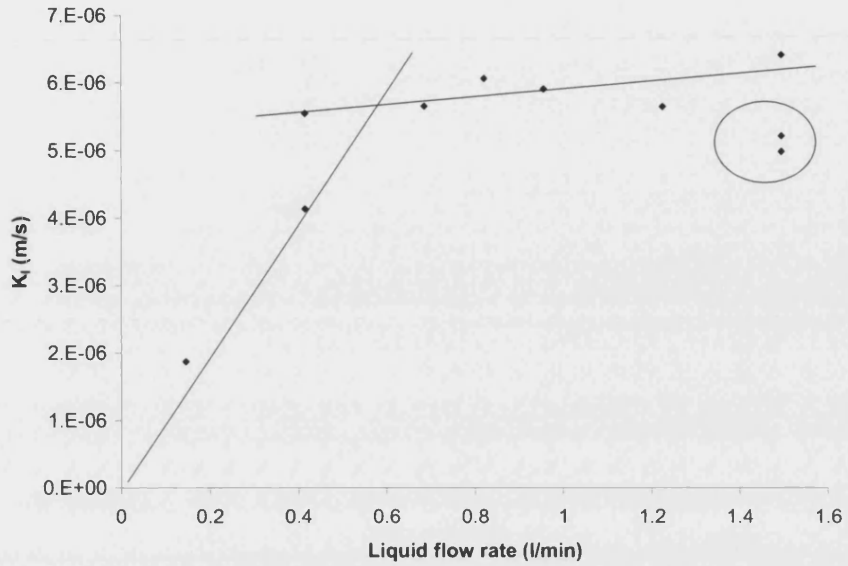

Figure 5.35 – Mass transfer coefficient calculated from the desorption of oxygen from solution 1 at varied liquid circulation rates [gas rate 3 l/min, ambient temperature, liquid inlet pressure 1.38barg, gas pressure minimum to sustain flow]

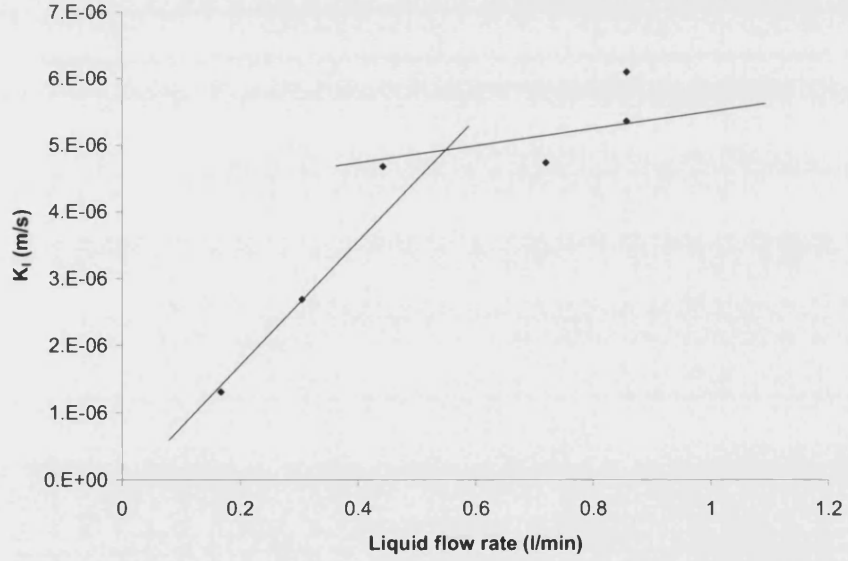

Figure 5.36 – Mass transfer coefficient calculated from the desorption of oxygen from solution 2 at varied liquid circulation rates [gas rate 3 l/min, ambient temperature, liquid inlet pressure 1.38barg, gas pressure minimum to sustain flow]

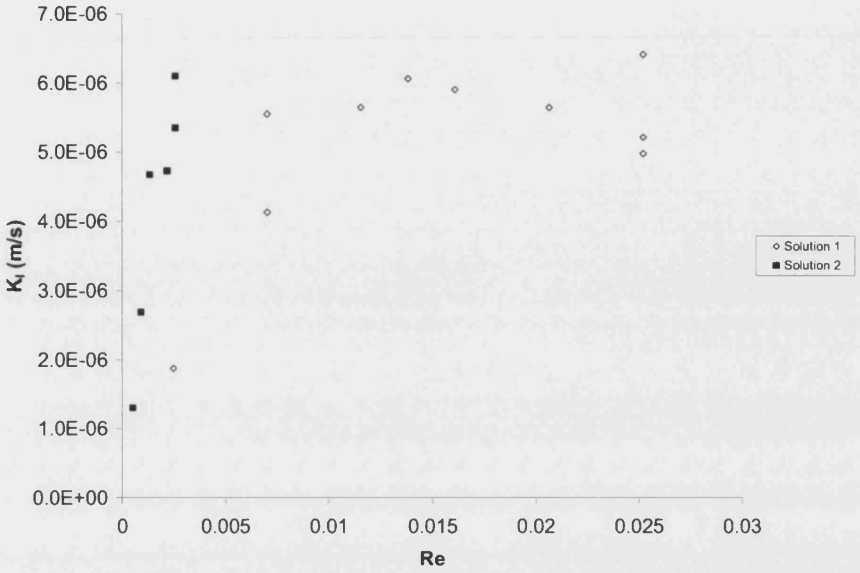

Figure 5.37 - Solutions 1&2 Mass transfer coefficient vs. liquid phase Reynolds Number, conditions as follows: gas rate 3 l/min, ambient temperature, liquid inlet pressure 1.38barg, gas pressure minimum to sustain flow

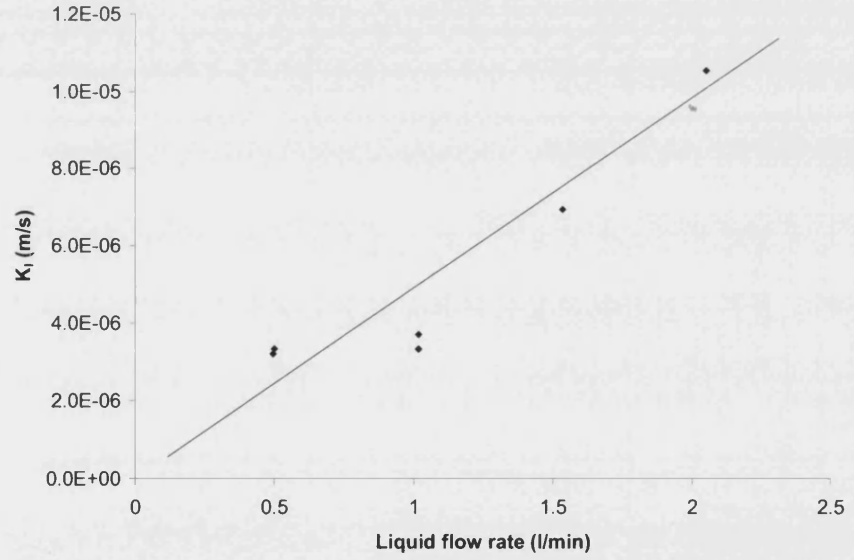

Figure 5.38 – Mass transfer coefficient calculated from the desorption of oxygen from solution 3 at varied liquid circulation rates [gas rate 3 l/min, ambient temperature, liquid inlet pressure 1.38barg, gas pressure minimum to sustain flow]

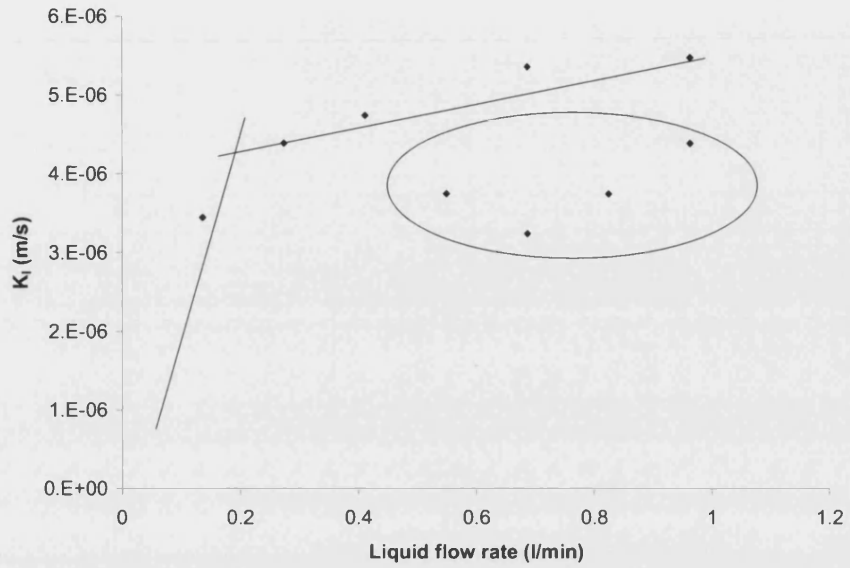

Figure 5.39 – Mass transfer coefficient calculated from the desorption of oxygen from solution 4 at varied liquid circulation rates [gas rate 3 l/min, ambient temperature, liquid inlet pressure 1.38barg, gas pressure minimum to sustain flow]

Solution 5 was not tested on the advice of the project sponsors who indicated that its similarity to solution 6 (see below) and its usage only in conjunction with other solutions meant its mass transfer performance (and that of solution 6) are less important than solutions 1-4 and solution 7.

Solution 6 (Figure 5.40), was the solution that exhibited the highest mass transfer rate – the mass transfer coefficient was higher by approximately 50% compared to the silicate solutions. The solution is essentially a suspension of solids in water. It could however be circulated much faster and more easily than other solutions owing to its viscosity being near that of water. Like solution 3 the rates of liquid flow tested were higher, this was however deliberate due to the low viscosity and difficulty maintaining module inlet pressure at very low flows (this was due to the after module valve being use in order to backpressure the system to 1.38barg at the inlet and the low viscosity meant that this was only reached at higher flows).

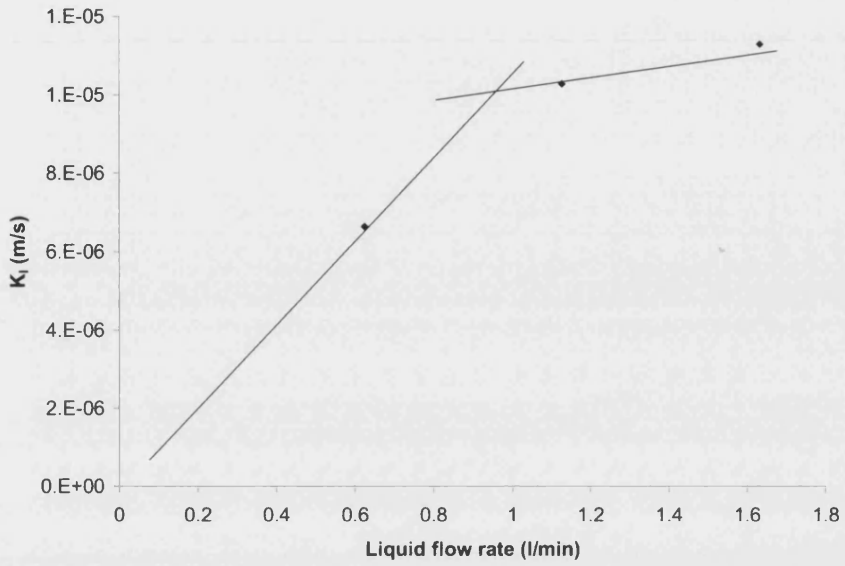

Figure 5.40 – Mass transfer coefficient calculated from the desorption of oxygen from solution 6 at varied liquid circulation rates [gas rate 3 l/min, ambient temperature, liquid inlet pressure 1.38barg, gas pressure minimum to sustain flow]

Solution 7 (Figure 5.41), this solution according to sponsors data was not drastically more viscous than the silicate solutions however this was not the experience found in the laboratory. The mass transfer rate is however as one would expect at higher viscosity, the lowest of all. The mass transfer coefficient is three to four times lower than for the previous silicate. The viscosity causes this by raising the liquid mass transfer resistance as the higher viscosity creates an effectively larger boundary layer (or mass transfer resistance layer). The shaper of the data is once again similar to that of the other silicate solutions with an initially fast rise in mass transfer followed by a region where there is a much slower rise in mass transfer coefficient.

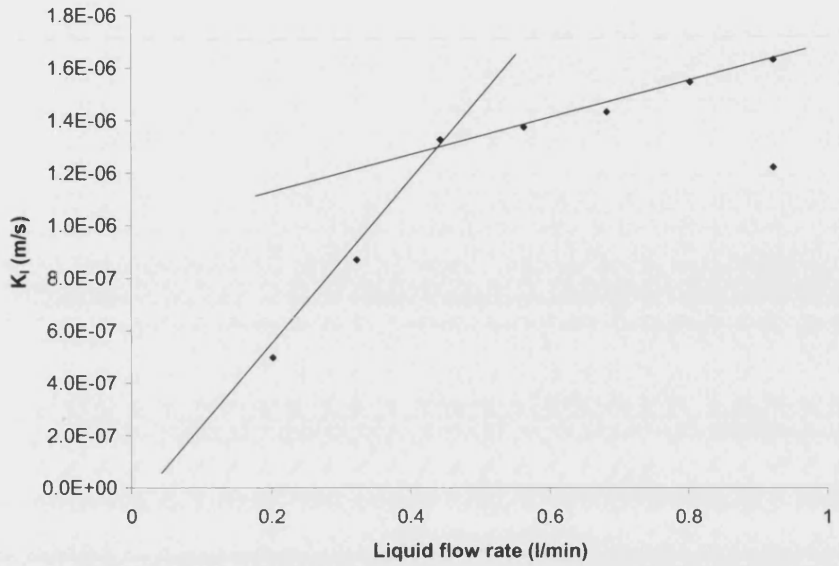

Figure 5.41 – Mass transfer coefficient calculated from the desorption of oxygen from solution 7 at varied liquid circulation rates [gas rate 3 l/min, ambient temperature, liquid inlet pressure 1.38barg, gas pressure minimum to sustain flow]

An overall summary chart showing all the solutions is presented following the results of this module with water tests

Water tests

Water tests were carried out and it is expected that water would yield the highest mass transfer rate as the least viscous solution. Figure 5.42 demonstates that this is essentially the case but that solution 6 is essentially close to the same performance. The probe was somewhat difficult to manage during the water tests (presumably due to months of testing in the more aggressive silicate solutions) hence the variability of the results. It is believed on calibration of the probe (several times) that the magnitudes of the DO removal are realistic just that the probe had a tendency to drift off calibration rapidly by this stage in testing.

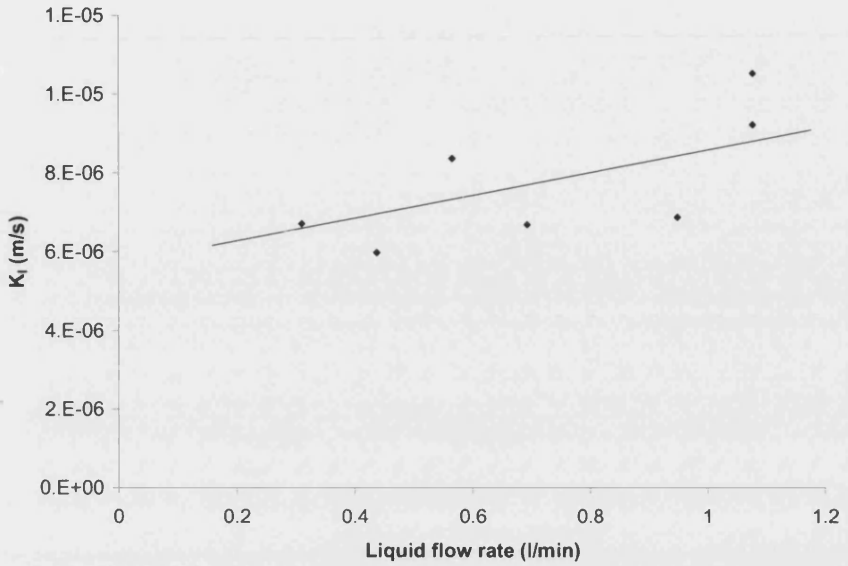

Figure 5.42 – Mass transfer coefficient calculated from the desorption of oxygen from water at varied liquid circulation rates [gas rate 3 l/min, ambient temperature, liquid inlet pressure 1.38barg, gas pressure minimum to sustain flow]

Overall mass transfer summary in polymeric module

The collated results from the individual solutions and water are presented in Figure 5.43 it can be seen that water and solution 6 stand out from the crowded region of data by being consistently higher values, solution 7 stands out for the opposite reason. The results for water seem slightly low compared to the literature values of [5, 18] where 1-6 × 10^{-5} was the order of magnitude for mass transfer in a polymeric module similar to this.

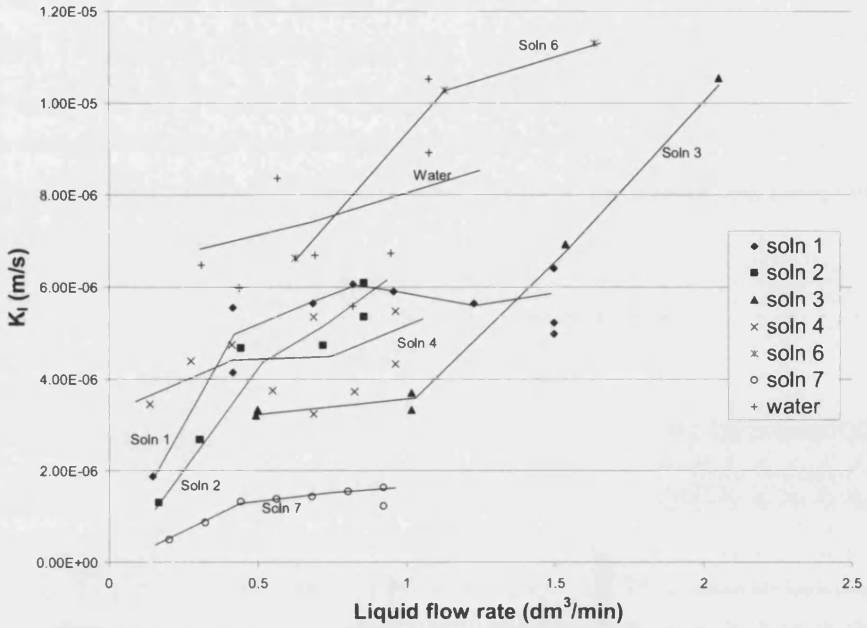

Figure 5.43 – Mass transfer coefficients for desorption of oxygen from all tested liquids at varied liquid flow rates [gas rate 3 l/min, ambient temperature, liquid inlet pressure 1.38barg, gas pressure minimum to sustain flow]

5.3 Mass transfer alternatives

Alternative methods of oxygen stripping would most simply involve dispersing the sweep gas within the liquid. The viscosity raises a problem however as the gas bubbles will not separate from the viscous liquid like they would from water or other less viscous liquids. As such a means to remove the gas must be used and ultrasound is a possibility investigated.

5.3.1 Mass transfer observed in leaking modules

The results in the ceramic module do not show one key observation made when taking the results. In some cases where high pressures were involved or in modules which had begun to leak gas it was noted that the ultrasonic bath used to remove bubbles from the tank prior to module tests could be employed in a continuous mode to remove bubbles during the progress of a run.

The liquid can be cycled through a second tank which is situated in the ultrasonic bath. The presence of bubbles even in the flow between module and this second tank has an effect on the mass transfer. Some experiments were carried out in order to investigate the effectiveness of simply feeding sweep gas into a circulating liquid loop where the module had been and removing the gas in a main tank using ultrasonic treatment was investigated.

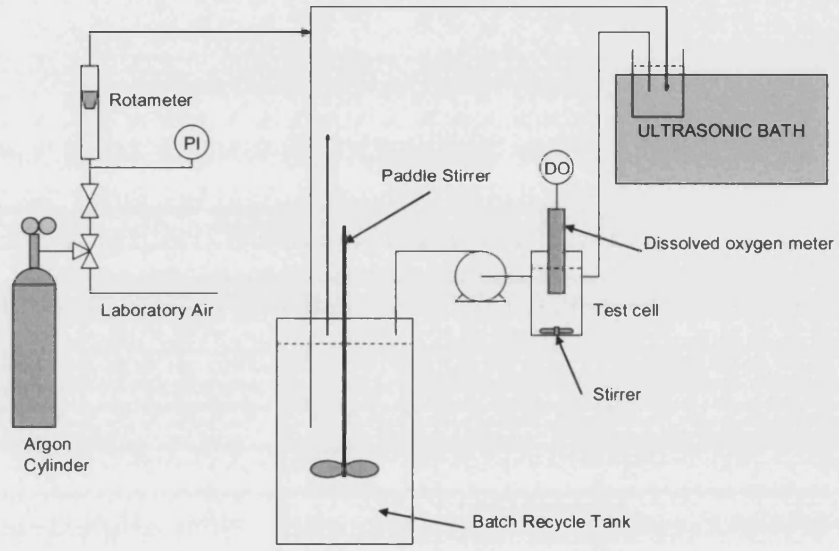

Figure 5.44 - Initial direct gas contact test set up

Figure 5.44 shows how the experimental system with the ultrasonic bath is put into continuous service. The decline of concentration of oxygen in the tank allows assessment of performance (oxygen concentration in all runs is normalised so the start value is 1). This gives us a comparison of the ceramic module runs with the directly fed gas runs. The feed of gas was qualitatively matched to rates that were similar to the amount of gas that would leak into the liquid with a module which had an average to severe leak. Higher gas rates could easily have been employed.

The result of these tests was quite telling – using modules the value of k reached 0.00706 s^{-1}, whilst without a module it was possible to reach values of 0.00489 s^{-1} and even a simulation of an average leak in a module yielded a value of 0.00226 s^{-1}. It

can be said that in runs where there was any leak there will have been some significant contribution to apparent mass transfer from the leak. It must also be stated that the rate of leaking in the module results above tended to be very low, runs where an average leak occurred tended to be impossible to maintain for long due to bubbles fouling the probe head and yielding false results.

5.3.2 Mass transfer by sparge and ultrasound

The magnitude of the rates of DO removal observed without a module led to the use of direct sparging of argon into a main tank with the pump merely circulating liquid to remove bubbles in an ultrasonic treatment tank in order for the DO level to be measured in bubble free liquid. In practice sparging without any re-circulation is perfectly acceptable and ultrasound can be used at the end of the process. Figure 5.26 shows the system set-up.

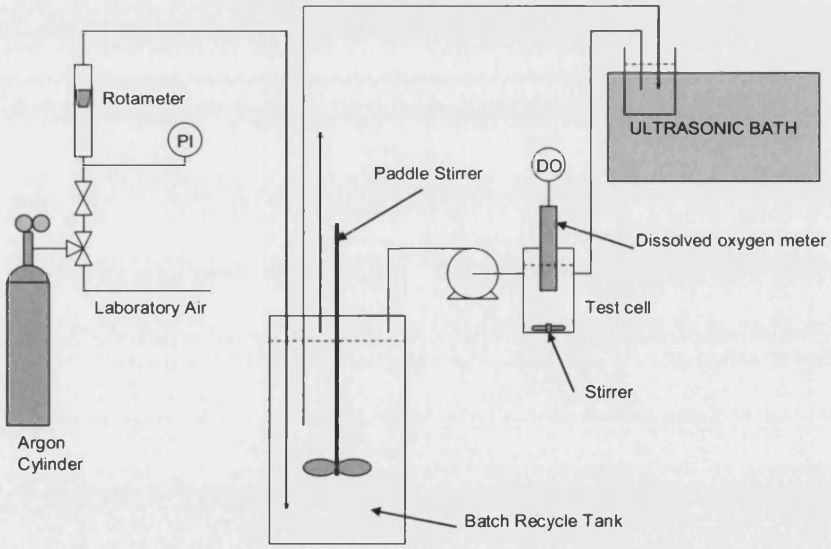

Figure 5.45 - Ultrasound and sparging system set up

In order to model this system the circulating loop is neglected and a mass balance o the liquid phase is conducted.

The rate of accumulation of oxygen in the tank is equal to the rate of mass transfer of oxygen to the gas phase, there is no flow in or out (neglecting the recirculation):

$$-V_T \frac{dC}{dt} = K_l A\left(C - C^*\right) \qquad \textbf{5.11}$$

Gives

$$\frac{dC}{dt} = K_l a C \qquad \textbf{5.12}$$

since $\frac{A}{V_T} = a$

and $C^* \approx 0$ so long as gas hold up is low this is not the case for all the gas a some becomes entrained but the vast majority of the gas does not become entrained. The low resistance to mass transfer in the gas phase also allows this approximation to be valid. These tests are intended to demonstrate the potential of the system and any future work would be improved by allowing methods of determining gas hold up and estimating C^* more precisely.

Rearranging equation 5.12 and integrating:

$$\int_{C_0}^{C_t} \frac{dC}{C} = \int_0^t K_l a \; dt \qquad \textbf{5.13}$$

$$K_l a = \frac{\ln \frac{C_0}{C_t}}{t} \qquad \textbf{5.14}$$

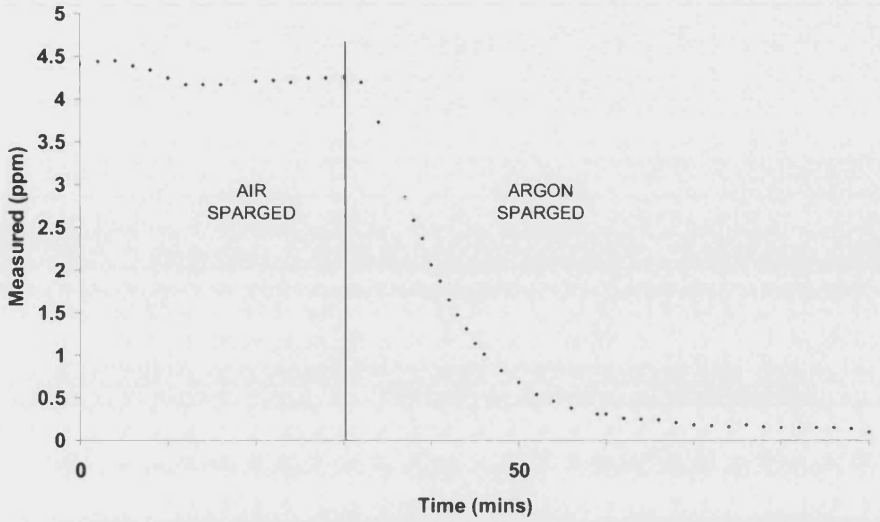

Figure 5.46 - Example of typical desorption curve using sparge and ultrasound in ambient conditions

Figure 5.46 shows a typical desorption experiment using the sparge and ultrasound method. The range of operability of this experiment was limited as is discussed in section 4.4.2 (page 121). In summary the system balances on the rate of gas feed, the recirculation rate and the rate at which gas can escape the system through the mechanical seal around the stirrer shaft. Without this deliberate 'leak' the contents of the main tank will all transfer to the ultrasonic measurement loop. The results are presented below in Table 5.18 as direct comparisons become difficult owing to the variable conditions – however the results indicate the order of magnitude of the mass transfer that is possible. The mass transfer coefficient cannot be separated from the parameter 'a' without estimating the interfacial area of the bubbles tank – though this could be done it is beyond the scope of this study. The highest value for $K_l a$ with a silicate solution is 0.069 s^{-1}, water achieved a value of 0.079 s^{-1} the two solutions based on SiO_2 suspensions (solns 5&6)are close to the water value it must be said that water and solutions 5 and 6 were tested at lower gas flows than the best results with silicate solutions – for similar flow rates silicate solutions only achieve values of the order 0.03 to 0.04 s^{-1}. Other methods which involve modules will be compared on the basis of $K_l a$ towards the end of this chapter. It appears from the results for the silicate solutions (solutions 1-4) that the flow rate of gas is influential as one would expect. The increase rate would however be due to the added area when more gas is

employed rather than the added volume of gas available for absorbing oxygen. It can be concluded that sparging removed the dissolved oxygen effectively as shown by Figure 5.46, while ultrasound appears to successfully remove bubbles which are entrapped in the solution.

Table 5.18 - Sparging with ultrasound mass transfer results and gas flow condition, temperature of all tests is ambient

Solution number	Gas flowrate (ml/min)	$K_l a$ (1/s)
2	Not measured	0.0304
2	200	0.02753
4	200	0.0354
4	190	0.03034
3	240	0.04246
1	440	0.03346
1	400	0.05966
water	220	0.0787
5	120	0.06208
6	70	0.06927
1	300	0.069

5.3.3 Mass transfer modules summary

Performance of ceramic modules with glass solution

A brief summary of module performance is included here to allow some comparison of module performance between ceramic modules and polymeric modules.

The water tests with ceramic modules at a liquid rate of 250 ml/min and pressure difference that did not cause obvious breakthrough of the gas into the liquid (i.e. disregarding the high points shown in Figure 5.24). These led to K_l values of approximately 6×10^{-6} m/s. Similar tests on water with the polymeric module (extrapolating from the data points shown in Figure 5.42 in order to compare at the

same liquid rate) yield a K_l value of 6.5×10^{-6} m/s. The best performing silicate solutions for the polymeric module at similar flow rates give values of 5.5×10^{-6} m/s.

The mass transfer coefficients are close for all the systems so following the guide laid down in Figure 5.32 we can suggest for similar conditions a mass transfer coefficient of between 5×10^{-6} m/s and 6×10^{-6} m/s for the ceramic module using silicate solution. The observed values are far lower at 1×10^{-6} m/s for runs where there was little evidence of gas leaking into the liquid phase. The principle conclusion drawn here is that the water results for the ceramic modules may well have been influenced by unobserved leaking of gas into the liquid side or were simply high due to a high liquid velocity. The latter is less likely since it was established that the liquid rate had little effect on performance. This is of course significant in assessment of ceramic module performance but the results were taken under conditions where no leaking was observed and as such must be assumed that no leaking occurred. There is a key note for future work to establish if leaking does occur through ceramic modules but this assessment could not realistically be made within this project. The experimentally observed value of the mass transfer coefficient is low and as such it is likely that the construction of such a ceramic module would be both expensive and would result in a significantly larger unit for the interfacial area required when compared to a polymeric module.

If however one assumes the ceramic module performed nearly as well as the polymeric module in water *without* leaking of gas into the water side. Then the further assumption is made that the mass transfer coefficient in the silicate solutions could have been similar to values seen in the polymeric module. The conclusion is therefore that ceramic modules are in fact a feasible solution for removing dissolved gas from aqueous solutions. However one would still expect to see a ceramic module of similar surface are to a polymeric module as being both expensive and large since it is very difficult to achieve such a high area per unit volume in ceramic modules compared to polymeric ones. This means in order to be competitive ceramic fibres must: (A) be made hydrophobic such there is no need to risk leaking of gas into the liquid (recalling that in the case of shifting of the gas interface the shift would need to be across 95% or more of the fibre wall which given the concerns raised with regard

to gas leakage is impractical). (B) Ceramic fibres must also be much smaller in diameter so as to limit module size and cost. (C) there must be clear evidence that the ceramic module will significantly outlast any polymeric unit (this arises principally because the suspected fears of polymeric modules suffering from the aggressive chemical environment did not materialise in the timescale of testing (several months). Polymeric fibres are almost certainly inexpensive enough to replace as regularly as required which would appear not to be very often (i.e. on a less than six monthly basis). Because of these points the type of ceramic fibres created in this study could be used but only in situations where which there is a major issue with chemical resistance and the product is of high enough value such that the size and cost ceramic units does not rule them out as feasible phase contacting devices.

$K_l a$ values

The sparge and ultrasound method was introduced as an alternative to the membrane as it was noted that use of ultrasound could eliminate the entrained gas bubbles from the glass solutions. Evaluation of this method was only possible to the extent of presenting some $K_l a$ values. These are the mass transfer coefficient presented in the other methods but factored against the surface area for mass transfer divided by the volume of the liquid phase in the mass transfer equipment. In effect this value is a measure of performance based on the size of the equipment. Fundamentally this is a more valuable measure of performance for the engineer as a rate of mass transfer achieved in the system per unit volume is arrived at. This allows comparison of different types of system. In effect despite the unit of s^{-1} the real unit is volume of solute transferred per volume of liquid phase per unit time whilst K_l alone measures volumetric rate of transfer per unit area per unit time. This is well and good for an appreciation of the nature mass transfer but the engineer designing a practical system in a confined space will not be interested in high values of K_l if the area per unit volume is very low. In summary a measure of K_l and $K_l a$ are useful together. For the sparge and ultrasound method there was no simple method to determine the value of a. This only leaves us the combined value of $K_l a$ to compare between membranes and sparging. A summary of typical values of $K_l a$ for both water and glass solution in the sparge and ultrasound system are presented below to maintain a fair comparison

judgement was used to pick typical runs. Those values quoted for the polymeric module based systems the liquid flow-rate was set as 1 l/min a typical value of flow. The best performing liquids were used. The ceramic module best values were chosen (these would have been at lower flow rates but far higher velocity across the membrane (afterall velocity and hence turbulence, regeneration of fresh bulk liquid to the membrane surface will be the key factors that arise from higher liquid flow rate) so effectively this is weighted in the advantage of the ceramic modules at least on the absolute figure. Table 5.19 shows the summary.

Table 5.19 - Typical $K_l a$ values (s^{-1}) based on all results gathered (where there are several results these figures are based on best mass transfer results obtained repeatably – where there are few results the figure quoted is the highest result that does not stand out significantly from others

Fluid	Ceramic module	Polymeric module	Sparge + US
Water	0.011	0.030	0.0787
Silicate (soln 1-4)	0.0014	0.021	0.033 - 0.035
Suspension (soln 6)	n/a	0.031	0.063 - 0.069

The values suggest that sparging with ultrasound is the best method, the polymeric module the second best and the ceramic module a distant last with silicate solutions. Liquid flow was expected to be the key factor for this process in modules and though the effect of higher rates was observed the increase in mass transfer at higher rates in the viscous systems was disappointing. Gas flow controls the sparging process and the system is difficult to control at high flow rates. This control issue is not just limited to the somewhat difficult to control equipment used but is a genuine reference to flooding caused when a very large volume of gas is within the bulk of the liquid at any one time. What is clear is that the ceramic module lags behind on this measure of performance – significant work in minimising size of units for a given mass transfer area is required. The area per unit volume of this system is between 3 and 7 times lower than the polymeric module depending if a structured or unstructured module is used. The difference in $K_l a$ for the silicate solutions was however nearly 15 times. This suggests that ceramic modules are unlikely to be suitable for the process especially as commercially available units have even lower area per unit volume values. The values for water and solution 5 do the polymeric module a disservice when compared to sparge and ultrasound since much higher liquid flows can be used

and the variability with liquid rate is much more significant, for example if one extrapolates to a liquid flow of 3 l/min for water and solution 5 the $K_l a$ values are nearer to the sparge and ultrasound values at around $0.06s^{-1}$.

Absolute values of DO measured in solution

For completeness an approximate figure for the absolute DO_{max} value (starting concentration) in the various solutions is included (Table 5.20). As has been discussed on several occasions the value measured may not be a true value but is only an indicative quantity that is assumed to scale correctly hence the presentation of these figures after assessment of the mass transfer performance where only ratio of concentration vs starting concentration is considered when using glass solutions.

Table 5.20 - Observed absolute DO_{max} values in each glass coating solution

Solution Number	Typical DO_{max} (ppm)
1	3.6
2	1.8
3	3.5
4	1.9
5	9.0
6	9.0-10.0
7	0.65

These values were obtained in the later runs with either the polymeric module or the sparge and ultrasound tests where relatively rapid approach to the figure was possible. An example of the profile is shown in Figure 5.47.

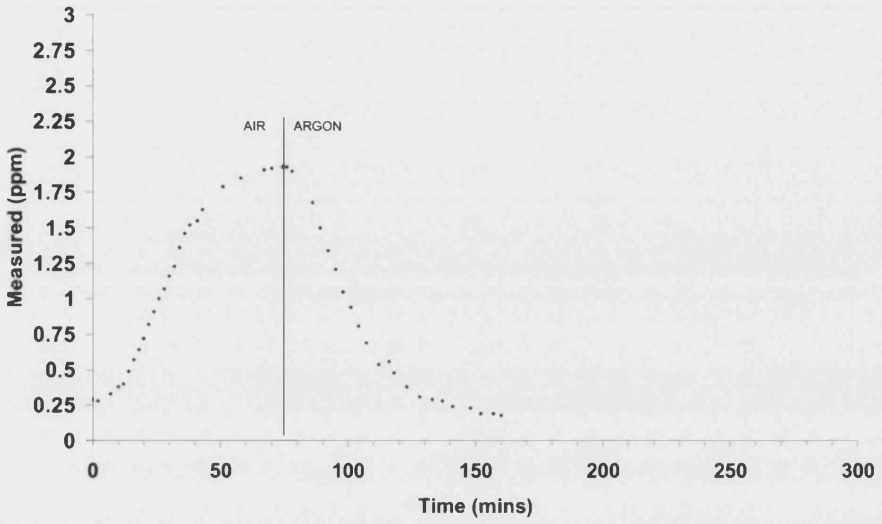

Figure 5.47 - Example of DO max determination curve

Nitrogen removal

For simplicity all results have been presented on the basis of dissolved oxygen but throughout it has been assumed that the relative value of DO (DO/DO_{max}) is equatable to the relative value for DN such that (DO/DO_{max}) = (DN/DN_{max}). As such when attempting to perform runs for the final application an attempt was made to reach values of (DO/DO_{max}) 0.1 or less. On this basis DN is assumed to be removed to a similar extent. Note there is no known maximum value of DN max in order to prevent the occurrence of bubbles in the produced glass.

5.4 Glass casting

The methods of casting the solution onto glass were discussed in section 4.5. In the relatively short period of testing that was possible none of the methods were successfully used to create glass products that were free of bubbles in the interlayer (glass coating is an interlayer in the final product). Each will be discussed in turn and reasons why bubbles remained are considered. The exact details of the solutions used are not included as the mass transfer performance is not being measured here. It is sufficient to say that in most cases the solutions were either the same as or blends of

the solutions used in the mass transfer tests. If the solution was the same as those used previously this is indicated where appropriate other solutions are simply listed as 'blended' or 'CIP solution' where the blend was specific to the cast in place method. Where the module was used liquid flows were as high as reasonably possible (within experience from mass transfer tests) Gas rate was as with the variable liquid flow test in the polymeric module (3 l/min displayed on an air rotameter which corresponds to approximately 2.7 l/min of argon). For sparge and ultrasound no measurement loop was used gas was sparged at 1 l/min measured (0.9 l/min actual).

Pour and Dry method

The pour and dry method was employed for several solutions which were successfully brought to within a value of $(DO/DO_{max}) = 0.1$. The principle cause of the failure of this method to work is believed to be the exposure of the poured solution to the atmosphere for a period of time prior to a skin being formed. The solution is poured over 30cm × 30cm plates at a thickness of 1-2 mm which gives a significant mass transfer area given the volume involved. A rapid uptake of nitrogen from the atmosphere is expected. Some examples of glass samples made using this method were photographed and some of these images are presented in Figure 5.48. During the testing a rough test of the re-sorbtion of oxygen was made the liquid was circulated for 30 mins after samples were taken and then air was run through the system for just 5 seconds (including flushing the headspace of the main tank) the air was then switched off and the absolute DO value rose from 0.05 ppm to 0.14ppm in three minutes. This is a fairly course test but it represents an example if how quickly the DO level rises. The level remaining in the tank was estimated at 5cm and the area of the liquid surface in the tank was smaller than the area of the samples which are exposed. This suggests that there is a severe re-sorbtion issue. There is however a word of caution in as much as the air flush of the system putting air across the surface of the membrane ($1.4m^2$ area).

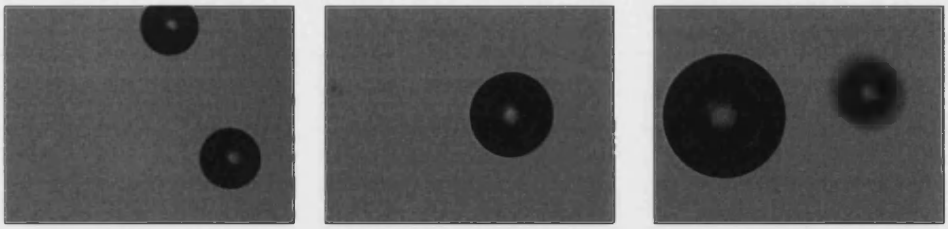

Control (solution 2) Control (solution 1) S&Ultrasound (solution 2)

Membrane (solution 2) Membrane (solution 1)

Figure 5.48 - Pour and dry glass sample images (dark regions are bubbles in the interlayer)

Tek Dry Method

The Tek dry method suffers from the same problems as the pour and dry method in that samples are exposed after pouring for a time. Once again some images of sample prepared are shown in Figure 5.49.

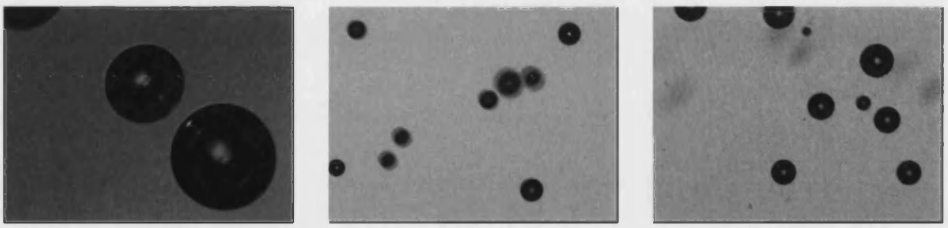

Ultrasound (Solution 2) Membrane (solution 2) Membrane (solution 7)

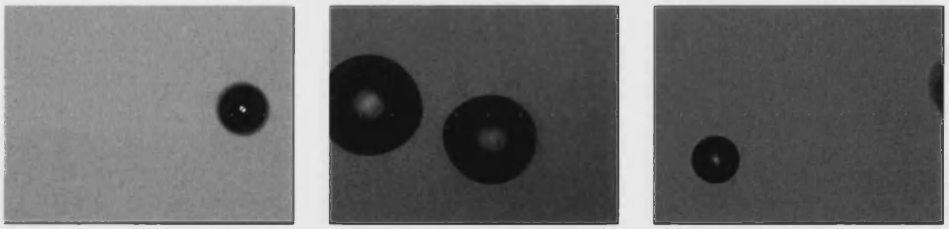

Membrane (CIP solution) Membrane (blended) Control (Solution 2)

Figure 5.49 - Tek Dry glass sample images (dark regions are bubbles in the interlayer)

Cast in Place Method

The cast in place method offered the most promising conditions for the system as the solution can be taken directly to glass and cast with virtually no exposure to air. There are however some significant issues with the system. Two halves of a mixture are prepared and when mixed the halves will solidify over time. The system was used to remove nitrogen from this solution in both a mixed method and in removing nitrogen from the half with the highest absolute measured DO. The pre-mixed solution showed no removal of DO. This may have been attributable to the probe simply not working in the solution or due to no mass transfer taking place. The latter seems unlikely as the project sponsors have existing methods for doing this to one half of the solution by concentration difference mass transfer. The other part of the solution is then added in their method. The attempt to remove the DO in one half of the solution was successful to a level of $(DO/DO_{max}) < 0.1$. The part of the solution treated was the half of the solution not treated by concentration difference mass transfer by the sponsors – hence both halves of the solution have been successfully treated in this way. This means that unless the reaction between the two halves prevents mass transfer it must be possible to remove dissolved gas and as such it is assumed the probe simply did not respond correctly when treating the pre-mixed solution. The solutions were hence treated on a time basis with 1 hour set as the running time on argon. The solutions used were also tested in the Pour and Dry method and Tek Dry method for comparison but in all cases bubbles were present in the interlayer. Figure 5.50 shows the images of these samples.

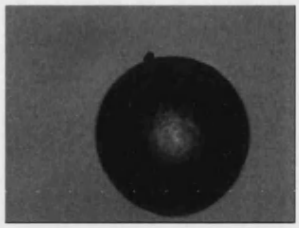

CIP method (solution 2)

Treated by membrane method

Figure 5.50 - CIP glass sample images (dark region is a bubble in the interlayer)

6 General Conclusions and summary discussion

6.1 Discussion of membrane manufacture details

The preparation of fibres from base spinning solutions of varied composition had the biggest effect on the median pore size. The variation was small with fibres that exhibited mean sizes from 0.2 to 0.5μm being prepared.

Summarising the effect of variables in the coating of the porous ceramic membranes used in this study there are some key points that arise. Firstly a lot of time and effort was spent attempting to influence the structure of the membrane at the surface in order to make a defect free membrane by means of a simple dipping technique. It was hoped to limit maximum pore size without restricting the median pore size. This proved difficult to achieve consistently owing to the delicate nature of coatings prior to sintering. However it was concluded that there was direct evidence for minimising of maximum pore size. Adding PVA to the dip coating mixture made the coating far more difficult to work with due to foaming when handling the liquid and bubbles at the surface then being trapped within the applied coating. The bubble issue tended to only affect a short section of fibre (around 1cm) which had been near the dip coating solution surface. PVA based coatings did however provided a rigid coating that remained adhered to membrane surfaces. Time limitations prevented extensive testing of these coatings but the successful operation of modules that used these fibres suggested that this technique improved consistency of coatings. Three of 5 modules made without a PVA based coating leaked at low gas side pressure (discounting module 1 which was used only for commissioning systems). All three modules made with a PVA based coating did not leak unless the pressure was turned up beyond 3 barg or higher. The lack of results from these modules owes more to the difficulties in achieving any measurable mass transfer in the ceramic units. The coatings that were studied in detail did little to alter mean (median) pore size, this was the intended result in order to maintain a maximum open surface area for contact.

6.2 Ceramic module mass transfer

The mass transfer achieved in the ceramic units was apparently poor with silicate solutions, compared to the polymeric module the mass transfer coefficient was significantly lower, this coupled with the lower mass transfer area per unit volume made the units far less effective at removing dissolved gas. This difference has a phenomenal impact on the removal of dissolved gas per unit time in a recycle system. Time is a serious issue in industrial application particularly in a batch process. In this system the only way to lower the time to the same order as a polymeric unit is to have a ceramic unit of several times the area.

If one assumes the experimentally observed rate of desorption in ceramic modules was accurate (i.e it was not unrealistically low due to the fibre being blocked while assumed to be clean) then the module would need to be 25 times the size (in volume terms) of a ceramic unit at least to approach the same mass transfer area. If one assume that the mass transfer coefficient could be the same in ceramic modules (compared to the polymeric module) then one would still need a unit some 4 times larger (in volume terms). Such units would be far more expensive. Put in stark terms the polymeric fibres are both more effective by mass transfer area and have significantly more area per unit volume.

The question must be asked then as to why the ceramic modules appeared to perform so poorly (assuming the silicate solution data observed is correct for a clean un-blocked module). Firstly their performance in water is apparently similar to the polymeric module this suggests some sort of performance drop related to the nature of the liquid tested.

It is already known that there was an issue with cleaning the units due to the liquid penetrating into the membrane wall unless very careful cleaning was performed the solution would dry in place and block the unit.

Assuming cleaning was effective, it is possible an extent of blocking occurred during the runs. This is because the immobilisation of the liquid in the pores during a run could also lead to drying of the solution. A gas flow next to an immobilised solution will inevitably evaporate some of the solvent, if this is the case the solids would come

out of suspension and block the membrane. It was observed that some water was ejected from the gas side of the membrane during runs, this supports the theory that water was being evaporated as the whole solution would have come through if the membrane was damaged. Finally the ceramic unit was laid out in a counter current mode. As alluded to in the review of literature a cross flow system is significantly better for achieving mass transfer. The polymeric unit used was a cross flow unit.

It was expected that the static fluid layer would impact negatively on mass transfer rate. It was planned to counteract this by driving the interface back across the membrane by control of gas side pressure. This was demonstrated by the most influential variable by far being the gas side operating pressure. It was demonstrated that the interface could be moved but at a certain point one gained little further movement of the interface and ran the risk of breakthrough of gas into the liquid side of the unit. In the units where sufficient data was obtained the movement was enough to leave the membrane wall 60-70% gas filled. The remaining 30-40% (of liquid filled wall) was still a very significant resistance to mass transfer. It is noted again however that the results with water must be taken at face value but may have been boosted by minute amounts of leaking gas.

The measurement of mass transfer was difficult in these units owing to their small size. Larger units would have achieved more transfer and led to the possibility of more results being generated. Figure 5.31 aptly shows that an experiment of nearly three hours in the original set-up yielded a drop in DO of barely 2-3% measuring such small changes when the oxygen probe reading varies by similar or larger amounts introduces error, clearly all that could be done with this data was to look at a general trend. The result was to work with smaller volumes where less time is taken to observe a significant concentration change.

6.3 Polymeric module mass transfer

Using the polymeric module was by far the simplest system to operate which is a significant engineering benefit. That said it is noted that a sparge and ultrasound system could potentially be cheaper and simpler dependant on the cost of ultrasonic

equipment. Cost of course being another key consideration industrially. The two systems both performed well in mass transfer studies but the polymeric module could potentially outperform the sparge system at very high liquid flow rates. As in most cases there was some relationship between liquid rate and mass transfer coefficient. The dependence on liquid flow was however not a significant as expected. It is also noted that at high rates of liquid flow there is such a pressure drop across the module that outlet pressure is not sufficient to prevent gas breakthrough (recalling that in the polymeric module it is important to retain a higher liquid pressure than gas pressure unlike in the ceramic modules). This is however a physical limitation of the module which is most likely designed for less dense and less viscous fluids. Hence a design which is less densely populated with fibres may achieve lower pressure drop. The drawback of this would be a larger unit for the same membrane surface area.

6.4 Sparge and ultrasound mass transfer

The sparge and ultrasound method presented itself unexpectedly during testing and outperformed modules slightly within the range of operation tested. On the principle of mass transfer per unit volume of the unit the performance was of a similar order to a polymeric module but as was noted in the results section higher liquid flows were easily achievable with the polymeric module while higher gas flows in the sparge system risked flooding. Further study of this system is desirable. The main issues with the method scientifically are the complex problem of balancing the loop in which DO measurement is carried out. There is a need to extract a two phase flow (principally a gas entrained as fine bubbles in a liquid) this gas and liquid are then separated by ultrasonic treatment. The liquid must then be fed back to the main tank, The main tank must be sealed or under positive sweep gas pressure to exclude air. The system is therefore needs an active control system in order to balance feed and take from the main tank as the system used here relied on positive pressure to drive the liquid and gas mixture out of the tank via a dip-leg and needed manual control of a pump to feed liquid back to the tank.

6.5 Method comparison

To conclude on method types – the ceramic modules may offer a significant benefit in chemical resistance in the long term but based on their performance in the silicate solution they were unable to match the performance of either the polymeric membrane system or the sparge and ultrasound system. The ceramic membranes are an order of magnitude less effective when compared by unit volume of the mass transfer device (K_la, based on silicate solution). As discussed however is it believed the high solids content and the general nature of the solution tended to restrict the effectiveness of the ceramic membranes due to blocking the pores. The ceramic membrane units performance in water suggests it would find application in alternative systems where there was low or zero solids content. The polymeric module performs well and is the simplest to operate and control. The doubts over chemical resistance remain but no degradation of the unit has been observed in the several runs made. The sparge and ultrasound system is also simple to operate (if no DO measurement is made) but flooding still imposes a limit on conditions. Significant improvements in the system can be made including better gas distribution but this is beyond the scope of this project. As such the polymeric module is concluded to be the best system with the following reservations.

- Chemical resistance needs to be investigated further but it appears the issues with chemical resistance in the polymeric unit do not appear as severe as expected.
- Ultrasound with sparging could be improved upon significantly with equipment directly designed for this operation
- The ceramic system could still be valid but only if the ceramic membrane can be made hydrophobic

None of the methods are suitable for the primary application based on the glass casting results. It would seem that far more removal of dissolved gas is necessary and hence a very large membrane unit could be required and it is still not proved that a membrane can sufficiently remove dissolved nitrogen. In addition The current method of gas blanketing has a relatively competitive value of surface area to volume ratio at around 300-500 m^2/m^3 compared to 500-1000 m^2/m^3 for ceramic modules only the polmeric modules at up to 3000-4000 m^2/m^3 have significantly more. The fact there is relative simplicity in the current method is a big advantage when handling such difficult material.

6.6 Liquids comparison

As expected the mass transfer coefficient in water was better than in all the other solutions. The silicate solutions all performed similarly which was slightly unexpected – the solutions with higher concentrations of silicate material and hence higher viscosity were expected to experience lower mass transfer but did not significantly. The potassium silicate was the only silicate type solution that performed significantly differently and it was visually observed that this solution was more viscous than any other despite the quoted viscosities from the project sponsor. The same liquid was used in the glass casting experiments and the liquid was visually less viscous than the batch used in mass transfer tests. No detailed mass transfer data was obtainable at the time of these tests so performance of the less viscous batch cannot be confirmed. The viscosity affects mass transfer by allowing thicker and hence more resistive boundary layers to exist which reduces the mass transfer rate. The solutions which were based on suspended solids performed somewhere in between water and the silicate solutions. That they did better than the silicate solutions is due to their lower viscosity, their performance was less good than water due to the solids content raising the viscosity slightly above that of water and the solids providing the possibility of extra surface to allow a greater boundary layer resistance. In effect the solids foul the surface of the membrane/or gas bubble and provide an aggregate in the solution to create a more robust boundary region.

6.7 Glass casting results

The inability to produce glass free of interlayer bubbles using the pour and dry method and the Tek-dry method are attributed to significant exposure to the atmosphere. The reasons for not being able to produce defect free inter-layers using the CIP method is more mysterious and is only explained by three possibilities.

Firstly the unlikely possibility that the reaction between the mixtures prevents any mass transfer taking place – this can essentially be ruled out as not being possible as

an explanation as there must be mass transfer between the gas and liquid provided there is some dissolved gas present in the liquid.

Secondly, simply the value of $(DN/DN_{max}) = 0.1$ was not low enough. This too seems unlikely as even if it was not 'low enough' then there should have been few bubbles in the coating layer rather than the large quantities that were observed.

The third and final possibility is that as the concentration could not be measured during these tests the time that the system was run for was insufficient because mass transfer was taking place more slowly than in other solutions. It is noted that the CIP solutions were cloudy and hence the level of entrained bubbles caused by fluid transfer, splashing etc was not clear. Large bubbles 1-2mm would have been detectable in the casting process but experience of the solutions suggests there could have been bubbles of smaller size present which would not necessarily have been detected.

The critical value of (DN/DN_{max}) is a significant unknown in the process and is a valuable figure to determine. This figure and the absolute values of DN in each solution are also values that would be of immense value.

6.8 Final summary

The performance of polymeric and ceramic modules was studied in a viscous liquid / gas system. The performance of the polymeric module suggests that this is a viable technology for rapid transfer of solutes to or from a viscous liquid. The ceramic modules suffer enormously from the mass transfer penalty imposed by having a stagnant region of liquid in the pore structure of the membrane. The application of this method with regard to this project was to remove DN from glass coating solutions. By analysis of a measurable dissolved gas it was shown that dissolved gas removal was achieved however the final result when the coating was used was not successful. It is believed that the reasons for this were down to the environment of transfer of the liquid from the system to the glass where exposure to air was not avoided. One system did achieve this but results were still unsuccessful the reasons

for this are unclear but are believed to be related to difficulties in removing dissolved gas from the particular combination of fluids and that the solution was not necessarily degassed to a sufficient extent. The use of membranes for this application is only recommended when the absolute dissolved gas removal duty is defined and the method of transfer of liquid from the membrane to the glass without exposure to atmosphere is fully designed. The system performance can then be re-assessed and the potential can be further established.

The ceramic membranes produced were shown to be able to remove dissolved gas from water and would find useful application in chemically aggressive systems with low or zero solids content and similar density and viscosity to water. The value of the product must also be high in order to balance the high cost of ceramic membranes.

The solutions used were able to show that membrane phase contacting in general can be used to remove dissolved gases from such solutions however the colloidal silicate solutions present a difficult challenge particularly in the ceramic membranes. The neutral silica sols showed themselves to be essentially as easy to de-gas as water despite their high solids content. This is due to their lower viscosity and the dense nature of the silica solids when compared to the colloidal silicates.

7 Future Work

Dip coating of membranes was identified as a method to remove or eliminate defects in membrane surfaces – using the solvent which was used in the original spinning of the fibre as a solvent in the dipping solution was attempted but presented problems with destroying the fibre. The results that were obtained hinted at the possibility of an appreciable alteration of the membrane pore size as such investigation of a diluted solvent based dip coating solution which does not seriously damage the overall structure could be of value.

The principal cause of poor mass transfer in the ceramic membranes was identified as the liquid filled region in the membrane wall. This is despite the fact that the liquid filled region could be minimised by elevating gas side pressure. As such making a hydrophobic ceramic membrane is the only serious alternative method for limiting or preventing liquid intrusion into the membrane wall. The process for production of such a membrane should be considered in future work.

The method of driving back the membrane interface is feasible if a far smaller pore diameter is used, this may impinge on the open area for gas liquid contact but a thin layer of pores an order of magnitude smaller than the rest of the membrane should allow a simple to manage fixed interfacial position owing to the high gas side pressure that could be comfortably used without risk of gas breakthrough.

Glass casting methods are difficult to control without clouding the performance of the membrane system, if one blankets the glass while casting and during the phase of the process where the solution forms a film then one can argue that the mass transfer based desorbtion is performed by the gas blanket. As such definition of the level of DN required for the system to work is necessary and then if this level is achieved using the unit the blanket can be applied during coating safe in the knowledge the bulk of the desorbtion duty was carried out by the membrane and with confidence the time for which the liquid is prevented from forming a film can be shortened.

The sparge and ultrasound method performed well (i.e. the kinetics of the mass transfer were fast) and is worthy of further investigation particularly to determine how well ultrasound removes bubbles from the liquid visually the liquid is clear but could there be tiny micro-bubbles present or even caused by the act of ultrasound at some frequencies.

A measurement directly of DN would be desirable, a best alternative would be a measurement of DO or another tracer substance that is not so sensitive to liquid stirring velocity, or trapped bubbles in the liquid. A development of such a technique is worthy of study as failure of the measurement of DO in the viscous liquid due to stirring failing or bubbles becoming trapped on the probe caused more abandoned experiments than any other problem encountered in the study.

A system of measuring mass transfer of dissolved gas out of the solutions when spread on glass would be a useful measure of the existing system's performance. Key obstacles to this are measuring DO or DN in a static liquid without any mixing permitted.

Finally a method of confidently establishing weather gas is leaked into the liquid side of the system must be assessed since in water it was not at all apparent unless there was a significant rate of gas flux. In silicate solution there would be no clear evidence other than a gradual increase in the number of apparent bubbles in the main tank. Given it is almost impossible to start with zero bubbles (due to splashing when handling the liquid) it is a very difficult observation to make.

8 Nomenclature

Table 8.1 details the symbols used in this work, in some cases specific subscripts are included for more general subscripts refer to Table 8.2

Table 8.1 - List of symbols

A	area
BP/GP	parameter as defined in section 5.1.1
C	concentration
D	diffusivity
d	diameter
Gr	Grasshof number ($d^2 v /Dl$)
H	Henry law constant
k	mass transfer coefficient
K	overall mass transfer coefficient
K	permeability coefficient
l	length
L	Length
M	Molecular weight
n	flux
p	pressure (partial pressure when indicated)
p_w	wetted perimeter
Q	volumetric flow rate
r	radius
R	universal gas constant
Re	Reynolds number (dv/υ)
Sc	Schmidt number (υ/D)
Sh	Sherwood number (kd/D)
t	time
T	temperature
u	axial velocity
v	velocity (radial where relevant)
V	volume
x	axial location from reference

α	contact angle
β_v	Parameter introduced in equation 3.18
δ	thickness (of membrane wall or layer within)
ε	porosity
ρ	density
σ	surface tension
τ	tortuosity
μ	dynamic viscosity
υ	kinematic viscosity

Table 8.2 – List of subscripts

0	inlet
A	component A
b	of the bulk
c	cross section
e	effective
e	exit (outlet)
g	gas phase
G	gas phase
i	component i
i	inner
l	liquid phase
L	liquid phase
m	of the membrane
o	outer
p	of a pore
t	of the tube
T	of the batch tank

Note in some cases subscripts are coupled, for example, p_{igb} refers to partial pressure of component i in the gas phase bulk region while p_{igm} refers to the partial pressure of component i in the gas filled portion of the membrane.

9 Bibliography

1. Fair, J.R., Steinmeyer D.E., Penney W.R., Crocker B.B., *Gas Absorption and Gas-Liquid System Design*, in *Perry's Chemical Engineers' Handbook*, R.H. Perry, Green, Don W., Maloney, James O, Editor. 1997, McGraw-Hill. p. 14-23 - 14-98.

2. Lee, J.C., *Gas-Liquid and Gas-Liquid-Solid Reactors*, in *Coulson & Richardson's Chemical Engineering*, J.F. Richardson, Peacock, D.G., Editor. 1994, Elsevier Science Limited. p. 196-197.

3. Gabelman, A. and S.T. Hwang, *Hollow fiber membrane contactors.* Journal of Membrane Science, 1999. **159**(1-2): p. 61-106.

4. Holden, D.W.,8th May 2003. *Silicate Solution Data.* E-mail to: B. Darragh.

5. Zhang, Q. and E.L. Cussler, *Microporous Hollow Fibers for Gas-Absorption .1. Mass-Transfer in the Liquid.* Journal of Membrane Science, 1985. **23**(3): p. 321-332.

6. Wickramasinghe, S.R., M.J. Semmens, and E.L. Cussler, *Better Hollow Fiber Contactors.* Journal of Membrane Science, 1991. **62**(3): p. 371-388.

7. Zhang, Q. and E.L. Cussler, *Microporous Hollow Fibers for Gas-Absorption .2. Mass-Transfer across the Membrane.* Journal of Membrane Science, 1985. **23**(3): p. 333-345.

8. Schoner, P., P. Plucinski, W. Nitsch, and U. Daiminger, *Mass transfer in the shell side of cross flow hollow fiber modules.* Chemical Engineering Science, 1998. **53**(13): p. 2319-2326.

9. Wickramasinghe, S.R., M.J. Semmens, and E.L. Cussler, *Mass-Transfer in Various Hollow Fiber Geometries.* Journal of Membrane Science, 1992. **69**(3): p. 235-250.

10. Wickramasinghe, S.R., M.J. Semmens, and E.L. Cussler, *Hollow-Fiber Modules Made with Hollow-Fiber Fabric.* Journal of Membrane Science, 1993. **84**(1-2): p. 1-14.

11. Yang, M.C. and E.L. Cussler, *Artificial Gills.* Journal of Membrane Science, 1989. **42**(3): p. 273-284.

12. Yang, M.C. and E.L. Cussler, *Designing Hollow-Fiber Contactors.* Aiche Journal, 1986. **32**(11): p. 1910-1916.

13. Bowen, W.R., *Membrane Separation Processes*, in *Coulson & Richardson's Chemical Engineering*, J.M. Coulson, Richardson, J.F., Backhurst, J.R., Harker, J.H., Editor. 1998, Butterworth-Heinemann: Bath, England. p. 885-889.

14. Kiani, A., R.R. Bhave, and K.K. Sirkar, *Solvent-Extraction with Immobilized Interfaces in a Microporous Hydrophobic Membrane.* Journal of Membrane Science, 1984. **20**(2): p. 125-145.

15. Prasad, R., S. Khare, A. Sengupta, and K.K. Sirkar, *Novel Liquid-in-Pore Configurations in Membrane Solvent-Extraction.* Aiche Journal, 1990. **36**(10): p. 1592-1596.

16. Prasad, R. and K.K. Sirkar, *Solvent-Extraction with Microporous Hydrophilic and Composite Membranes.* Aiche Journal, 1987. **33**(7): p. 1057-1066.

17. Shindo, M.Y., Takashi. Kamada, Kensuke, *Gas transfer process with hollow fiber membrane.* 1981: United States.

18. Costello, M.J., A.G. Fane, P.A. Hogan, and R.W. Schofield, *The Effect of Shell Side Hydrodynamics on the Performance of Axial-Flow Hollow-Fiber Modules.* Journal of Membrane Science, 1993. **80**(1-3): p. 1-11.

19. Crowder, R.O. and E.L. Cussler, *Mass transfer in hollow-fiber modules with non-uniform hollow fibers.* Journal of Membrane Science, 1997. **134**(2): p. 235-244.

20. Dindore, V.Y. and G.F. Versteeg, *Gas-liquid mass transfer in a cross-flow hollow fiber module: Analytical model and experimental validation.* International Journal of Heat and Mass Transfer, 2005. **48**(16): p. 3352-3362.

21. Kim, K.J., A.G. Fane, R. Benaim, M.G. Liu, G. Jonsson, I.C. Tessaro, A.P. Broek, and D. Bargeman, *A Comparative-Study of Techniques Used for Porous Membrane Characterization - Pore Characterization.* Journal of Membrane Science, 1994. **87**(1-2): p. 35-46.

22. Koros, W.J. and G.K. Fleming, *Membrane-Based Gas Separation.* Journal of Membrane Science, 1993. **83**(1): p. 1-80.

23. Hernandez, A., J.I. Calvo, P. Pradanos, and F. Tejerina, *Pore size distributions in microporous membranes. A critical analysis of the bubble point extended method.* Journal of Membrane Science, 1996. **112**(1): p. 1-12.

24. Ho, W.S.W. and K.K. Sirkar, eds. *Membrane Handbook.* Membrane Handbook, ed. . 1992, Chapman and Hall: New York.

25. *Product Tour* [Online]. Available from: http://www.liqui-cel.com/page.cfm?page=tour [Accessed 19th September 2005]

26. *Hollow Fiber Membranes - Overview* [Online]. Available from: http://www.kochmembrane.com/prod_hf.html [Accessed 19th September 2005]

27. *Microfiltration - Filtration Overview* [Online]. Available from: http://www.kochmembrane.com/sep_mf.html [Accessed 19th September 2005]

28. *Standard / Lab / Pharmaceutical Products* [Online]. Available from: http://www.microdyntech.com/ [Accessed 19th September 2005]

29. *Product List* [Online]. Available from: http://direct.millipore.com/catalogue.nsf/webitemlist?open&search_criteria=cat_id%3D68LPWW [Accessed 19th September 2005]

30. *Products* [Online]. Available from: http://www.ceparation.com/ceramic-membranes-1.html [Accessed 19th September 2005]

31. Xu, H., X. Jian, T.T. Meek, and Q. Han, *Degassing of molten aluminum A356 alloy using ultrasonic vibration.* Materials Letters, 2004. **58**(29): p. 3669-3673.

32. Meidani, A., *A study of hydrogen bubble growth during ultrasonic degassing of Al-Cu alloy melts.* Journal of materials processing technology, 2004. **147**(3): p. 311-320.

33. Mulder, M., *Basic Priciples of Membrane Technology.* 2nd ed. 1996: Kluwer Academic Publishers. 12-13.

34. Mulder, M., *Basic Priciples of Membrane Technology.* 2nd ed. 1996: Kluwer Academic Publishers. 71-88.

35. Gore, R.W., *Very highly stretched polytetrafluoroethylene and process therefor.* 1976: United States.

36. Loeb, S. *Pressure-retarded osmosis revisited: the prospects for osmotic power at the Dead sea.* in *Euromembrane '95.* 1995. University of Bath, United Kingdom: European Society for Membrane Science and Technology.

37. Loeb, S., L. Titelman, E. Korngold, and J. Freiman, *Effect of porous support fabric on osmosis through a Loeb-Sourirajan type asymmetric membrane.* Journal of Membrane Science, 1997. **129**(2): p. 243-249.

38. Moreno, R., *The Role of Slip Additives in Tape-Casting Technology .1. Solvents and Dispersants.* American Ceramic Society Bulletin, 1992. **71**(10): p. 1521-1531.

39. Descamps, M., M. Mascart, B. Thierry, and D. Leger, *How to Control Cracking of Tape-Cast Sheets.* American Ceramic Society Bulletin, 1995. **74**(3): p. 89-92.

40. Hotza, D. and P. Greil, *Aqueous Tape Casting of Ceramic Powders.* Materials Science and Engineering a-Structural Materials Properties Microstructure and Processing, 1995. **202**(1-2): p. 206-217.

41. Liu, S.M., X.Y. Tan, K. Li, and R. Hughes, *Preparation and characterisation of SrCe0.95Yb0.05O2.975 hollow fibre membranes.* Journal of Membrane Science, 2001. **193**(2): p. 249-260.

42. Terpstra, R.A., J.P.G.M. Van Eijk, and F.K. Feenstra, *Method for the production of ceramic hollow fibres.* 1998: United States.

43. Brinkman, H.W., J. van Eijk, H.A. Meinema, and R.A. Terpstra, *Innovative hollow fiber ceramic membranes.* American Ceramic Society Bulletin, 1999. **78**(12): p. 51-55.

44. Wang, D., K. Li, and W.K. Teo, *Polyethersulfone hollow fiber gas separation membranes prepared from NMP/alcohol solvent systems.* Journal of Membrane Science, 1996. **115**(1): p. 85-108.

45. Wang, D., K. Li, and W.K. Teo, *Porous PVDF asymmetric hollow fiber membranes prepared with the use of small molecular additives.* Journal of Membrane Science, 2000. **178**(1): p. 13-23.

46. Wang, D., K. Li, and W.K. Teo, *Preparation of poly(ether sulfone) and poly(ether imide) hollow fiber membranes for gas separation: Effect of interval coagulant*, in *Membrane Formation and Modification.* 2000. p. 96-109.

47. Li, K., J.F. Kong, D. Wang, and W.K. Teo, *Tailor-made asymmetric PVDF hollow fibers for soluble gas removal.* AIChE Journal, 1999. **45**(6): p. 1211-1219.

48. Deshmukh, S.P. and K. Li, *Effect of ethanol composition in water coagulation bath on morphology of PVDF hollow fibre membranes.* Journal of Membrane Science, 1998. **150**(1): p. 75-85.

49. Kong, L.F. and K. Li, *Preparation of PVDF hollow-fiber membranes via immersion precipitation.* Journal of Applied Polymer Science, 2001. **81**(7): p. 1643-1653.

50. Albrecht, W., K. Kneifel, T. Weigel, R. Hilke, R. Just, M. Schossig, K. Ebert, and A. Lendlein, *Preparation of highly asymmetric hollow fiber membranes from poly(ether imide) by a modified dry-wet phase inversion technique using a triple spinneret.* Journal of Membrane Science, 2005. **262**(1-2): p. 69-80.

51. Tai-Shung Chung, Z.-L.X., Wenhui Lin,, *Fundamental understanding of the effect of air-gap distance on the fabrication of hollow fiber membranes.* Journal of Applied Polymer Science, 1999. **72**(3): p. 379-395.

52. Barth, C., M.C. Goncalves, A.T.N. Pires, J. Roeder, and B.A. Wolf, *Asymmetric polysulfone and polyethersulfone membranes: effects of thermodynamic conditions during formation on their performance.* Journal of Membrane Science, 2000. **169**(2): p. 287-299.

53. Mulder, M., *Basic Priciples of Membrane Technology.* 2nd ed. 1996: Kluwer Academic Publishers. 99-104.

54. Yeow, M.L.,September 2002. *Personal Communication.* Discussion with: B. Darragh.

55. Li, K.,August 2002. *Personal Communication.* Discussion with: B. Darragh.

56. Tan, X., S. Liu, and K. Li, *Preparation and characterization of inorganic hollow fiber membranes.* Journal of Membrane Science, 2001. **188**(1): p. 87-95.

57. Loeb, S., *The Loeb-Sourirajan Membrane - How It Came About.* Abstracts of Papers of the American Chemical Society, 1980. **180**(AUG): p. 1-9.

58. Reuvers, A.J., J.W.A. Vandenberg, and C.A. Smolders, *Formation of Membranes by Means of Immersion Precipitation .1. A Model to Describe Mass-Transfer During Immersion Precipitation.* Journal of Membrane Science, 1987. **34**(1): p. 45-65.

59. Reuvers, A.J. and C.A. Smolders, *Formation of Membranes by Means of Immersion Precipitation .2. The Mechanism of Formation of Membranes Prepared from the System Cellulose-Acetate Acetone Water.* Journal of Membrane Science, 1987. **34**(1): p. 67-86.

60. Smolders, C.A., A.J. Reuvers, R.M. Boom, and I.M. Wienk, *Microstructures in Phase-Inversion Membranes .1. Formation of Macrovoids.* Journal of Membrane Science, 1992. **73**(2-3): p. 259-275.

61. Boom, R.M., I.M. Wienk, T. Vandenboomgaard, and C.A. Smolders, *Microstructures in Phase Inversion Membranes .2. The Role of a Polymeric Additive.* Journal of Membrane Science, 1992. **73**(2-3): p. 277-292.

62. Cabasso, I., E. Klein, and J.K. Smith, *Polysulfone Hollow Fibers .1. Spinning and Properties.* Journal of Applied Polymer Science, 1976. **20**(9): p. 2377-2394.

63. Cabasso, I., E. Klein, and J.K. Smith, *Polysulfone Hollow Fibers .2. Morphology.* Journal of Applied Polymer Science, 1977. **21**(1): p. 165-180.

64. Yamasaki, A., R.K. Tyagi, A.E. Fouda, T. Matsuura, and K. Jonasson, *Effect of gelation conditions on gas separation performance for asymmetric polysulfone membranes.* Journal of Membrane Science, 1997. **123**(1): p. 89-94.

65. Yamasaki, A., R.K. Tyagi, A.E. Fouda, T. Matsuura, and K. Jonasson, *Effect of solvent evaporation conditions on gas separation performance for asymmetric polysulfone membranes.* Journal of Applied Polymer Science, 1999. **71**(9): p. 1367-1374.

66. Mok, S., D.J. Worsfold, A.E. Fouda, T. Matsuura, S. Wang, and K. Chan, *Study on the Effect of Spinning Conditions and Surface-Treatment on the Geometry and Performance of Polymeric Hollow-Fiber Membranes.* Journal of Membrane Science, 1995. **100**(3): p. 183-192.

67. Pinnau, I. and W.J. Koros, *Influence of Quench Medium on the Structures and Gas Permeation Properties of Polysulfone Membranes Made by Wet and Dry Wet Phase Inversion.* Journal of Membrane Science, 1992. **71**(1-2): p. 81-96.

68. Pesek, S.C. and W.J. Koros, *Aqueous Quenched Asymmetric Polysulfone Hollow Fibers Prepared by Dry Wet Phase-Separation.* Journal of Membrane Science, 1994. **88**(1): p. 1-19.

69. Pesek, S.C. and W.J. Koros, *Aqueous Quenched Asymmetric Polysulfone Membranes Prepared by Dry Wet Phase-Separation.* Journal of Membrane Science, 1993. **81**(1-2): p. 71-83.

70. Lafreniere, L., M., *Effect of polyvinylpyrrolidone additive on the performance of polyethersulfone ultrafiltration membranes.* Industrial & engineering chemistry research, 1987. **26**(11): p. 2385-2389.

71. Wang, D.L., K. Li, and W.K. Teo, *Polyethersulfone hollow fiber gas separation membranes prepared from NMP/alcohol solvent systems.* Journal of Membrane Science, 1996. **115**(1): p. 85-108.

72. Wang, D., *Phase-Separation Phenomena of Polysulfone Solvent Organic NonsolventT and Polyethersulfone Solvent Organic Nonsolvent Systems.* Journal of applied polymer science, 1993. **50**(10): p. 1693-1700.

73. Khayet, M., C.Y. Feng, K.C. Khulbe, and T. Matsuura, *Preparation and characterization of polyvinylidene fluoride hollow fiber membranes for ultrafiltration.* Polymer, 2002. **43**(14): p. 3879-3890.

74. Khayet, M. and T. Matsuura, *Preparation and characterization of polyvinylidene fluoride membranes for membrane distillation.* Industrial & Engineering Chemistry Research, 2001. **40**(24): p. 5710-5718.

75. Yeow, M.L., Y.T. Liu, and K. Li, *Preparation of porous PVDF hollow fibre membrane via a phase inversion method using lithium perchlorate (LiClO4) as an additive.* Journal of Membrane Science, 2005. **258**(1-2): p. 16-22.

76. Liu, Y., Xiaoyao Tan, K. Li,, *SrCe0.95Yb0.05O3-alpha hollow-fiber membrane and its property in proton conduction.* AIChE journal, 2006. **52**(4): p. 1577-1585.

77. Liu, S.M., K. Li, and R. Hughes, *Preparation of porous aluminium oxide (Al2O3) hollow fibre membranes by a combined phase-inversion and sintering method.* Ceramics International, 2003. **29**(8): p. 875-881.

78. Tan, X.Y., S.M. Liu, and K. Li, *Preparation and characterization of inorganic hollow fiber membranes.* Journal of Membrane Science, 2001. **188**(1): p. 87-95.

79. Smid, J., C.G. Avci, V. Gunay, R.A. Terpstra, and J. VanEijk, *Preparation and characterization of microporous ceramic hollow fibre membranes.* Journal of Membrane Science, 1996. **112**(1): p. 85-90.

80. Hsieh, H.P., *Inorganic Membrane Reactors.* Catalysis Reviews-Science and Engineering, 1991. **33**(1-2): p. 1-70.

81. Falamaki, C., *Dip-coating technique for the manufacture of alumina microfilters using PVA and Na-CMC as binders: a comparative study.* Journal of the European Ceramic Society, 2006. **26**(6): p. 949-956.

82. Pan, X.L., N. Stroh, H. Brunner, G.X. Xiong, and S.S. Sheng, *Deposition of sol-gel derived membranes on alpha-Al2O3 hollow fibers by a vacuum-assisted dip-coating process.* Journal of Membrane Science, 2003. **226**(1-2): p. 111-118.

83. Okubo, T., K. Haruta, K. Kusakabe, S. Morooka, H. Anzai, and S. Akiyama, *Preparation of a Sol-Gel Derived Thin Membrane on a Porous Ceramic Hollow Fiber by the Filtration Technique.* Journal of Membrane Science, 1991. **59**(1): p. 73-80.

84. Yasuda, H. and J.T. Tsai, *Pore Size of Microporous Polymer Membranes.* Journal of Applied Polymer Science, 1974. **18**(3): p. 805-819.

85. Hopfinger, E.J. and M. Altman, *Experimental Verification of the Dusty-Gas Theory for Thermal Transpiration through Porous Media.* The Journal of Chemical Physics, 1969. **50**(6): p. 2417.

86. Mulder, M., *Basic Priciples of Membrane Technology.* 2nd ed. 1996, Dordrect: Kluwer Academic Publishers. 157-187.

87. Jakobs, E. and W.J. Koros, *Ceramic membrane characterization via the bubble point technique.* Journal of Membrane Science, 1997. **124**(2): p. 149-159.

88. Rocek, J. and P. Uchytil, *Evaluation of Selected Methods for the Characterization of Ceramic Membranes.* Journal of Membrane Science, 1994. **89**(1-2): p. 119-129.

89. Crowshaw, D.,25th February 2004. *GC suitability.* E-mail to: B. Darragh.

90. *Hach Ultra Analytics* [Online]. Available from: www.orbisphere.com [Accessed 30th September 2005]

91. Spencer, N.,19th January 2004. *Dissolved Nitrogen.* E-mail to: B. Darragh.

92. McNeil, C.L., B.D. Johnson, and D.M. Farmer, *In-Situ Measurement of Dissolved Nitrogen and Oxygen in the Ocean.* Deep-Sea Research Part I-Oceanographic Research Papers, 1995. **42**(5): p. 819-826.

93. Lide, D.R., ed. *CRC Handbook of Chemistry and Physics.* 86th ed. 2005, CRC Press: Boca Raton, FL.

94. Skelland, A.H.P., *Diffusional Mass Transfer.* 1974, New York: Wiley-Interscience. 142-176.

95. Heaton, H., H.S., *Heat transfer in annular passages -- Simultaneous development of velocity and temperature fields in laminar flow.* International journal of heat and mass transfer, 1964. **7**(7): p. 763-781.

96. Siegel, R., R., *Steady laminar heat transfer in circular tube with prescribed wall heat flux.* Applied scientific research, 1958. **7**(5): p. 386-392.

97. Goldberg, P., *M. S. Thesis*, in *Department of Mechanical Engineering.* 1958, Massachusetts Institute of Technology.

98. Leveque, J., Amm. Mines, 1928. **13**(12).

99. Smith, J.M., *Chemical Engineering Kinetics.* 3rd ed. 1981, New York: McGraw-Hill. 197-208.

Appendix I – Furnace Programs and Programming

Furnace programming commands:

Ramp t – A timed ramp in temperature, inputs are target temperature and intended duration in minutes

Ramp r – A ramp in temperature with a designated ramp rate, inputs include a ramp rate in °C/min and a target temperature

Dwell – A timed period at a sustained temperature inputs include a duration in minutes. The temperature will be that at the end of the previous instruction.

End – There are various end types including 'end dwell' (select type: dwell)which results in the final temperature being maintained indefinitely until further instruction and 'end stop' (select type: stop) which terminates all heating control.

Notes on furnace programs:

A typical furnace program will used in this study tries to achieve the desired maximum temperature in as fast a time as is possible in the furnace used. Due to the nature of the furnace this heating rate or 'ramp rate' is quite low and results in long furnace programs with apparently slow gentle heating. The maximum rate ever used in the furnace was 5.3 °C/min, though early in the study this was limited to 5 °C/min and later following a number of failures of key parts in the furnace notably the work tube and the platinum based thermocouples the limit was established at 4°C/min.

Due to these rates a program conducting a 5 hour heating at the specified maximum temperature will take considerable time to complete its program. This is accentuated by the fact that beyond approximately 1000-1200 °C there is a need to slow the ramp rate as power cannot be supplied quickly enough to achieve the set rate of between 4 and 5.3 °C/min. Usually the rate is then lowered again at around 1300°C, finally cool down usually at the maximum rate of 4°C/min is only achieved down to a

temperature of circa. 800 °C, beyond this the controller continues to demand the set rate but insulation around the work tube prevents sufficient heat loss.

A typical program to 1500 °C would be as follows:

Table A1.1 – Typical furnace program

Step No	Start Temp	End Temp	Rate/Duration	Type
1	amb	1100	5.3	Ramp R
2	1100	1350	2.5	Ramp R
3	1350	1350	300	Dwell
4	1350	amb	5.3	Ramp R
5	amb	amb	-	End D

Below is a plot of how this program would look starting at ambient temperature matched to how the program actually performs

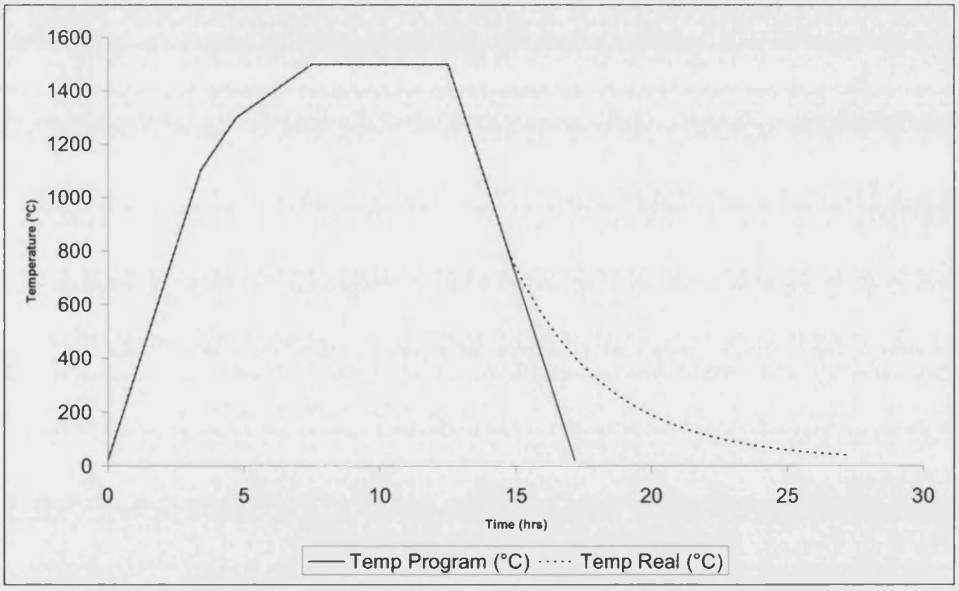

Figure A1.1 - Typical sintering program showing actual and real temperature

Appendix II – Spinning solution compositions

No.	Total	1NMP	2PES	3PEG(400)	4(1um)	5(0.3um)	6(0.01/0.02um)	7Citric Acid	8PVP
1	50.42	20.06	5.04	0	23.47	1.04	0.56	0	0.25
wt%	100	39.7858	9.996033	0	46.54899	2.06267	1.110670369	0	0.49583
2	50.19	19.83	5.03	0	22.04	2.03	1.01	0	0.25
wt%	100	39.50986	10.02192	0	43.91313	4.04463	2.012353058	0	0.49811
3	50.3	20.22	4.98	0	20.08	3.01	2.01	0	0
wt%	100	40.19881	9.900596	0	39.92048	5.9841	3.996023857	0	0
4	49.47	19.86	5.01	0	18.02	4.56	2.02	0	0
wt%	100	40.14554	10.12735	0	36.42612	9.21771	4.083282798	0	0
5	26.57	12.04	2.02	0	10.03	1.49	0.99	0	0
wt%	100	45.31426	7.602559	0	37.74934	5.60783	3.726006775	0	0
6	50.96	20.96	5.03	0	14.98	7.02	2.97	0	0
wt%	100	41.1303	9.870487	0	29.3956	13.7755	5.828100471	0	0
7	16.28	10.35	5.93	0	0	0	0	0	0
wt%	100	63.57494	36.42506	0	0	0	0	0	0
8	49.88	20.24	4.01	0	20.06	4.01	1.02	0	0.54
wt%	100	40.57739	8.039294	0	40.21652	8.03929	2.044907779	0	1.0826
9	54.72	20.01	8.3	1.59	9.82	12.97	2.03	0	0
wt%	100	36.56798	15.16813	2.905702	17.94591	23.7025	3.709795322	0	0
10	33.7	18.81	6.27	1.62	0	0	7	0	0
wt%	100	55.81602	18.60534	4.807122	0	0	20.77151335	0	0
11	48.47	19.02	6.34	1.5	20.01	0	0	1.6	0
wt%	100	39.24077	13.08026	3.094698	41.28327	0	0	3.3010109	0
12	56.87	18.66	6.22	0	0	0	31.99	0	0
wt%	100	32.81168	10.93723	0	0	0	56.251099	0	0
13	49.19	19.03	6.46	2.11	19.99	0	0	1.6	0
wt%	100	38.68672	13.13275	4.28949	40.63834	0	0	3.2526936	0
14	42	20	5	0	15	0	2	0	0
wt%	100	47.61905	11.90476	0	35.71429	0	4.761904762	0	0
15	357.72	133.91	33.49	3.34	148.47	31.95	6.56	0	0
wt%	100	37.43431	9.362071	0.933691	41.50453	8.93157	1.83383652	0	0
16	108.5	82	19.94	2.31	0	0	0	0	4.25
wt%	100	75.57604	18.37788	2.129032	0	0	0	0	3.91705
17	187.56	65	20	2.49	85.07	10.01	4.99	0	0
wt%	100	34.65558	10.66325	1.327575	45.35615	5.33696	2.660481979	0	0
18	202.51	80	20.02	2.51	85	9.99	4.99	0	0
wt%	100	39.50422	9.885932	1.239445	41.97324	4.93309	2.464075848	0	0
19	217.49	95	19.99	2.51	85	9.99	5	0	0
wt%	100	43.68017	9.191227	1.154076	39.08226	4.59331	2.298956274	0	0
20	232.44	110.01	20.01	2.51	84.92	9.99	5	0	0
wt%	100	47.32834	8.608673	1.079849	36.53416	4.29788	2.151092755	0	0
21	404.03	160.02	40	4.01	149.98	39.01	11.01	0	0
wt%	100	39.60597	9.900255	0.992501	37.12101	9.65522	2.72504517	0	0
22	404.46	160.01	40	4.45	160	30	10	0	0
wt%	100	39.56139	9.88973	1.100232	39.55892	7.4173	2.472432379	0	0
23	204.01	160.01	40	4	0	0	0	0	0
wt%	100	78.43243	19.60688	1.960688	0	0	0	0	0
24	52.97	32.12592	8.030979	0.803098	12.01	0	0	0	0
wt%	100	60.64928	15.16137	1.516137	22.67321	0	0	0	0
25	59.67	31.30238	7.825107	0.782511	19.76	0	0	0	0
wt%	100	52.45916	13.11397	1.311397	33.11547	0	0	0	0
26	69.61	27.569	6.891819	0.689182	34.46	0	0	0	0
wt%	100	39.60494	9.900616	0.990062	49.50438	0	0	0	0
27	150	75	25	0	0	30	20	0	0
wt%	100	50	16.66667	0	0	20	13.33333333	0	0
28	48.14	15.9061	3.976276	0.397628	27.86	0	0	0	0
wt%	100	33.04133	8.259817	0.825982	57.87287	0	0	0	0
29	200.01	75.01	25	0	100	0	0	0	0
wt%	100	37.50312	12.49938	0	49.9975	0	0	0	0
30	100	75	25	0	0	0	0	0	0
wt%	100	75	25	0	0	0	0	0	0
31	0	0	0	0	0	0	0	0	0
wt%									
32	0	0	0	0	0	0	0	0	0
wt%									
33	0	0	0	0	0	0	0	0	0
wt%									
34	270.03	120.02	30	0	120.01	0	0	0	0
wt%	100	44.44691	11.10988	0	44.44321	0	0	0	0
35	359.81	119.704	29.926	30	180.18	0	0	0	0
wt%	100.00	33.27	8.32	8.34	50.08	0.00	0.00	0.00	0.00
36	709.93	260.02	40	10.01	264.94	114.97	19.99	0	0

wt%	100	36.62615	5.634358	1.409998	37.31917	16.1946	2.815770569	0	0
37	729.95	260.08	80	10	319.87	39.99	20.01	0	0
wt%	100	35.62984	10.95965	1.369957	43.82081	5.47846	2.74128365	0	0
38	270	120	30	0	120	0	0	0	0
wt%	100	44.44444	11.11111	0	44.44444	0	0	0	0
39	360	130.01	40	0	159.99	20	10	0	0
wt%	100	36.11389	11.11111	0	44.44167	5.55556	2.777777778	0	0
40	300.02	120.01	29.99	0	120.02	30	0	0	0
wt%	100	40.00067	9.996	0	40.004	9.99933	0	0	0
41	329.91	120.01	30	0	179.9	0	0	0	0
wt%	100	36.37659	9.093389	0	54.53002	0	0	0	0

Appendix III – Start up and shut down procedures

Rig Preparation procedure

1. The equipment should be connected as shown in Figure 4.2 prior to spinning.
2. The outlet valves on the bottom of baths 1 and 2 should be closed and the three baths should be filled with the desired non-solvent, in this work the non-solvent is exclusively tap water the temperature can be raised using hot water if required. The temperatures should be noted.
3. The desired air gap should be set by positioning the outlet point of the spinnerette the desired distance above the surface of the non-solvent in bath 1.
4. The air stop valve prior the solution tank should be closed and the desired air pressure to drive the extrusion process should be set on the cylinder.
5. The supply tank prior to the metering pump should be filled with the desired non-solvent, in all cases in this work this is distilled water. The metering pump should be started such that the non-solvent primes the pump and fills the outlet tube for a distance of 2-4 cm after the pump head the flow on the metering pump should then be set to 5 ml/min and the pump stopped.
6. The solution tank should be opened and the spinning solution poured in. Note: if a valve is in place between the solution tank and the spinnerette it should be closed prior to pouring in the solution. The solution will take some time to pour so can be left pouring for a few moments
7. The sponge surface on the motor driven roller should be made wet and the roller should be started at a drive speed of 20 rpm.
8. The solution should have poured by this stage and the solution tank should be closed tightly.

Spinning Rig Shut down/clean down procedure

1. When gas begins to come from the extrusion head the air stop valve should be closed and the metering pump switched off.
2. The valves on the outlets from both baths 1 and 2 should be opened once the last of the fibre has reached tank three. Approximately the last one meter of fibre made should be discarded.

3. The air cylinder should be closed.
4. The solution tank should be opened and disconnected from the spinnerette such that the tube between the solution tank and spinnerette remains attached to the solution tank.
5. The tank can be cleaned by filling with water and removing solution as it solidifies on contact with the water. The spinnerette can be cleaned in a similar manner though certain parts of the spinnerette which do not contact the solution can be removed first.
6. The tube still attached to the solution tank can be disconnected once the tank is clean and one end should have solidified (the end which was attached to the solution tank). By pushing a stiff wire which has been wetted with tap water through the tube from the spinnerette end all the solution can be removed either by pushing it out or solidifying it on the wire using a pipe cleaning (back and forth action) action.
7. All parts should be thoroughly rinsed and then dried by placing them in an oven at 50-65°C

Mass transfer rig start up procedure

Notes on start up: the start up procedure outlined below is a full version for use of a silicate solution or water to test mass transfer – the same procedure applied for washing with sodium hydroxide after silicate solution has been used but some instructions are not required if only cleaning is being carried out more guidance is provided below in the "Shut down/clean down" section.

Start up:

1. The batch recycle tank was weighed using a suitable scale measuring in excess of 8 kg was used for this purpose.
2. The chosen liquid was added to the tank and the tank re-weighed, the system charge was be calculated.
3. All connections to the batch recycle tank were made.
4. In systems where the test cell is employed the liquid side valve prior to the test module was fully closed. A rubber bung with a 1.5mm hole was placed in

test cell in the free port for the DO probe and a 50 ml capacity syringe placed in the 1.5 mm hole in the bung. The syringe was used to draw liquid into the test cell – by repeatedly withdrawing the plunger, removing the syringe from the bung, resetting the plunger and replacing the syringe if necessary. When the test cell was filled the syringe was left in the bung in a ready to draw liquid position.

5. The valves on the liquid side flow were both fully opened.
6. The pump control was set to zero and all equipment was switched on at the mains.
7. In a ceramic membrane system a gas side pressure of 200 kPa is required for start up and was provided using lab air or cylinder air. A rate of 1 dm^3/min was normal for start up.
8. The pump was switched on and it was ensured that the indicated pump speed was zero and that the pump did not appear to be turning. Gently the pump speed was raised to 10-15%, liquid will begin to rise out of the test cell and out of the batch recycle tank. If this was the case the pump speed was increased to 30-40% gently for silicate solution (80-100% for water or water like solutions). If liquid failed to move the test cell was re-primed by returning to instruction 4. If a second failure to pump occurred instruction 11 was followed, if this failed a moving seal in the pump head usually required re-setting. Once liquid reached the pump head it flowed quickly throughout the rest of the rig.
9. Both liquid side pressure gauges usually made minimal movement – possibly going as high as 10 psi (68.94 kPa) at the maximum. If the pressure went higher the pump was stopped immediately. Both liquid side valves were checked and should ave been found to be open fully. If the valves were in order and the pressure roses again on restart at 30-40% then the pump was stopped again and the system drained – shut down/clean down instructions were followed (see below).
10. If the liquid flowed normally with no great pressure rise the liquid flow was dropped quickly to 10-15% for silicate solution and 30-40% for water or water like solutions so as to allow the flow to gently fill the system. Start up continued from instruction 12.

11. If instruction 8 failed to prime the pump then manual priming was carried out. The inlet tube to the pump was disconnected from either the main tank or test cell dependant on the set-up. The inlet tube was held by hand such that the tube end faced upwards and could be filled with liquid. The tube was filled with liquid from the batch recycle tank by syringe. The pump was switched on and the level in the tube usually dropped as the pump speed is gently increased to 5-10%. If this was the case all rig connections were be re-made and instructions proceeded again from instruction 8. If pumping did not proceed the pump usually needed its internal moving seal to be reset. In this case the system was drained and when the pump was ready the instructions began again from instruction 1.
12. The level in the test cell dropped as liquid was drawn from it by the pump. This liquid was initially replaced by air in the tube which connected the batch recycle tank to the test cell (it was not sufficiently narrow to avoid rapid draining after the test cell had been filled in instruction 5). As such the pump was stopped and the module inlet liquid valve fully closed. The syringe was used to reload the test cell, once again the syringe remained in the bung in a ready to draw position. The liquid valve was fully opened once again and the pump re-started.
13. Liquid would quickly emerge from the recycle tube which feeds from the module back to the batch recycle tank. If silicate solution was being used the tube was held above the liquid level to avoid bubbling of the air in the system (air from within the system being forced out ahead of the advancing front of liquid).
14. The system was now allowed to pump for some time to eliminate pockets of gas in the system areas known to hold gas such as tubing corners were tapped gently. The module was manoeuvred by hand in order to dislodge trapped gas pockets.
15. The liquid side valves were adjusted to give the desired liquid side pressures in most cases this was achieved by the after module valve.
16. If using a polymeric membrane air could be fed to the gas side, both gas side valves were fully opened and air was supplied at any rate desired within the operational limits given by the manufacturer provided the gas side inlet

pressure remained a minimum of 5 psi (34.47 kPa) below the liquid side outlet pressure.

17. The DO meter was calibrated if required (usually only first start up on any day).
18. Once the system is settled and no pockets of gas were coming through the recycle tube the stirrer in the batch recycle tank was started.
19. The DO meter was located in its correct position which is dependant on the set-up. If it was placed in a test cell the pump was stopped while the probe was swapped for the bung and syringe and then re-started. Depending on location of the test cell relative to the tank level the test cell could fill or drain slowly on removal of the bung so the probe was inserted quickly. Ideally the level (in terms of height not tank volume) in the test cell was as close as possible to the level in the batch recycle tank to prevent this.
20. The argon cylinder should was opened and the regulator set to 3 bar for polymeric membranes and to 6 bar for ceramic membranes.

The system is now ready for experiments and the DO measurement procedure can be followed.

Mass transfer rig shut down/clean down procedure

1. Air should have been running on the gas side of the membrane for ceramic modules. All gas side flow for the polymeric module was stopped.
2. The pump rate was slowed to 10-15%. The outlet from the batch recycle tank was lifted clear of liquid surface and the pump was switched off when all liquid remaining in the lines reached the pump. If using a test cell there was still some residual liquid in the test cell.
3. The DO meter was removed from the main tank or test cell and rinsed thoroughly with plenty of tap water – the protective DO meter cap was fitted.
4. The liquid line valve prior to the module was closed. The module was disconnected from the pump upstream of the liquid line valve. The module was raised to a position such that the liquid could drain to the batch recycle tank and the closed liquid line valve was re-opened. Once open the liquid could drain to the tank, some manoeuvring of the module was be necessary to remove all the liquid.

5. The batch recycle tank was drained by returning silicate solution to its container – pouring water to drain or returning sodium hydroxide to its container if it has been used in the main tank.
6. All connections on the module were re-made and the start up procedure implemented with a 5 wt% solution of sodium hydroxide (used for coarse wash see above) unless water was in use in which case there is no need for the alkali rinse and instruction 9 was carried out. Note: Water was NEVER used to rinse after silicate solution as it causes solidification of components in the solution. The rinse solution was not used in the batch recycle tank (though it could have been) and no stirring of the batch recycle tank or rinse solution is required in this time. The rinse was fed direct from a lab bottle of 1 dm^3 capacity. The DO probe must not be put into the system. Sodium hydroxide was circulated through the system for several minutes, and retained for future coarse washes. A second 5wt% of solution used for fine wash (see above) should not be run through the system.
7. For ceramic membrane units gas flow was periodically be stopped during the flush and the liquid module outlet closed – liquid was driven through the membrane wall into the gas side and was observed in the lines. Liquid would readily flow into the gas side if the membrane was not blocked if it did not there may have been dried silicate in or on the membrane wall and a long period of such flushing was be required to clear it. For extremely severe blockages the blockage clearance procedure was followed. Once liquid was observed in the gas lines the liquid side valve was re-opened and gas flow was re-started. This procedure was NEVER used with polymeric membranes.
8. The procedure is now repeated, by draining down and rinsing with water unless silicate solution was to be used on next run. Once the water rinse was complete instruction 9 could be carried out.
9. All electrical connections to the rig were disconnected. The air supply was switched off if on lab supply or the air cylinder closed. The remaining gas in the lines was vented through the gas side of rig. The argon cylinder was closed and vented argon from lines through the gas side of rig.
10. The batch recycle tank was cleaned with water if silicate solution has been used and then left open to dry.

Blockage clearance:

Blockages in the module usually arise from deviation from the operating procedure such as leaving silicate in the system overnight but failure to turn off the gas supply which can dry out the silicate which is static in the module. In the case of a blockage being identified in the start up instructions a sodium hydroxide solution of >10 wt% should be used as the start up liquid (blockages are usually only encountered as partial blockages so water and liquids of similar viscosity should pass through the module without causing excess liquid side pressure). The sodium hydroxide should be run and refreshed as it becomes contaminated for several hours (8 or more is typically required). For ceramic membranes some use of the technique described in "Shut down/clean down" instruction 6 may be required.

Sparge and ultrasound start up procedure:

1. The batch recycle tank and ultrasound cell were charged with the chosen liquid and all connections made as shown in Figure 4.10. The mass of the container from which the chosen liquid was poured was measured before and after charging and the mass added to the system was noted.
2. The batch recycle tank was closed and a large excess of sealant grease was fed into the stirrer seal as this provided semi-controlled pressure relief from the tank.
3. The test cell was charged with the liquid under the same procedure used in membrane mass transfer measurements start up.
4. The pump was set on a speed of 0%. All electrical items on the rig were switched on.
5. The pump speed was raised 10-15% until the lines between the pump and the tests cell and the test cell and ultrasonic cell were filled. The pump was briefly stopped and the test cell refilled with the syringe. The DO probe was placed in the test cell.
6. The air flow to the batch recycle reactor was set such that it was suitable for the experiment that is to be carried out.
7. The ultrasonic bath was switched on.

8. If flow of liquid from the batch recycle tank towards the ultrasound cell began after a few moments the sealant grease seal on the stirrer was successful and start up could continue. If liquid did not flow the stirrer seal adjuster had to be tightened (this forced more sealant grease into the gap between the stirrer and stirrer seal components. Liquid would begin to flow towards the ultrasound cell. If this still did not occur all other seals on the tank were checked and application of more grease to the stirrer seal may have been required. Flow would begin once seals were correct.
9. Balancing of the raising and lowering of the level in the ultrasound tank was by adjustment of the pump rate. A higher rate lowered the level and a lower rate would see the level rise.
10. Bubble free liquid would flowing to the test cell and the DO meter would have no bubbles around its tip. If this was not he case the pump and air were stopped and the tip cleaned and re-inserted to the system. The pump and air were then be restarted.

<u>Sparge and ultrasound shut down/clean down procedure:</u>

1. Gas and pumping were be stopped.
2. The batch recycle tank was disconnected from the system and drained along with the ultrasound test cell and DO test cell. The disconnected lines were drained also at this time. The two lines either side of the pump were NOT disconnected from the pump.
3. If silicate solution had been used the lines and pump needed to be cleaned otherwise all gases were be switched off, pressure in lines vented and electrical equipment turned off.
4. The fully disconnected lines were washed with water and allowed to dry.
5. The pump should was cleaned if by placing the free end of the feed line into sodium hydroxide (coarse wash used in membrane mass transfer clean down can be used) the liquid from the free end of the pump outlet line was collected. So that the same liquid can be pumped through five times.
6. Finally water was pumped through the pump for ten-fifteen minutes.

Note: sodium hydroxide need not be used for cleaning on all parts of this system as there are no narrow channels except in the pump and hence any solids formed on contact with water are easily flushed away. The method requires the delicate balance of pressure and suction in order to run wit the one pump that was available as such wide ranging conditions could not be tested.